SURFACE IMMOBILIZATION OF NATURAL WETTING AND LUBRICATING AGENTS FOR THE DEVELOPMENT OF NOVEL BIOMIMETIC CONTACT LENSES

SURFACE IMMOBILIZATION OF NATURAL WETTING AND LUBRICATING AGENTS FOR THE DEVELOPMENT OF NOVEL BIOMIMETIC CONTACT LENSES

By
MYRTIDIOTISSA KOROGIANNAKI
Dipl. Ing. (B. Eng, M. Eng.), M.A.Sc

A Thesis
Submitted to the School of Graduate Studies
in Partial Fulfilment of the Requirements for the
Degree of Doctor of Philosophy

McMaster University
Hamilton, Ontario

DOCTOR OF PHILOSOPHY (2018) McMaster University

(Chemical Engineering) Hamilton, Ontario

TITLE: Surface immobilization of natural wetting and lubricating agents for the development of novel biomimetic contact lenses

AUTHOR: Myrtidiotissa Korogiannaki

Dipl. Ing (B. Eng, M. Eng) – University of Patras, Greece

M.A.Sc – McMaster University, Canada

SUPERVISOR: Professor Heather Sheardown

NUMBER OF PAGES: xxiii, 252

Abstract

Despite the effort to optimize soft contact lens performance, almost half of the 140 million contact lens wearers worldwide experience symptoms of ocular dryness and discomfort, especially towards the end of the day. These symptoms are attributed to reduced compatibility between the contact lens and the ocular surface and are the main reason for contact lens discontinuation. As the interactions of the contact lens-eye interface are dynamic, the surface properties play a key role in improving ocular compatibility, comfort and overall performance of contact lenses. One promising method to reduce adverse interfacial interactions between the contact lens and the ocular surface is to modify the contact lens surface with a biomimetic layer inspired by the ocular surface and the tear film. Hyaluronic acid (HA) is a non-sulfated glycosaminoglycan naturally found in the ocular environment providing ocular hydration and lubrication. Proteoglycan 4 (PRG4), a mucin-like glycoprotein naturally produced at the ocular surface contributes to natural lubrication during blinking and to tear film stability. Surface modification with HA or PRG4 has been shown to result in improved wetting, lubricating and antifouling properties. Moreover, HA and PRG4 have been previously found to interact and synergistically reduce friction further.

In the current work, novel HA and PRG4-grafted soft contact lens surfaces were prepared, and the impact of the surface tethered layer on important contact lens properties was assessed. Furthermore, the potential synergistic effect between HA and rhPRG4 on the examined properties was evaluated.

Surface immobilization of HA on model conventional (pHEMA) and silicone (pHEMA-*co*-TRIS) hydrogel contact lenses was achieved by thiol-ene "click" chemistry, while full-length recombinant human PRG4 (rhPRG4) was surface grafted via carbonyldiimidazole (CDI) linking chemistry respectively. The chemical structure after each modification step was determined by attenuated total reflectance FTIR (FTIR-ATR) and X-ray photoelectron spectroscopy (XPS) analyses. HA-grafted model soft contact lenses were characterized by improved surface wettability, antifouling and water retentive properties, while a decreasing trend in boundary friction was observed but only for the HA-grafted pHEMA-*co*-TRIS materials. Surface-tethering of rhPRG4 was found to effectively enhance the surface wettability and boundary lubricating properties of pHEMA-*co*-TRIS hydrogels only, whereas both rhPRG4-grafted pHEMA and pHEMA-*co*-TRIS materials exhibited lower protein sorption and dehydration rate. Overall, the surface immobilization processes followed herein did not alter the optical transparency of the

model soft contact lenses or their *in vitro* compatibility with human corneal epithelial cells. Finally, there was evidence that HA and rhPRG4 synergistically interacted, further improving the contact lens properties. However, the degree of HA/rhPRG4 synergy was found to be dependent on the configuration of the formed HA/rhPRG4 complex as well as the composition of the substrate hydrogel material, with the noted improvement being more significant for the model silicone hydrogels.

This is the first study to examine surface grafted full-length rhPRG4 and the effect of this modification on contact lens properties. Moreover, the study is the first to investigate the interactions between covalently tethered rhPRG4 and solutions containing HA. The results of this thesis demonstrate that HA and rhPRG4 are good candidates for the development of novel biomimetic surfaces, especially for silicone hydrogel contact lenses. The potential for using these compounds in synergy was also demonstrated, with wetting solutions of HA showing promise for modifying rhPRG4 modified materials to improve symptoms of discomfort. These naturally occurring ocular agents have the potential to improve the management of ocular dryness and discomfort, thus optimizing the overall soft contact lens performance.

Acknowledgements

This thesis is the final stop of a long journey of educational endeavors and I would like to thank all those who helped me along the way to reach a goal that no one can easily achieve alone. All of you together are greater than the parts.

First of all, I would like express my sincere gratitude to my supervisor, Professor Heather Sheardown, for your invaluable guidance through this journey by inspiration, scientific skills, passion and encouragement, especially in times of struggle and doubt. Your confidence and support over the years have given me the opportunity to discover new horizons as well as to grow and develop as a researcher and an individual. I would also like to thank you for giving me the opportunity to participate in some many conferences all over the world, and thus meet and get inspired by so many interesting and top researchers of the bioengineering and contact lens field. Thank you for believing in me and allow me to become a patient (half)-marathon runner in the lab and in real life! It has been a true honor and great privilege to work with you!

I would also like to sincerely thank my supervisory committee members, Dr. Lyndon Jones and Dr. Carlos Filipe, for your guidance, help and feedbacks, for providing your critical perspective on my PhD project and for teaching me how to think outside the box but also to narrow down my focus so as not to spend the rest of my "life" in the lab!

Moreover, this work would not have been possible without the collaboration of Dr. Tannin Schmidt and his research group. Dr. Schmidt, thank you for sharing your expertise in the field of biotribology and for your helpful feedback, insightful thoughts and guidance. A special thank to Dr. Michael Samsom for his help in conducting the friction experiments.

I would like to express my appreciation to Dr. John Vlachopoulos for your unreserved help and encouragement since the first day I came to McMaster University, for sharing your tremendous knowledge while guiding me in the right academic directions and for always being available and supportive, especially when things were not easy.

I have been fortunate to be part of the Sheardown group that truly made working in the lab, day or night, a joy! I would like to thank all the students within the Sheardown group that throughout the years helped me and contributed to my unforgettable graduate experience. Most of all, I would like to thank Lina Liu for her endless help, patient support and for always answering with a smile to my unending barrage of questions. Our lab is very lucky to have you! Special

thanks to Fran for being my "ask-me-anything" person and being resourceful since day one, Alysha for our long contact lens-related conversations and funny Starbucks writing moments, and Vidooni for being such a good listener during our coffee time in the office and for not getting mad at my pranks. I will always cherish these moments! I also want to thank my summer students, especially Jeff and Moiz, for helping with the loads of my samples! I would also like to acknowledge Dr. Jianfeng Zhang and Dr. Talena Rambarran for their help and insightful advice regarding my chemistry questions, Dr. Megan Dodd for her assistance with the cytotoxicity assay; and from the Biointerface Institute Dr. Danielle Covelli for her help obtaining the XPS spectra and Dr. Marta Princz for administrative support.

This journey would not be meaningful without the people that I met along and became true friends with. I owe you all so much and I apologize if I was MIA during the last part of writing my thesis. Effro, Thano, Pedram, Shayan, Lili, Kaveh and Hajir, thank you for all those crazy moments of laugh and happiness but also for cheering me up throughout the ups and downs of this journey!

Last but not least, I would like thank my friends and family in Greece for giving me a tremendous amount of support and encouragement over the years, for always being there for me – no matter the distance – and for making this whole process an adventure that made me the person who proudly I am today. Dad, thank you for always trying to understand my challenges as an engineer. Mom, thank you for your words of wisdom, for teaching how to believe in myself and never give up in order to follow my dreams. Alex, thank you for all your wise advices and for being the best brother and friend I could ever ask for! Words are not enough to express my gratitude about my family, as this journey would not have been possible for me without them. I owe you more than you know! This thesis is dedicated to you!

Sapere aude…

Horace, Epistularum liber primus

Preface

This Ph.D. dissertation is organized in a sandwich style based on published, submitted and prepared for submission articles as described below:

Chapter 3

M. Korogiannaki, J. Zhang, H. Sheardown, Surface modification of model hydrogel contact lenses with hyaluronic acid via thiol-ene "click" chemistry for enhancing surface characteristics. J Biomater Appl. 2017 Oct;32(4):446-462. doi: 10.1177/0885328217733443.

In Chapter 3, all experiments were conducted by myself, M. Korogiannaki. Dr. J. Zhang provided assistance in the synthesis of the materials. The paper was initially drafted by myself, M. Korogiannaki, and edited for the final version by Dr. Heather Sheardown.

Chapter 4

M. Korogiannaki, L. Jones, H. Sheardown, The impact of a hyaluronic acid-grafted layer on the surface properties of model silicone hydrogel contact lenses. Submitted to *Langmuir*, Manuscript ID: la-2018-01693k (May 2018).

In Chapter 4, all experiments were conducted by myself, M. Korogiannaki. The paper was initially drafted by myself, M. Korogiannaki, and edited for the final version by Dr. Lyndon Jones and Dr. Heather Sheardown.

Chapter 5

M. Korogiannaki, M. Samsom, T. A. Schmidt, H. Sheardown**,** Surface functionalized model contact lenses with a novel bioinspired Proteoglycan 4 grafted layer. Submitted to *ACS Applied materials & Interfaces*, Manuscript ID: am-2018-09755d (June 2018).

In Chapter 5, synthesis and surface characterization experiments were conducted by myself. In vitro friction measurements were conducted by Michael Samsom. The paper was initially drafted by myself and edited for the final version by Dr. Tannin Schmidt and Dr. Heather Sheardown.

Chapter 6

M. Korogiannaki, M. Samsom, A. Matheson, T. A. Schmidt, H. Sheardown, Investigating the synergistic interactions of surface immobilized and free natural ocular lubricants for contact lens applications: A comparative study between hyaluronic acid and proteoglycan 4 (Lubricin).

In Chapter 6, synthesis and surface characterization experiments were conducted by myself, M. Korogiannaki. *In vitro* friction measurements were conducted by Michael Samsom and Austyn Matheson. The paper was initially drafted by myself, M. Korogiannaki, and edited for the final version by Dr. Tannin Schmidt and Dr. Heather Sheardown.

Table of Contents

List of Figures

List of Tables

List of Abbreviations

^{1}HNMR	Proton nuclear magnetic resonance
Acr Cl	Acryloyl chloride
AFM	Atomic force microscopy
ANOVA	Analysis of variance
AR-XPS	Angle-resolved - X-ray photoelectron spectroscopy
ATRP	atom transfer radical polymerization
ATS	artificial tear solution
BSA	bovine serum albumin
B&L	Bausch&Lomb
CLPC	contact lens papillary conjunctivitis
CDI	N,N'-carbonyldiimidazole
Dk	oxygen permeability
Dk/t	oxygen transmissibility
DTT	1,4-dithiothreitol
ECM	extracellular matrix
EDC	1-ethyl-3-(3-dimethylaminopropyl) carbodiimide
EDTA	ethylenediaminetetraacetic acid
EGDMA	ethylene glycol dimethylacrylate
EGF	Epidermal Growth Factor
EWC	equilibrium water content
FDA	U.S. Food and Drug Administration
FTIR-ATR	Fourier transform infrared spectroscopy - attenuated total reflectance
HA	Hyaluronic Acid
HA-SH	Thiolated Hyaluronic Acid
HA_{sol}	physisorbed HA
HEMA	poly(2-hydroxyethyl methacrylate)
HEX	hemopexin
HCEC	human corneal epithelial cells
HOBt	hydroxybenzotriazole
HSA	human serum albumin

HPMC	hydroxypropyl methylcellulose
I184	Irgacure® 184
I2959	Irgacure® 2959
IgG	Immunoglobulin G
IPN	interpenetrating network
ISO	International Organization for Standardization
LIPCOF	lid parallel conjunctival folds
LWE	lid-wiper epitheliopathy
MPC	2-methacryloyloxyethyl phosphorylcholine
MTT	3-(4,5-dimethylthiazol-2-yl)-2,5-diphenyltetrazolium bromide
MW	molecular weight
NSERC	Natural Sciences and Engineering Research Council of Canada
NVP	N-vinylpyrrolidone
PBS	phosphate buffer saline
PEG	poly(ethylene glycol)
pI	isoelectric point
PMMA	polymethylmethacrylate
pMPC	poly(2-methacryloyloxyethyl phosphorylcholine)
PoLTF	post-lens tear film
PreLTF	pre-lens tear film
PRG4	Proteoglycan 4
PVA	polyvinyl alcohol
PVP	polyvinylpyrrolidone
RH	relative humidity
rhPRG4	recombinant human PRG4
$rhPRG4_{sol}$	physisorbed rhPRG4
SMB	somatomedin
SD	standard deviation
SEALs	superior epithelial arcuate lesions
SEM	standard error of the mean
SiHy	silicone hydrogel

TBUT	tear film break-up time
TCEP	tris(2-carboxyethyl)phosphine
TEMPO	(2,2,6,6-tetramethylpiperidin-1-yl)oxidanyl
TRIS	3-methacryloxypropyl-tris-(trimethylsiloxy)silane
UV-vis	ultraviolet – visible
XPS	X-ray photoelectron spectroscopy

Chapter 1

1.1. Introduction

It is estimated that there are more than 140 million contact lens wearers worldwide, with soft contact lenses continuing to dominate the market [1]. Approximately 90% of the newly fitted and refitted contact lenses are conventional and silicone hydrogel contact lenses, with the latter accounting for the two-thirds of the prescribed soft contact lenses [2]. Conventional hydrogel contact lenses, although well-accepted for daily use, were characterized by limited oxygen permeability for extended wear [3]. The introduction of highly oxygen permeable silicone hydrogels to the contact lens market overcame such hypoxia-related complications of conventional hydrogel materials as corneal edema, limbal hyperaemia and corneal vascularization [4,5], allowing for overnight wear. However, the surface mobility of the inherently hydrophobic siloxane components compromised the surface hydrophilicity of these materials, which in turn created issues associated with surface wettability and deposition [6]. Different techniques have been used over the years aiming to improve their surface wettability, reduce deposits and ultimately provide higher degree of comfort, either by incorporating hydrophilic monomers or high MW polymers, synthetic analogues or networks during synthesis, or by modification of the silicone hydrogel surface post synthesis [7–10].

Despite the efforts to optimize soft contact lens characteristics and their overall performance, up to 50% of contact lens wearers continue to experience sensations of dry eye and discomfort, particularly towards the end of the day [11–13]. These symptoms are considered to be the primary reason for limiting or even discontinuing contact lens wear [14–16], creating a significant drain on the overall growth of the contact lens wear base [16]. Moreover, the issue of contact lens discomfort is of great concern for novel applications of soft contact lenses in the future, including control of myopia, ocular drug and stem cell delivery and their use as biosensors, since the success of these applications relies on long-term comfortable and successful wear by the patients in order to receive the benefits from these innovations [17].

The factors that affect contact lens performance are complex, multifactorial and can independently or synergistically result in a specific etiology for poor ocular compatibility [18]. Upon insertion, a soft contact interacts *in situ* with the cornea, the perilimbal conjunctiva and the eyelids while is in direct contact with the tear film. In turn, changes in tear film physiology,

dynamics and nature of dispersal occur [19,20]. Thinning of tear film in the presence of a soft contact lens, which is not as wettable as the natural corneal surface, often in combination with more incomplete or infrequent blinking may interrupt the tear film reformation and increase the tear film break-up time and evaporation rate. This subsequently would result in tear film instability, irrespectively of the soft contact lens material [6,20]. Disruption of tear film stability is reported to be a major contributing factor to deposit formation and lack of lubrication which in turn degrade the quality of contact lens surface over time and frequently may be accompanied by reduced vision, mechanical irritation, ocular surface alterations, epithelial trauma or even stimulation of an immune response [14].

Ideally a biocompatible contact lens should be characterized by adequate wettability and lubricity to support the formation of a stable and continuous tear film, be resistant to accumulation of tear deposits and to biofouling, provide the oxygen requirements and have the mechanical properties of the cornea while causing minimum interruption of the ocular surface function during wear; thus allowing for clear vision and good performance/comfort throughout the day. Since the contact lens is dynamically interacting with the ocular surface and the tear film during wear, the surface properties of the contact lens play a critical role in its ocular compatibility, comfort and overall performance [21]. Currently, friction is the only variable from the contact lens properties known to directly associate with discomfort *in vivo* [22]. Other variables such as contact lens dehydration and poor surface wettability, uncontrolled protein and lipid deposition and denaturation, modulus (stiffness), oxygen deficiency, contact lens (edge) design as well as compromised tear film physiology and stability may also contribute to ocular dryness and discomfort during contact lens wear but to a lesser extent [23,24].

With contact lenses being the most widely studied ophthalmic material and contact lens technology constantly trying to get improved, the current statistics suggest that there is still some considerable margin of improvement in the surface characteristics of soft contact lenses. One promising method with the potential to reduce the adverse interfacial interactions between the contact lens and the ocular surface and thus improve its ocular compatibility and performance, is to modify the contact lens surface with a biomimetic layer inspired by the ocular surface and the tear film. In native tear film, the glycocalyx which is composed by mucins is responsible for anchoring the tear film on the otherwise hydrophobic corneal surface and provide adequate lubrication to the eye to prevent any damage of the ocular tissues from the shear-induced forces

developed by the eyelid during blinking. Therefore, naturally occurring ocular wetting and lubricating agents, such as hyaluronic acid (HA) and proteoglycan-4 (PRG4), could be used for the functionalization of the contact lens surface.

Hyaluronic acid (HA) is a linear, anionic non-sulfated glycosaminoglycan naturally found at the ocular surface and tear film [25–28] contributing to ocular hydration and epithelial regeneration [29]. Taking advantage of its ocular compatibility and unique hygroscopic, rheological and lubricating properties, HA has also been used in artificial tears and in contact lens products, including packaging and multipurpose solutions, alleviating the symptoms of dry eye disease [30–32] and contact lens related dryness and discomfort [16,33]. PRG4, a mucin-like glycoprotein present in meibomian gland secretions and at the corneal surface [34,35], is postulated to contribute to tear film stability and natural lubrication of the ocular surface during blinking and eye movements [34,36,37]. A recent clinical study [38] showed that eye drops containing full-length recombinant human PRG4 (rhPRG4) were effective in the treatment of dry eye disease, likely by restoring the glycocalyx layer thus enhancing tear film homeostasis. Moreover, several studies have shown the surface modification with HA or PRG4 provided antiadhesive [39–41], antifouling [42–44] as well as wetting and lubricating properties [45–47]. Finally, both HA and PRG4 function as boundary lubricants creating a low friction boundary layer preventing physical contact during sliding [48,49]. Boundary friction occurs at low sliding speeds and/or high contact pressures, as in the case of compromised synovial fluid in the joints or tear film in the eye. Interestingly, HA and PRG4 have been shown to interact with each other and by forming an HA/PRG4 complex to synergistically reduce friction to a greater extent than either agent would alone [34,50,51]. Therefore, the natural wetting and boundary lubricating properties of HA and PRG4 could be exploited for the modification of contact lens surfaces that ultimately would allow for enhanced compatibility between the contact lens and the ocular environment.

Based on the hypothesis that coating the surface of soft contact lens materials with a natural, ocular friendly layer with inherent hydrophilic and lubricating properties can improve their surface characteristics long-term under physiological conditions without altering their bulk properties, the overall goal of this thesis work is to investigate the potential of surface immobilized HA and rhPRG4 to allow for the development of innovative surfaces with well controlled interfacial properties for soft contact lens applications. In addition, this study aims to gain a greater

understanding of the synergistic interactions developed between HA and rhPRG4 biomolecules and their impact on important contact lens properties.

Therefore, the main objectives of this research work are to covalently attach HA or full-length rhPRG4 on the surface of model conventional and silicone hydrogel materials and characterize *in vitro* the developed hydrogels by assessing the following contact lens-related properties, surface wettability, dehydration profile, resistance to protein deposition and boundary friction against corneal tissue. Moreover, the interactions developed between HA and PRG4 were evaluated and the impact of the configuration of the HA/PRG4 complex (HA-grafted+$PRG4_{sol}$ or PRG4-grafted+HA_{sol}) on the following contact lens-related properties, surface wettability, dehydration profile, resistance to protein deposition and boundary friction against corneal tissue was investigated as well.

1.2. Thesis outline

Chapter 1 is a brief introduction to the subject matter related to the content of this thesis work, the main objectives of this research work and the thesis outline.

Chapter 2 provides a literature overview regarding the anatomy of the ocular surface, soft contact lens materials, the material-related interactions and complications developed between soft contact lenses and the ocular surface, important surface properties for improved contact lens performance and methods for surface modification of polymer materials with biomolecules.

Chapter 3 describes the covalent attachment of HA on the surface of poly(2-hydroxyethyl methacrylate) (pHEMA) model conventional hydrogels via nucleophile-mediated thiol-ene "click" chemistry. The HA-grafted pHEMA hydrogels developed were characterized *in vitro* in respect to surface wettability, dehydration rate, lysozyme and albumin deposition, and transparency. The *in vitro* cytocompatibility of the HA-grafted pHEMA hydrogels with human corneal epithelial cells was also assessed. This work has been published in *Journal of Biomaterials Applications* [52].

Chapter 4 reports the synthesis of surface functionalized poly(2-hydroxyethyl methacrylate-*co*-3-methacryloxypropyl-tris-(trimethylsiloxy)silane) (pHEMA-*co*-TRIS) model silicone hydrogel materials with grafted HA via UV-induced thiol-ene "click" chemistry. The surface wettability, dehydration rate, lysozyme and albumin deposition, transparency, and compatibility to human

corneal epithelial cells were determined *in vitro* for the HA-grafted pHEMA-*co*-TRIS materials. This work has been submitted to *ACS Langmuir*, Manuscript ID: la-2018-01693k (May 2018)

Chapter 5 provides a simple two-step method of synthesizing novel rhPRG4-grafted surfaces of model pHEMA and pHEMA-*co*-TRIS hydrogels via carbonyldiimidazole (CDI) chemistry, following by the *in vitro* characterization of their surface wettability, affinity to deposited lysozyme and albumin and frictional properties under boundary conditions using a cadaveric human cornea. The impact of the surface modification on the transparency and on potential cytotoxicity against human corneal epithelial cells was also evaluated *in vitro*. To the best of our knowledge this is the first report of rhPRG4 being chemically tethered to the surface of soft polymeric materials such as hydrogel contact lenses. This work has been submitted to *ACS Applied Materials & Interfaces*. Manuscript ID: am-2018-09755d (June 2018)

Chapter 6 investigated the interactions between HA and rhPRG4 on the surface modified model conventional and silicone hydrogels synthesized in Chapters 3-5 and their effect on surface wetting, water retentive, antifouling and boundary lubricating properties, when one agent was grafted to the surface and the other one was in solution thus physisorbed on the modified surface. In addition, a systematic study about the impact of the configuration of the formed HA/rhPRG4 complex (HA-grafted+$PRG4_{sol}$ or PRG4-grafted+HA_{sol}) on the above properties was also conducted. This chapter is in preparation for submission.

Chapter 7 provides a summary of all the results presented in this thesis and some suggestions to consider as a continuation of this research work that would be valuable additions to the optimizing process and understanding the nature of required surface characteristics for the development of contact lens materials that exhibit good compatibility with the ocular surface and provide higher degree of comfort during wear.

***Appendix* contains the published version of Chapter 3.**

This thesis is written in a "sandwich" thesis format, therefore there is some repetition in the introduction as well as in the materials & methods sections regarding the synthesis of the HA and rhPRG4-grafted pHEMA and pHEMA-*co*-TRIS hydrogel materials in Chapters 3-6.

Chapter 2

Literature Review

2.1. The anatomy of the ocular surface

The human eye is one of the most complex organs in the body. It can be divided into two main parts, the anterior segment and the posterior segment. At the front of the eye, there is a well-integrated unit mainly consisting of the cornea and the sclera separated by the limbus, and the conjunctiva as depicted in Figure 2.1. Together, these form the ocular surface [53]. The eyelids and the lacrimal drainage system work with these structures, and are responsible for the production, distribution and elimination of the tear film. The exposed ocular surface is constantly covered by the tear film. Overall, the role of the ocular surface is to maintain corneal transparency by regulating its hydration as well as by protecting it from pathogenic agents and from mechanical trauma in order to provide vision.

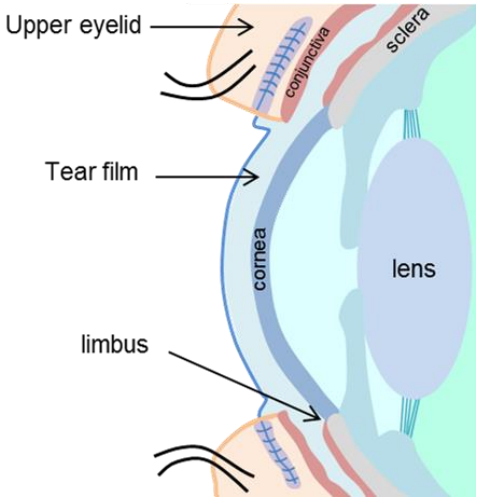

Figure 2.1: A schematic illustration of a cross-section of the anterior segment of the human eye

2.1.1. The Cornea

The cornea is an optically transparent tissue that provides the majority of refractive power to the eye [54]. In order to be transparent, the cornea is avascular and thus the growth factors and nutrients are received by diffusion either from the tear film or the aqueous humor, while the oxygen of the surrounding air is dissolved into the tears and diffuses throughout the cornea [54]. Additionally, the cornea is among the most densely innervated tissues in the human body as it is

broadly subjected to environmental challenges [55]. Structurally, it consists of five layers, starting from the top surface: the epithelium, Bowman's membrane, the corneal stroma, Descemet's membrane and the endothelium layer [56] (Figure 2.2).

The corneal epithelium covers the outermost part of the cornea. The numerous microvilli and microplicae of the superficial corneal epithelial cells have filaments that protrudes into the glycocalyx [57] which in turn contains proteoglycans, glycolipids and cell surface-associated mucins [58]. Due to its dense mucinous structure, the glycocalyx renders the surface of the corneal epithelium hydrophilic, allowing for uniform tear spreading and thus a smooth wettable corneal surface. Along with the tight junctions, the glycocalyx is also responsible for the barrier function of the corneal epithelium that protects the cornea against pathogenic organisms [59]. Bowman's layer, produced by the corneal epithelium, is a thin acellular transition zone, 10–17 μm thick [60,61] that contributes to the maintenance of the corneal structural integrity [62]. Beneath Bowman's layer, the stroma is a transparent collagenous tissue that is the major structural part of the cornea since it is approximately 85-90% of the total corneal thickness [63]. It is essential for the maintenance of the corneal transparency through the regulation of hydration. Immediately posterior to the corneal stroma lies Descemet's membrane, a thin acellular layer secreted by the endothelial cells with a thickness dependent on age (10 μm thick in an adult human cornea) [64]. Finally, the corneal endothelium is a non-regenerating cellular monolayer approximately 5 μm thick, arranged in a honeycomb-like structure (hexagonal-shaped cells). Serving as a pump, it is responsible for the diffusion of solutes and nutrients from aqueous humor to the corneal stroma and the removal of fluid by active transport from the stroma to the aqueous humor, thus maintaining stromal hydration [65–67]. The corneal endothelium is the primary contributor to the maintenance of corneal transparency, hence compromised barrier functions of the endothelium normally result in a loss of visual acuity [64].

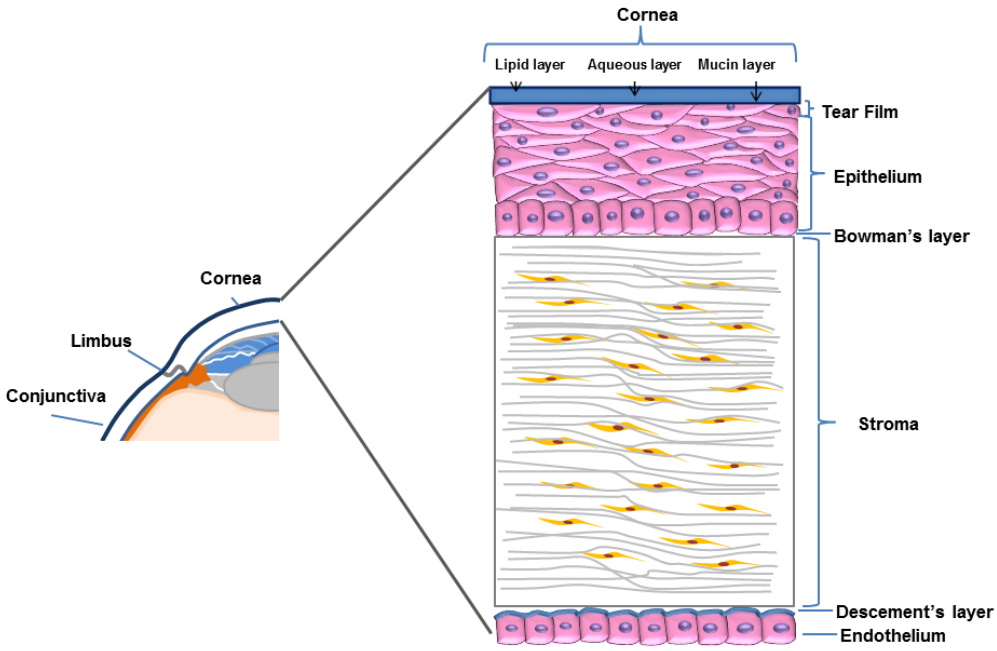

Figure 2.2: Schematic illustration of the structure of the cornea (Adaptation from [68]).

2.1.2. The Sclera

The sclera is the protective outer layer of the eye and is connected to the cornea anteriorly and to the optical nerve posteriorly [69]. It contains primarily glycosaminoglycans, collagen (type I, III, V and VI) and elastin fibers [70]. The irregularity of the orientation of the scleral collagen fibers gives the white color to the eye and it is completely opaque so as to prevent light from entering anywhere within the eye except the cornea. Forming the five-sixths of the connective tissue coat of the posterior part of the globe and generally comprising 95% of the ocular surface area, the sclera is responsible for maintaining the shape of the globe. The border between the cornea and the sclera is designated by the corneoscleral limbus, the pathway of the aqueous humor outflow [71]. Limbal vessels provide the nearest point of access to blood-borne defense mechanisms of cornea since cornea itself is avascular.

2.1.3. The Conjunctiva

The conjunctiva is a thin, vascularized and translucent mucous membrane that covers two-thirds of the ocular surface, from the corneal rim to the lid margin [72]. It is divided into three topographic zones: the bulbar (or ocular), the palpebral (or tarsal) and the forniceal conjunctiva.

The conjunctival epithelium has a similar barrier function as that of the corneal epithelium [73]. Along with the cornea and the limbus, conjunctiva forms the epithelium of the ocular surface. Moreover, the palpebral conjunctiva, which is the most posterior layer of the eyelid, contains goblet cells that synthesize and secrete soluble mucins that will eventually end in tears through the lid wiper surface [74]. Located on the conjunctival side of the inner (ie, posterior) lid margin of the upper and lower eyelids and opposed to the globe, the lid wiper acts as an internal lubrication system that is responsible for reducing friction between the lid margin and the globe during blinking [55]. It is believed to be the only part of the lid margin that comes in direct contact with the globe [53,75]. Hence, the conjunctiva plays a significant role for the formation and stability of tear film, essential factors for the maintenance of corneal transparency and ocular lubrication.

2.1.4. The Eyelids

The upper and lower eyelids are divided into the anterior lamella, which includes the skin and orbicularis oculi muscle of the eyelid and the posterior lamella, which includes to the retractors, the tarsal muscle, the tarsal plate, the palpebral conjunctiva, and the lid margin [76]. Underneath and within the tarsal plate lie the meibomian glands which secrete the lipid layer of the tear film once the upper and lower eyelids come in contact [77]. The lid margin is responsible for the distribution of the mucins secreted into the preocular tear film allowing for ocular lubrication by blinking. Finally, Marx's line is a narrow line of squamous cells that extends along the crest of the of the posterior lid margin of both upper and lower eyelids and is usually visualized as a thin strip by staining with rose Bengal or lissamine green vital dyes. It has been suggested that Marx's line may be involved in contacting the ocular surface [78]. Overall, the eyelids serve as the first line of defense to the eye against foreign bodies and control the quantity of light that enters the eye [76,79].They contribute to the formation of the tear film and play an essential role for the distribution and drainage of the precorneal tears through blinking, facilitating corneal metabolism as well as ocular hydration and lubrication [80]. Therefore, blinking is necessary for corneal health and integrity. There are two types of blinking, spontaneous blinking which is the most common type, and reflex blinking which is involuntary and occurs under external stimulation.

2.1.5. The Preocular Tear Film

The preocular tear film is characterized by a complex structured environment of hydrophilic, amphiphilic and lipophilic components creating an interface between the ocular epithelium and the air. It can be considered as a special form of extracellular matrix component for the ocular surface [81]. The tear film is mainly responsible for providing an environment that protects the ocular surface from any injury and infection, supplies the cornea with adequate oxygen and nutrients, and maintains hydration, lubrication and a smooth ocular surface to allow for light refraction during and between blinks [82]. Hence, maintaining tear film homeostasis, volume and stability are major parameters for a healthy eye.

In humans, the thickness of the precorneal tear film is estimated to be approximately 4-7 μm thick, depending on the method of assessment [83,84], and approximately 4–10 μl in volume [85,86]. Human tears exhibit non-Newtonian shear-thinning behavior, which is essential for the proper lubrication of the ocular surface during blinking [87,88]. In normal subjects they have a surface tension is approximately two-thirds that of water or saline [89]. Moreover, the mean value of the tear film pH ranges from 7.2 to 7.5, similar to the pH of the plasma [90]. Interestingly, the tear film changes its composition in response to environmental and bodily conditions; and tears have been classified into basal, reflex, emotional, and closed-eye tears.

2.1.5.1. Structure of Precorneal Tear Film

The tear film components work in harmony to continuously perform multiple vital optical and physiologic functions. Wolff [91] was the first to describe the unique three-layered structure of the precorneal tear film that consists of the outermost thin lipid layer, the middle aqueous layer and the innermost mucous layer that covers the epithelium of the ocular surface (Figure 2.3). Although this layered preocular tear film model is still favored, it is currently proposed that it would be more accurate to describe the aqueous and mucous layers as a continuous phase [92] whose mucin density is reduced towards the lipid layer [93,94], while it is noted that components from each layer can be found throughout the entire film [95].

The thin superficial lipid bilayer (13-100 nm thick [96]), produced by the Meibomian glands (Meibum secretion), consists of the outer layer that contains non-polar lipids and the inner layer that contains polar lipids, and is adjacent to the aqueous layer. The non-polar lipids found in the

lipid layer include cholesterol esters, non-polar wax esters and triacylglycerol, cholesterol and free fatty acid [97], whereas phospholipids are the main polar lipids of the lipid layer [95]. The lipid layer reduces the surface tension and maintains the viscosity and elasticity of tear film, contributing to uniform tear film spreading over the corneal surface during blinking [98]. This in turn inhibits the early tear film break-up time (TBUT), helps to maintain the integrity of the ocular surface, and prevents the spillage of the tears over the eyelid margins. Tear film lipids have been shown to contribute to boundary lubrication, facilitating eyelid movement and preventing any damage of the ocular surface due to the high shear forces generated during blinking [99,100]. The absence of a continuous lipid layer was found to result in a four-fold increase in the rate of tear evaporation [101]. As the outer layer of the tear film, it also acts as the first line of defense against the entrance of debris or other contaminants from the environment [102].

The intermediate aqueous layer (6.5-7.5 μm thick [103]), is largely secreted by the main lacrimal gland as well as by the accessory lacrimal glands of Wolfring and Krause [104] and contains proteins, electrolytes, salts, oxygen, enzymes, growth factors and mucins. Some of the major proteins of the aqueous layer, including lysozyme, lipocalin, immunoglobulin A and lactoferrin, as well as enzymes such as peroxidase that function as protective components with antimicrobial activity [105]. Tear film electrolytes are responsible for maintaining a normal tear osmolarity and physiological pH, allowing for protein solubilization, enzymatic activity, maintenance of cellular homeostasis, and secretory function [106]. Significantly elevated tear osmolarity, associated with decreased tear secretion or increased tear film evaporation, has been reported in a variety of ocular surface abnormalities and during contact lens wear [107–109]. Moreover, tear film growth factors can regulate corneal and conjunctival epithelial cell growth, and contribute to the wound healing of the ocular surface [110] and the mucins present in the aqueous layer contribute to the lubrication of the ocular surface [111]. Overall, the aqueous layer is responsible for spreading the tear film over the ocular surface, maintaining tear film stability, while contributing to a trophic and protective environment for the ocular surface epithelium [111].

Finally, the innermost mucous layer is mainly comprised of heavily glycosylated high-molecular weight glycoproteins known as mucins [57,111] that are primarily produced by the conjunctival goblet cells, by the corneal and conjunctival squamous epithelial cells and to a lesser extent by the lacrimal gland [112,113]. The mucins of the mucous layer are categorized into secretory which are further divided into gel-forming (MUC5A) and small soluble into the aqueous

layer mucins (MUC7); and cell-associated mucins which can be either membrane-spanning mucins or shed into the tear film (i.e MUC1, MUC2, MUC4 and MUC16) [114]. The transmembrane mucins associate with the mucinous glycocalyx of the ocular epithelium, subsequently anchoring the overlaying aqueous layer to the eye [115,116]. Chemical interactions between the glycocalyx and the mucins of the mucous and aqueous layers play a significant role in tear film spreading and ocular surface wetting. Hence, the mucous layer acts as a surfactant and by lowering the tear film surface tension, it creates a hydrophilic and wetting cover that facilitates the retention and even distribution of the aqueous tear film layer on the otherwise relatively hydrophobic ocular surface [46,115]. The mucous layer is primarily responsible for the viscosity of the tear film, however, recently it was suggested that protein and lipids synergistically contribute as well [87,88]. Due to its non-Newtonian rheological properties, the mucous layer protects the ocular surface from shear forces generated during blinking, providing lubrication and anti-adhesive properties [88]. It also contributes to the epithelial barrier protection against pathogens and foreign objects that can damage the ocular surface [117]. Overall, the mucin layer of the tear film has vital functions for protecting the human sight and together with the aqueous layer account for 90% of the tear film thickness [118]. Hence, a decrease in the production or functionality of tear film mucins would be reflected in a decrease in tear film stability.

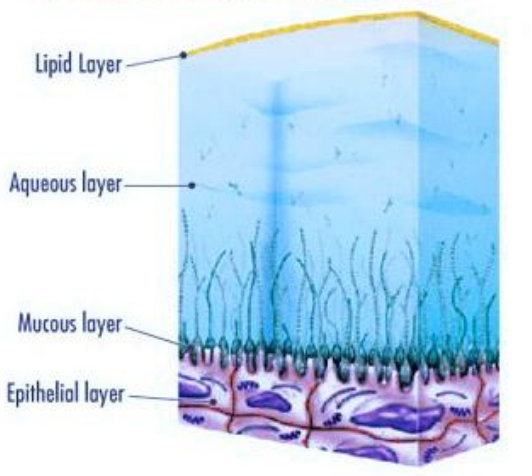

Figure 2.3: Schematic representation of the structure of the precorneal tear film [55].

2.2. Contact Lens Materials

Contact lenses are one of the most widely used biomedical devices in the world, with an estimate of 140 million contact lens wearers worldwide [1,2]. They have a remarkable history that goes back more than 500 years. Leonardo da Vinci is often credited for the first conception of the contact lens idea in 1508, in Codex of the Eye, Manual D, where he described a way to manipulate the corneal power. Throughout the years, numerous other developments have taken place in an effort to correct vision by placing glass-based devices on the eye. In the late 1880s, Fick [119] and Müller [120] were the first to develop thick glass-blown scleral contact lenses. For several decades, only this type of contact lenses was available for the correction of the optical power of the eyes [121–123]. However, the choice of glass as a contact lens material was very problematic as it caused severe hypoxic adverse events and discomfort [122,123]. In the beginning of the 20th century (1930), the development of the plastic polymethylmethacrylate (PMMA), widely known as Plexiglas, allowed for the manufacture of the first polymeric contact lenses. Initially used as scleral lenses for therapeutic purposes and then as the first hard corneal contact lenses for the correction of ametropia, PMMA based contact lenses were significantly thinner, lighter and more convenient. One of the more limiting disadvantages of the hard contact lenses was again the limited oxygen transmissibility [122,123]. This led to development of rigid gas permeable (RGP) contact lenses that were silicone-based, and thus oxygen-permeable, but still rigid polymeric materials.

Wichterle and Lím [124] introduced the concept of using hydrogel materials which conform to the shape of the eye as contact lens devices, leading to the production of the first soft hydrogel contact lenses. Gradually, soft hydrogel contact lens evolved with great success. To date, soft contact lenses are the most prescribed contact lenses because of their comfort, affordability, ease-of-wear and convenience [2]. Soft contact lenses are categorized into conventional hydrogel and silicone hydrogel contact lenses.

2.2.1. Conventional hydrogel contact lenses

Hydrogels have been extensively used in the medical and pharmaceutical fields since they resemble natural tissue more than any other type of synthetic biomaterial. They consist of hydrophilic polymer chains connected together by crosslinkers leading to the formation of a three-dimensional network that can swell in water and biological fluids up to an equilibrium state without

dissolving [125]. The presence of crosslinks in the chemical structure of the hydrogel provides a characteristic physical integrity upon hydration and thus it is of great significance. Hydrogel materials, based on either natural or synthetic components, have been extensively used in the field of biomedical engineering as tissue engineering scaffolds, drug delivery systems, medical and biological sensor, micro-device bases and contact lenses [126–128].

In 1960s, Wichterle and Lim [124] were the first to suggest the use of synthetic hydrogels based on the 2-hydroxyethyl methacrylate (HEMA) monomer, for the development of the first generation of soft contact lenses. The main benefits of the poly(2-hydroxyethyl methacrylate) (pHEMA) contact lens materials were biocompatibility and the ability to absorb and retain water, providing significantly improved flexibility and comfort during wear. Bausch & Lomb eventually bought the patents, obtained FDA approval and introduced the Softlens (polymacon) contact lenses to the market, the first pHEMA-based hydrogel contact lenses as a device for the correction of refractive errors [122]. In the following years, the demand for contact lens functions and comfort increased leading to the continuous development of new monomers and synthetic methods. Incorporation of other hydrophilic monomers, including methacrylic acid (MA), N-vinylpyrrolidone (NVP), vinyl alcohol (VA) and others, to poly(HEMA)-based hydrogel lenses led to higher-water-content conventional contact lenses with lower modulus and higher surface wettability and hydration, parameters that were considered to be important for improved contact lens performance.

Another very important parameter for contact lens performance and safety is the oxygen permeability of the contact lens. During contact lens wear, oxygen delivery to the cornea depends on both the oxygen permeability (Dk) of the material and the thickness (t) of the lens [10]. For conventional hydrogel contact lenses, diffusion of oxygen to the ocular surface occurs through the aqueous phase; thus Dk is directly related to its water content. In fact, Dk was found to increase logarithmically with increasing the water content of the conventional hydrogel contact lenses [5]. Despite the increase in the water content, the oxygen provided to the cornea through the aqueous phase was not adequate enough for overnight or extended wear even in the case of the higher-water-content hydrogel contact lenses [122]. Limited oxygen permeability compromised the corneal physiology causing hypoxia-related complications, such as corneal edema and neovascularization as well as epithelial microcycts or even cell damage that can potentially affect

corneal function [4,5]. Corneal infections, such as microbial keratitis, were also observed during extended wear [129,130].

Moreover, high-water-content contact lenses resulted in increased protein deposits [131–134] and dehydration rates [135,136], as well as low tear strength compared to lower water-content hydrogel contact lenses [137]. The mechanical properties, such as strength and elasticity, were also negatively impacted thus reducing their life-span [138]. Therefore, mid- or high- water content materials have dominated the market primarily in a modality that they were disposed of between a day and one month. Synthetic analogues such as phosphorylcholine (PC) or glycerol methacrylate (GMA) have been also included in the pHEMA lenses to solve the problem of on-eye dehydration and fouling [7,8]. However, the mechanism of oxygen transport in conventional hydrogel cannot change in order to substantially increase the oxygen permeability, despite the different components used for modification. Currently, conventional hydrogels are mainly used as daily disposable contact lenses [2]. As a result, the development of materials with a different oxygen transport mechanism was necessary.

2.2.2. Silicone Hydrogel Contact Lenses

In the late 1990s, the contact lens industry was revolutionized by the development of the silicone hydrogel contact lenses. In silicone hydrogel contact lenses, siloxane and fluoro monomers or macromers, such as methacryloxypropyl tris(trimethylsiloxy)silane (TRIS) or monomethacrylated polydimethylsiloxane (PDMS), are combined with hydrophilic monomers that are typically used in conventional lenses, including HEMA, NVP and/or N,N-dimethylacrylamide (DMA) [139]. The introduction of the silicone domains in hydrogel materials was an important breakthrough in the evolution of contact lenses since the oxygen solubility in these domains is significantly higher than in the aqueous phase. As a result, this type of soft contact lenses are characterized by superior oxygen permeability (up to five times higher than conventional hydrogels), permitting them to be safely worn overnight and on an extended or continuous basis for periods of up to thirty days, while avoiding any hypoxia-related complications [139–141]. Contrary to conventional hydrogel contact lenses where both oxygen and ion permeability are governed by the hydrophilic domains and thus they are both dependent on the water content of the hydrogel material, the oxygen permeability of silicone hydrogel lenses is mainly governed by the presence of the hydrophobic siloxanes whereas the hydrophilic domains present are mainly

responsible for ion and water permeation that in turn is necessary for the on-eye movement of the contact lens [139].

The development of highly oxygen permeable silicone hydrogel contact lens materials was a pivotal moment for vision correction contact lenses. Significant challenges were overcome in order to successfully merge hydrophobic and hydrophilic monomers without phase separation for the production of optically clear contact lens materials. In addition, the migration of hydrophobic siloxane components to the surface was another significant impediment in the development of silicone hydrogel contact lenses. The presence of surface-active silicone chains led to surfaces of low wettability and increased deposition of tear film components [142], rendering these materials unsuitable for contact lens application. For successful contact lens wear, contact lenses materials should possess suitable surface characteristics that would not alter the physiology of the ocular surface while providing vision correction. Along with the evolution of silicone hydrogel contact lenses, developing novel silicone hydrogel materials with appropriate surface properties was always in the centre of attention. Different approaches have been used for the manufacture of silicone hydrogel contact lens materials over the years in an effort to minimize the undesired interactions between the contact lens and the ocular surface.

Initially, the surface properties of the first-generation of extended wear silicone hydrogel lenses were improved by treating their surface post synthesis using gas plasma techniques. More specifically, Bausch & Lomb applied the technique of plasma oxidation for the balafilcon A (PureVision®) lens to modify siloxane groups to silicate, forming well distributed hydrophobic glassy "islands" on the surface of the contact lens [138,143]. On the other hand, CIBA Vision applied to silicone hydrogel contact lenses a high-refractive-index plasma coating of a proprietary polymer that forms a homogenous thin (25 nm) grafted layer on the surface of the lotrafilcon A and lotrafilcon B (Focus Day & Night™ and O_2 Optix™) [143]. In both cases, surface modification led to more wettable surface characteristics and reduced protein and lipid deposition, without affecting the oxygen permeability of the underlying material [139,143].

Another approach is the incorporation of a wetting agent in the bulk of the silicone hydrogel leading to materials of higher water content while maintaining oxygen permeability. For the second-generation silicone hydrogel contact lenses, high MW polyvinylpyrrolidone (PVP) was added via direct entrapment during the synthesis of the galyfilcon A and senofilcon A silicone hydrogel lenses (HydraClear™ technology for Acuvue® Advance™ and Acuvue® Oasys™,

Johnson & Johnson Vision). PVP is a highly hydrophilic polymer that, when entrapped as an internal wetting agent, can migrate to the surface to improve lens wettability and lubricity, yielding a more stable tear film [144–146]. Recently, Bausch & Lomb developed the samfilcon A silicone hydrogel contact lenses (MoistureSeal technology for B&L Ultra®) based on a two-step reaction sequence, forming a semi-interpenetrating network (IPN) post synthesis that is also used as an internal wetting agent. This method was reported to lead to higher amounts of PVP present in the matrix of the samfilcon A contact lenses compared to that of senofilcon A [147].

For the third-generation silicone hydrogel lenses, different hydrophilic functionalized silicone-based macromers were used in combination with hydrophilic monomers [148]. This included the comfilcon A (Biofinity®), enfilcon A (AVAIRA™) and somofilcon A (Clariti Elite and 1 Day) silicone hydrogel lenses developed by CooperVision. The non-TRIS chemistry used in some of these silicone hydrogel lenses allows for enhanced compatibility between the silicone moieties and the hydrophilic domains, while using less silicon, providing high oxygen permeability, water content and inherently wettable surfaces without however requiring the addition of a surface coating or a wetting agent [144,148]. Interestingly, these lenses break the traditional inverse relationship between oxygen permeability and water content by having a significantly higher oxygen permeability than expected based on their water content [149].

The driving force for the development of silicone hydrogel contact lenses was that the increased oxygen availability to the cornea would decrease the rate of corneal infections associated with the overnight lens wear [150]. Studies indicated, however, that despite the obvious reduction in hypoxia with silicone hydrogel materials, the risk of inflammatory events and corneal infections, such as microbial keratitis, and more importantly the rate of loss of vision due to those complications were similar regardless of the contact lens material used with extended wear [151–155]. Additionally, an increase in clinically adverse events during the first generations of silicone hydrogel contact lens wear was observed due to mechanical irritation, particularly in the case of the extended wear modality, including contact lens papillary conjunctivitis (CLPC), superior epithelial arcuate lesions (SEALs) and mucin ball production [156–158]. Therefore, progress in both sophisticated materials science and manufacturing methods over the last decade allowed for the development of silicone hydrogel contact lenses that can be nowadays used as daily lenses with scheduled replacement (from two weeks up to a month), resulting in significantly lower complications during contact lens wear [159,160]. Accounting for approximately 60% of all soft

contact lens fits worldwide, biweekly or monthly disposable silicone hydrogel lens materials remain the most widely prescribed type of contact lenses [2]. However, issues with inflammation and care solution compatibility arose as silicone hydrogels were developed for daily wear use. Hence, daily disposable silicone hydrogel contact lenses that are single-use only, were introduced in the market in 2008, in an effort to further reduce the risk of infection, deposits, and clinical complications as well as care solution-induced corneal staining, while providing the additional physiological benefits of higher oxygen transmissibility [161–163]. It is noteworthy that 2017 marked the first year in which the number of prescribed daily disposable silicone hydrogel contact lenses was higher than that of the conventional hydrogel contact lenses [2].

Recently, delefilcon A (Dailies® Total 1) by Alcon, a daily disposable silicone hydrogel contact lens with a unique water-gradient structure was launched in the market. It has a silicone hydrogel core (water content ~ 33%) that transitions to a thin (5-6 μm) water-gradient surface of crosslinked polymeric wetting agents that form a hydrogel layer with a very low modulus (water content > 80%) [164–167]. So far, delefilcon A has the highest oxygen transmissibility of any daily disposable contact lens and a very low coefficient of friction [166,167], two properties that are considered advantageous for improved contact lens performance [168–170]. Overall, the surface properties of silicone hydrogel lenses are more complex than those of conventional hydrogels and do not correlate directly with water content but they are dependent on the approach used to overcome the inherent wettability problems of silicone hydrogel materials.

Apart from improving the surface properties of the silicone hydrogel materials, the modulus of elasticity has also been targeted over the years. The presence of the silicone domains generally renders the silicone hydrogels more rigid (stiffer) than the majority of conventional hydrogels. Therefore, silicone hydrogel contact lenses initially were not as comfortable as the conventional lenses [9,171]. A shift from high modulus-lower water content to low modulus-higher water content silicone hydrogel lenses occurred in an effort to improve comfort during wear. During the advancement of silicone hydrogel contact lenses, the water content of silicone hydrogel contact lenses has increased (24-74%) and the modulus has significantly decreased (1.4-0.3 MPa). As a result, the prevalence of some mechanical complications that have been linked to the lower water content/higher modulus silicone hydrogel lenses appears to be reduced with the more recently introduced silicone hydrogel materials [172–174]. However, the oxygen permeability values have

not shown a similar simple trend over time and thus silicone hydrogel lenses were divided into extended-wear capability (Dk > 100) and those intended for daily wear only (Dk < 100).

Despite the extensive progress that the contact lens technology has undergone in order to minimize the undesired interactions of the contact lens with the ocular surface and thus improve ocular compatibility for a successful contact lens overall performance; contact lens induced dryness and discomfort remain the primary reason for discontinuation of contact lens wear [12,175–177]. Interestingly, a recent study reported that there was no significant difference in the rate of adverse events between conventional and silicone hydrogel lenses when used on a daily disposable basis [178].

2.2.3. Classification of soft contact lenses

The conventional hydrogel contact lenses are classified into four groups by the U.S. Food and Drug Administration (FDA), based on their water content (lower or higher than 50%) and surface charge (ionic, non-ionic) [179]. This categorization is useful for predicting their interactions with the tear film components as well as their potential incompatibility when used with lens care product solutions [180]. However, silicone hydrogel contact lenses exhibit different interaction patterns with tear film components and lens care solutions, potentially due to their complex chemical structure and morphology. Hence, silicone hydrogel contact lens would make a new separate group to address these differences. The introduction of silicone hydrogel contact lenses as a fifth Group in the FDA classification has been proposed [181–183] and has now been implemented into the most current conventional group [184] (Table 2.1).

Table 2.1: Classification of soft contact lenses according to FDA and ISO [184].

FDA Group	Subgroup	Water Content	Ionic Charge	Surface Treatment
I	-	<50%	No	-
II	-	>50%	No	-
III	-	<50%	Yes	-
IV	-	>50%	Yes	-
V	A	<50%	No	Yes
	B1 & B2	<50%	No	Incorporated hydrophilic monomer & Semi-IPN
	C	>50%	No	-
	D	No Specification	Yes	-

IPN: interpenetrating network

2.3. Ocular surface and soft contact lenses

Upon contact lens insertion, soft contact lenses are surrounded and in direct contact with the tear film and its components. In addition, the anterior contact lens surface interacts with the palpebral conjunctiva and the eyelid margins, while the posterior contact lens surface is in close contact with the cornea, the limbus and the surrounding bulbar conjunctiva (Figure 2.4). Understanding the interactions that occur between soft contact lens, the ocular surface and the tear film, and more specifically focusing on contact lens-related factors that contribute to adverse responses, is crucial for the design and development of contact lenses with improved compatibility with the ocular surface, allowing for the maintenance of the normal physiological activities of the eye while providing vision correction and comfort during contact lens wear.

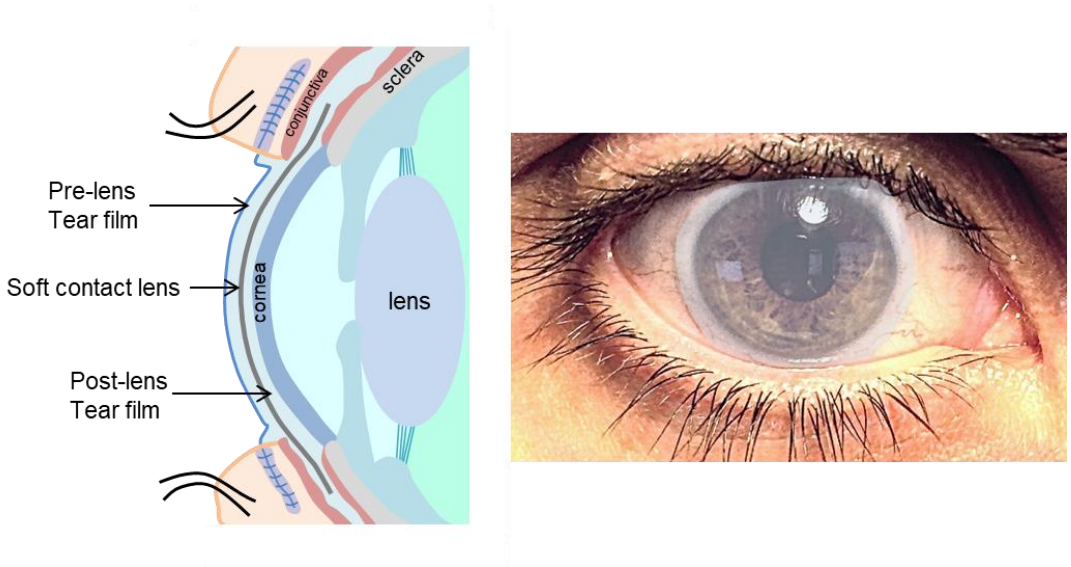

Figure 2.4: Schematic illustration of the on-eye position of soft contact lenses on the ocular surface.

2.3.1. Contact lens-induced changes in the cornea

The presence of soft contact lenses has a number of effects on corneal homeostasis. It has been suggested that the majority of corneal responses during contact lens wear can be traced to the epithelium, including epithelial thinning and erosion, increased cell size, and a greater number of epithelial microcysts when compare to non-lens wearers [5,172,185,186]. Increased corneal staining, an accepted clinical measure of epithelial integrity, is often observed in contact lens wearers and particularly in extended wear modality, and can be caused by desiccation as well as hypoxic, mechanical, inflammatory, allergic and toxic effects [5]. The degree of corneal epithelium thinning is affected to varying degrees by oxygen permeability and the contact lens type [5], while several mechanisms may be involved for corneal erosion, including contact lens adhesion, long-term hypoxia, reduced epithelial density, and mechanical damage from aggravated corneal thinning and contact lens dehydration [187]. Chronic wear of soft contact lenses may also lead to thinning of the corneal stroma [188]. Another adverse corneal event associated with soft contact lens wear is the superior epithelial arcuate lesion (SEAL) which can be explained as mechanical chaffing at the area of the ocular surface covered by the upper eyelid [189]. The increased adhesive shear forces on the corneal epithelium from the contact lens, which in turn are

induced by the upper eyelid during blinking, are suggested to be the primary reason for the development of SEAL [173].

Contact lens-related hypoxia may also cause corneal swelling, which usually accompanies epithelial edema [190] and corneal neovascularization with the latter often being associated with an inflammatory process, especially in the case of low oxygen transmissible (Dk/t) soft contact lenses [191,192]. Even though all contact lenses induce some level of corneal edema, silicone hydrogel contact lenses induce less than 3% overnight central corneal edema which is not considered different from that observed in non-lens wearers [193]. Mechanical effects were also found to contribute to corneal edema but to a lower extent [194]. Furthermore, contact lens wear can deteriorate corneal sensitivity due to hypoxic conditions, with loss in sensitivity being inversely related to the oxygen transmissibility of the lens material [195]. Decrease in corneal sensitivity may lead to a reduction in tear production or blinking frequency subsequently causing contact lens induced dry eye [196–198]. Hypoxia and reduced tear secretion during contact lens wear have been associated with reduction of the corneal barrier function as well [199,200].

2.3.2. Contact lens-induced changes in limbal region

The physiological effects of the limited oxygen permeability in combination with mechanical pressure applied from the contact lens periphery contact lenses result in a hyperemic response referred as limbal hyperemia or limbal redness [201,202]. Limbal hyperemia is more common for extended wear low Dk/t hydrogel contact lenses where a significant increase in neovascularization is also observed [203]. The opposite was reported for silicone hydrogel contact lenses, with vascular response being similar to that of no-lens wearers [203,204]. Chronic limbal hyperemia is a stimulus for corneal vascularization, a non-reversible condition [203,205]. It has been suggested that soft contact lens wear may also result in limbal stem cell deficiency, potentially due to hypoxia and/or mechanical friction on the limbal tissue from the contact lens edge [206,207]. This may be problematic for contact lens performance, causing abnormalities on corneal surface which are often accompanied by decreased vision since the ability of the cornea to constantly replace its epithelium and to quickly repair superficial damages depend on the capacity of the limbal stem cells to continuously proliferate in appropriate circumstances and at high rates [5,206].

2.3.3. Contact lens-induced changes in the conjunctiva

Contact lens wear can induce distinct morphological and structural changes at the conjunctiva around the limbus due to the frictional forces of the contact lens on the conjunctival epithelial cell surface [208]. These changes can be considered reversible upon cessation of contact lens wear. Contact lens wear can also cause a conjunctival epithelial thinning effect which has been attributed to mechanical and metabolic effects, the same mechanism which leads to corneal thinning with contact lens wear [209]. Conjunctival hyperemia may be present due to the combination of the contact lens material (modulus of elasticity), design, dehydration rates, hypoxia and solution used [5], and in extreme circumstances it can be associated with a vascular response of the cornea [203]. Moreover, contact lens-induced conjunctival staining, also referred as circumlimbal staining, and conjunctival epithelial flaps are caused by the direct contact of the contact lens edge with the ocular surface, while bulbar staining away from the limbus is believed to be mainly associated more with poor tear film stability and increased evaporation [210]. These symptoms normally recede with contact lenses discontinuation [211–213]. Bulbar staining has been associated with dry eye symptoms in contact lens wearers while contact lens-induced conjunctival and bulbar staining have been reported to affect comfort during wear [210,212,213]. Moreover, lid parallel conjunctival folds (LIPCOF) are small folds in the lateral, lower quadrant of the bulbar conjunctival likely caused by increased friction and hydrodynamic pressure between the contact lens and the conjunctiva during blinking [214]. LIPCOF have been shown to significantly link to tear film stability, symptoms of ocular dryness and with the percentage of complete blinks [215]

An immunological response of the upper palpebral/tarsal conjunctiva which is postulated to be the consequence of mechanical trauma and/or hypersensitivity reaction caused by the contact lens material, tear-film deposits accumulated on the contact lens surface, or multipurpose solutions is known as contact lens-induced papillary conjunctivitis (CLPC) [173]. It is a clinically significant condition as it is accompanied by mucus production causing discomfort and intolerance during contact lens wear which in turn can lead to contact lens discontinuation [5]. In general, the encountered mechanical complications in the conjunctiva are considered to be greater with silicone hydrogel materials than with conventional hydrogel materials due differences in their modulus [172,173].

2.3.4. Contact lens-induced interactions with the eyelids and the impact of blinking

The eyelids play an important role for the movement and settlement of soft contact lenses over the ocular surface during blinking. Blinking is a dynamic rather than static process, where the eyelids exert a backwards squeeze pressure on the contact lens (normal force), and a shearing force that is parallel to its anterior surface [216,217]. In turn, these forces are transferred to the cornea, the limbus and the bulbar conjunctiva as the soft contact lens moves. Contact lenses are estimated to increase the average pressure exerted by the eyelid from 1-5 kPa [218,219] into pressures in the range of 12.3-17.6 kPa [74,220,221]. Moreover, contact lens movement during blinking allows for tear fluid exchange. The degree of contact lens movement during blinking is affected by the developed frictional interactions of the eyelid with the contact lens together with the elastic properties of the contact lens [9], and thus varies depending on the lens type and fitting characteristics [53]. The interblink location of the contact lens is determined by the elastic properties of the contact lenses material. Therefore, the frictional forces experienced by the ocular surface during blinking with contact lens wear are significantly higher than normal, and in the case of poor tear film stability, there is a risk of contact lens-induced epithelial damage [4]. Although soft contact lenses are generally more tolerable, their acceptance is significantly influenced by various material properties, such as water content, rigidity, oxygen permeability and surface wettability [53]. The differences in the stresses generated between the ocular surface and the different contact lens subtypes during blinking, may explain the development of a variety of mechanical complications, such as lid-wiper epitheliopathy (LWE).

For contact lens wearers, LWE is a clinically observable alteration of the epithelium of the upper lid margin (the lid wiper) and it is believed to be the outcome of the increased shear stress that occurs between the lid wiper and the anterior contact lens surface during eyelid movement [215,222]. LWE was also found to traumatize the corneal epithelium, and increase corneal sensitivity during blinking [223]. Since LWE and LIPCOF are significantly correlated with dry eye symptoms in contact lens wearers, it is postulated that in both cases the mechanical interactions at the eye-contact lens interface derive from insufficient tear film or reduced wettability of the contact lens surface [215,221,222,224]. LWE and LIPCOF are more prevalent and more severe in contact lens wearers than in non-lens wearers, while they both increase significantly in symptomatic contact lens wearers [214,215,222–226]. As they are postulated to have a common

frictional origin, they are considered related clinical signs and good predictors for contact lens-induced dry eye [214,224,227]. They are thought to represent an indirect, *in vivo* measurement of ocular surface contact lens induced-friction during blinking, while recently LWE and LIPCOF have been suggested as a useful tool for the prediction of contact lens discomfort and successful contact lens performance [53,224,226,228].

2.3.5. Tear film and contact lenses

In situ, contact lenses divide the tear film into the pre-lens tear film (PreLTF) and post-lens tear film (PoLTF), creating new interfaces with and within the ocular environment (Figure 2.5). The presence of the contact lens can dramatically change the tear film thickness, structure and dynamics [229]. Contact lens wear may also affect the nature of tear film dispersal [19]. The PreLTF helps maintain a smooth and optically clear surface and reduces friction, while the PoLTF ideally facilitates a continuous tear exchange underneath the contact lens allowing for oxygen transmission, metabolic processes and debris removal while it also acts as a cushion for the lens-ocular epithelium interface [230,231]. The PreLTF and PoLTF are thinner than the preocular tear film prior to contact lens insertion [232,233], while this compartmentalization was found to alter tear film composition due to the changes in biophysical and biochemical properties [23]. A decrease in the pH [234,235] and volume over time [231,236], and an increase in tear film osmolarity [109] during contact lens wear has been also observed. In addition, the PreLTF and PoLTF between the contact lens cause capillary attraction that prevents the contact lens from falling out of the eye.

Changes in tear film composition can also influence the tear film quality and stability over time [237,238], irrespectively of the contact lens material [239–241]. Compared to preocular tear film, for instance, the PreLTF contains less polar lipids, which are responsible for tear film spreading in the preocular tear film, and more non-polar lipids [237]. As a result, the lipid layer of the PreLTF is thinner and less stable than that of the precorneal tear film [239]. Lipid turn-over is generally much slower than the aqueous tear flow and turn-over in contact lens wear [242]. In turn, compromised PreLTF lipid layer cannot fully cover the aqueous layer during interblink periods resulting in increased PreLTF evaporation and faster tear film break-up [19,243,244] with the amount of on-eye dehydration for conventional hydrogel contact lenses, especially for the high-water content lenses, being higher than that of silicone hydrogels lenses [245–247]. Contact lens

parameters such as water content and thickness as well as the on-eye fit and movement were found to influence the stability of the PreLTF [20,230]. Contact lenses with a firmer fit and less on-eye movement favour the formation of a more stable PreLTF. A deterioration of tear film stability during contact lens wear can lead to corneal staining [16,101,243] while PreLTF thinning and reduced contact lens wettability are considered potential mechanisms for the creation of evaporative dry eye [196,197].Therefore, the stability of both PreLTF and PoLTF together with adequate PoLTF exchange rate are essential factors for the maintenance of a healthy tear film. A healthy and stable tear film upon contact lens insertion is essential for successful contact lens wear and comfortable vision.

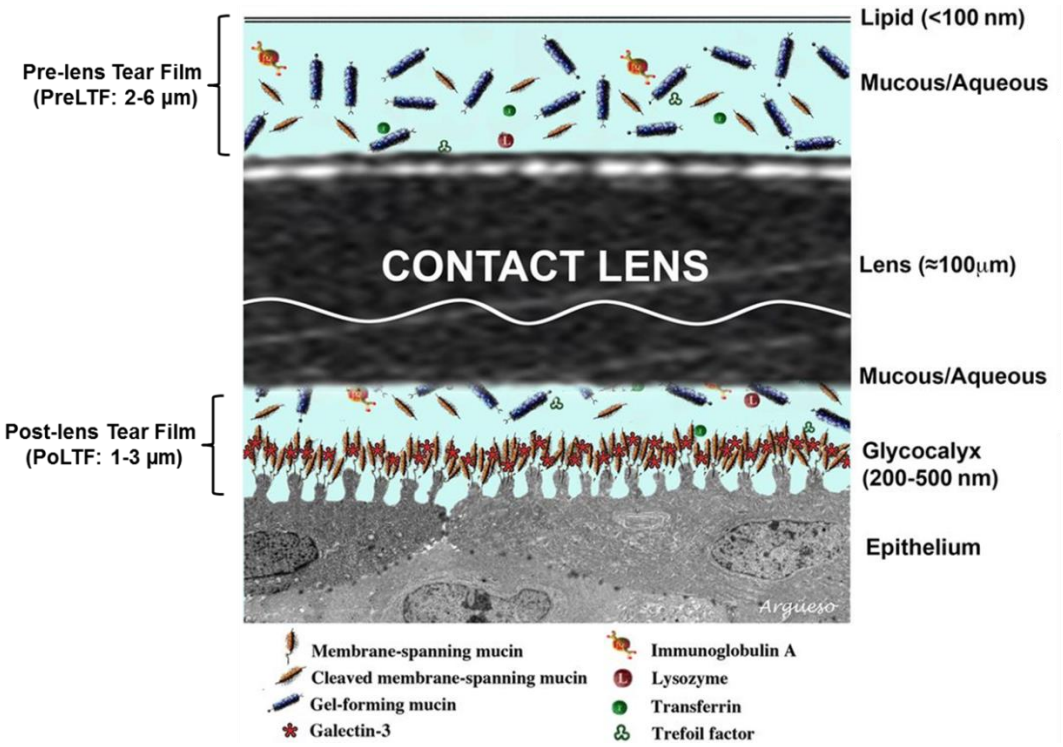

Figure 2.5: Contact lens-induced compartmentalization of tear film on the ocular surface. (Adaptation from [4]).

Finally, interactions between the lens and the tear film components occur within minutes of contact lens insertion. The contact lens-tear film interactions are dependent both on the properties of the contact lens material, including water content, ionicity, modulus and surface properties, as well as the tear composition and chemistry of the individual wearer [23]. Attraction of tear derived substances creates a physiologically normal coating, a biofilm or pellicle, which ensures good

compatibility between the ocular surface and the contact lens. This coating starts to adhere to the lens and progressively builds-up over time. However, when the coating around the contact lens changes in a potential pathological manner, the adherent proteins, lipids or mucins are considered deposits [248]. Due to the semipermeable nature of hydrogel contact lens materials, protein, lipids and mucins can get both absorbed into the lens and adsorbed on the surface, resulting in varying degrees of sorption. The extent of contact lens fouling and the state of the deposits are significant factors for the ocular compatibility and thus overall performance of the contact lens.

2.3.5.1. Interactions of tear proteins with the contact lenses

The presence of the contact lens in the tear film can cause a cascade or up-regulation of processes leading either to the generation of new proteins and peptides or changes in the concentration of existing proteins in order to retain the ocular homeostasis [249–253]. In addition, the presence of the contact lens may alter the stability of the blood-barrier, thus stimulating vascular leakage in the conjunctiva, which in turn results in the influx of plasma derived proteins into the tears, such as albumin [254,255]. The binding and deposition of tear film protein on the contact lens surface is a highly complex process. Over 100 proteins have been identified in the proteomic profile adhered on contact lens surfaces [256]. All proteins in the tear film can potentially form deposits on contact lenses. However, the type, quantity and structure of such deposits are ultimately influenced by several factors, including both tear composition and the chemical characteristics of the contact lens material [257]. Tear film proteins that are frequently detected and examined on soft contact lenses include lysozyme, lactoferrin, lipocalin and albumin [257].

Although not definite, the FDA groups for the contact lenses can provide a useful guide to predict the different interaction patterns between the tear film and the contact lens material [258]. Over all groups, Group I (non-ionic; <50% water) is typically characterized by the lowest amount of deposited proteins, followed by similar amounts for Group II (non-ionic, >50%) and Group III (ionic; <50% water) conventional contact lenses. The highest level of accumulated proteins is found at Group IV (ionic, >50%) conventional contact lenses, which is approximately 10 times higher than Group I [257,259,260]. Despite the high amount of protein adhesion on ionic hydrogel contact lenses, the protein was found to mostly retain its activity. According to both *in vitro* [261]

and *ex vivo* (worn contact lenses) [262] studies, the percentage of active lysozyme is typically more than two times higher on ionic contact lens materials compared to non-ionic hydrogel contact lenses. On the other hand, silicone hydrogel contact lenses tend to exhibit lower levels of adhered proteins than conventional hydrogel contact lenses materials [263,264]. However, a high proportion of the deposited proteins on the surface of silicone hydrogel materials tends to be inactive or denatured [261,265]. The relative amount of denatured protein detected on silicone hydrogel contact lenses is typically higher than that of the conventional hydrogel contact lenses [261,263,265]. Further analysis of the driving forces and parameters causing protein deposition on soft contact lenses is presented in the next section of this chapter.

A correlation between protein sorption and contact lens discomfort has not been fully established yet [22]. However, it has been suggested that the conformational state of the deposited protein may have a greater influence than the total amount of deposited proteins on contact lens performance [266], though further research with regard the degree of protein activity is required to confirm such relation. Moreover, increased/uncontrolled protein fouling and, more importantly, denaturation during contact lens wear are related to adverse ocular effects, including reduced vision, itching, redness, irritation or even inflammation. More specifically, it has been associated with CLPC [267–270] and bacterial adhesion [262,271,272]. Bacterial accumulation on contact lens surface has been linked to microbial keratitis which can ultimately cause vision loss if left untreated [273,274].

2.5.3.2. Interactions of tear lipids with contact lenses

Apart from the dissolved in the tear film lipids, when the aqueous layer becomes too thin due to evaporation or drainage, the lipids of the compromised lipid layer can interact directly with the contact lens surface [275]. The driving forces for attracting lipids are the surface hydrophobicity and the specific chemistry of the underlying contact lens material. Lipid deposition was found to be strongly related to the monomeric composition of the contact lens material, with increased lipid spoilation being associated with Group II conventional hydrogel lenses, particularly those containing N-vinyl pyrrolidone (NVP) [260]. In contrast, silicone hydrogel contact lenses tend to deposit higher amounts of lipids than conventional hydrogel contact lenses, regardless of the type of silicone hydrogel material [275,276]. Lipid deposition on soft contact lenses appears to be cumulative, with no plateau occurring over time [277]. In a similar manner to proteins, lipids

may progressively diffuse into the lens matrix following their adherence to the surface. Unlike surface lipid deposits, the quantity and quality of the lipids present in the contact lens matrix were found to be influenced by the lens type and the wear schedule [278]. Lipid degradation due to the oxidation of lipid deposits on contact lens surfaces has been also observed [279]. The interactions between the proteins and the lipids on a lens surface are of considerable interest since both are thought to play a role in the deposit formation and profile of each other [280].

Increased lipid deposition can alter the surface characteristics of contact lenses, leading to symptoms of dryness and impaired quality of vision [23,281–283]. Although some studies suggest that lipid oxidation may eventually contribute to contact lens discomfort, there is insufficient evidence in the literature to conclude whether lipid deposition and/or degradation can significantly reduce comfort during contact lens wear [22,279,284]. Finally, lipid spoliation has not yet been associated with ocular inflammatory responses [285]. In fact, Omali et al. [286] showed that the presence of cholesterol on silicone hydrogel contact lenses was not important for the modulation of bacterial adhesion on the contact lens surface.

2.5.3.3. Interactions of ocular mucins with contact lenses

The presence of a contact lens on the ocular surface can alter mucin production [249], which in turn may influence the tear film characteristics. Even though previous work indicated that mucin production is reduced during contact lens wear [215,287,288], the overall results regarding the amount and expression of tear film mucins are neither consistent nor conclusive [23,289–291]. This is likely due to the different methods, techniques and contact lens materials used resulting in the examination of different variables making it impossible to elucidate patterns of behavior.

Mucins were found to adhere and deposit in a non-selective manner at the surface of conventional and silicone hydrogel contact lenses [290,292–294]. Proust et al. [295] showed that mucin adsorption *in vitro* was proportional to the vinyl pyrrolidone content of the hydrogel materials, resulting in higher degree of mucin deposition on vifilcon A than etafilcon A contact lenses. It is thus suggested that the surface chemistry of contact lens materials may significantly impact the deposition profile of mucins *in vitro*. Additionally, the presence of mucin in certain conventional (etafilcon A) and silicone hydrogel lenses (balafilcon A and lotrafilcon A) was found to improve their wettability [196,296], potentially leading to more tolerable contact lenses. Even though mucin coated model contact lenses were found to reduce corneal damage *in vitro* [297],

there is no evidence linking mucin deposition with contact lens discomfort so far [215,298]. However, both contact lens induced LWE and LIPCOF have been reported to be significantly associated with reduced quality and quantity of mucins during wear [215,299].

The mechanical interactions of the contact lens with the underlying mucin layer of the PoLTF and the epithelial surface due to the sliding or shearing forces exerted anteriorly by the lid during blinking result in the formation of mucinous particulates, known as mucin balls. The mucin balls (20-200 μm [173]) cause temporary, spherical indentation in the corneal epithelium [300]. The frequency of mucin balls is similar for both conventional and silicone hydrogel contact lenses, with the latter exhibiting higher amounts of mucin balls on their surface [301,302]. Though, the presence of mucin balls is not associated with compromised vision or contact lens performance; while patients with mucin balls are usually asymptomatic [300,303]. The clinical significance of this biochemical change in the PoLTF is unclear since it is not a pathological finding [173,304], while they might prevent the development of corneal infiltrates, by either aiding in the separation of the contact lens from the corneal or by contributing to the presence of a more protective viscous pre-corneal mucin layer [305].

Finally, electrolyte deposition, such as that of calcium and iron, has been observed as well, though it is less prevalent [306].

2.4. Surface properties affecting the compatibility of contact lens with ocular surface and its overall performance

Contact lens wearers have a higher incidence (up to 50%) of adverse ocular sensations than non-contact lens wearers, generally described as ocular dryness or discomfort during wear, particularly toward the end of the day [307,308]. The symptoms of contact lens dryness and discomfort which decrease after lens removal [13] and may or may not be part of a prior dry eye condition, remain the primary reason for limiting or even discontinuing contact lens wear [12,308]. Despite the progress in the design of new contact lenses, it has been estimated that the number of wearers who cease contact lens wear each year is similar to the newly fitted wearers [16]. Therefore, successful contact lens wear is highly influenced by the degree of comfort provided, while managing contact lens discomfort remains still a challenge. In addition, the success of the novel applications of contact lenses, such as drug and cell delivery devices, biosensors or their use

as a means of controlling the development of myopia, relies on the design of contact lens materials in order to allow for years of comfortable wear.

Although there is a multitude of factors that influence the overall contact lens performance, the compatibility of a contact lens with the ocular environment is a key factor, particularly since contact lens discomfort has been attributed to the reduced ocular compatibility of contact lenses [309]. The dynamics that affect successful contact lens wear can be contact lens-related, patient-related and environmental, and they can independently or synergistically lead to a specific etiology for poor contact lens performance causing discomfort during wear only [176,310]. For patients who do not display any dry eye signs or experience any pre-existing symptoms prior to fitting (asymptomatic), contact lens-related parameters such as manufacturing methods, material, design, fit and wear, and lens care play an essential role [18].

A contact lens material should be considered as the extension of the cornea [310]. A biocompatible contact lens should be able to remain on the ocular surface without affecting the natural biological processes that take place in the surrounding ocular environment. Therefore, it should promote tear film physiology and stability, allowing for tear film components to retain their native state while minimising the accumulation of deposits and bacteria, permit normal oxygenation of the cornea, and resist to the shear forces induced by the eyelids during blinking. Hence, the material-based contact lens properties that are necessary in order to achieve that are ion and oxygen permeability, mechanical/modulus and surface characteristics [310].

Upon insertion, the surface of the contact lens comes first into contact with the tear fluid and the physicochemical properties of the contact lens surface directly affect its interactions with the tear film. Consequently, the surface properties that play a crucial role in the interactions of the contact lens with the ocular environment include surface wettability, resistance to protein deposition, and low friction. Further analysis on the importance of the major surface properties of contact lenses on the compatibility and overall contact lens performance is discussed below.

2.4.1. Surface wettability and contact lenses

One of the most fundamental requirements for a contact lens material is to allow the tear film to maintain its stability and integrity during wear. Wettability can be defined as the tendency of the fluid to spread over a solid [311]. For contact lenses, it typically describes the ability of the tear film to spread and remain on the surface during wear [22,312], and it is considered one of the

main parameters defining contact lens interaction with the ocular surface [6]. Wettable and hydrophilic contact lens surfaces are essential to support normal interblink tear film and tear structure reformation after blink [310]. Poor front surface lens wettability has been linked to rapid and increased surface deposition [140,313], reduced optical quality [314,315], and discomfort [6,316,317]. Therefore, it is an important parameter that needs to be considered in order to assess the compatibility of a contact lens, particularly for silicone hydrogels, due to the inherent surface hydrophobicity of the silicone domains.

Despite the different approaches used to improve the surface wettability of soft contact lenses, including the surface modification with hydrophilic layers, incorporation of internal or releasable wetting agents in the bulk of the contact lens as well as the addition of surface active agents in the contact lens care solutions, soft contact lenses still reduce tear film stability. Therefore, the development of a contact lens material that would support a PreLTF similar to the precorneal tear film is highly desirable.

2.4.1.1. Surface free energy and wetting

The *surface energy* or *surface tension* represents the excess energy that is present at a surface of a material compared to the bulk due to intermolecular forces. The surface energy or interfacial tension of a solid–vapour and solid–liquid interface is an important thermodynamic parameter that plays a key role in the wetting and adhesive properties, and the adsorption processes of polymeric materials. It is directly related to the intermolecular interactions between the interfaces. Hence, it is particularly relevant in the development of biomaterials and their biocompatibility, since they come in contact with living tissues and biological fluids.

Wetting refers to the process of a liquid covering a solid surface due to intermolecular interactions and *wettability* refers to the ability of a liquid to remain in contact with a solid surface. Good wetting involves the spreading of the liquid over the surface, displacing the fluid that was initially in contact with the surface, or the penetration of a liquid into a porous solid medium [318]. The degree of wetting of a surface is the result of a force balance between adhesive and cohesive forces developed at the interface of the solid surface and the deposited liquid. Stronger intermolecular forces, and thus increased attraction between the solid and the liquid lead to lower interfacial tension and higher degree of wetting.

The surface energy can be indirectly determined through the measurement of the contact angle formed at a solid/liquid/vapor interface when a liquid droplet is deposited on a solid surface. Taking into consideration a thermodynamic equilibrium between the three phases, the contact angle (θ_c) is defined by the Young's equation [319]:

$$\cos(\theta_c) = \frac{\gamma_{sv} - \gamma_{sl}}{\gamma_{lv}} \qquad (2.1)$$

where γ_{sv}, γ_{sl} and γ_{lv} are the solid-vapor, solid-liquid and liquid-vapor interfacial tensions respectively (Figure 2.6). The effect of the vapor phase on the surface energy of the solid-liquid is negligible when exposed to air. Therefore, the γ_{sv} can also be referred as the surface free energy of the solid (γ_s) and the γ_{lv} can be referred as the surface tension of the liquid (γ_l). Consequently, the molecular involvement of the solid-liquid phase is significant as it determines the interfacial tension between them [320]. The contact angle in Young's equation (equation 2.1) depends on the physicochemical nature of the three phases and is independent of gravity [321]. Hence, the contact angle values represent the state of the three-phase system that has then minimum Gibbs energy. The smaller the contact angle, the more wettable a solid surface is. The most common techniques for the determination of the contact angle are the sessile drop technique, the captive bubble technique (Figure 2.6) and the Wilhelmy plate technique [322].

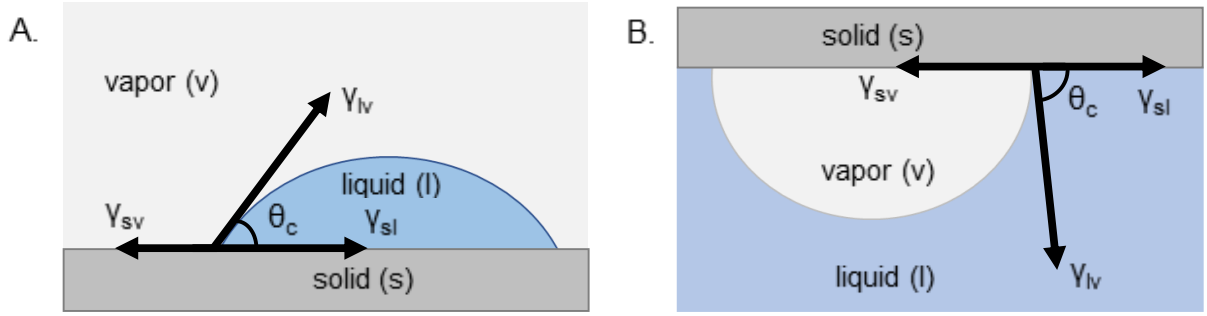

Figure 2.6: Schematic illustration of the contact angle (θ_c) measured with (A) the sessile drop technique and B. the captive bubble technique.

The derivation of the Young's equation assumes that the solid surface is an ideal surface, with smooth, homogeneous, non-reactive and non-deformable characteristics, and as a result a unique static contact angle would be expected for a given solid-liquid-fluid system in equilibrium [321]. However, real surfaces are characterized by roughness, chemical heterogeneity to some

extent, and metastable states with each state having its own associated contact angle. As a result, the static equilibrium contact angle poorly represents the surface of a material, significantly disregarding the surface characteristics. For this reason, the dynamic contact angle is more useful than the static angle, including the *advancing* (liquid expands over solid surface – maximum metastable state) and the *receding* contact angle (liquid retreats from the solid surface – minimum metastable state) [323]. The difference between the advancing and the receding contact angle is called *contact angle hysteresis*. The presence of hysteresis is an indication of surface roughness, physical and chemical heterogeneity (thermodynamic hysteresis, independent of time and frequency [324]) .

In the case of hydrogel materials, it is thought to also occur due to reorientation of the surface functional groups and molecular mobility, surface swelling and liquid penetration [313], and possibly due to surface deformability (kinetic hysteresis, time or frequency dependent) [325,326]. Hysteresis can also derive from solution impurities adsorbed on the examined surface. Therefore, determination of the dynamic contact angle and its hysteresis can provide information about the stability of the intrinsic wettability of the surface layer.

2.4.1.2. Surface wettability, contact angles and soft contact lenses

Contact angle analysis has become a widely accepted method for the evaluation of the wetting characteristics of contact lenses *in vitro* or *ex vivo* (after removal of worn contact lens) [327]. According to the contact lens literature, the sessile drop and the captive bubble technique and less frequently the Wilhelmy plate technique are used for contact angle determination [320]. Yet there is no standard method accepted for the determination of the contact angle for soft contact lens applications [320], since each method has its own advantages and disadvantages when characterizing the surface of a material.

In the case of dynamic contact angle measurements, the advancing contact angle is postulated to correspond to the situation when the eyelids close and the PreLTF spreads over a partially or fully dehydrated contact lens surface, whereas the receding contact angle corresponds to the phase where the eyelids open and the PreLTF starts to retract at the interblink period of a blinking cycle. The advancing contact angle can be important in modeling the initial spreading of the PreLTF over the examined contact lens surface and the receding contact angle may be an indicator of the PreLTF stability and integrity upon blinking [196]. Consequently, determination

of advancing and receding contact angles is important, since both contact angles are clinically relevant for the clinical assessment of contact lens wettability. Maldonaldo-Codina et al. [312] suggested that the static contact angle measured with sessile drop technique can be analogous to the advancing angle, while the contact angle measured with the captive bubble technique is considered to be analogous to receding contact angle. Reducing hysteresis and achieving dynamic contact angles of zero degrees is one of the ultimate goals in contact lens research and development [196,328], as complete wetting of the contact lens would translate into spontaneous spreading of tears during wear and prevent PreLTF instability, allowing for smooth and unimpeded blinking [196].

The contact angle results are shown to be methodologically dependent, with parameters such as the experimental conditions (temperature, humidity and the liquid probe used), the conditioning and the age of the contact lens playing an important role [312]. The impact of drop size in contact angle analysis remains elusive [320]. Contact angles are often quoted by manufacturers in their marketing literature; however, comparison of the published values should be done with caution and only when the same technique is followed under the same conditions. Overall, the wettability of a contact lens *in vivo* is largely dependent on the surface tension of the tears, the surface free energy of the contact lens, the interfacial tension between them, the surface chemistry of the contact lens, which is dynamic in an ocular environment, and the types of deposits on the contact lens surface during the earliest stages of the wear cycle [329,330]. Unworn contact lenses were characterized by lower contact angles in the presence of tear film components *in vitro* [329]. Similar results were observed on the contact angles of worn contact lenses after removal (*ex vivo*) [171], suggesting that is important to mimic *in vivo* conditions for contact angle measurements on unworn contact lenses while also *ex vivo* contact angle analysis on worn contact lenses might be more informative for the *in vivo* behavior of soft contact lenses. Finally, a single contact angle measurement cannot easily predict the complex interaction of the tears with a lens, thus it is suggested that a more complete surface energy characterisation would be necessary to better model the *in vivo* contact lens behaviour [316].

Although contact angles studies for both unworn and worn soft contact lens materials have provided useful clinical information [196,328,329], a robust correlation between the clinical measures of on eye contact lens wettability with physical wettability or comfort is yet to be

established [22]. However, an association between compromised tear film kinetics *in vivo* and discomfort was recently reported [317].

2.4.2. Proteins and contact lenses

Upon contact lens insertion, tear film proteins can adhere within the first few minutes to the contact lens surface. The interactions between the contact lens surface and the tear film components should be dynamic in order to maintain ocular compatibility, thus allowing for successful contact lens wear. Although many factors can be attributed to the appearance of contact lens-related complications, protein deposition may be one of the most concerning. Therefore, the development of contact lenses with antifouling properties it is of great importance both from the perspective of comfort and clinical performance of contact lenses.

2.4.2.1. Principles of protein adsorption and deposition

When a biomaterial surface (synthetic or natural) comes in contact with a biological fluid, a cascade of interdependent events occurs. Native proteins coat the surface of the biomaterial in a rapid process that is both complex and competitive. Protein adherence is likely considered the most significant process in determining the biological fluid - biomaterial interactions. *Adsorption* is the accumulation and adhesion of atoms, molecules, ions and larger particles to a surface only, without penetrating into the bulk.

The behaviour of proteins at the interfaces is the net result of various types of interactions between the protein molecules, the sorbent surface, the solvent (water) molecules and any other solutes present, such as low molecular weight (MW) ions. At constant temperature and pressure, the thermodynamic principle governing the *adsorption* involves enthalpic and entropic terms (equation 2.2). Independently of the mechanism and the kinetics of protein adsorption, the process can occur spontaneously only if the Gibbs free energy (G) of the system decreases [331]:

$$\Delta_{ads}G = \Delta_{ads}H - T\Delta_{ads}S < 0 \qquad (2.2)$$

where H, S and T stand for enthalpy, entropy and temperature of the system, while Δ_{ads} indicates the change in the thermodynamic functions of state resulting from the adsorption process. The dynamics of protein adsorption are strictly related to the physicochemical properties of the protein

(size, charge, structure stability, concentration, unfolding rate, functionalities and protein-protein interactions), the sorbent surface (chemical composition, free energy, hydrophilicity, relative charge distribution and polarity), the solvent (pH, ionic strength, temperature) and the presence of pre-adsorbed molecules [332].

The different modes of interactions between the proteins and the surface result in different degrees of selectivity, thus leading to *specific* and *nonspecific* protein adsorption. *Specific* adsorption occurs when proteins exhibit a high affinity of binding to a very defined chemistry and preferentially adhere on surfaces (e.g. ligand-receptor interactions). *Nonspecific* protein adsorption is a dynamic process that occurs very quickly, typically only seconds after the protein comes in contact with the surface, and is largely dominated by the electrostatic, hydrophobic and dispersive forces, and by the conformational stability of the protein molecule [333]. *Nonspecific* protein adsorption, also known as protein fouling, is considered a dominant factor in the failure of many biomedical implants and devices. Most protein adsorption to biomaterial surfaces is essentially governed by non-specific interactions, forming a thin monolayer (2-10 nm), which in turn may trigger a cascade of biological events. Upon adsorption, proteins may alter their secondary, tertiary or quaternary structures in order to energetically adapt to the surrounding environment. In the case of minimum structural change, the protein adsorption is considered reversible, whereas when the surface bound protein undergoes a conformational change the protein adsorption is considered irreversible (non-equilibrium state) [333,334]. In general, the interactions between a protein and an aqueous solution are energetically unfavourable as they tend to increase the Gibbs free energy of the system, rendering the aqueous environment unfavourable for protein adsorption [335]. Therefore, surface characteristics and more importantly the degree of surface hydrophilicity contribute significantly to the protein adsorption profile [336].

In the case of predominantly hydrophilic (polar) interactions between the sorbent surface and the protein, the hydration layer of the surface retained water molecules can prevent intimate contact between the surface and the protein [333]. For protein adsorption on hydrophilic surfaces, the structural stability of the protein needs to be considered. *"Hard"* proteins are those that exhibit high structural stability and thus adsorb at hydrophilic surfaces only if electrostatically attractive forces are developed, whereas structurally labile *"soft"* proteins may gain sufficient degrees of conformational entropy upon adsorption to anchor even on an electrostatically repellent surface (flexible proteins with low conformational stability). In the case of hydrophobic (nonpolar)

surfaces, the exposed protein will rearrange or even unfold its structure, in order to reduce the net hydrophobic surface area of the system once adsorbed (hydrophobic effect), which in turn is accompanied by the release of water molecules from the interface into the aqueous solution. Protein adsorption on a hydrophobic surface is energetically favourable and can occur even in the presence of electrostatic repulsive forces [333]. The degree of hydrophobic interactions at the surface-protein interface determines the strength of the bond and the degree of the change in protein configuration, which may be irreversible [337].

In complex multiprotein solutions such as the tears or blood, there can be sequential adsorption and exchange processes of proteins to surfaces that are determined by protein mobility and concentration, known as the *Vroman effect*. *Vroman effect* is a dynamic and competitive process during which low-molecular weight proteins of higher concentration that typically adsorb to surfaces first are displaced subsequently by less abundant proteins higher of molecular weight under the condition that they are able to form stronger interactions with the surface over time [338]. The surface and the solution conditions determine the relative adhesion strengths at the surface-protein interface.

As previously mentioned, proteins tend to rearrange their structure upon adsorption to lower Gibbs energy [335]. The irreversible conformational changes and unfolding of the tertiary structure of a surface bound protein is termed *protein denaturation* [336]. A denatured protein obtains a random coil conformation which in turn leads to alternation in its original properties since a protein performs its biological function only in this native conformation. Denaturation of irreversibly bound protein is suggested to disrupt the competitive binding [339]. Hence, denatured proteins can interact with other proteins and cells, and may cause protein aggregation and adverse clinical events, such as triggering an immune response. It is well established that this phenomenon is more likely to occur on hydrophobic surfaces rather than hydrophilic surfaces [334]. Other factors that can induce protein denaturation include the contact time of the protein with the surface, the chemical composition of the sorbent surface as well as the surrounding pH and temperature [335].

2.4.2.2. Protein sorption and deposition on soft contact lenses

In vitro, *ex vivo* and *in vivo* studies have all been extensively used to understand and describe protein binding and deposition on contact lens materials [340–342]. The formation of a protein film on the contact lens surface is a highly complex process driven by different protein-surface

forces, including hydrogen bonds, van der Waals, hydrophobic and electrostatic interactions [336,343].

Initially, the deposited proteins form a monolayer that covers the contact lens surface [344]. Hydrophobic dehydration of the contact lens surface due to protein binding that may lead to higher protein adsorption [339]. Therefore, the pattern of this monolayer may impact subsequent deposition of other tear components, creating a competitive adsorption profile that is of great relevance and significance to the design of antifouling contact lens materials. For instance, it has been reported that lactoferrin can associate with albumin [345], while Sariri et al. [346] found that sequential absorption of proteins onto soft contact lenses involves almost total displacement of pre-adsorbed proteins *in vitro*. Apart from protein-protein interactions, the interactions of proteins with mucins and lipids have been reported to affect the protein deposition profile as well [280,347].

Protein penetration into the matrix of the soft contact lenses has been also observed [348,349]. As a result, the uptake of proteins by soft contact lenses is likely due to a combination of surface adsorption and absorption, referred herein as *protein sorption*. For conventional hydrogel contact lenses, the ionic and/or high-water content contact lenses are more likely to allow for diffusive penetration of proteins into their bulk. Hence, electrostatic interactions and high degree of porosity mainly explain why ionic Group IV conventional contact lenses tend to attract higher quantities of small, charged proteins like lysozyme [259,264] forming a thick protein-based layer on their surface [262], when compared to non-ionic hydrogel contact lenses. For silicone hydrogel contact lenses, the significantly lower amount of sorbed proteins, compared to conventional hydrogel contact lenses, can be attributed to their different surface characteristics and small pore size [257,263,264]. The protein deposition profile on contact lens surfaces is influenced by many factors, including the contact lens properties such as material type, surface chemistry, charge, pore size, water content and roughness, degree of hydrophilicity, contact lens manufacturing technique and the dehydration rate. Intrinsic protein characteristics, including net charge, molecular weight, conformation and concentration in addition to the tear film pH and ionic strength also play a role [257,262,343,350]. In addition, the length of contact lens wear, protein-protein interactions and protein-contact lens surface interactions followed by the drying and wetting cycle between blinks *in vivo* are important factors that need to be also considered for protein fouling [258].

Although conventional contact lenses tend to accumulate higher levels of proteins than silicone hydrogel contact lenses, the activity of the sorbed proteins remains higher. Apart from the surface hydrophobicity and chemistry of the contact lens, protein denaturation can be significantly impacted by the contact time with the surface, the type of protein, the surrounding pH and temperature, the dehydration rate of the contact lens and solution interaction [23,265]. Protein denaturation will exhibit different binding strengths and rates of exchange, further affecting the fouling process of contact lens materials [339]. Protein adhesion, in-matrix penetration and/or denaturation can influence the physical and/or chemical characteristics of contact lenses, including water content, oxygen permeability [351,352], and the optical transparency (thin, semi-opaque superficial layer of distinct surface deposits) [353], while removal of denatured proteins from contact lenses can be harder as they are more tightly bound than the native proteins [354]. It is therefore clear that protein fouling can reduce the compatibility of the contact lens with the ocular surface, compromise quality of vision and potentially contact lens intolerance [281,355], and cause severe immunologic reactions such as contact lens papillary conjunctivitis [267–270] and bacterial adhesion [262,271,272]. These adverse effects may weaken the contact lens wearing experience of the patient and eventually lead to discontinuation of wear.

Taking into consideration that the interfacial tension between the contact lens surface and the tear film component is a primary driving force for surface fouling, the minimum interfacial tension hypothesis of biocompatibility suggests that low interfacial tension results in thermodynamically unfavourable conditions for protein sorption and denaturation, and thus a higher degree of biocompatibility [356,357]. Hence, surface wettability and hydrophilicity are considered as key determinants for protein adsorption and deposition processes.

2.4.2.3. Lysozyme and albumin as model proteins

The deposition profile of lysozyme and albumin on soft contact lens materials have been extensively studied [23,257,267,350]. Both proteins have been used as markers for protein deposition, including in the study herein, due to their prevalence in tear film, important roles, and significant differences in charge, size and conformation.

2.4.2.3.1. Tear lysozyme and soft contact lenses

Lysozyme is a glycosidic enzyme and bioactive protein with antibacterial, antiviral, and antifungal properties. In humans, the highest concentration of lysozyme is found in tears, saliva and milk. It is a compact globular protein molecule of relatively low MW (15 kDa) with a slightly ellipsoidal shape and a net positive charge (pI 10.7) at physiological pH [358]. It is a major component of human tear film, accounting for approximately 40% of tear film proteins, and is derived from the acinar and ductal epithelial cells of both main and accessory lacrimal glands [358,359]. In addition, lysozyme interacts with other major tear film proteins, including lipocalin and lactoferrin [360], and either alone or in combination with lactoferrin, lysozyme exhibits bactericidal properties against certain species of gram-positive bacteria, such as *Staphylococcus epidermidis* [358,361]. Native lysozyme has been also reported to have anti-inflammatory activity in the tear film, though the exact mechanism of action has yet to be determined [267].

Lysozyme is one of the major proteins deposited on soft contact lenses (approximately 36-95% depending on contact lens type [267]). Lysozyme adsorption occurs readily after contact lens insertion, and depending on the contact lens type, the protein tends to undergo conformational changes which might end in denaturation. Compared to other major tear film proteins, lysozyme is a relatively small and stable protein [262]. Due to its high internal stability, lysozyme does not normally adsorb to hydrophilic surfaces unless there is electrostatic attraction [331]. This explains why the greatest affinity between lysozyme and soft contact lens material was observed in the case of group IV hydrogel contact lenses and more specifically for the negatively charged contact lens, etafilcon A [263]. Despite the high amount of adhered lysozyme on ionic convention hydrogel contact lenses, the protein was found to mostly retain its activity [262,263,362]. In contrast, even though the amount of lysozyme in silicone hydrogel contact lenses was significantly lower, the amount of denatured lysozyme was found to be higher when compared to conventional hydrogel contact lenses [261,263,362].

In most of the studies investigating the deposition and conformation of lysozyme on contact lens materials, hen egg-white lysozyme is used as a model protein instead of human lysozyme (MW 14 kDa, pI~11). Hen egg-white lysozyme shares a high degree of similarity with human lysozyme in primary, secondary and tertiary structures and catalytic properties, though it exhibits a weaker enzymatic/antibacterial activity when compared to the human lysozyme [358]. Data agreement between *in vitro* studies using hen egg-white lysozyme [264,363] and *ex vivo*

[266,364,365] studies of worn soft contact lenses on lysozyme deposition and conformation, suggests that hen egg-white lysozyme is an appropriate candidate to be used as a model protein in contact lens research.

2.4.2.3.2. Human serum albumin in tears and soft contact lenses

Albumin is the most abundant protein in human serum and is also the most prominent soluble protein in the body of all vertebrates. It contributes to the stability of osmotic blood pressure and blood pH, and transports various biomolecules including hormones and fatty acids, and drugs in the blood stream [118]. It is a relatively large protein (66 kDa) with a three-dimensional heart-shaped structure and a net negative charge (pI 4.9) at physiological pH [366]. Albumin is not an indigenous lacrimal gland protein, but it is synthesized mainly in the liver. Due to its high concentration in plasma and relatively low MW, albumin can transverse the conjunctival (blood-tear) capillary layer to the tear fluid [350]. Hence, it can act as an effective indicator of the integrity of the blood-tear barrier and for vascular leakage into the ocular environment [359]. The concentration of albumin in tears is very irregular (0.01 - 1.1 mg/ml for asymptomatic subjects [118]). Albumin influx into tears as a consequence of contact lens wear, especially during overnight wear, has been observed [118,255] while albumin concentration has been found to rapidly decrease upon contact lens removal [367].

Albumin is known to be a “soft” protein with low conformational stability when binding to solid surfaces, such as soft contact lenses [345,350]. For soft contact lenses, albumin exhibited higher binding affinity to lower water-content contact lenses (highest amount for group I and lowest for group IV conventional contact lenses) and to less hydrophilic surfaces [347,368]. Due to is relatively large size, albumin was found to primarily deposit on the surface of soft contact lenses [349,350,368]. Silicone hydrogel contact lenses tend to accumulate less albumin compared to conventional hydrogel contact lenses. Moreover, it is suggested that binding of albumin to any of the lens surfaces was strong in comparison to the binding of other protein types [347], and thus the fact that albumin can compete with other proteins on contact lens surfaces may be of clinical significance.

In general, the structure of albumin is resilient towards denaturation. Although conformational changes of adherent albumin on soft contact lenses occur shortly after insertion, irreversible binding of albumin is a slow process that might be governed by the kinetics of protein

denaturation [369,370]. Analysis of the conformational state and/or degree of denaturation of deposited albumin on soft contact lenses is fairly limited in the contact lens literature [369,371]. Finally, the presence of surface bound albumin was found to increase the adhesion of bacteria that is associated with ocular infections [251,372,373]. Tan et al. [374] reported that albumin deposits were higher on the surface of extended wear contact lenses from patients with contact lens-induced papillary conjunctivitis. Although it is not clear if the observed increase in tear albumin during contact lens wear is causative or consequential, minimizing albumin deposition seems to be desirable for reducing bacterial colonization.

Bovine serum albumin and human serum albumin are characterized by similar amino acid sequences and biological properties but their physicochemical properties and conformation are slightly different [345,375]. Therefore, bovine serum albumin is commonly used as a model protein in many *in vitro* studies, including contact lens deposition research, instead of human serum albumin due to its higher availability and lower cost. However, comparative studies between these two proteins should be carefully done, since they are not completely identical.

2.4.2.4. Techniques used for protein deposition studies on contact lenses *in vitro*

Protein deposition on contact lenses has been studied using several photometric, microscopic and imaging techniques [376]. Quantification of the sorbed proteins on contact lens materials has been achieved using biochemical techniques of increased sensitivity and accuracy, including Enzyme-Linked Immunosorbent Assay (ELISA), Sodium Dodecyl Sulphate Polyacrylamide Gel Electrophoresis (SGS-PAGE) (with/without immunoblotting [265]), and colorimetric assays [376]. These techniques are useful especially in the case of *ex vivo* (worn) contact lenses; however, they typically require complex extraction procedures for the protein and resuspension in solution which can affect the efficiency and accuracy of the results. *In vitro* quantification of adhered proteins can be determined by labelling the protein(s) of interest either fluorescently [377] or radiochemically [378].

Radiochemical experiments attach radioactive atoms to proteins, allowing for direct quantification of the protein of interest that is sorbed in the bulk and/or on the surface of the contact lens materials without the need for scintillation fluid or chemical extraction. Radiolabeling the proteins is suggested to not affect the protein properties and deposition profile [378], while also allowing for direct quantification of single proteins from multicomponent fluids (artificial tear

solution). It is a reproducible and sensitive technique with low detection limit (nanograms), compatible with all the soft contact lenses, provided that the adequate steps are taken to limit any interaction of the free iodine tracer with the contact lens materials [378], while it can assess a large number of samples in a short period of time. The isotope I^{125} has been extensively used for radiolabeling tear film proteins, such as lysozyme, albumin and lactoferrin in the contact lens literature [376,379].

2.4.3. Ocular Friction and Lubrication

Blinking is essential for maintaining a healthy ocular surface and clarity of vision. Taking into consideration that we blink about 14000 times per day, the dynamic interaction between the contact lens and the ocular surface is of great significance. During blinking, the compression and shearing forces are transferred from the eyelid to the contact lens over the cornea, and bulbar conjunctiva for soft contact lenses. Therefore, the frictional and elastic properties of the contact lens material play a significant role in contact lens performance [9]. In healthy wearers, the tear film acts as lubricant between the contact lens and the eye, producing a thin layer that covers the interfacial asperities, reducing friction and preventing wear. However, the tear film components that are rapidly attracted to the soft contact lenses upon insertion, particularly proteins and lipids, may change the contact lens surface characteristics and thus alter the friction forces during blinking [365]. Moreover, progressive dehydration during wear, further deposit formation and tear film break-up can compromise the surface wettability and lubricity of the contact lenses which in turn might increase friction forces during blinking. This is more likely to increase blink rate [380–382] and could be responsible for end-of-day discomfort. In fact, there is enough evidence based on the results of separate clinical and laboratory studies that soft contact lenses with lower friction coefficients are more likely to be linked to higher degree of *in vivo* comfort [168,169,383–387].

Moreover, studies have suggested that compromised frictional properties of contact lenses can lead to the formation of SEAL and the development of CLPC, with the latter potentially induced by mechanical trauma [269]. For both complications there is a patient-related as well as material influence. Clinical complications of the eyelid related to inadequate lubrication during contact lens wear include the LWE and LIPCOF which are postulated to be correlated with each other and have the same friction origin [215,224]. However, a direct relationship between LWE and LIPCOF with contact lens friction coefficient has not yet been discerned.

Therefore, the frictional properties of contact lenses should be considered in the design and fabrication of soft contact lenses as well. The need for the development of contact lenses with controlled friction and lubrication mechanisms while providing the required contact lens function and high degree of comfort still remains. Moreover, understanding the frictional forces that take place at the contact lens-eye interface may also provide insight into the relationship between the surface properties and the overall contact lens performance *in vivo*.

2.4.3.1. Important concepts in tribology and biotribology

Tribology investigates interactive surfaces in relative motion; thus the type of interaction between the two surfaces determines their tribological behavior. The type of forces developed between the sliding surfaces depends on the nature of the interacting surfaces and the medium between them. Adhesion, which is the process of attraction between two particles or surfaces to bring them together, plays a crucial role in tribological phenomena, particularly in friction and wear. The tribological behavior of two surfaces in contact is primarily determined by the nature of the interfacial junctions formed between them. The study of friction, lubrication and wear in biological systems constitutes the field of *biotribology*, an area of growing importance in promoting a better understanding of the ocular compatibility of contact lenses.

Friction is defined as the force that resists the relative motion between two objects that are in contact. According to Amonton's laws of friction, friction force is directly proportional to the applied load and it is independent of the contact area. Hence, the friction coefficient (μ) between two sliding surfaces, expressed as a metric for resistance to sliding, is defined as the ratio of the friction force (F) by the normal force (N) applied to the surfaces:

$$\mu = \frac{F}{N} \qquad (2.3)$$

Amonton's empirical rules of "dry" friction were based on the observation of solid macroscopic objects sliding (load-controlled friction), and thus the mechanical origin of the linearity between friction and normal forces is considered to arise from the asperity-asperity contacts that define the real area of contact between hard solid surfaces [388]. However, the frictional behavior of hydrogels, such as soft contact lenses, and its dependencies do not conform to Amonton's law (equation 2.3) since the asperities of soft materials are speculated to deform and

thus a deviation from the linearity between friction and normal forces occurs [389]. Taking into consideration the different chemical structures of hydrogels, the inter-molecular interactions (contact junctions), the surface area of contact (asperities) and the surface topography of the opposing surfaces, the three basic aspects currently thought to be responsible for sliding friction are the molecular adhesion, surface roughness, and deformations [390,391]. Measurement conditions also play an important role. Finally, when a confined fluid is sheared between two solid surfaces, viscosity-controlled friction takes place and, in this case, the fluid can minimize the inter-molecular interactions between the adjacent surfaces and separates the asperities from direct contact. Therefore, this type of friction is dependent on the viscosity, rheological properties and flow rate of the fluid at the interface [391]. Viscosity-controlled friction also occurs for surface coated or grafted materials, where the surface layer is thicker (high MW polymers) than the asperities of the substrate and has an adequate conformation freedom to exhibit fluid-like behavior despite the restricted surface mobility [392]. If the surface energy of the surface layer is low and consequently the work of adhesion is low as well, a general correlation with low friction coefficients is expected. This suggests that thick hydrophilic surface layers can provide reduced friction in a hydrophilic medium, such as water [9,393,394].

Euler was the first to distinguish between two modes of friction, *static friction* and the *dynamic or kinetic friction* [395]. S*tatic friction* is the force required to initiate motion which maintenance of motion at steady state is the *dynamic or kinetic friction*. The *static friction coefficient* (μ_{static}) is higher than the *kinetic friction coefficient* ($\mu_{kinetic}$) when the normal load remains constant.

Lubrication is the process that controls friction and prevents wear of interactive surfaces in relative motion. It is mediated by introducing a modifying material called a *lubricant* that can prevent direct surface-to-surface contact. The frictional behaviour of sliding surfaces follows a well-established pattern described by the Stribeck curve (Figure 2.7) [396]. This is a semi-empirical model that follows the sliding on journal bearings lubricated by a hydrocarbon fluid film, and links the friction coefficient to fluid film viscosity, relative shear velocity and load (contact pressure), demonstrating the different lubrication regimes. Hence, the Stribeck curve is more representative for hard-hard than soft-soft tribopairs. The three distinct lubrication regimes shown are the *boundary* lubrication regime, the *intermediate or mixed* lubrication regime and the *fluid-film* or *hydrodynamic* lubrication regime.

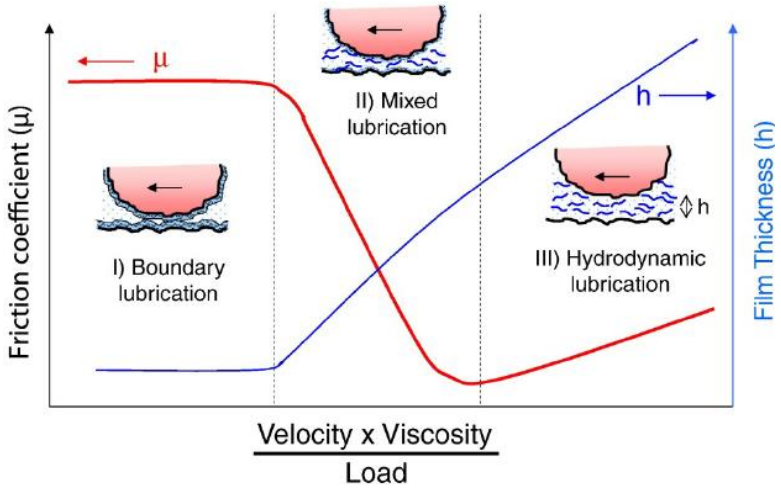

Figure 2.7: Model Stribeck curve and schematic representation of three distinct lubrication regimes. Friction coefficient (left, red line) and fluid film thickness (right, blue line) as a function of fluid viscosity, shear velocity and load (Hersey number) under hydrodynamic conditions, for I) boundary, II) mixed lubrication and III) hydrodynamic lubrication regimes [397].

Boundary lubrication occurs when the sliding surfaces are either in "solid contact" with the asperities of both surfaces being in direct contact (dry friction) or in "physical contact" where a thin surface-bound molecular film (boundary lubricant) prevents the direct contact of the sliding surfaces [398]. As a result, boundary lubrication is normally associated with higher friction coefficients. An effective boundary lubricant provides low surface energy and is either strongly adhered (chemisorbed or physisorbed) to the surface to avoid being sheared away, or can quickly adsorb to the surface from the solution replacing the sheared-off lubricating molecules [397]. Therefore, the intermolecular forces (strength of adhesion) between boundary lubricant and the substrate are of great significance [399,400]. Boundary friction depends on the type and MW of the intermediate fluid-film/lubricant and the nature of the solid surfaces. Boundary lubrication is suggested to reduce the susceptibility to wear during shearing. In many biological systems, it plays the essential role of the last mechanism of lubrication preventing the direct contact of the biointerface and thus the potential complications [401,402].

Recently, advances in the study of the lubricating and frictional properties of polymer brushes in biomedical applications necessitated the redefinition of boundary lubrication into three subtypes, the thin film (monolayer), the intermediate (tens of nanometers) and the thick film (up

to many micrometers) boundary lubrication [392]. Hydration layer-mediated thin film boundary lubrication is present at biological surfaces where load and shear stress remain low, as in the case of cellular processes [403]. Water is a unique dipole molecule that can form a quasi-structured layer at hydrophilic surfaces able to reduce other molecular interactions at this surface. Despite the narrow operational temperature window, the low viscosity and surface energy which in turn limit its efficiency as a boundary lubricant under larger compressive loads, water's contributions to more complex macroscale multimodal biological systems is pivotal [404,405]. Intermediate film boundary lubrication is also often observed in biological systems, including articular joints and the eye, that use lipids, short-chain polysaccharides (e.g. hyaluronic acid), mucins and highly glycosylated glycoproteins (e.g. proteoglycan 4) to modulate friction. These biological lubricating agents can contribute to reducing friction through steric repulsion and repulsive hydration forces, hydrophobic interactions, and their intrinsic viscoelastic properties. A typical example is the thick layer on the cartilage surface where hyaluronic acid (HA), proteoglycan 4 (PRG4), collagen and phospholipids are interconnected in order to contribute to boundary lubrication during locomotion. Thick boundary layer extends past the interfacial asperities preventing not only direct/solid contact but also physical contact, even under significantly high loads [401]**.**

Mixed lubrication occurs as the lubricant becomes partially entrained between the two surfaces and describes the transition regime from the load-controlled boundary (maximum friction) to the viscosity-controlled hydrodynamic lubrication (minimum friction). Mixed lubrication is a type of multimodal lubrication where friction forces occur due to mechanical interactions between the contacting surface asperities and hydrodynamic processes in the confined interfacial fluid-film [392]. Therefore, different lubrication mechanisms are present simultaneously, contributing, often synergistically, to friction reduction and shear-induced wear/damage prevention.

In hydrodynamic lubrication, the sliding surfaces are fully separated by the pressurized fluid film, leading to low friction. In this regime, friction is controlled by the shear rate and not by the load. Thus, it is dependent on the fluid properties, including effective viscosity, dynamic rheological behavior and film thickness. This is typically the most desirable mode of lubrication since both physical contact and wear are prevented. *In vivo*, hydrodynamic regimes are expected at high sliding speeds and low contact pressures, as in the case of cornea-eyelid biointerface in the presence of a continuous tear film, where the mucous and lipid layer inhibit the contact of the ocular tissues [406]. For soft and elastic surfaces, including most of the biological surfaces and

many biomaterials, the hydrodynamic pressure developed by the sheared fluid will cause elastic deformations and this type of lubrication is called elastohydrodynamic [407]. However, elastohydrodynamic processes can be extremely complex. Understanding and modeling of these systems is still in process.

In general, biolubrication systems are often characterized by more than one lubrication process or mode that can either contribute synergistically or can adapt from one mechanism to another depending on the operating conditions and biological function.

The deformation occurring between the sliding materials can be reversible or irreversible and can take place both on and beneath the surface of the sliding materials [408]. The irreversible deformation and loss of material from a surface due to friction forces is known as *wear*. Although wear can be related to friction, there is no direct relationship between friction and wear for different materials. For instance, reduced friction coefficients with an increase in wear has been previously reported for HA-grafted biological surfaces [50].

2.4.3.2. Friction and lubrication mechanisms during contact lens wear

The blinking cycle includes a fast phase with the eyelid reaching a maximum slip velocity on the order of 100 mm/s when it transverses the ocular surface and a slow phase with sliding speeds below 10 mm/s at the initiation and termination of the blinking process [167]. The effective lubrication process during contact lens wear in the presence of a healthy tear film involves a transition from intermediate and thick boundary friction to hydrodynamic lubrication, at increasing blink speed, in order to maintain low shear throughout the blinking cycle (Figure 2.8) [409]. More specifically, hydrodynamic lubrication occurs during the fast phase and in the presence of a continuous healthy tear film [410], and thus the eye-contact lens interface is well-separated allowing for normal tribology at the ocular surface to take place with relatively low friction coefficients [167]. No wear is expected in the hydrodynamic regime under these conditions [409]. In addition, it is the properties of tear film and more specifically its shear thinning and viscoelastic behavior that govern the hydrodynamic friction [34]. As the shear rate increases, approaching the slower phase of blinking, the friction becomes elastohydrodynamic due to the low modulus of soft contact lenses and their elastic deformations [406].

At lower ocular velocities and under constant eyelid pressure, as in the beginning and the end points of blinking cycle, the tear film is squeezed between the conjunctiva and eyelid and thus

boundary friction is predominant resulting in higher friction coefficients [164,410,411]. Boundary lubrication is also observed in the case of inadequate tear film quantity and quality or even under closed-eye conditions [5]. During boundary friction, the properties of the contacting biointerface and the surface interactions of the latter with the confined thin tear film are responsible for preventing direct lens-eye contact [164]. Hence, the PreLTF acts as a lubricating layer between the anterior contact lens surface and the eyelids and the PoLTF acts as a cushioning and lubricating layer between the posterior contact lens surface and the cornea. In the eye, the glycocalyx and the associated mucous layer of the tear film contribute to lower interfacial shear stresses for both hydrodynamic and boundary ocular lubrication, due to their high hydration and through the generation of repulsive steric and electrostatic forces, preventing the wear and damage of the ocular surface epithelium [57,409]. Additionally, the presence and adhesion of mucins on contact lenses are considered to likely reduce friction during wear [292,298].

For soft contact lenses materials, the friction of the eye-contact lens biointerface was found to be dependent on the applied load, the sliding speed as well as the thickness and rheological properties of the tear film [318]. Since the surface roughness of soft contact lens was found to be comparable to that of the ocular surface [412], the material properties that are important are the elastic modulus and the thickness of the soft contact lens. Intermolecular and surface forces, including van der Waals, electrostatic, steric, hydrophobic interactions and hydrogen bonding, were also found to influence the tribological properties of the system [23].

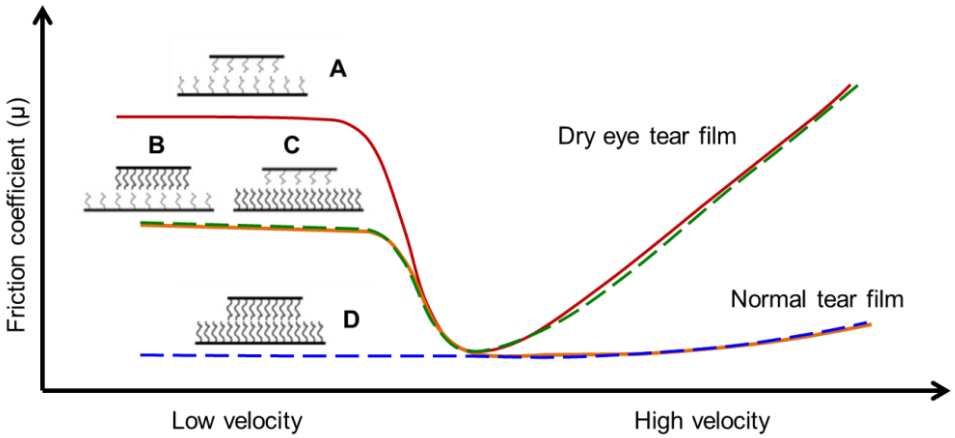

Figure 2.8: Friction coefficient for a low- and high-friction coefficient contact lens-eyelid biointerface in the presence of normal or dry eye tear film layer as a function of sliding velocity (blinking speed). A (red line): High friction coefficient contact lens with dry eye tear film. B (orange line): High friction coefficient contact lens with normal tear film. C (green dashed line): Low friction coefficient with dry eye tear film. D (blue dashed line): Low friction coefficient with normal tear film. (Adaptation from [409])

The presence and retention of a robust lubricious surface layer is vital for the normal contact lens induced friction mechanism. Although surface wettability is a necessary property, it is not a surface property criterion. Determination of the dynamic contact angle provides information for the stability of the intrinsic surface wettability (open-eye conditions), whereas measuring the friction coefficients under physiological conditions is essential for determining the stability of the wetting layer during blinking. Consequently, the determination of the frictional forces between the contact lens and the ocular surface interface in combination with the evaluation of the PreLTF and PoLTF composition and tear exchange may allow for a further understanding the correlation of *in vivo* wettability with contact lens performance and comfort.

In contact lens biotribology studies, there is no current industry standard for the measurement of friction coefficient or an accepted current technique for direct measurement of friction *in vivo*. Different methods that have been employed over the years to determine the friction coefficients of soft contact lenses *in vitro*, including atomic force microscopy [167,413,414], the inclined plane method [415] and, more commonly, techniques using a microtribometer or a tribometer of different

configurations [297,385,416–418]. However, the great differences in the techniques, methodology and conditions used resulted in various and noticeably different friction coefficient values. According to the literature, the chemistry of the hydrogel material, the water content, the testing media, the applied load and the sliding velocity were found to influence the results [419]. Generally, comparative studies should be between friction coefficients generated by the same instrument under identical conditions. Interpretation of the friction results from different instruments and under different conditions are challenging and should be done with caution.

More recently, in an effort to develop a method that examines the frictional behavior of contact lens under closer to *in vivo* conditions, the Schmidt lab used a biomechanical tester for the determination of the boundary friction coefficients of a human eyelid or cornea-contact lens biointerface [386]. The designed set-up ensured constant contact of the interacting surfaces, throughout the experiment, by preventing fluid infiltration during motion. This technique was used in the current work since it allows for the determination of the static and kinetic friction coefficients in a range of sliding speed and applied pressure similar to those that occur in the eye during contact lens wear under boundary conditions.

2.5. Improving the ocular compatibility and performance of soft contact lenses

Throughout the contact lens history, there has been a continuous effort to optimize their surface properties, particularly surface wettability [22]. Modification approaches for soft contact lens materials with improved surface characteristics, and overall contact lens performance has been traditionally achieved with the use of demulcents, surfactants or biomimetic components that act as moisturizing and lubricating agents. This has been accomplished by their incorporation as internal or releasable wetting agents in the bulk of the contact lens material or by their immobilization on the surface of the contact lenses as a grafted layer. Typical examples of the comforting agents used in the development of soft contact lenses over the years include monomers such as methacrylic acid (MA), N-vinylpyrrolidone (NVP), or 2-methacryloyloxyethyl phosphorylcholine (MPC) [140,141] or hydrophilic polymers of relatively high MW and viscoelastic properties, such as polyvinyl alcohol (PVA), hydroxypropyl methylcellulose (HPMC), polyvinylpyrolidone (PVP), and poly(ethylene oxide) (PEO) [420–425]. Rewetting and lubricating agents are also increasingly used in packaging and contact lens care solutions as well as in eye drops in an attempt to promote contact lens comfort, both on contact lens insertion and during wear

by promoting hydration and lubrication of the eye-contact lens interfaces. Instillation of eye drops was found to reduce lysozyme denaturation on silicone contact lenses [426] and alleviate symptoms of LWE and discomfort [5,427,428]. However, the drawback of using releasable wetting agents to improve the surface properties and thus overall contact lens performance is their relatively short-term duration and associated inconvenience during wear, especially in the case of extended wear contact lenses.

2.5.1. Biological Wetting Agents and Boundary Lubricants for Biomimetic Surface Modification

The design of biomimetic surfaces is a well-established method for the development of surface engineered materials that can simulate the natural surface and control interfacial phenomena without causing adverse reactions [429]. This allows for integration of the biomaterial with the natural tissue or the biological environment without affecting its functional performance while improving host acceptance and thus biocompatibility. One promising approach for the creation of biomimetic surfaces is to mimic the highly hydrated state of cell membranes, and more specifically that of the glycocalyx in order to confer protection from adverse physiological responses that is naturally provided by the glycocalyx *in vivo* [429]. The glycocalyx mainly contains highly glycosylated proteins (mucins) and lipids, exposing a pattern of polysaccharide chains that form a dense hydrophilic layer on the outer surface of the cell membrane of the otherwise hydrophobic epithelium [430]. This mucous-based layer directs intercellular specific interactions, while at the same time it can act as a lubricant [431] and limit any undesired nonspecific interaction, such as the nonspecific adsorption of extracellular proteins, due to the steric repulsion provided by the carbohydrate side-chains [432,433]. In the eye, tear film biomolecules, and mainly the gel-forming mucins, interact with the glycocalyx of the corneal and conjunctival epithelia, forming a hydrated complex with a brush-like surface conformation, which in turn plays a crucial role in the wettability, hydration and lubrication of the ocular surface, promoting tear film stability and protection against foreign bodies and pathogens [57,59,100]. Several approaches have been followed for the development surfaces that mimic the non-adhesive properties of the cell surface glycocalyx, including surface-bound polysaccharides such as hyaluronic acid, mucins and model glycoproteins as well as glycocalyx-mimetic peptoids, containing glucose or β-D-maltose side chains, and dextran-based bioinspired polyelectrolyte

copolymers. All were characterized by protein antifouling and low friction properties [297,430,434–437].

Maintaining tear film stability at the eyelid-cornea biointerface plays a pivotal role in the hydration, lubrication and overall maintenance of anterior-segment ocular homeostasis. Taking into consideration that a contact lens material should be well hydrated by tears, prevent protein deposition and accumulation, and provide a low-shear-strength interface, the agents chosen for the modification of the model contact lenses in this study are biomolecules that are naturally present at the human ocular surface and tear film and exhibit wetting, antifouling and lubricating properties. The polysaccharide hyaluronic acid (HA) and the mucin-like glycoprotein Proteoglycan 4 (PRG4) were used in this study since they are considered good potential candidates for their application in soft contact lenses.

2.5.1.1. Hyaluronic Acid

Hyaluronic acid (HA), also known as hyaluronan, is a linear non-sulfated glycosaminoglycan (GAG) composed of alternating units of the disaccharide β1-4D-glucuronic acid (GlcA) and β1-3N-acetyl-D-glucosamine (GlcNAc) (Figure 2.9). Each disaccharide dimer of HA has an approximate MW of 450 Da and the entire polymer can consist of 2,000 to 25,000 dimers depending on the tissue from which it was derived. Commercially, HA is available with a MW up to 5 million Da [438]. It was first discovered in 1934 by Meyer and his coworkers in the vitreous humor, while 3 years later it was found in the cell coat of *Streptococcus* bacteria [439,440]. Hyaluronan is synthesized in the cellular plasma membrane and is a major structural component of the extracellular matrix (ECM), promoting the formation and hydration of the ECM in various tissues throughout the body as well as enabling their mechanical functionality and stability [441]. In the human body, HA can be found in the skin, umbilical cord, synovial fluid, cartilage, connective tissues and in the eye [442].

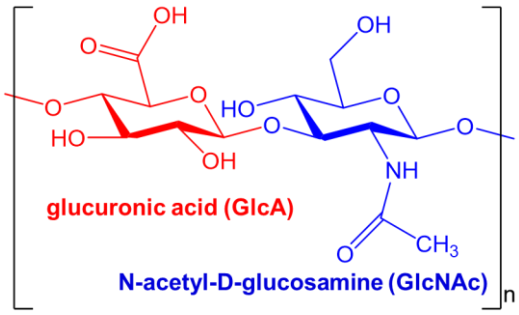

Figure 2.9: Schematic illustration of HA structure, comprised by alternating β1-4D-glucuronic acid (GlcA) and β1-3N-acetyl-D-glucosamine (GlcNAc) disaccharide units

Despite its simple chemical structure, HA exhibits various biological functions because of its intrinsic properties. Apart from its anionic nature (pKa ~3-4) under physiological conditions, HA is also considered a relatively weak polyelectrolyte [443]. The stiff HA chains with an extended random-coil configuration (radius of gyration ~ 200 nm) occupy enormous molecular domains that can form an entangled network in solution [444]. The random coil structure of HA is responsible for its unique high water-binding and retention capacity, and its viscoelastic properties [445,446]. Interestingly, it is estimated that HA may retain water up to 1,000 times its own weight [447]. In addition, it exhibits shear-thinning and viscoelastic behaviour in aqueous solutions [448], which are likely the most distinctive properties of HA, making it an ideal biological lubricant [446]. In turn, this justifies its presence in the soft connective tissues as well as the cartilaginous and ocular surfaces of the human body. The physicochemical properties of HA are dependent on its MW and concentration as well as the pH and iconicity of the solution [449,450].

HA is biocompatible, non-immunogenic, non-toxic, non-fouling and biodegradable [451,452]. It has been also reported to suppress inflammation [453] and promote wound healing [454]. Hence, HA is a versatile candidate for numerous cosmetic, medical and pharmaceutical applications, including angiogenesis, viscoprotection, tissue engineering and drug delivery [451,455–457]. HA formulations have been also studied in cancer therapy because this glycosaminoglycan specifically binds to the CD44 receptor which is overexpressed in several types of cancers [458]. Commercial preparations containing HA have also been used to promote wound healing, in treating osteoarthritis as a viscosupplement, and in surgery to prevent post-operative adhesions and scar formation.

2.5.1.1.1. Ophthalmic applications of HA

In the human eye particularly, HA is a component of the vitreous humor, the lacrimal gland, the conjunctiva, the corneal epithelium and the tear film [442]. It provides several biological benefits to ocular tissues, including corneal stroma hydration, corneal epithelial migration and wound healing, while also it modulates inflammation, and protects the cornea from oxidative damage as well as from the toxic effects of the preservatives of ophthalmic solutions [29]. Moreover, its ocular compatibility in combination with its unique hygroscopic, viscoelastic, shear-thinning and thus lubricating properties, render HA well-suited for applications of the anterior ocular segment [459]. Initially, HA was used for vitreous and aqueous humor replacement in ocular surgery [460], however, currently HA is also used for corneal protection during cataract surgery and in corneal transplant surgeries in order to provide better graft transparency [461].

The presence of HA in the tear film is considered to contribute to tear film stability [28]. More specifically, HA has been shown to interact with the glycans of the mucous layer on the ocular surface [462,463] and enhance the spreading of the tear film [464]. Due to its hygroscopic, non-Newtonian shear-thinning and mucoadhesive properties along with its tolerability and biodegradability, HA allows for long-lasting hydration of the ocular surface by enhancing the tear stability and lubrication [30,465]. Hence, one of the most prominent ocular applications of HA is its use as a wetting and lubricating agent in artificial tear solutions and over-the-counter eye drops for the management and treatment of ocular dryness and dry eye syndrome [33,427,466]. In addition, HA has been used as an active excipient in therapeutic eye drops in order to prolong the precorneal residence time of the drug, reduce systemic drainage and thus improve bioavailability and therapeutic efficacy while improving patient compliance [467]. A commercially available topical solution that contains HA is Hyalcrom NF launched by Bausch & Lomb for the treatment of allergic conjunctivitis.

In contact lens applications, HA has been used as conditioning agent in commercial contact lens rewetting drops, such as Aquify® Long-lasting Comfort Drops (Ciba Vision) and Blink Contacts® Lubricating Eye Drops (Abbott Medical Optics), and in a multipurpose solution (Biotrue™ by Bausch & Lomb) [468]. As noted, the presence of the contact lens in the eye disrupts tear film structure, while the surface tension at the boundary of the cornea-lens interface is increased, causing alterations in tear film stability [469]. During lens wear, HA is thought to evenly cover the surface of the contact lens upon blinking due to its shear-thinning behavior, retaining

water molecules close to the ocular surface thus reducing contact lens dehydration. HA-containing eye drops were found to increase tear film thickness (measurement without contact lens) [470] and volume [471], stabilize the tear film, increase tear break-up time, and alleviate symptoms of ocular dryness during contact lens wear [33,465,472]. Moreover, the high MW HA used in Biotrue™ solution was reported to readily sorb on a variety of pHEMA-based and silicone hydrogel contact lenses during storage time, thus improving their surface wettability [473]. Despite the short residence time of HA in tears compared to the daily period of contact lens wear [474], Biotrue™ was reported to clinically improve end-of-day discomfort [475].

Moreover, HA has been examined as an internal [43,476–478], a releasable wetting agent [479–481], and as a component of an interpenetrating network (IPN) [482] for conventional and silicone hydrogel contact lenses. According to the results, extended release of HA was achieved in a controlled manner, while the water content, surface wettability and hydrophilicity, and resistance to protein deposition of the tested HA-containing hydrogel materials were improved. Reduced lysozyme denaturation and boundary friction were also observed when HA was covalently immobilized in the bulk of model silicone hydrogel contact lenses [483,484]. Deposition of a self-assembled chitosan/HA multilayer coating, via electrostatic interactions using the layer-by-layer (LbL) technique, also improved surface characteristics, such as wettability, dehydration and resistance to protein sorption [485,486]. Surface immobilization of contact lenses with HA-binding peptides was found to locally attract and concentrate exogenous HA, creating a thin HA coating able to delay contact lens dehydration [487]. Finally, resistance to protein deposition, bacterial adhesion and biofilm formation was observed when HA was used as a surface layer [488–492], further supporting its functionality as an efficacious surface layer for contact lens applications. Hence, all of these properties suggest that HA is an excellent biomimetic candidate in contact lens applications.

2.5.1.1.2. HA as a boundary lubricant

HA is believed to have an important function in the boundary biolubrication of articular cartilage and the ocular surface, contributing to their protection against abrasive wear and damage [493–495]. However, the efficiency of HA as a boundary lubricant has been disputed in the literature. HA exhibited low compressibility when it was physically adsorbed to negatively and positively charged model surfaces under high loads, with the polyelectrolyte being sheared away

and expelled from the contacting surfaces under high loads [47,297,496,497]. According to the classical theory of boundary lubrication, a lubricant needs to be strongly bound to the surface it lubricates and have the appropriate conformation in order to provide reduced friction [493]. Therefore, the poor adhesion of HA *in vitro* has been ascribed for minimal or no impact on both boundary lubrication and wear protection [47,297,496,497]. However, HA was found to effectively reduce boundary friction when it was mechanically trapped in soft porous surfaces, such as articular cartilage [401,495] and cornea-polydimethylsiloxane (PDMS) or silicone hydrogel [48,49] biointerfaces. Reduced friction and wear were also observed when HA was covalently attached or crosslinked (*hylan*) to various substrates [50,297,484,493,498]. The boundary lubricating ability of surface-grafted HA was reported to be similar when PBS and an artificial tear solution were used [297]. Furthermore, surface modification with HA-binding peptides led to the formation of a non-covalently bound HA layer that exhibited reduced boundary friction coefficients [499,500]. The boundary lubricating properties of HA were found to be concentration and MW dependent, with higher MW and thus thicker HA films exhibiting lower frictions coefficients, when an eye-mimicking tribological model was used [297]. Finally, it has been suggested that HA functions more as a viscoadditive excipient enhancing hydrodynamic rather than boundary lubrication [497,501]. In hydrodynamic lubrication, viscous films result in lower friction coefficients preventing thus surface contact.

2.5.1.2. Proteoglycan 4

Proteoglycan 4 (PRG4), also referred as lubricin or superficial zone protein, is a mucin-like glycoprotein expressed by the PRG4 gene. PRG4 (MW ~230 kDa) has a extensively glycosylated central domain via O-linked β(1–3)Gal-GalN-acetylgalactosamine (β(1–3)Gal-GalNAc, 50% w/w) that is mostly capped with sialic acid (NeuAc) in a “bottle-brush” configuration, as well as a somatomedin-B (SMB)-like and a hemopexin (PEX)-like globular end domain that flank the protein backbone at the N’ and C’- terminals, respectively (Figure 2.10) [502]. It is an asymmetric molecule with a weight average contour length of approximately 220 nm and 1-2 nm in diameter that has a partially extended and flexible rod conformation [503]. PRG4 is able to lubricate in the absence of a thick fluid film and hence can act as a boundary lubricant [386]. The end hydrophobic globular domains carry most of the positive charge present in PRG4 and are considered to play a significant role in the binding ability of PRG4 to a surface, which is crucial for boundary

lubrication [45,504,505]. Additionally, these domains are of special interest since they play specific roles in cell-cell and cell-ECM interactions [506]. The abundant negatively charged polysaccharides of the central domain provide a high degree of hydrophilicity and generate strong repulsive forces through hydration and steric-entropic forces, contributing to lubricating property of PRG4 [45,503,507,508]. Therefore, the lubricating function of PRG4 is structure dependent, supporting the notion that intact PRG4 is required for lubrication, particularly under boundary conditions. In its native state, PRG4 can form intra and intermolecular disulfide bonds between the cysteine (Cys) residues of its end domains, leading to extended supramolecular loops that in turn can aggregate into dimers or even oligomers [397,503]. Overall, the composition of PRG4 is typical of mucin proteins that are responsible for forming the mucous coating in order to provide lubrication at epithelial surfaces [46].

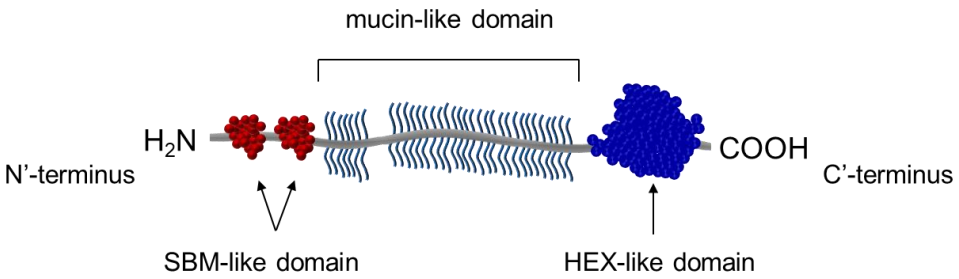

Figure 2.10: Schematic representation of Proteoglycan 4 (PRG4) molecule, depicting the end somatomedin (SBM)-like and hemopexin (HEX)-like domains at its N' and C'-terminus respectively, and the central mucin like domain.

In human body, PRG4 has been discovered in synovial fluid, articular cartilage, menisci, tendons, ligaments and at the ocular surface. Its diverse biological properties can likely be attributed to the multiple protein domains contained within the glycoprotein. PRG4 is a major component of synovial fluid, highly expressed and secreted by chondrocytes and synoviocytes; as a boundary lubricant in joints it protects the cartilaginous surfaces against wear and damage, cell adhesion and protein deposition [46,509]. In the eye, PRG4 was found to be transcribed, translated and expressed by corneal and conjunctival epithelial cells [34] and in meibomian gland secretions [36,37]. Deficiency of functional PRG4 was reported to result in lack of ocular lubrication, as in the case of dry eye, contributing to wear and damage to the ocular surface [34,35]. It is thus

suggested that PRG4 is responsible for preventing tear film evaporation and for protecting the ocular surface against the significant shear forces generated during blinking.

PRG4 was first isolated from bovine synovial fluid by Swan et al. in 1981 [510]. The naturally occurring PRG4 used initially for the *in vitro* studies was extracted and purified from bovine stifle joints, a time- and money-consuming process that often resulted in low yields. Recent advances in molecular biology allowed for the expression of full-length recombinant human PRG4 (rhPRG4) in Chinese hamster ovary (CHO) cells. Significant characteristics regarding rhPRG4, including higher order structure (monomeric and disulfide bonded dimeric structure), O-linked glycosylation, protein identity and lubricating properties were found to be consistent with that of the naturally occurring PRG4 present at the ocular surface [511]. According to a recently published clinical trial, rhPRG4-containing eye drops were able to rapidly reduce signs and symptoms of dry eye disease without causing any adverse events, by significantly improving the damage to the ocular surface epithelium, reducing inflammation on the eyelid and the conjunctiva as well as restoring a competent teat film [38]. Interestingly, the clinical results showed that PRG4 supplementation was superior to that observed with commercial HA-containing eye drops [38], further supporting the notion that PRG4 may be a new promising candidate for the treatment of corneal and conjunctival epitheliopathies as well as dry-eye related symptoms such as Sjögren's syndrome, graft vs host disease, Stevens-Johnson syndrome, refractive surgery and dry eye disease.

PRG4 was also found to reduce the boundary friction *in vitro* between synthetic and idealized surfaces [47,502,507,512] as well as cartilage [513] and cornea-eyelid [34,35] biointerfaces, further supporting the case that it is a highly surface-active mucinous glycoprotein. PRG4 adhesion to the substrate is thought to occur by hydrogen bonding, hydrophobic and electrostatic interactions. The lubricating properties of PRG4 were found to differ depending on the surface chemistry and charge, the PRG4 surface density and conformation, and the ionic strength of the solution. Physisorbed PRG4 adopts a "loop-like" conformation on hydrophobic or negatively charged surfaces, resulting in friction-lowering behavior [502,503,512]. The observed reduction in boundary friction and wear by PRG4 has been attributed to the steric-entropic and hydration repulsive forces caused by its central extensively glycosylated mucinous domain that gains a unique "loop" conformation similar to a telechelic polymer "brush-like" structure (~100 nm thick), once its C', N'-terminal domains are strongly bound to the underlying surface [502,503]. Long-

range electrostatic interactions are postulated to play an important but secondary role. In contrast, on hydrophilic surfaces the molecule adopts an extended "tail-like" conformation, while for positively charged surfaces the conformation is speculated to be more complicated [502,503,512]. Restriction of the conformational freedom of the adhered PRG4 led to compromised boundary lubrication for these surfaces. In the case of soft polymeric materials, and more specifically for hydrogel contact lenses, physisorbed PRG4 acted as good boundary lubricant for PDMS and for certain model or commercial non-surface pretreated silicone hydrogel contact lenses, but not for the more hydrophilic conventional hydrogel contact lens materials [48,49,386,484,511]. Therefore, it is suggested that not all surfaces are good candidates for PRG4 to function as boundary lubricant.

Finally, it has been reported that the extensive *O*-linked glycosylation of the central mucinous domain of PRG4 can improve wettability on hydrophobic surfaces and cartilage. Besides the lubricating property and protection form wear, PRG4 has been shown to exert anti-adhesive action preventing cell attachment while protecting the underlying cells [45,514,515]. This antiadhesive character of exogenous PRG4 was able to manifest wound healing and tissue regenerative properties *in vivo* [516]. Antifouling properties against protein deposition [514,517] and bacterial adhesion and proliferation for PRG4-coated surfaces were also observed [39,518]. Therefore, PRG4 can be an advantageous biomimetic candidate in contact lens applications.

2.5.1.3. Synergistic interactions of HA and PRG4 in boundary lubrication

PRG4 and HA were first reported to interact and synergistically reduce boundary friction at a latex-glass interface under high contact pressures [47]. Decrease in boundary friction was also observed *in vitro* when free PRG4 and HA were sorbed together on cartilage–cartilage [495,519], cornea-eyelid [34] as well as cornea-PDMS or silicone hydrogel [48,49] biointerfaces. For idealized model surfaces, however, synergistic lubrication between HA and PRG4 was observed only when HA was surface-grafted and not adsorbed [50,51,496,512]. Recently, synergistic reduction in boundary friction was observed when HA was covalently immobilized in the bulk of certain model silicone hydrogel contact lenses materials and PRG4 was physisorbed, but not for the respective hydrogel conventional hydrogel materials [484]. Moreover, the molecular weight of HA was not found to significantly impact the synergistic lubrication of the physisorbed PRG4 and HA complex at a cartilage-cartilage biointerface [520], whereas high MW of HA was found to be

more effective in its interactions with PRG4 for protection against wear at cartilage-glass biointerface [401].

Understanding the mechanism for the PRG4-HA synergistic interactions for boundary lubrication has been challenging. It is postulated that PRG4 and HA interact directly, through non-specific interactions [51], forming a partially entangled and physically crosslinked weak hydrogel complex. For HA-immobilized surfaces, physisorbed PRG4 was reported to form a stable PRG4-HA complex that led to reinforced steric and electrostatic repulsion between the contacting surfaces, further reducing friction while providing wear protection in a PRG4 and HA concentration-dependent manner [51,519]. In contrast, HA was not found to interact to the same extent with PRG4-coated idealized surfaces [512], further supporting that the interactions between PRG4 and HA are physical rather specific site-dependent binding interactions. Overall, some studies suggested that the surface bound PRG4 induced HA deposition [521,522], whereas others reported that surface tethered HA is responsible for PRG4 sorption [401,520] for the formation of the PRG4-HA complex at the interface that is in turn responsible for the observed synergistic effect. Hence, the relationship between the PRG4-HA interactions and structure with boundary lubrication remains to be fully elucidated.

Taking advantage of the commercial contact lens-related HA products and the promising results of PRG4 eye drops for the treatment of ocular dryness, these two wetting and lubricating agents may have significant potential to work synergistically for alleviating ocular dryness and discomfort during contact lens wear.

2.5.2. Controlled interfacial interactions: Protein antifouling and low friction properties

The composition and behavior of surfaces and interfaces plays a pivotal role in dictating the biocompatibility and overall efficiency of a biomaterial. Modification of the surface properties of a biomaterial allows for the modulation of the interfacial interactions with the biological environment without however altering the bulk properties that are also required for performance. In the case of contact lenses, surface modification has been used to improve surface wettability, lubricity and resistance to protein deposition while retaining bulk properties, such as oxygen permeability and elastic modulus [523]. A promising approach to optimize the surface properties of a biomaterial is via the deposition of a thin-film of a naturally occurring or synthetic polymer that possesses appropriate physical and chemical properties [524–526].

Surface modification can be achieved by many strategies, including self-assembled monolayers, physisorption or chemisorption of polymer chains or biomolecules. In the case of physisorption, the form coating is non-covalently tethered to the surface through molecular interactions, such as electrostatic or hydrophobic interactions. As the interactions developed between the chains and the substrate are relatively weak and can be reversible, the deposited coating can be unstable and may be easily depleted upon a change in the physicochemical conditions (pH, temperature and ionic strength) [527]. On the other hand, chemisorption involves the formation of a covalent bond between the surface and the layer, a process also known as grafting. Surface grafted layers are characterized by improved long-term chemical stability due to the nature of the immobilization bond, minimizing delamination over time [527].

Surface grafting with polymer chains can be classified as either *grafting from* and *grafting to*, depending on the nature of the grafting strategy (Figures 2.11A and B). *Grafting from* is a surface-initiated polymerization reaction where an initiator is immobilized or generated on the substrate and polymer chains grow directly "from" the reactive sites surface *in situ* [524]. *Grafting from* polymerization strategies that have been studied include conventional radical, controlled radical, and atom transfer radical polymerization (ATRP). The latter grafting technique allows for controlled functionality, density, and thickness of the polymer brushes and can be an effective method for the formation of thick and high-density functional polymer brushes in a controlled fashion. *Grafting to* involves the covalent coupling of the functionalized groups of adsorbed polymer chain with complimentary functional groups present on the surface of interest via a chemical reaction [524]. In contrast to *grafting from* technique, this method is using well-defined polymers with a narrow molecular weight distribution that can be characterized prior to the grafting reaction. Moreover, it is considered a less challenging facile method from a chemical point of view as it does not involve elaborate synthetic procedures, while it allows the simultaneous surface immobilization of different polymer chains. However, it can be difficult to achieve high graft density due to steric-hindrance effects, particularly as the chain length increases, and thus "grafting to" is considered a self-limiting process [528]. Parameters such as the chemistry, the nature of the polymer chain and the experimental conditions (pH, temperature, ionic strength and polymer concentration) determine the conformation, thickness and grafting density of the surface layer as well as its long-term and chemical stability [524].

A high degree of surface grafting of end-functionalized polymers to the surface can lead to the formation of polymer brushes, as the polymer chains obtain an elongated conformation due to steric repulsion and volume exclusion effect [529]. However, surface grafting of naturally occurring polysaccharides, such as hyaluronic acid (HA), to the substrate occurs through one or more of the side repeating functional groups present. Hence, each chain can be grafted to the surface at several points and the obtained conformation is that of loops and/or tails (Figure 2.11C) [530]. The resulting conformation of the grafted layer is dependent on immobilization conditions, such as degree of polymer chain functionalization (pinning density), conformation in solution and affinity for the surface of interest. When the substrate is completely covered with a relatively dense stretched monolayer of the grafted chains, "brush-like" layers are formed due to the excluded volume effect. Polymer "loops" have been suggested as a good alternative to polymer brushes because of the reported low degree of chain interpenetration under normal load [531].

Polymer brush coatings on surfaces have gained great attention in recent years because of their outstanding stability, multifunctionality and chemical robustness. According to the literature, biomaterials with surface tethered hydrophilic polymer layers are characterized by a steric barrier at the interface allowing for controlled short and long-range interfacial interactions, often associated with low adhesion properties, resistance to non-specific protein adsorption and lubricity in an aqueous environment allowing for improved biocompatibility [392,532,533]. The steric and/or electrostatic repulsion, the repulsive hydration layer and the decrease in the interfacial tension are considered the key mechanisms for this effect in an aqueous medium [532,534,535]; and are primarily affected by the chemical structure, and the surface density, thickness, morphology and architecture of the surface immobilized layer [535–537]. The formation of dense and tightly-tethered surface layers of long polymer chains is preferred. Therefore, development of a surface grafted-layer with a brush or a brush-like conformation provides a versatile tool for surface modification and functionalization in a well-controlled and adjustable manner with great applicability in biomedical implants and devices, such as catheters, prosthetic devices, stents and contact lenses where protein resistance and low friction is desired, as well as in applications where antifouling properties are more important than the frictional as such as surgical grippers, immunoassays and biosensors [538]. Various types of polymer surface layers that were designed based on non-ionic hydrophilic polymers such as and poly(ethylene glycol) PEG and PEG-based copolymers, zwitterionic polymers, polyelectrolytes and polysaccharides were reported to exhibit

superior resistance to non-specific protein adsorption, and lubricating properties, [539–545] allowing for improved biocompatibility.

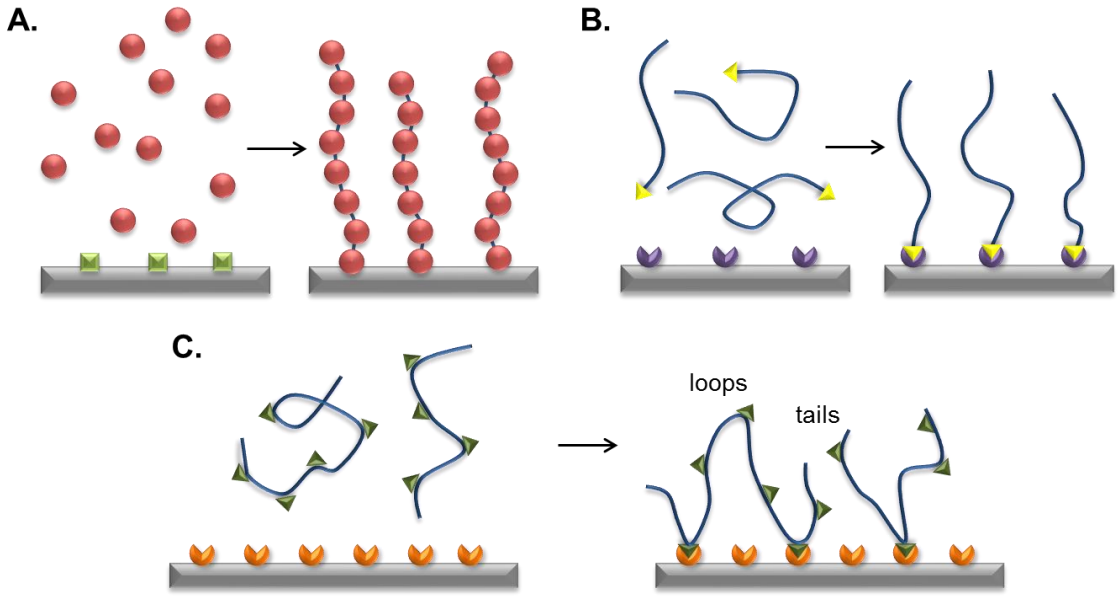

Figure 2.11: Schematic illustration of the grafted polymer A. brushes via "grafting from" (i.e. surface initiated polymerization), B. brushes via "grafting to" technique; and C. "brush like" chains grafted via side functional groups (loops and tails behave similar to polymer brush).

2.6. Thiol-ene click chemistry

Click chemistry, introduced by Sharpless and colleagues in 2001 [546], is characterized by modularity, high efficiency, regioselectivity, stereospecificity and orthogonality, resulting in high yields with minimal or no inoffensive byproducts and proceeds under mild reaction conditions with readily available materials having a wide range of applications. The high reaction rate and efficiency of *click chemistry* are the result of thermodynamically driven reactions that have low energies of activation and high affinity between the reactant groups.

An attractive and widely used "click" process is the century-old *thiol-ene coupling* which involves the addition of a thiol (-SH) group to a carbon-carbon double bond (C=C) (Figure 2.12), such as norbornenes, acrylates, maleimides or unactivated alkenes. The "click" character is attributed to thiol-ene chemistry due to its chemo and region-selectivity, good tolerance for

functional groups, versatility, high reaction rates and efficiency that results in the formation of a highly specific product which requires either little or no purification in the absence of toxic transition-metal catalysts and under very mild or even ambient conditions, including the presence of water, salts and oxygen [547]. Thiol-ene "click" reactions make use of the high nucleophilicity of the sulfhydryl moiety and follow either base/nucleophilic catalyst-mediated thiol-Michael addition or free radical addition mechanisms resulting in a thioether product with anti-Markovnikov orientation. The thioether linkage is very stable under physiological conditions, in strong basic or acidic media and to reducing agents; however, it is susceptible to oxidizing agents. Depending on the reaction conditions, both mechanisms may be active simultaneously [548].

Thiol-ene chemistry was extensively used in the 1950s for the formation of crosslinked networks [549]. Taking advantage of the features of "click" chemistry along with the availability of various thiol-functionalized (bio)molecules that simplify both the reaction processing and the product isolation, thiol-ene "click" chemistry has been recently exploited in synthesizing, functionalizing and modifying a wide range of (bio)molecules and (bio)materials with controlled physical, chemical and mechanical properties. Hence, it has become an attractive synthetic tool for biomedical applications, including controlled drug delivery, tissue engineering and surface modification [547,550,551]. The thiol–acrylate "click" chemistry has been widely implemented for dendrimer and block copolymer synthesis, hydrogel formation, surface and particle modification [552–555]. For surface modification processes, thiol-Michael addition and particularly radical mediated thiol-acrylate "click" chemistry have been successfully used for the development of well-defined surface functionalities with fine temporal and spatial control, allowing for improved wettability, antiadhesive and antifouling properties [556–560].

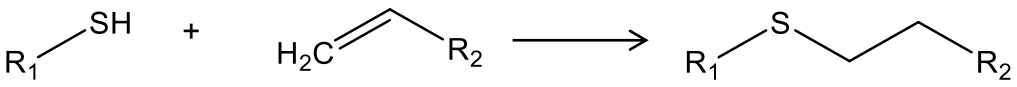

Figure 2.12: Schematic illustration of the thiol-ene reaction.

2.6.1. Nucleophile-mediated thiol-Michael addition "click" reactions

Thiol-Michael addition reaction can be initiated using a wide-range of precursor materials due to the versatility of the weak sulfur-hydrogen bond, proceed under mild reaction conditions

and yield a highly efficient modular "click" reaction in the presence of mild catalysts [547,561]. Compared to base catalysts used for the thiol-Michael "click" reactions, the nucleophile catalysts have been shown to catalyze the thiol-Michael addiction reaction much more rapidly and efficiently with minimal or no side reactions, under facile ambient conditions, even with significantly lower catalyst concentrations [562–565]. Nucleophilic catalysts for thiol-Michael addition include simple primary/secondary amines as well as certain tertiary phosphines, while tertiary amines were found incapable of initiating the reaction because of their limited nucleophilicity and increased steric hindrance of their nitrogen [561]. During a nucleophile-mediated thiol-Michael addition reaction, the nucleophile undergoes conjugate addition to the activated C=C bond creating a strong enolate base or carbanion, which in turn deprotonates the thiol and forms a thiolate anion (strong nucleophile) and an inert catalyst-derived byproduct. Subsequently, the thiolate anion enters an anionic chain process in which it undergoes direct thiol-Michael addition resulting in the rapid formation of a thioether product with anti-Markovnikov orientation (Figure 2.13).

It is worth noting that the significantly rapid rates of nucleophile-mediated thiol-Michael addition reactions are attributed to the anionic chain-like process. Moreover, the structure of the thiol and ene functional groups, the type and concentration of the catalyst and the type, polarity and pH of the solvent are crucial parameters for the efficiency and kinetics of thiol-Michael addition reactions [561]. A Michael acceptor in thiol-Michael addition reactions is typically an electron-deficient *ene* group such as an acrylate group. Electron-deficient alkenes are necessary due to the creation of the thiolate anion and the reaction between the thiolate and the alkene. Therefore, the more electron deficient the C=C bond is, the more reactive it is typically towards a Michael addition reaction. In addition, acidic thiols with lower pKa values exhibit faster kinetics than basic thiols due to ease of deprotonation [561,565]. The nucleophilicity of the catalyst used also has an impact on the reaction rate. More specifically, increasing the nucleophilicity of the catalyst results in the generation of more thiolate anion intermediates leading to higher reaction rates of the thiol-Michael addition reactions. For instance, tertiary phosphines (such as (tris(2-carboxyethyl)phosphine (TCEP) and dimethylphenylphosphine (DMPP)) were found provide the fastest reaction and when used in small catalytic amounts to achieve quantitative yields of the desired compounds without any significant undesired byproducts [561]. However, the thiol content

determines the kinetic profile of the reaction in this case since the reactant thiols are the only protic species that react with the anionic intermediate during the anion chain-like process [561,565,566].

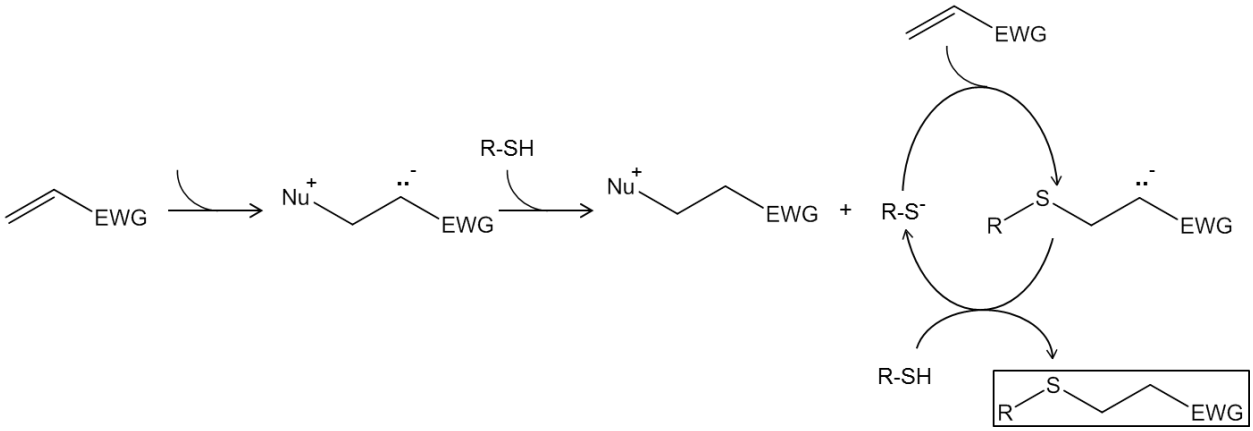

Figure 2.13: Schematic illustration of the nucleophile-catalyzed thiol-Michael addition "click" reaction.

2.6.2. Radical-mediated thiol-ene reaction

The radical-mediated thiol-ene reaction can be readily initiated thermally or photochemically (with or without photoinitiator) and involves the hydrothiolation of an alkene, commonly in a terminal position following a mechanism similar to the chain-growth free radical polymerization processes. A typical radical thiol–ene reaction mechanism, in a similar manner to other radical-initiated polymerization and reaction processes, encompasses three necessary distinct reaction processes: the initiation, the polymerization or coupling reaction, and the termination (Figure 2.14). The termination reaction is suggested to involve typical radical-radical coupling processes [567], though the details of this step remain elusive. The resulting thioether product is formed in essentially quantitative yield with anti-Markovnikov orientation. In the presence of unsaturated electron deficient alkenes such as acrylates and acrylamides, the carbon radical can react with another -ene functional group as well, resulting in a mixed mode of step-growth and chain-growth processes. Hence, the radical-mediated thiol-ene reactions are associated with byproduct formation since complete conversion of unsaturated alkenes cannot easily equate to complete thiol conversion [551,568]. However, radical-mediated thiol-ene reactions are not oxygen inhibited,

yielding more rapid reaction kinetics compared to the free radical chain-growth reaction. Overall, thiol-ene radical additions are advantageous as "click" reactions because of the step growth (alternating propagation and chain transfer cycles) process [568].

The chemical structure of the thiol and the alkene group are important parameters for the rate and the efficiency of the radical-mediated thiol-ene reaction. Electron-rich unsubstituted and strained alkenes react more rapidly with thiols than electron-poor alkenes [569]. Although the literature regarding the thiol contribution to this type of thiol-ene chemistry is limited, some general trends suggest that thiols based on propionate esters and glycolates esters are significantly more reactive than the alkyl thiols. This was attributed to a potential weakening of the S-H bond by hydrogen bonding of the thiol hydrogen groups with ester carbonyls [569]. Thiol-ene stoichiometry, type of solvent, competitive chain growth processes, specific thiol and alkene substitution and solubility, also influence the overall radical-mediated thiol-ene kinetics. In addition, controlled time, dose and/or intensity of light exposure can be used to control the rate and extent, and thus the characteristics of the thiol-ene reactions. The spatial and temporal control of light exposure can be used for materials and surfaces with gradient characteristics and/or chemical patterns [553].

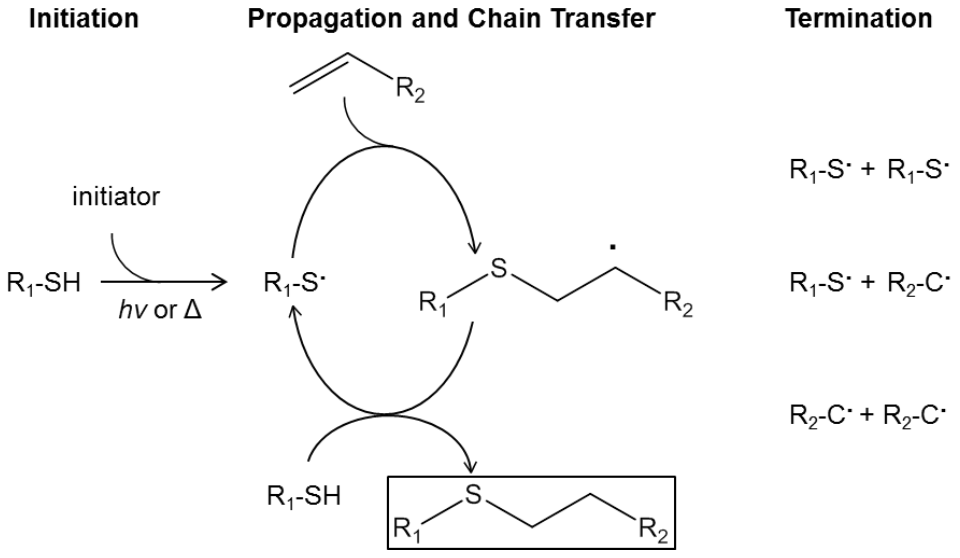

Figure 2.14: Schematic illustration of the radical-mediated thiol-ene "click" reaction

Chapter 3

Surface modification of model hydrogel contact lenses with hyaluronic acid via thiol-ene "click" chemistry for enhancing surface characteristics

Authors: Myrto Korogiannaki, Jianfeng Zhang, Heather Sheardown

Publication Information:

This chapter has been published in J Biomater Appl. 2017 Oct;32(4):446-462. doi: 10.1177/0885328217733443.

Abstract

Discontinuation of contact lens wear as a result of ocular dryness and discomfort is extremely common; as many as 26% of contact lens wearers discontinue use within the first year. While patients are generally satisfied with conventional hydrogel lenses, improving on-eye comfort continues to remain a goal. Surface modification with a biomimetic, ocular friendly hydrophilic layer of a wetting agent is hypothesized to improve the interfacial interactions of the contact lens with the ocular surface. In this work, the synthesis and characterization of poly(2-hydroxyethyl methacrylate) (pHEMA) surfaces grafted with a hydrophilic layer of hyaluronic acid (HA) are described. The immobilization reaction involved the covalent attachment of thiolated HA (20 kDa) on acrylated pHEMA via nucleophile-initiated Michael addition thiol-ene "click" chemistry. The surface chemistry of the modified surfaces was analyzed by Fourier transform infrared spectroscopy - attenuated total reflectance (FTIR-ATR) and X-ray photoelectron spectroscopy (XPS). The appearance of N (1s) and S (2p) peaks on the low resolution XPS spectra confirmed successful immobilization of HA. Grafting HA to the pHEMA surfaces decreased the contact angle, the dehydration rate and the amount of nonspecific sorption of lysozyme and albumin in comparison to pristine hydrogel materials, suggesting the development of more wettable surfaces with improved water-retentive and antifouling properties, while maintaining optical transparency (>92%). *In vitro* testing also showed excellent viability of human corneal epithelial cells with the HA-grafted pHEMA surfaces. Hence, surface modification with HA via thiol-ene "click"

chemistry could be useful in improving contact lens surface properties, potentially alleviating symptoms of contact lens related dryness and discomfort during wear.

Keywords

conventional hydrogel contact lenses; 2-hydroxyethyl methacrylate (HEMA); Hyaluronic Acid (HA); wettability, protein deposition; dehydration

3.1. Introduction

It is estimated that there are more than 140 million contact lens wearers worldwide, with approximately 44 million in the United States alone [1]. Studies suggest that as many as 50% of the contact lens wearers experience symptoms of dryness and discomfort, particularly towards the end of the day [2,3]. In fact, these symptoms are considered to be the primary reason for discontinuation of use [4–6]. The compatibility of the lens with the ocular surface is a critical design criterion in the development of comfortable contact lenses, since the contact lens comes in direct contact with the tear fluid and the ocular tissue during wear [7]. Ideally a contact lens candidate material must remain well hydrated, sustain stable and continuous tear fluid flow, be resistant to deposition of tear film components and provide adequate surface lubrication. Poor surface properties such as low wettability and lubricity along with increased protein deposition and denaturation, all of which are directly related to surface chemistry and surface morphology [8–10], can lead to reduced vision, altered inflammatory response and symptoms of discomfort. The bulk properties of a contact lens material, including water content, transparency, elasticity, and tear strength are of equal importance and are dictated mainly by the nature of the polymer. Hence, it is important to develop contact lens materials with both appropriate bulk and surface properties, which may lead to a necessity for surface modification.

Conventional contact lens materials consisting of poly (2-hydroxyethyl methacrylate) (pHEMA) and/or similar hydrophilic materials currently account for approximately 10% of all newly fitted soft contact lenses worldwide [11]. It is been reported that a considerable amount of protein can bind to pHEMA-based hydrogels [12,13]. Different approaches have therefore been investigated in order to improve the surface characteristics of conventional lenses including copolymerization with other monomers such as methacrylic acid (MA) or N-vinylpyrrolidone (NVP) [14], use of releasable or immobilized wetting agents, or surface coating. Most of the

demulcents explored, including polyvinyl alcohol (PVA) [10,15], carboxymethyl cellulose (CMC) [16], hydroxypropyl methylcellulose (HPMC) [16–18], polyvinylpyrolidone (PVP) [19] and poly(ethylene oxide) (PEO) [20,21], are highly hydrophilic moisturizing agents, more preferably of high molecular weight, with viscoelastic, antifouling and lubricating properties. In another approach, modification with 2-methacryloyloxyethyl phosphorylcholine (MPC), a biomimetic component of the cell membrane with zwitterionic nature resulted in higher tear film stability as well as significantly reduced protein deposition and bacterial adhesion [22]. Recently, Bengani et al. [23] copolymerized HEMA with surfactants whose chemical structure was similar to those being widely used in ophthalmic applications, resulting in hydrogels with higher water uptake as well as improved surface wettability and lubricity. Today, commercially available conventional contact lenses contain agents that are releasable (PVA, PEG, HPMC for nelfilcon A), tethered into the bulk (MPC for omafilcon A) or have their surface modified with a surfactant that mimics the lipid layer of the tear film (HyperGel material for nesofilcon A), aiming ultimately at the creation of a cushioning layer on the lens surface capable of enhancing interactions between the lens-eye and lens-eyelid interface [10,15,24–26]. However, problems associated with contact lens related ocular dryness, protein deposition, surface lubricity, dehydration and overall discomfort remain unsolved.

Over the past decade, of particular interest is the use of hyaluronic acid (HA) in contact lens applications. Commercially, HA has been used as a releasable conditioning agent in a multi-purpose care solution for soft contact lenses (Biotrue, Bausch and Lomb), rewetting eye drops (Blink Contacts, Abbott Medical Optics and Aquify® Long-lasting Comfort Drops, CIBA Vision) and in the blister package solution of the daily pHEMA-based contact lenses (methafilcon A, Safigel™) targeting enhanced comfort during wear.

Hyaluronic acid (HA) is a high molecular weight, linear, anionic and non-sulfated glycosaminoglycan found naturally throughout the human body. As a major component of synovial fluid, it plays an important role in joint lubrication [27,28], while in the eye it can be found as a component of the vitreous and lacrimal gland, as well as in the conjunctiva, corneal epithelium and tear film [29–33]. HA has been found to be involved in promoting corneal stroma hydration [34], corneal epithelial wound healing as well as in modulating inflammation [34–37]. Due to its biocompatibility and unique physicochemical properties, it has been widely used in ophthalmic applications [38–40]. Additionally, HA exhibits unique viscoelastic, shear thinning

and hygroscopic properties, allowing for improved tear film stability, ocular hydration and effective lubrication [33,41,42] affording protection to the ocular surface [43]. HA has been used for more than 20 years in artificial tears and over-the-counter eye drops for the treatment of ocular dryness and Sjögren's syndrome [42,44,45]. Moreover, it was found to significantly reduce protein deposition [46–48] and bacterial adhesion [49–51] when used as a coating layer. Hence, all of these properties suggest that HA is an excellent biomimetic candidate as a wetting agent in contact lens applications.

In model conventional contact lens materials, HA of different molecular weights has been evaluated as a releasable [52–54] or internal [55–57] wetting agent, as a component of an interpenetrating network (IPN) [58] or of a coating layer [59]. As releasable wetting agent, HA could be released in a controlled manner for up to 10 days, increasing the swellability, surface wettability and hydration of the materials without affecting their transparency, modulus and ion permeability [52–54]. However, the impact of releasable HA on important clinical parameters such as protein sorption and lipid uptake is as yet unknown. Immobilization of HA in the bulk, extensively studied in the Sheardown lab, was achieved by photopolymerization of methacrylated HA during synthesis [57] or post synthesis by covalent tethering of a dendrimer-modified HA [55,56]. Independent of the immobilization process, all HA-containing pHEMA hydrogels were optically clear, highly wettable and low fouling surfaces [55–58]. Surface modification with HA was achieved using either direct or indirect methods. Deposition of a physically adsorbed chitosan/HA layer by layer (LbL) self-assembled multilayer film on the surface of chitosan-containing 1-Day Acuvue contact lenses (etafilcon A) resulted in improved surface characteristics [59], while surface immobilization of HA binding peptides was found to locally attract and concentrate exogenous HA, delaying the contact lens dehydration [60]. Recently, Deng et al. [61] were able to improve the surface characteristics of pHEMA hydrogels by HA immobilization via hydrazone bonds using aldehyde-hydrazide chemistry. Although improved surface properties were observed, there are drawbacks with the methods used to synthesize the HA-hydrazide and the aldehyde-modified pHEMA surfaces, which limit control over the reaction and may also limit the scalability of the system. For example, the functionalization of HA with hydrazide was carried out using difunctional adipic acid dihydrazide which can lead to crosslinking, and as a result, a large excess of the modifier was used in an attempt to minimize this outcome. Deng et al. [61] also noted that undesired side reactions were observed between the aldehydes formed by the laccase/TEMPO

oxidation and the hydroxyl groups on pHEMA surface, impeding the degree of surface functionalization. Additionally, there are potential concerns with the presence of residual unreactive functional groups in the material, since, it has been reported that aldehydes for example can cause local toxicity due to their ability to react with proteins via their amine groups [62]. Therefore, in the current work an alternative type of "click" chemistry, the thiol-ene "click" coupling, was investigated for the surface grafting of HA to the surface of pHEMA hydrogels aiming for more control over the synthesis and yield better surface characteristics, including wetting and antifouling properties.

Thiol-ene "click" chemistry has been widely examined and shown to be a powerful approach for synthesizing novel materials in the field of polymer chemistry and nanotechnology as well as for engineering multifunctional surfaces in modular fashion [63]. It involves the reaction of a thiol with an α,β-unsaturated derivative or an unactivated olefin via a base/nucleophile-catalyzed Michael addition reaction or anti-Markonikov's radical addition mechanism [64]. Nucleophile-mediated Michael addition thiol-ene chemistry, characterized by the same general features of a typical radical-mediated thiol-ene "click" reaction [65], benefits from mild reaction conditions in the presence of very low amount of catalysts, as well as high functional group and oxygen tolerance, chemoselectivity, bio-orthogonality and conversion, requirements that make it attractive for efficient surface functionalization [64,66]. Compared to a base-catalyzed thiol-Michael addition reaction, this reaction type occurs significantly more efficiently [67–69]. Among the catalysts suggested in the literature, phosphine based catalysts were reported to be very reactive, leading rapidly to thiol-ene reactions [63] with high efficiency and minimal or no side product formation when used in catalytic amounts [70]. Due to the insolubility of HA in organic solvents, commercially available tris(2-carboxyethyl)phosphine (TCEP) was chosen herein since it is a very reactive and efficient catalyst for thiol–ene reactions in aqueous media [70], without affecting the biocompatibility of biomaterials *in vitro* [71] or *in vivo* [72]. Although TCEP has been previously used in biomedical applications as a catalyst, to the best of our knowledge, there is no published report of its use as a catalyst in a surface modification reaction of a biomedical device.

In this study, it is hypothesized that coating the surface of a conventional contact lens with a biomimetic HA layer can provide long-term improvement to surface characteristics, such as surface wettability and hydrophilicity while minimizing protein sorption under physiological conditions without affecting bulk properties. It is presumed that this will ultimately improve ocular

compatibility and comfort during wear. HA was covalently attached to the surface of model pHEMA hydrogels by the "grafting to" approach via TCEP-mediated Michael addition thiol-based "click" chemistry. The effect of the grafted HA layer on properties including surface wettability, protein deposition, dehydration and transparency was investigated.

3.2. Materials and methods

3.2.1. Chemicals and reagents

Hyaluronic acid (HA) (sodium hyaluronate) with an average molecular weight (MW) of 20 kDa was obtained from LifeCore Biomedical (Chaska, MN, USA). Hydroxybenzotriazole (HOBt) was purchased from Toronto Research Chemicals Inc. (Toronto, ON, Canada), while the UV photoinitiator 1-hydroxy-cyclohexyl-phenyl-ketone (Irgacure® 184) was generously donated by BASF Chemical Company (Vandalia, IL, USA). All other chemicals, reagents and proteins used were purchased from Sigma Aldrich (Oakville, ON, Canada).

3.2.2. Synthesis and characterization of thiolated hyaluronic acid (HA-SH)

For the synthesis of HA-SH, a two-step reaction protocol was followed. Initially, HA (20 kDa) was dissolved in Milli-Q water (16.6mg/ml) (pH 7.4), while an aqueous solution of 1-ethyl-3-(3-dimethylaminopropyl) carbodiimide (EDC)/HOBt (1:1 molar ratio) (4 equivalents to -COOH of HA, 10 ml water) and a cystamine dihydrochloride solution (2 equivalents to -COOH of HA, 10 ml water) were prepared separately. The EDC/HOBt solution was added dropwise into the HA solution and the mixture was stirred for 1.5 hours, while maintaining the pH at 6.8-7 (using NaOH 1M) for the activation of the carboxyl groups on HA. Cysteamine dihydrochloride solution was then added dropwise to modify HA keeping the pH stable at 7 (NaOH 1M) (HA-SS-R). The amidation reaction was mixed for 24 hours (pH 7, NaOH 0.1M) at room temperature. The product was then extensively dialyzed against Milli-Q water using a dialysis membrane with a MWCO of 3.5 kDa (Spectrapore, Spectrum Labs, CA). For the cleavage of the disulfide bond of the intermediate HA-SS-R product, TCEP HCl (5 equivalents to -COOH of HA) was added in the HA-SS-R solution while maintaining the pH at 5 (NaOH 1M) for five hours at room temperature. The final concentration of TCEP in the solution was 35 mM. Following the reaction, the pH was reduced to 3.5. The final product was then purified by dialyzing it extensively against Milli-Q

water (pH 3.5). After five days of dialysis at 4°C, HA-SH was freeze-dried and the final product was stored in the freezer (-20°C) and under nitrogen to protect the free thiols from being oxidized.

Thiolated HA (HA-SH) and the intermediate HA-SS-R product were characterized by ^{1}HNMR (20 mg/ml) on a Bruker AVANCE 600 MHz (256 scans, room temperature) spectrometer using D_2O as the solvent (D, 99.96%, Cambridge Isotope Laboratories, Inc.) as well as by Raman spectroscopy (Renishaw, laser = 785 nm, 30 mW).

3.2.3. Ellman's Test – Quantification of free thiols of HA-SH

The quantification of the free thiols of HA-SH was achieved spectrophotometrically, using Ellman's reagent (5,5'-dithiobis (2-nitrobenzoic acid), DTNB) [73]. Briefly, unmodified HA, HA-SS-R and HA-SH were dissolved in sodium phosphate buffer (0.1M, pH 8) containing 1mM ethylenediaminetetraacetic acid (EDTA), while L-cysteine was used for the calibration curve (2-20 nmol, R^2=0.9987). Samples and L-cysteine standards were mixed with a solution of Ellman's reagent and incubated for 15 minutes at room temperature under dark conditions, at which time the absorbance was measured at 412 nm using a UV-vis spectrophotometer (Spectramax Plus 384, Molecular Devices Corp.).

3.2.4. Synthesis of model pHEMA hydrogels

Initially, HEMA monomer and the ethylene glycol dimethylacrylate (EGDMA) crosslinker were passed through a column to remove the polymerization inhibitor monomethyl ether hydroquinone (MEHQ). As model contact lens materials, pHEMA hydrogels were prepared by mixing HEMA (3 g) and EGDMA (2 mol%) for 10 minutes followed by the addition of the photoinitiator Irgacure® 184 (0.5 wt%). After five minutes of constant stirring, the prepolymer mixture was injected into a custom-made UV-transparent acrylic mold equipped with a 0.5 mm thick spacer that was in turn placed into a 400 W UV chamber (λ=365 nm) (Cure Zone 2 Con-trol-cure, Chicago, IL, USA) for 10 minutes. Following an overnight post-curing period at room temperature, the hydrogels were removed from the mold and placed into Milli-Q water to swell and subsequently punched into discs of 6.35mm (1/4") diameter. The discs were then extracted in a 1:1 (v/v) methanol:water solution and in Milli-Q water only, to remove unreacted monomers. Finally, dry hydrogel discs were stored in room temperature.

3.2.5. Surface acrylation of pHEMA hydrogels

For the surface acrylation of pHEMA hydrogels (AcrpHEMA), acryloyl chloride (Acr Cl, 29 mM per disc) was added dropwise into an anhydrous dichloromethane solution (DCM) that contained the pHEMA discs, previously dried overnight under vacuum, and pyridine (0.1 equivalent to Acr Cl used) which was used as the catalyst. The reaction was carried out at room temperature for three hours under dark conditions. For the removal of unreacted chemicals and reaction by-products, the AcrpHEMA discs were initially rinsed in dimethylformamide (DMF) for five minutes (three rinses) and then washed with Milli-Q water (three cycles) for 24 hours. Afterwards, the discs were stored in foil covered glass vials containing 10ml phosphate buffer saline (PBS) (0.1M, pH 8) at room temperature until further use.

3.2.6. Surface grafting of HA-SH on AcrpHEMA surface (HA-pHEMA) – Phosphine-mediated Michael Addition Thiol-ene "click" reaction

In a 20 ml vial covered with foil, HA-SH 20 kDa (240 mg, 21.12 mM -SH) was initially dissolved into PBS (0.1M pH 8). Fully hydrated in PBS AcrpHEMA discs (6 discs per batch) were then submerged into the HA solution. TCEP (0.7 equivalent to -SH) was then added dropwise and the final pH set at 8.5-8.7 (NaOH 0.1M). The Michael addition thiol-acrylate reaction proceeded at room temperature for 36 hours under stirring (vortex mixer, 1100 rpm), ensuring that both surfaces of each hydrogel disc were equally exposed to the reaction mixture. All of the steps were done under N_2 in order to minimize free thiol oxidization. Since the presence of phosphates can deleteriously affect TCEP stability [74–76], fresh TCEP solution was made before every reaction. At the end of the reaction, the hydrogel discs were thoroughly washed for 24 hours with PBS (1M, pH 7.4) and Milli-Q water to ensure that only grafted HA remained on the surface. AcrpHEMA discs were also soaked in the HA-SH solution as above without the presence of TCEP for comparative studies. In all cases, control refers to the unmodified pHEMA discs unless otherwise specified.

3.2.7. Surface chemistry characterization

3.2.7.1. Fourier Transform Infrared Spectroscopy - Attenuated Total Reflectance (FTIR – ATR)

The surface chemistry of dehydrated pHEMA discs before and after surface acrylation and HA grafting was analyzed using FTIR-ATR mode (Vertex 70 FTIR spectrometer, Bruker Instruments, Billerica, MA, USA) equipped with a diamond ATR cell. The absorption spectra used for the characterization were measured at room temperature in the range of 600-4000 cm^{-1} (64 scans, 4 cm^{-1} resolution).

3.2.7.2. X-ray Photoelectron Spectroscopy (XPS)

Elemental composition analysis of the control and modified pHEMA discs under dry conditions was performed using PHI Quantera II XPS spectrometer (Physical Electronics (Phi), Chanhassen, MN, USA) equipped with an Al anode source for X-ray generation and a quartz crystal monochromator for focusing the generated X-rays. A monochromatic Al K-α X-ray (1486.7 eV) source was operated at 50W and 15kV. The operating pressure did not exceed 2.0 $x10^{-8}$ Torr. Elements present were identified from survey spectra. A pass energy of 280 eV was used to obtain survey spectra with the photoelectron take off angle set at 45°, while a dual beam charge compensation system was used for neutralization of all samples (beam diameter 200 μm). The instrument was calibrated using a sputter-cleaned piece of Ag, where the Ag $3d_{5/2}$ peak had a binding energy of 368.3 ± 0.1 eV and full width at half maximum for the Ag $3d_{5/2}$ peak was at least 0.52 eV. Data manipulation of low resolution spectra was performed using PHI MultiPak Version 9.4.0.7 software. At least two different spots per sample surface (n=4 discs per sample) were examined.

3.2.8. Contact angle measurements – captive bubble and sessile drop techniques

The surface wettability of the hydrogel surfaces was assessed by measuring the contact angle using the captive bubble and the sessile drop techniques (Optical Contact Angle Analyzer - OCA 35, Dataphysics, Germany). Briefly, the discs were fully swollen in Milli-Q water and the surface was blotted with a Kimwipe® to remove any excess water before measuring the contact angle. For

the captive bubble technique, the disc was initially immersed into a chamber filled with Milli-Q water and a 10 µl air bubble was placed on the surface of the disc. The Milli-Q water in the chamber was replaced before each set of samples was assessed. For the sessile drop technique, a 5 µl drop of Milli-Q water was placed on the surface of the disc. In both techniques, the drop was allowed to settle on the surface and the contact angle between the bubble/drop and the hydrogel surface was calculated with a video-based software (SCA 20, Dataphysics Instruments, Germany). To account for potential non-homogeneities on the surface of the samples, the contact angle of three different spots from both sides of each disc was measured (n=6 discs per sample). All measurements were made at ambient humidity and temperature.

3.2.9. In vitro protein deposition – lysozyme and human serum albumin

For the quantification of the physically adsorbed lysozyme (from chicken egg white) and human serum albumin (HSA) on the modified pHEMA surfaces, proteins were radiolabeled with $I^{125}Na$ using the iodine monochloride method (ICl) [56]. Following iodination, each labelled protein solution was passed through two columns packed with AG 1-X4 (Bio-Rad, Hercules, CA, USA) to remove unreacted iodide. The columns were then rinsed with PBS (pH 7.4) to collect the I^{125}-labeled protein. The hydrogel discs, swollen in PBS (pH 7.4) (n=6 per sample) were individually incubated into 250 µl of each I^{125}-labeled protein/PBS (pH 7.4) solution (1mg/ml, I^{125}-protein 5%) for 6 hours at room temperature and then washed three times with PBS (pH 7.4) (5-minute intervals) to remove loosely adherent protein. Each disc was then blotted dry with a Kimwipe® and placed in a counting vial (5 ml non-pyrogenic, polypropylene round-bottom tube). The radioactivity of the hydrogels was measured using a Gamma Counter (Perkin Elmer Wallac Wizard 1470 Automatic Gamma Counter, Wellesley, MA, USA). The radioactivity associated with the surfaces was converted into a protein amount using a standard calibration curve. The results are presented as the mass of protein sorbed per disc surface area.

3.2.10. Optical transparency

The optical transparency of the materials was determined by measuring the light transmittance (%) of fully hydrated hydrogel discs (n=6 discs per sample) immersed in 100 µl

Milli-Q water, using a UV–Vis spectrophotometer (Spectramax Plus 384, Molecular Devices, Corp, Sunnyvale, CA, USA) over the range of 400-750 nm.

3.2.11. Water content and dehydration study

The equilibrium water content (EWC) of the materials was calculated based on the equation below:

$$\text{EWC}\ (\%) = \frac{W_{wet} - W_{dry}}{W_{wet}} \cdot 100\% \qquad (3.1)$$

Briefly, dry hydrogel samples were weighed (W_{dry}) and then immersed in Milli-Q water to swell for 24 hours, under stirring at ambient temperature. The swollen discs were removed, blotted with a Kimwipe® to remove excess water and then weighed (W_{wet}) to determine the mass change (n=6 discs per sample).

In order to determine the water dehydration rate of the hydrogels, the mass change of blotted swollen discs (n=6 discs per sample) was measured over time using a closed chamber digital balance with an incorporated digital hygrometer (La Crosse Technology, WT-137U, RH=30% at 24°C). The water loss (%) used to express the dehydration rate was calculated based on the equation below:

$$water\ loss\ (\%) = \frac{W_{wet} - W_t}{W_{wet} - W_{dry}} \cdot 100\% \qquad (3.2)$$

where W_{wet} is the weight of fully swollen disc (t=0), W_t is the weight of the disc at each time point t (t=1-150 mins) and W_{dry} is the weight of the disc after being dried overnight in a 50°C oven. In between the measurements, discs were placed vertically on a holder in the chamber in order for both surfaces to be equally exposed for evaporation.

3.2.12. *In vitro c*ell viability - MTT Assay

To evaluate the impact of surface modification of pHEMA discs with HA on cell viability, the 3-(4,5-dimethylthiazol-2-yl)-2,5-diphenyltetrazolium bromide (MTT) cellular viability assay was performed. This assay provides an indication of metabolic activity of the cells through the conversion of soluble yellow chromogen MTT into the water-insoluble formazan salt via the dehydrogenases that are present in viable cells. Immortalized human corneal epithelial cells

(HCEC) (HCE-2 [50.B1] ATCCR CRL-11135™ from the American Type Culture Collection; Rockville, MD, USA) were cultured in Keratinocyte Serum Free Medium (KSFM) supplemented with human recombinant Epidermal Growth Factor 1-53 (EGF 1-53) and Bovine Pituitary Extract (BPE) in a humidified 5% CO_2 environment at 37°C. For the cytotoxicity assay, 1.5×10^4 HCEC in 100 µl culture medium per well were seeded in a flat bottom 96-well culture plate and incubated for 24 hours to ensure adhesion. At this time, the supernatant was gently removed and fresh KSFM was added (250 µl). Swollen discs were washed twice with sterilized PBS pH 7.4 for 6 hours prior to beginning the test. The nearly confluent HCEC were exposed to pHEMA, AcrpHEMA and HA-grafted pHEMA samples. The discs were placed vertically in the wells and incubated for 24 hours at 37°C in a cell culture incubator (n=4 discs per sample). At the end of the incubation period, the discs and the media were discarded, following a gentle wash of each well with PBS pH 7.4. For the MTT assay, 10 µl of the MTT solution (5 mg/ml in PBS pH 7.4) and 100 µl of PBS were added to each well, and the plate was covered with foil and placed in the incubator. After four hours of incubation, 85 µl of the above solution was replaced with 50 µl of DMSO for solubilization of the formazan crystals, and the absorbance of the resulting solution was measured at 540 nm using a UV–Vis spectrophotometer (Spectramax Plus 384, Molecular Devices, Corp, Sunnyvale, CA, USA). The reported cell viability (%) was expressed relative to that of cells grown in the absence of hydrogel discs (cell-only).

3.2.13. Statistical analysis

Statistical analyses were carried out using a single-factor analysis of variance (ANOVA) and Tukey HSD test in Statistica 10.0 (StatSoft Inc., Tulsa, OK, USA). In all cases, data are shown as mean ± standard deviation (SD), while a confidence interval of 95% (or $p<0.05$) was established for statistically significant results.

3.3. Results and Discussion

3.3.1. Synthesis and characterization of thiolated HA (HA-SH)

For the synthesis of HA-SH, a two-step reaction was chosen (Figure 3.1). Initially, the carboxyl group of HA was activated by EDC and HOBt coupling agents, following its reaction with the primary amine of cystamine dihydrochloride forming the intermediate product HA-SS-R.

The EDC/HOBt condensation reaction was set at a pH 6.8-7 because under mildly acidic conditions, the unstable intermediate *O*-acylisourea can rearrange irreversibly to the energetically more favoured *N*-acylurea [77,78] due to the absence of nucleophiles [79]. However, *N*-acylurea is unreactive towards the primary amines of cysteamine dihydrochloride, reducing thus the efficiency of the amidation reaction. In addition, removal of the stable N-acylurea is extremely difficult as it is covalently attached the backbone of HA [80]. Following, TCEP was used for the cleavage of the disulfide bond of the intermediate HA (HA-SS-R) product to generate HA with free thiols (HA-SH), since it is suggested to be a stronger reducing agent than 1,4-dithiothreitol (DTT) [81] due to the presence of phosphine which is more nucleophilic than the DTT thiols [82]. Compared to DTT, TCEP is a faster and stronger reducing agent over a wider range of pH (1.5 – 8.5) and more stable against oxygen [76], facilitating its use in many biochemical applications. The pH of the dialysate was maintained at around 3.5 to avoid HA degradation which occurs at lower pH as well as oxidation of the thiol groups that occurs at basic pH. The yield of this two-step reaction was 90%.

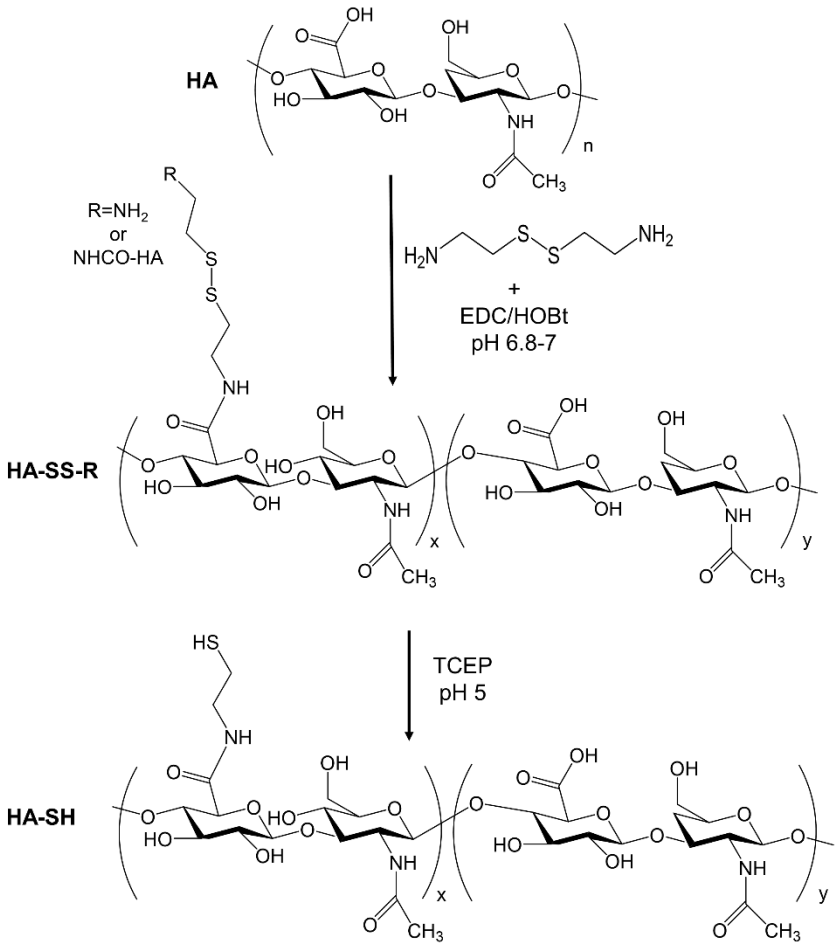

Figure 3.1: Schematic of synthesis of thiolated-HA (HA-SH).

The structures of HA-SS-R and HA-SH were confirmed by ^{1}HNMR (Figure 3.2). The peak at 2.01 ppm (δ_1) was attributed to the N-acetyl glycosamine group of HA whereas the peaks from 3.35 to 3.9 ppm corresponded to the methine groups on the six-membered rings of HA backbone (Figure 3.2(a)). Compared to the spectrum of unmodified HA, the new peaks at 3 and 3.18 ppm (δ_{2+3}) corresponded to the side chain methylene groups (C**H**$_2$C**H**$_2$NH) (Figure 3.1 (b)), while the appearance of the two triplets at 2.9-2.7 ppm (δ_{4+5}) further confirmed successful linking of thiol groups on HA-SH (C**H**$_2$C**H**$_2$S**H)** (Figure 3.2 (c)).

Following, Raman spectroscopy is a common method for the detection and analysis of free thiol groups [83]. The S-H stretching vibration is located between 2535-2600 cm^{-1} and gives a strong signal in Raman spectra [84]. Figure 3 shows a clear peak, similar to that found by Dhanasingh et al. [85], at 2576 cm^{-1} which was attributed to the free thiols of the HA-SH after

TCEP reduction further suggesting successful reaction (Figure 3.3). Using Ellman's method, the HA-SH synthesized herein for the modification of the model pHEMA hydrogels was determined to have a free thiol content of 352 ± 3.93 nmol SH/mg HA, corresponding to a 14.1 ± 0.15 free thiols per 100 repeat units of HA. No free thiol content was detected in the control and intermediate HA-SS-R product. The low degree of HA thiolation was thought to be favourable for the modification of the surface of pHEMA discs, as lower degree of HA thiolation would lead to fewer anchoring sites per HA chain on the AcrpHEMA surface resulting in a grafted HA layer with a more mobile and flexible structure. As well, a low degree of HA thiolation means fewer basic thiol groups, allowing HA to retain its hydrophilic anionic character through the presence of the sufficient carboxyl groups, a significant parameter for the desired surface properties. It was also assumed that the presence of a low thiol content should not negatively impact the bioactivity and toxicity of HA [83,86].

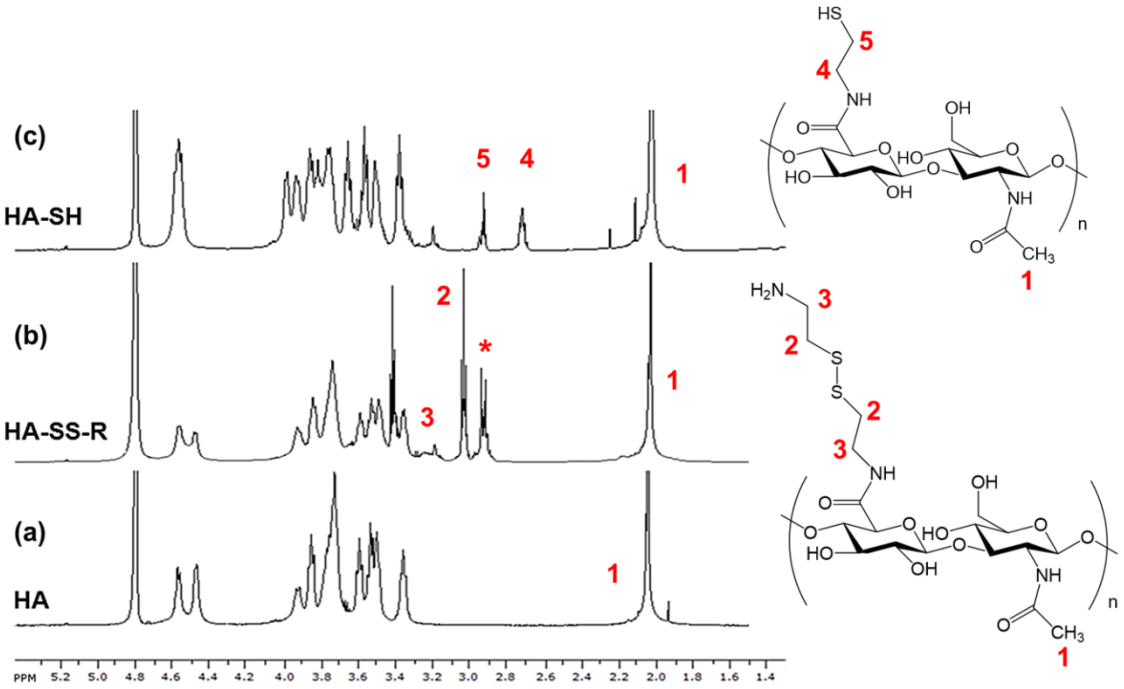

Figure 3.2: Representative ^{1}HNMR spectra of (a) unmodified HA (20 kDa), (b) HA-SS-R and (c) HA-SH. Chemical shift impurities from 1-ethyl-3-(3-dimethylaminopropyl) urea (EDU) in the course of amide coupling reaction are represented with the symbol *.

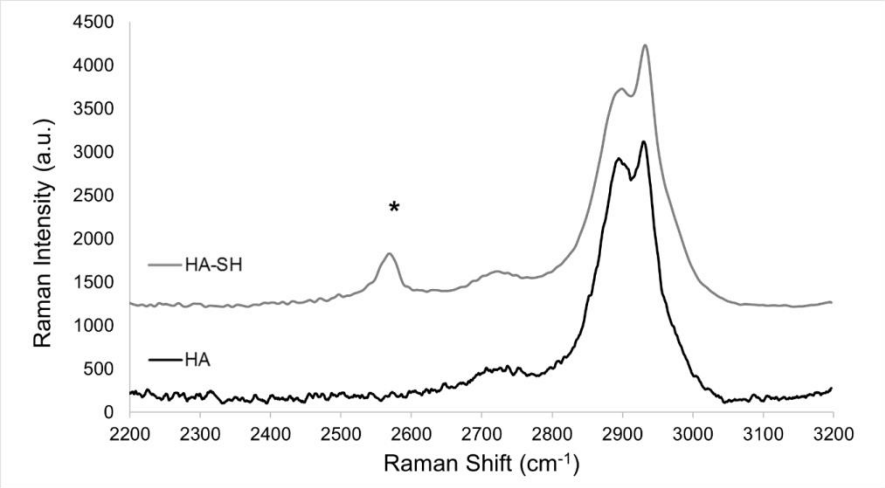

Figure 3. 3: Raman spectrum analysis of unmodified HA and thiolated-HA (HA-SH).

3.3.2. Synthesis and surface chemistry characterization of AcrpHEMA grafted with thiolated-HA (HA-SH)

The initial step for the attachment of HA on the model pHEMA contact lenses using thiol-based "click" chemistry involved the esterification of the hydroxyl (-OH) groups of pHEMA discs with Acr Cl for the introduction of acrylate groups (AcrpHEMA) (Figure 3.4 (b)). Acrylates have been shown to react considerably faster than other unsaturated esters and were therefore chosen as standard conjugated unsaturated partners [87,88]. For the acrylation reaction, anhydrous DCM was chosen as the organic solvent since pHEMA discs did not swell in this solvent (data not shown), while Pyr was selected as the nucleophilic catalyst to combine with the liberated HCl. Optimization of the Acr Cl and Pyr concentration and ratio as well as time of reaction was based on the impact of these parameters on the water content and optical transparency of the hydrogel discs. Subsequently, HA-SH was grafted to the surface of AcrpHEMA hydrogels via TCEP-initiated Michael addition thiol-acrylate reaction. The expected mechanism of this reaction is the addition of the nucleophilic TCEP to the electron-deficient alkene of the acrylate group (intermediate enolate based) which in turn is responsible for the deprotonation of the thiol of HA-SH (thiolate anion, $HA\text{-}S^-$), followed by the hydrothiolation of the double carbon bond creating the final thioether linkage between HA and pHEMA surface [70] (Figure 3.4 (c)).

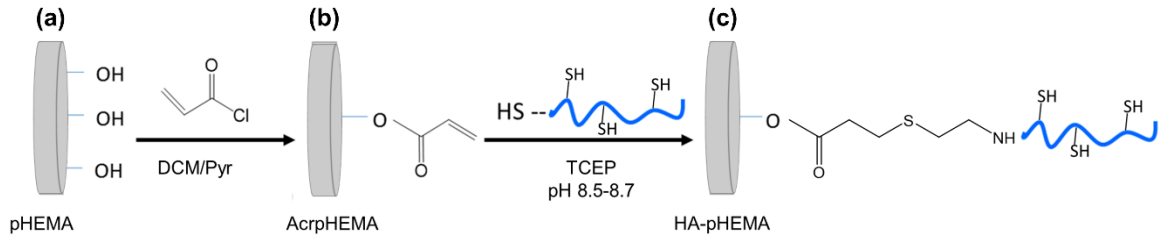

Figure 3.4: Schematic illustration of the synthesis of surface grafted HA-pHEMA hydrogel *via* TCEP-mediated thiol-acrylate "click" chemistry.

The chemistry of the surfaces was initially determined by FTIR-ATR. The decrease in the broad absorption band at approximately 3405 cm^{-1} corresponding to the -OH stretching vibration, in combination with the appearance of a new peak at 1635 cm^{-1} attributed to the bending vibrations of C=C bonds, suggested successful surface acrylation of pHEMA surfaces (Figure 3.5 (b)). For the HA-modified surfaces, the FTIR-ATR spectra did not show the expected characteristic peaks of HA (Figure 3.5 (c)). Since the surface grafted layer is expected to have a thickness on the order of several tens of nanometers, XPS was therefore used to confirm modification as the sampling depth at <10 nm is much smaller than FTIR-ATR sampling depth.

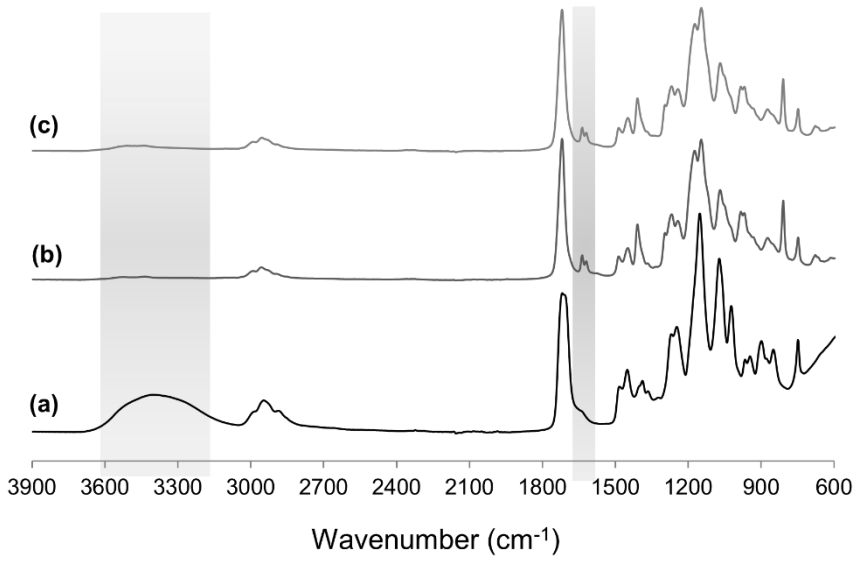

Figure 3.5: FTIR-ATR absorption spectra of (a) unmodified pHEMA, (b) AcrpHEMA and (c) HA-pHEMA surfaces (n=4).

Low resolution XPS spectra provided quantitative elemental compositions of the surface of the hydrogels. The C (1s), O (1s), N (1s) and S (2p) signals were detected, as anticipated. The surface composition is reported in terms of percent atomic composition in Table 3.1. The ubiquitous contaminant, Si (2p), was thought to originate from the silicone oil in the syringes used for the pHEMA polymerization and surface acrylation reactions. As the pHEMA hydrogel prior to the modification steps did not present nitrogen (N) and sulfur (S) on its structure, the presence of these two elements was used to confirm and monitor the amount of HA tethered to the surfaces. Based on the results, the percentage of N (1s) on the AcrpHEMA samples was very low and within the experimental error of technique, suggesting that any unreacted Pyr was successfully removed during the first washing step. Compared to pHEMA and AcrpHEMA discs, the N (1s) and S (2p) signals were significantly increased on the HA-grafted pHEMA discs, suggesting successful HA covalent attachment via TCEP-catalyzed thiol-ene reaction on the AcrpHEMA surfaces. Additional proof of successful HA grafting is the decrease observed in the Si (2p) signal on the HA-grafted pHEMA surfaces. Finally, no traces of phosphorus were detected on the surface of HA-grafted pHEMA surfaces, indicating that the catalytic amount of TCEP used was adequate for the reaction and there were no side reactions as has been previously observed [70].

Table 3.1: Atomic composition (%) from low resolution XPS spectra of the surface of pHEMA, AcrpHEMA and HA-grafted pHEMA hydrogel discs (n=4).

sample	C (1s)	N (1s)	O (1s)	S (2p)	Si (2p)
pHEMA	72.9 ± 3.8	0	25.9 ± 3.8	0	1.2 ± 0.3
AcrpHEMA	67.8 ± 1.2	0.2 ± 0.1	28.7 ± 1.0	0	3.1 ± 0.6
HA-pHEMA	70.8 ± 1.9	1.8 ± 0.4	24.6 ± 1.4	0.6 ± 0.2	0.9 ± 0.2

TCEP-mediated Michael addition thiol-acrylate chemistry has been used successfully for polymer–biomolecule conjugation and surface immobilization reactions [66,88–91]. This type of thiol-Michael addition chemistry, under non-demanding conditions (i.e. no heat or light required) with very small amounts of catalyst, enables the rapid, modular and bio-orthogonal addition of thiols to electron-deficient vinyl groups [64,66]. Previously, surface modification through TCEP-catalyzed thiol-Michael addition allowed for quantitative substrate modification in a relatively short reaction time [72], with an *in situ* linear adsorption profile [66,88,89]. The protocol used for

the HA surface grafting reaction was carefully optimized to minimize the impact of TCEP on the optical transparency of the modified discs and to minimize the potential formation of side products that could affect the cytocompatibility of the materials. In addition, pH plays a significant role in TCEP-initiated thiol addition reactions. Li et al. found that at acidic pH, by-products can be also formed [70]; hence the pH of the reaction was set above 8 to favour the creation of the thiolate anion ($R\text{-}S^-$), allowing for a higher degree of grafting. The dual role of TCEP in this study, for the reduction of thiols and as a conjugation catalyst, could prove useful for minimizing the steps for the development of HA-modified contact lenses, allowing potentially for a one-pot synthesis as has been previously shown for thiol-ene reactions [66,72].

3.3.3. Surface wettability - contact angle measurements

The *in vitro* surface wettability of a contact lens is thought to be somewhat predictive of *in vivo* behavior [92]. Surface wettability is an important parameter for the design of comfortable contact lenses, since more wettable contact lenses allow for improved tear film stability which in turn leads to increased surface lubrication of the lens-ocular surface biointerface, permitting adequate on-eye movement. Previous studies have found a correlation between reduction in comfort and surface wettability over time [93,94]. In this study, the surface wettability of the HA-modified pHEMA hydrogels was assessed by measuring contact angles using the captive bubble and sessile drop techniques. According to Maldonaldo – Codina et al. [95], the captive bubble technique can be used to measure the receding contact angle, an indication of the tear film stability on a fully hydrated lens surface during blinks, while the sessile drop technique measures the advancing angle which is presumably indicative of the ease with which the eyelids reform the tear film over a fully or partially dehydrated lens surface. Hence, these two techniques are of equal importance even though they measure two different types of contact angle. For both techniques, lower contact angles suggest improved surface wettability.

According to Figure 3.6, the contact angle of AcrpHEMA hydrogels was higher than that of the pristine pHEMA sample ($p<0.01$), as expected, due to substitution of the hydroxyl groups of HEMA with the less hydrophilic acrylate groups. Upon HA immobilization on the surface of AcrpHEMA, a significant (>40%) decrease in the contact angle was observed compared to the pristine sample (captive bubble: $p<0.0005$ and sessile drop: $p<0.0002$). The hysteresis, defined as

the difference between the advancing and the receding contact angle, was calculated as the difference in the contact angles measured using the two techniques. The hystereses of the pHEMA control, AcrpHEMA and HA-grafted pHEMA samples were 37.5 ± 1.8^{o}, 45.1 ± 2.6^{o} and 14.5 ± 1.3^{o} respectively. The decrease in the contact angles for HA-grafted pHEMA discs, despite the low degree of HA thiolation, suggests the formation of more wettable surfaces due to the hydrophilic nature of the HA polysaccharide. The hysteresis observed for the HA-grafted pHEMA sample was 60% lower than that seen with pristine pHEMA ($p<0.0002$), indicating the presence of rigid HA polymer chains with decreased surface roughness and heterogeneity [92]. Decreasing hysteresis is in fact one of the primary goals in contact lens research and development [96,97]. Additionally, the hysteresis between the sessile drop and advancing water contact angles has been suggested as a potential predictor of the clinical performance of the contact lens [95]. Holy et al. [98] attributed the relative large hysteresis of pHEMA hydrogels to the reorientation of the mobile surface polymer side chains and segments depending on the nature of the adjacent phase. Therefore, the improvement observed in the surface wettability of modified discs is consistent with the covalent attachment of the hydrophilic HA on the pHEMA surfaces.

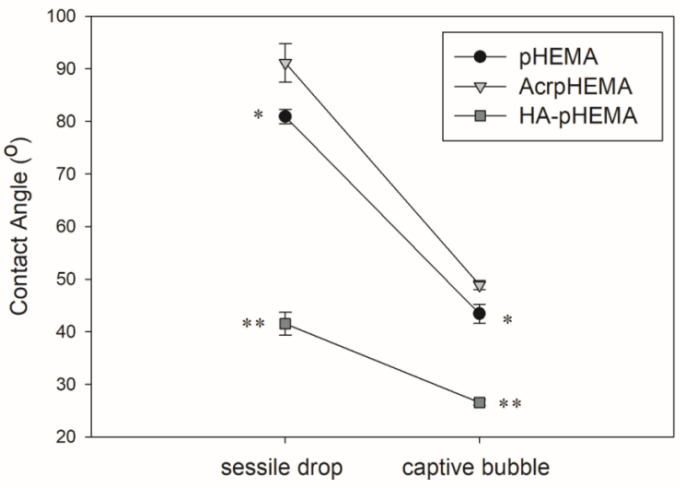

Figure 3.6: Static water contact angle (±SD) of unmodified pHEMA, AcrpHEMA and HA-pHEMA hydrogels (n=6) assessed by captive bubble and sessile drop techniques (*$p<0.01$ and **$p<0.0002$ compared to pristine pHEMA).

3.3.4. Protein antifouling properties - *in vitro* protein deposition

To examine the potential antifouling ability of HA-grafted layer on pHEMA surfaces, the amount of I^{125} lysozyme and human serum albumin (HSA) deposited on the modified surfaces was determined. Lysozyme and albumin were chosen as model proteins since they are two of the major protein components of tear film and are found in abundance on worn contact lenses [99], especially on conventional pHEMA based contact lenses [100]. Under physiological conditions, lysozyme (MW 14 kDa, pI 11) bears a net positive charge in tear fluid, HSA is a bigger protein (MW 66 kDa, pI 4.7) with an overall net negative charge, while HA is negatively charged due to the presence of the carboxyl groups (pKa 3-4). In addition to being associated with reduced comfort, protein deposition and denaturation can lead to immunological responses such as contact lens-induced papillary conjunctivitis [101,102], acute red eye [103] or even bacterial adhesion [104–106]. An ideal contact lens material should allow proteins to be loosely bound on the surface in their native state, creating an environment similar to that found in the absence of the contact lens, which would also allow proteins to be readily removed when exposed to contact lens care solutions [9].

Protein deposition can occur by both nonspecific adsorption and absorption in hydrogel materials, such as contact lenses. For the AcrpHEMA surface, lysozyme and HSA deposition (1.5 ± 0.22 and 0.22 ± 0.02 μg/cm^2 respectively) was significantly higher than on the pristine pHEMA surfaces (0.92 ± 0.06 and 0.13 ± 0.01 μg/cm^2 respectively) ($p<0.0002$) (Figure 3.7). This increase was attributed to the lower than the control hydrogels surface wettability of the intermediate AcrpHEMA samples. Contrary, the amount of both lysozyme (0.18 ± 0.02 μg/cm^2) and HSA (0.09 ± 0.01 μg/cm^2) present on HA-grafted pHEMA surfaces was significantly decreased ($p<0.0007$), leading to an 80% and 30% reduction in surface density of lysozyme and HSA respectively compared to unmodified pHEMA samples. The HA-grafted pHEMA hydrogel materials exhibited antifouling characteristics similar to those previously observed by our group [46,51,57,107], demonstrating that the thiol-based immobilization method did not alter the HA bioactivity. In addition, the amount of lysozyme deposited on all hydrogel materials was found to the consistently higher than the respective amount of HSA ($p<0.0002$), presumably due to the absorption of the smaller lysozyme into the grafted HA layer and the matrix of pHEMA hydrogels; and also due to the weaker interactions of bulkier HSA with the substrates [13]. The HA-modified pHEMA surfaces were less resistant to nonspecific HSA deposition than to lysozyme deposition, despite

the electrostatic repulsion expected between the negatively charged HSA and HA layer. This could be due to differences in the conformational stability of the proteins examined since proteins with low conformational stability, such as HSA, tend to adsorb on all surfaces independent of electrostatic interactions [13,108].

Interestingly, the HA-grafted layer using thiol-ene "click" chemistry exhibited superior antifouling properties, especially against lysozyme deposition, when compared to previously developed HA-grafted pHEMA surfaces via aldehyde/hydrazide chemistry [61], despite the significantly smaller MW of HA used. In addition to surface chemistry, parameters such as surface grafting density, layer thickness and chain conformation play a key role in achieving protein repellent properties [109].Typically, increasing the MW of the surface grafted layers and thus its thickness is expected to lead to improved antifouling characteristics, when grafting density is the same or similar [110,111]. Therefore, it can be speculated that surface immobilization of HA via thiol-ene chemistry resulted in greater grafting density than what was observed with the aldehyde-hydrazide chemistry, although the degree of HA functionalization was significantly lower (DS for HA-SH 14% vs HA-Hzd 52%). This could be also supported by the slightly higher N (1s) (%) (XPS results) of thiol-ene grafted HA-pHEMA surfaces, taking into consideration the difference in the MW (20 kDa vs 300 kDa) as well as the type and the degree of HA modification.

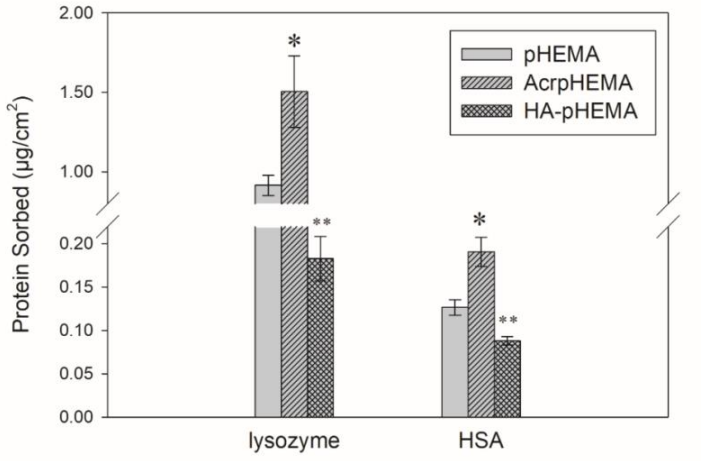

Figure 3.7: The amount (±SD) of lysozyme and albumin (HSA) deposited on the surface of unmodified pHEMA, AcrpHEMA and HA-pHEMA hydrogel discs (n=6) (*$p<0.0002$, **$p<0.0007$ compared to pristine pHEMA).

3.3.5. Optical transparency

The optical transparency is an important parameter that needs to be considered for the design of contact lens-based applications. As shown in Figure 3.8, the optical acuity of the intermediate AcrpHEMA and HA-grafted pHEMA materials was slightly decreased (2% for both cases) but remained within an acceptable range of transparency for contact lens applications (> 92%), suggesting that the grafting of HA to the pHEMA surfaces did not alter significantly the optical properties of the materials. Also, it should be noted that these materials have a thickness of 0.5 mm which is approximately 5 times higher than that of the commercial contact lenses. As a result, it is assumed that the impact of the HA layer would be even less in a material with thinner dimensions, and thus would not be of any clinical significance.

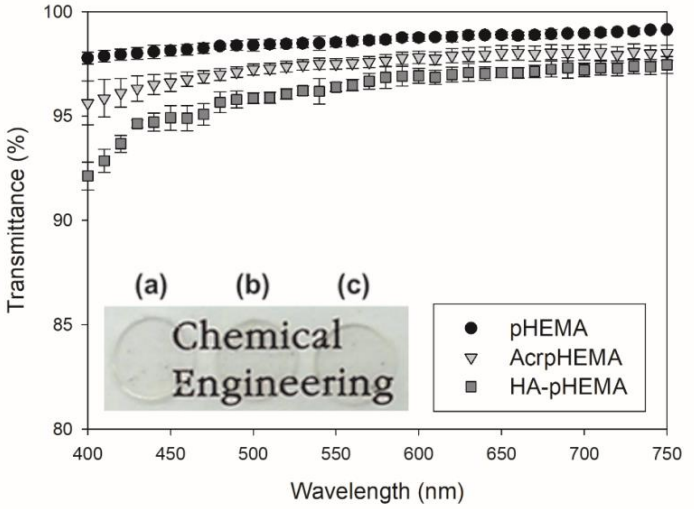

Figure 3.8: The transmittance spectra (±SD) and a photograph of the (a) unmodified pHEMA, (b) AcrpHEMA and (c) HA-pHEMA hydrogel discs (n=6).

3.3.6. Swellability and dehydration rate

For conventional contact lenses, the water content is a crucial determining factor for oxygen permeability. The impact of the HA-grafted layer on the swellability of the hydrogel materials was determined by calculating the equilibrium water content (EWC) using equation 3.1. The intermediate esterification reaction for the surface acrylation (AcrpHEMA) well as the thiol-ene reaction for the covalent immobilization reaction of HA on the surface of the pHEMA hydrogels

(HA-pHEMA) did not cause any changes in the water content of the materials (p=1) (Table 3.2). The equilibrium water content of the hydrogels remained within an acceptable range for contact lens wear.

Table 3.2: Equilibrium water content (EWC) (%) of the pHEMA control, AcrpHEMA and HA-grafted pHEMA hydrogel discs (n=6)**.**

sample	**EWC (%)**
pHEMA	34.1 ± 1.3
AcrpHEMA	32.7± 0.5
HA-pHEMA	32.5 ± 0.9

Moreover, the dehydration rate which was expressed through the water loss (%) from equation 3.2 using the gravimetric method was also assessed. Based on the water loss profiles depicted in Figure 3.9, surface grafting of the hydrophilic HA on the surface of pHEMA hydrogels significantly delayed the water evaporation, compared to the unmodified pHEMA samples ($p<0.05$). The hygroscopic nature of HA apart from improving the surface wettability of the hydrogel discs, was also able to control dehydration rate by prolonging water retention when compared to pHEMA control samples. This may lead to a higher degree of comfort in contact lens applications since the surface dehydration of contact lenses has been correlated with the feeling of ocular dryness during contact lens wear [4,5]. Parameters such as changes in temperature and humidity of the closed chamber during measurements, the sensitivity limit of the scale used, the thickness of the samples as well as the different amounts of water absorbed may potentially affect the dehydration profile. Therefore, the results herein should be used only for comparison of the unmodified and modified surfaces. These results are in agreement with previous findings when HA used in the formation of chitosan/HA multilayer coating that led to conventional contact lenses with good moisture retention properties [112].

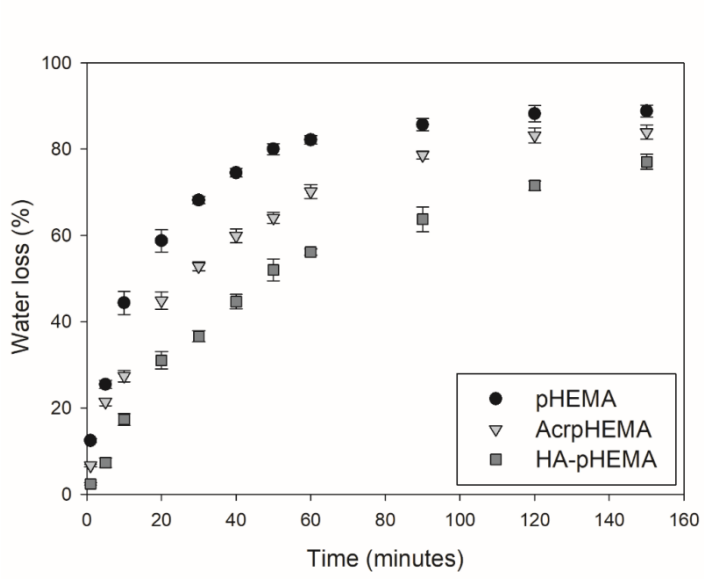

Figure 3.9: The dehydration profile expressed as water loss (%) (±SD) from the unmodified pHEMA, AcrpHEMA and HA-pHEMA hydrogels was calculated over time in a closed cha**m**ber (T=24°C, RH=30%) (n=6).

3.3.7. Cytotoxicity Study

The cytotoxicity of the materials was assessed using an MTT assay with human corneal epithelial cells. Immortalized HCEC, such as those used in this study, have been shown to be adequate as an *in vitro* model of human ocular surface in toxicity and inflammation studies for front-of-the-eye biomaterial applications, such as contact lenses [113,114]. As shown in Figure 3.10, the MTT assay did not show any statistically significant difference ($p>0.05$) in HCEC viability with exposure to AcrpHEMA and HA-grafted pHEMA hydrogel discs for 24 hours, when compared to control pHEMA discs, suggesting that the washing steps upon surface acrylation and thiol-ene reaction successfully removed any unreacted chemical components and by-products. Consistent with the current results, previous studies showed that materials involving thiolated HA (HA-SH) and its derivatives or TCEP mediated thiol-ene reactions exhibited little or no cytotoxic effects *in vitro* [71,73,115] and *in vivo* [72,116–119]. Hence, the modified materials are considered to exhibit acceptable compatibility to HCEC.

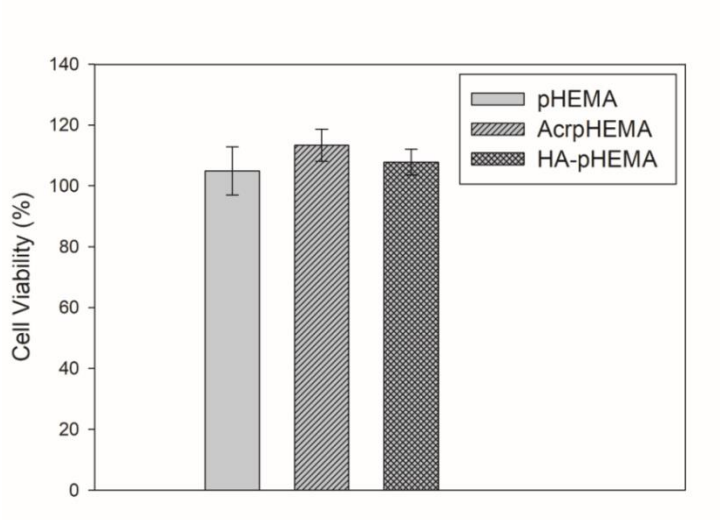

Figure 3.10: Cell viability (%) (±SD) of the HCEC upon incubation with unmodified pHEMA, AcrpHEMA and HA-pHEMA discs (n= 4) for 24 hours, in respect to control (cell-only).

3.4. Conclusions

In this study, TCEP-mediated Michael addition thiol-ene "click" chemistry was used to covalently attach thiolated HA (HA-SH) to the surface of acrylated pHEMA hydrogels. FTIR-ATR and XPS confirmed the intermediate surface acrylation and HA immobilization on the pHEMA surfaces. The HA-grafted pHEMA surfaces were characterized by significantly improved wettability, resistance to protein deposition and water retentive properties, while remaining optically transparent and showing no cytotoxic effects. Therefore, these novel surface-modified model contact lens materials with controlled interfacial properties could allow for enhanced compatibility between the lens and the ocular environment under physiological conditions; and ultimately could alleviate contact lens induced dryness and discomfort during wear.

3.5. Acknowledgements

The authors would also like to thank Danielle Covelli (Biointerfaces Institute, McMaster University) for her help acquiring the XPS spectra and Megan Dodd for her help with the cytotoxicity assay.

3.6. Funding

This work was funded by Natural Sciences and Engineering Research Council (NSERC) of Canada; and the 20/20 NSERC Ophthalmic Materials Research Network.

3.7. References

[1] J.J. Nichols, Contact lenses 2014., Contact Lens Spectr. 30 (2015) 22–27.

[2] G. Young, J. Veys, N. Pritchard, S. Coleman, A multi-centre study of lapsed contact lens wearers, Ophthalmic Physiol. Opt. 22 (2002) 516–527.

[3] K. Dumbleton, C.A. Woods, L.W. Jones, D. Fonn, The impact of contemporary contact lenses on contact lens discontinuation., Eye Contact Lens. 39 (2013) 93–99.

[4] D. Fonn, P. Situ, T. Simpson, Hydrogel lens dehydration and subjective comfort and dryness ratings in symptomatic and asymptomatic contact lens wearers., Optom. Vis. Sci. 76 (1999) 700–704.

[5] N. Efron, N.A. Brennan, A.S. Bruce, D.I. Duldig, N.J. Russo, Dehydration of hydrogel lenses under normal wearing conditions., CLAO J. 13 (1987) 152–156.

[6] D. Fonn, Targeting contact lens induced dryness and discomfort: what properties will make lenses more comfortable., Optom. Vis. Sci. 84 (2007) 279–285.

[7] P.L. Valint, D.M. Ammon, G.L. Grobe, J.A. McGee, In-Situ Surface Modification of Contact Lens Polymers, in: Surf. Modif. Polym. Biomater., Springer US, Boston, MA, 1996: pp. 21–26.

[8] C.D. Leahy, R.B. Mandell, S.T. Lin, Initial in vivo tear protein deposition on individual hydrogel contact lenses., Optom. Vis. Sci. 67 (1990) 504–511.

[9] D. Luensmann, L. Jones, Protein deposition on contact lenses: The past, the present, and the future, Contact Lens Anterior Eye. 35 (2012) 53–64.

[10] R.C. Peterson, J.S. Wolffsohn, J. Nick, L. Winterton, J. Lally, Clinical performance of daily disposable soft contact lenses using sustained release technology, Contact Lens Anterior Eye. 29 (2006) 127–134.

[11] N.J.J. Morgan PB, Woods C, Tranoudis IG, Helland M, Efron N, Knajian R, Grupcheva C, Jones D, Tan K, Pesinova A, Santodomingo J, Vodnyanszky E, Erdinest N, Hreinsson I H,

Montani G, Itoi M, Bendoriene J, van der Worp E, Hsiao J, Phillips G, González-Méijome J M, International contact lens prescribing in 2009, Contact Lens Spectr. 25 (2010) 30–53.

[12] O. Moradi, H. Modarress, M. Noroozi, Experimental study of albumin and lysozyme adsorption onto acrylic acid (AA) and 2-hydroxyethyl methacrylate (HEMA) surfaces, J. Colloid Interface Sci. 271 (2004) 16–19.

[13] M.S. Lord, M.H. Stenzel, A. Simmons, B.K. Milthorpe, The effect of charged groups on protein interactions with poly(HEMA) hydrogels, Biomaterials. 27 (2006) 567–575.

[14] P.C. Nicolson, J. Vogt, Soft contact lens polymers: an evolution., Biomaterials. 22 (2001) 3273–3283.

[15] L.C. Winterton, J.M. Lally, K.B. Sentell, L.L. Chapoy, The elution of poly (vinyl alcohol) from a contact lens: The realization of a time release moisturizing agent/artificial tear, J. Biomed. Mater. Res. Part B Appl. Biomater. 80B (2007) 424–432.

[16] C.J. White, C.R. Thomas, M.E. Byrne, Bringing comfort to the masses: A novel evaluation of comfort agent solution properties, Contact Lens Anterior Eye. 37 (2014) 81–91.

[17] L.C. Thai, A. Tomlinson, P.A. Simmons, In vitro and in vivo effects of a lubricant in a contact lens solution, Ophthalmic Physiol. Opt. 22 (2002) 319–329.

[18] C.J. White, M.K. Mcbride, K.M. Pate, A. Tieppo, M.E. Byrne, Extended release of high molecular weight hydroxypropyl methylcellulose from molecularly imprinted, extended wear silicone hydrogel contact lenses., Biomaterials. 32 (2011) 5698–56705.

[19] F. Yañez, A. Concheiro, C. Alvarez-Lorenzo, Macromolecule release and smoothness of semi-interpenetrating PVP–pHEMA networks for comfortable soft contact lenses, Eur. J. Pharm. Biopharm. 69 (2008) 1094–1103.

[20] I. Toki, M. Komatsu, Y. Shimizu, Y. Hara, Surface modification of contact lenses using adsorption of ethylene oxide branched copolymers, J. Appl. Polym. Sci. 127 (2013) 3657–3662.

[21] D. Bozukova, C. Pagnoulle, M.-C. De Pauw-Gillet, N. Ruth, R. Jérôme, C. Jérôme, Imparting Antifouling Properties of Poly(2-hydroxyethyl methacrylate) Hydrogels by Grafting Poly(oligoethylene glycol methyl ether acrylate), Langmuir. 24 (2008) 6649–6658.

[22] J. Wang, X. Li, Enhancing protein resistance of hydrogels based on poly(2-hydroxyethyl methacrylate) and poly(2-methacryloyloxyethyl phosphorylcholine) with interpenetrating

network structure, J. Appl. Polym. Sci. 121 (2011) 3347–3352.

[23] L.C. Bengani, G.W. Scheiffele, A. Chauhan, Incorporation of polymerizable surfactants in hydroxyethyl methacrylate lenses for improving wettability and lubricity, J. Colloid Interface Sci. 445 (2015) 60–68.

[24] N.J. Schwarz S., Effectiveness of lubricating daily disposable lenses with different additives, Optician. 231 (2006) 22–26.

[25] G. Young, R. Bowers, B. Hall, M. Port, Six month clinical evaluation of a biomimetic hydrogel contact lens., CLAO J. 23 (1997) 226–236.

[26] M.A. Lemp, B. Caffery, K. Lebow, R. Lembach, J. Park, G. Foulks, B. Hall, R. Bowers, S. McGarvey, G. Young, Omafilcon A (Proclear) soft contact lenses in a dry eye population., CLAO J. 25 (1999) 40–47.

[27] A. Engström-Laurent, Hyaluronan in joint disease, J. Intern. Med. 242 (1997) 57–60.

[28] S. Mori, M. Naito, S. Moriyama, Highly viscous sodium hyaluronate and joint lubrication., Int. Orthop. 26 (2002) 116–121.

[29] E.A. Balazs, G. Armand, Glycosaminoglycans and Proteoglycans of Ocular Tissues, in: Glycosaminoglycans Proteoglycans Physiol. Pathol. Process. Body Syst., S. Karger AG, Basel, 1982: pp. 480–499.

[30] K. Yoshida, Y. Nitatori, Y. Uchiyama, Localization of glycosaminoglycans and CD44 in the human lacrimal gland., Arch. Histol. Cytol. 59 (1996) 505–513.

[31] L. Lapcík L Jr and, L. Lapcík, S. De Smedt, J. Demeester, P. Chabrecek, Hyaluronan: Preparation, Structure, Properties, and Applications., Chem. Rev. 98 (1998) 2663–2684.

[32] L.E. Lerner, D.M. Schwartz, D.G. Hwang, E.L. Howes, R. Stern, Hyaluronan and CD44 in the Human Cornea and Limbal Conjunctiva, Exp. Eye Res. 67 (1998) 481–484.

[33] M.Y. Fukuda K, Miyamoto Y, Hyaluronic acid in tear fluid and its synthesis by corneal epithelial cells., Asia-Pacific J Ophthalmol. 40 (1998) 62–65.

[34] A. Davies, J. Gormally, E. Wyn-Jones, D.J. Wedlock, G.O. Phillips, A study of hydration of sodium hyaluronate from compressibility and high precision densitometric measurements, Int. J. Biol. Macromol. 4 (1982) 436–438.

[35] T. Nishida, M. Nakamura, H. Mishima, T. Otori, Hyaluronan stimulates corneal epithelial

migration., Exp. Eye Res. 53 (1991) 753–758.

[36] N. Volpi, Therapeutic Applications of Glycosaminoglycans, Curr. Med. Chem. 13 (2006) 1799–1810.

[37] J.M. Delmage, D.R. Powars, P.K. Jaynes, S.E. Allerton, The selective suppression of immunogenicity by hyaluronic acid., Ann. Clin. Lab. Sci. 16 (1986) 303–310.

[38] G. Kogan, L. Soltés, R. Stern, P. Gemeiner, Hyaluronic acid: a natural biopolymer with a broad range of biomedical and industrial applications., Biotechnol. Lett. 29 (2007) 17–25.

[39] M.J. Rah, A review of hyaluronan and its ophthalmic applications., Optometry. 82 (2011) 38–43.

[40] N. Volpi, J. Schiller, R. Stern, L. Soltés, Role, metabolism, chemical modifications and applications of hyaluronan., Curr. Med. Chem. 16 (2009) 1718–1745.

[41] J.R.E. Fraser, T.C. Laurent, U.B.G. Laurent, Hyaluronan: its nature, distribution, functions and turnover, J. Intern. Med. 242 (1997) 27–33.

[42] P.D. O'Brien, L.M.T. Collum, Dry eye: diagnosis and current treatment strategies., Curr. Allergy Asthma Rep. 4 (2004) 314–319.

[43] Szczotka-Flynn LB, Chemical properties of contact lens rewetters., Contact Lens Spectr. 21 (2006) 11–9.

[44] J.C. Stuart, J.G. Linn, Dilute sodium hyaluronate (Healon) in the treatment of ocular surface disorders., Ann. Ophthalmol. 17 (1985) 190–192.

[45] M.J. Doughty, S. Glavin, Efficacy of different dry eye treatments with artificial tears or ocular lubricants: a systematic review., Ophthalmic Physiol. Opt. 29 (2009) 573–583.

[46] X. Liu, R. Huang, R. Su, W. Qi, L. Wang, Z. He, Grafting hyaluronic acid onto gold surface to achieve low protein fouling in surface plasmon resonance biosensors., ACS Appl. Mater. Interfaces. 6 (2014) 13034–13042.

[47] M. Ombelli, L. Costello, C. Postle, V. Anantharaman, Q.C. Meng, R.J. Composto, D.M. Eckmann, Competitive protein adsorption on polysaccharide and hyaluronate modified surfaces., Biofouling. 27 (2011) 505–518.

[48] R. Huang, X. Liu, H. Ye, R. Su, W. Qi, L. Wang, Z. He, Conjugation of Hyaluronic Acid onto Surfaces via the Interfacial Polymerization of Dopamine to Prevent Protein

Adsorption, Langmuir. 31 (2015) 12061–12070.

[49] Y. Wang, L. Guo, L. Ren, S. Yin, J. Ge, Q. Gao, T. Luxbacher, S. Luo, A study on the performance of hyaluronic acid immobilized chitosan film., Biomed. Mater. 4 (2009) 1–7.

[50] X. Hu, K.-G. Neoh, Z. Shi, E.-T. Kang, C. Poh, W. Wang, An in vitro assessment of titanium functionalized with polysaccharides conjugated with vascular endothelial growth factor for enhanced osseointegration and inhibition of bacterial adhesion, Biomaterials. 31 (2010) 8854–8863.

[51] M. Morra, C. Cassineli, Non-fouling properties of polysaccharide-coated surfaces, J. Biomater. Sci. Polym. Ed. 10 (1999) 1107–1124.

[52] C.A. Scheuer, K.M. Fridman, V.L. Barniak, S.E. Burke, S. Venkatesh, Retention of conditioning agent hyaluronan on hydrogel contact lenses, Contact Lens Anterior Eye. 33 (2010) S2–S6.

[53] M. Ali, M.E. Byrne, Controlled release of high molecular weight hyaluronic Acid from molecularly imprinted hydrogel contact lenses., Pharm. Res. 26 (2009) 714–726.

[54] F.A. Maulvi, T.G. Soni, D.O. Shah, Extended release of hyaluronic acid from hydrogel contact lenses for dry eye syndrome., J. Biomater. Sci. Polym. Ed. 26 (2015) 1035–10350.

[55] M. Van Beek, L. Jones, H. Sheardown, Hyaluronic acid containing hydrogels for the reduction of protein adsorption., Biomaterials. 29 (2008) 780–789.

[56] A. Weeks, L.N. Subbaraman, L. Jones, H. Sheardown, The Competing Effects of Hyaluronic and Methacrylic Acid in Model Contact Lenses, J. Biomater. Sci. Polym. Ed. 23 (2012) 1021–1038.

[57] A. Weeks, D. Morrison, J.G. Alauzun, M. a Brook, L. Jones, H. Sheardown, Photocrosslinkable hyaluronic acid as an internal wetting agent in model conventional and silicone hydrogel contact lenses., J. Biomed. Mater. Res. A. 100 (2012) 1972–1982.

[58] H.-J. Kim, G.-C. Ryu, K.-S. Jeong, J. Jun, Hydrogel lenses functionalized with polysaccharide for reduction of protein adsorption, Macromol. Res. 23 (2015) 74–78.

[59] X.H. Hu, H.P. Tan, D. Li, M.Y. Gu, Surface functionalisation of contact lenses by CS/HA multilayer film to improve its properties and deliver drugs, Mater. Technol. 29 (2014) 8–13.

[60] A. Singh, P. Li, V. Beachley, P. McDonnell, J.H. Elisseeff, A hyaluronic acid-binding contact lens with enhanced water retention, Contact Lens Anterior Eye. 38 (2015) 79–84.

[61] X. Deng, M. Korogiannaki, B. Rastegari, J. Zhang, M. Chen, Q. Fu, H. Sheardown, C.D.M. Filipe, T. Hoare, "Click" Chemistry-Tethered Hyaluronic Acid-Based Contact Lens Coatings Improve Lens Wettability and Lower Protein Adsorption, ACS Appl. Mater. Interfaces. 8 (2016) 22064–22073.

[62] P.J. O'Brien, A.G. Siraki, N. Shangari, Aldehyde sources, metabolism, molecular toxicity mechanisms, and possible effects on human health., Crit. Rev. Toxicol. 35 (2005) 609–62.

[63] A.B. Lowe, Thiol-ene "click" reactions and recent applications in polymer and materials synthesis, Polym. Chem. 1 (2010) 17–36.

[64] J.W. Chan, C.E. Hoyle, A.B. Lowe, M. Bowman, Nucleophile-initiated thiol-Michael reactions: Effect of organocatalyst, thiol, and ene, Macromolecules. 43 (2010) 6381–6388.

[65] C.E. Hoyle, C.N. Bowman, Thiol-Ene Click Chemistry, Angew. Chemie Int. Ed. 49 (2010) 1540–1573.

[66] S. Kumari, B. Malvi, A.K. Ganai, V.K. Pillai, S. Sen Gupta, Functionalization of SBA-15 Mesoporous Materials using "Thiol–Ene Click" Michael Addition Reaction, J. Phys. Chem. C. 115 (2011) 17774–17781.

[67] M. Liu, B.H. Tan, R.P. Burford, A.B. Lowe, Nucleophilic thiol-Michael chemistry and hyperbranched (co)polymers: synthesis and ring-opening metathesis (co)polymerization of novel difunctional exo-7-oxanorbornenes with in situ inimer formation, Polym. Chem. 4 (2013) 3300.

[68] J.W. Chan, B. Yu, C.E. Hoyle, A.B. Lowe, The nucleophilic, phosphine-catalyzed thiol–ene click reaction and convergent star synthesis with RAFT-prepared homopolymers, Polymer (Guildf). 50 (2009) 3158–3168.

[69] J.W. Chan, H. Wei, H. Zhou, C.E. Hoyle, The effects of primary amine catalyzed thio-acrylate Michael reaction on the kinetics, mechanical and physical properties of thio-acrylate networks, Eur. Polym. J. 45 (2009) 2717–2725.

[70] G.-Z. Li, R.K. Randev, A.H. Soeriyadi, G. Rees, C. Boyer, Z. Tong, T.P. Davis, C.R. Becer, D.M. Haddleton, Investigation into thiol-(meth)acrylate Michael addition reactions using amine and phosphine catalysts, Polym. Chem. 1 (2010) 1196–1204.

[71] L. Wong, M. Kavallaris, V. Bulmus, Doxorubicin conjugated, crosslinked, PEGylated particles prepared via one-pot thiol-ene modification of a homopolymer scaffold: synthesis and in vitro evaluation, Polym. Chem. 2 (2011) 385–393.

[72] M.W. Jones, G. Mantovani, S.M. Ryan, X. Wang, D.J. Brayden, D.M. Haddleton, Phosphine-mediated one-pot thiol–ene "click" approach to polymer–protein conjugates, Chem. Commun. 2 (2009) 5272–5274.

[73] H. Wang, H. Sun, H. Wei, P. Xi, S. Nie, Q. Ren, Biocompatible hyaluronic acid polymer-coated quantum dots for CD44+ cancer cell-targeted imaging, J. Nanoparticle Res. 16 (2014) 2621.

[74] D.O. Lambeth, G.R. Ericson, M.A. Yorek, P.D. Ray, Implications for in vitro studies of the autoxidation of ferrous ion and the iron-catalyzed autoxidation of dithiothreitol., Biochim. Biophys. Acta. 719 (1982) 501–508.

[75] J.A. Burns, J.C. Butler, J. Moran, G.M. Whitesides, Selective reduction of disulfides by tris(2-carboxyethyl)phosphine, J. Org. Chem. 56 (1991) 2648–2650.

[76] J.C. Han, G.Y. Han, A procedure for quantitative determination of tris(2-carboxyethyl)phosphine, an odorless reducing agent more stable and effective than dithiothreitol, Anal. Biochem. 220 (1994) 5–10.

[77] X.Z. Shu, Y. Liu, Y. Luo, M.C. Roberts, G.D. Prestwich, Disulfide Cross-Linked Hyaluronan Hydrogels, Biomacromolecules. 3 (2002) 1304–1311.

[78] F. Kurzer, K. Douraghi-Zadeh, Advances in the Chemistry of Carbodiimides, Chem. Rev. 67 (1967) 107–152.

[79] P. Bulpitt, D. Aeschlimann, New strategy for chemical modification of hyaluronic acid: preparation of functionalized derivatives and their use in the formation of novel biocompatible hydrogels., J. Biomed. Mater. Res. 47 (1999) 152–169.

[80] S. Santhanam, J. Liang, R. Baid, N. Ravi, Investigating thiol-modification on hyaluronan via carbodiimide chemistry using response surface methodology., J. Biomed. Mater. Res. A. 103 (2015) 2300–2308.

[81] D.J. Cline, S.E. Redding, S.G. Brohawn, J.N. Psathas, J.P. Schneider, C. Thorpe, New water-soluble phosphines as reductants of peptide and protein disulfide bonds: reactivity and membrane permeability., Biochemistry. 43 (2004) 15195–15203.

[82] P.C. Jocelyn, Biochemistry of the SH group: the occurrence, chemical properties, metabolism and biological function of thiols and disulphides., 2nd ed., Academic Press, London, 1972.

[83] A. Köwitsch, M. Jurado Abreu, A. Chhalotre, M. Hielscher, S. Fischer, K. Mäder, T. Groth, Synthesis of thiolated glycosaminoglycans and grafting to solid surfaces., Carbohydr. Polym. 114 (2014) 344–351.

[84] G. Socrates, Infrared and raman characteristic group frequencies : tables and charts., 3rd ed., John Wiley & Sons, Chichester ; New York, 2001.

[85] A. Dhanasingh, J. Salber, M. Moeller, J. Groll, Tailored hyaluronic acid hydrogels through hydrophilic prepolymer cross-linkers, Soft Matter. 6 (2010) 618–629.

[86] S. Ouasti, R. Donno, F. Cellesi, M.J. Sherratt, G. Terenghi, N. Tirelli, Network connectivity, mechanical properties and cell adhesion for hyaluronic acid/PEG hydrogels., Biomaterials. 32 (2011) 6456–6470.

[87] M.P. Lutolf, N. Tirelli, S. Cerritelli, L. Cavalli, J.A. Hubbell, Systematic Modulation of Michael-Type Reactivity of Thiols through the Use of Charged Amino Acids, Bioconjugate Chem. 12 (2001) 1051–1056.

[88] S. Slavin, D.M. Haddleton, An investigation into thiol–ene surface chemistry of poly(ethylene glycol) acrylates, methacrylates and CCTP polymers via quartz crystal microbalance with dissipation monitoring (QCM-D), Soft Matter. 8 (2012) 10388.

[89] M. Heggli, N. Tirelli, A. Zisch, J.A. Hubbell, Michael-type addition as a tool for surface functionalization., Bioconjug. Chem. 14 (2003) 967–73.

[90] D.L. Elbert, A.B. Pratt, M.P. Lutolf, S. Halstenberg, J.A. Hubbell, Protein delivery from materials formed by self-selective conjugate addition reactions, J. Control. Release. 76 (2001) 11–25.

[91] B. Schyrr, S. Pasche, G. Voirin, C. Weder, Y.C. Simon, E.J. Foster, Biosensors Based on Porous Cellulose Nanocrystal–Poly(vinyl Alcohol) Scaffolds, ACS Appl. Mater. Interfaces. 6 (2014) 12674–12683.

[92] D. Campbell, S.M. Carnell, R.J. Eden, Applicability of Contact Angle Techniques Used in the Analysis of Contact Lenses, Part 1, Eye Contact Lens Sci. Clin. Pract. 39 (2013) 254–262.

[93] C. Cassinelli, M. Morra, A. Pavesio, D. Renier, Evaluation of interfacial properties of hyaluronan coated poly(methylmethacrylate) intraocular lenses., J. Biomater. Sci. Polym. Ed. 11 (2000) 961–977.

[94] M.C. Lin, T.F. Svitova, Contact lenses wettability in vitro: effect of surface-active ingredients., Optom. Vis. Sci. 87 (2010) 440–447.

[95] C. Maldonado-codina, P.B. Morgan, In vitro water wettability of silicone hydrogel contact lenses determined using the sessile drop and captive bubble techniques, J. Biomed. Mater. Res. Part A. 83A (2007) 496–502.

[96] L. Cheng, S.J. Muller, C.J. Radke, Wettability of silicone-hydrogel contact lenses in the presence of tear-film components., Curr. Eye Res. 28 (2004) 93–108.

[97] S. Tonge, L. Jones, S. Goodall, B. Tighe, The ex vivo wettability of soft contact lenses., Curr. Eye Res. 23 (2001) 51–59.

[98] F.J. Holly, M.F. Refojo, Wettability of hydrogels I. Poly(2-hydroxyethyl methacrylate), J. Biomed. Mater. Res. 9 (1975) 315–326.

[99] C. Baleriola-Lucas, M. Fukuda, M.D. Willcox, D.F. Sweeney, B.A. Holden, Fibronectin concentration in tears of contact lens wearers., Exp. Eye Res. 64 (1997) 37–43.

[100] S.L. McArthur, K.M. McLean, H.A.. St. John, H.J. Griesser, XPS and surface-MALDI-MS characterisation of worn HEMA-based contact lenses, Biomaterials. 22 (2001) 3295–3304.

[101] A.D. Porazinski, P.C. Donshik, Giant papillary conjunctivitis in frequent replacement contact lens wearers: a retrospective study., CLAO J. 25 (1999) 142–147.

[102] P.C. Donshik, Contact lens chemistry and giant papillary conjunctivitis., Eye Contact Lens. 29 (2003) S37-39-59, S192-194.

[103] M. Kotow, B.A. Holden, T. Grant, The value of regular replacement of low water content contact lenses for extended wear., J. Am. Optom. Assoc. 58 (1987) 461–464.

[104] S.I. Butrus, S.A. Klotz, Contact lens surface deposits increase the adhesion of Pseudomonas aeruginosa, Curr. Eye Res. 9 (1990) 717–724.

[105] R.L. Taylor, M.D.P. Willcox, T.J. Williams, J. Verran, Modulation of Bacterial Adhesion to Hydrogel Contact Lenses by Albumin, Optom. Vis. Sci. 75 (1998) 23–29.

[106] S.I. Butrus, S.A. Klotz, R.P. Misra, The Adherence of Pseudomonas aeruginosa to Soft

Contact Lenses, Ophthalmology. 94 (1987) 1310–1314.

[107] M. van Beek, A. Weeks, L. Jones, H. Sheardown, Immobilized hyaluronic acid containing model silicone hydrogels reduce protein adsorption., J. Biomater. Sci. Polym. Ed. 19 (2008) 1425–1436.

[108] Q. Garrett, R.C. Chatelier, H.J. Griesser, B.K. Milthorpe, Effect of charged groups on the adsorption and penetration of proteins onto and into carboxymethylated poly(HEMA) hydrogels., Biomaterials. 19 (1998) 2175–2186.

[109] S. Chen, L. Li, C. Zhao, J. Zheng, Surface hydration: Principles and applications toward low-fouling/nonfouling biomaterials, Polymer (Guildf). 51 (2010) 5283–5293.

[110] I. Szleifer, Protein adsorption on tethered polymer layers: effect of polymer chain architecture and composition, Phys. A Stat. Mech. Its Appl. 244 (1997) 370–388.

[111] A. Chen, D. Kozak, B.J. Battersby, M. Trau, Particle-by-particle quantification of protein adsorption onto poly(ethylene glycol) grafted surfaces, Biofouling. 24 (2008) 267–273.

[112] M. Kolasińska, P. Warszyński, The effect of nature of polyions and treatment after deposition on wetting characteristics of polyelectrolyte multilayers, Appl. Surf. Sci. 252 (2005) 759–765.

[113] J. Bednarz, M. Teifel, P. Friedl, K. Engelmann, Immortalization of human corneal endothelial cells using electroporation protocol optimized for human corneal endothelial and human retinal pigment epithelial cells, Acta Ophthalmol. Scand. 78 (2000) 130–136.

[114] E.A. Offord, N.A. Sharif, K. Macé, Y. Tromvoukis, E.A. Spillare, O. Avanti, W.E. Howe, A.M. Pfeifer, Immortalized human corneal epithelial cells for ocular toxicity and inflammation studies., Invest. Ophthalmol. Vis. Sci. 40 (1999) 1091–1101.

[115] J. Ding, R. He, G. Zhou, C. Tang, C. Yin, Multilayered mucoadhesive hydrogel films based on thiolated hyaluronic acid and polyvinylalcohol for insulin delivery., Acta Biomater. 8 (2012) 3643–3651.

[116] H. Li, Y. Liu, X.Z. Shu, S.D. Gray, G.D. Prestwich, Synthesis and biological evaluation of a cross-linked hyaluronan-mitomycin C hydrogel., Biomacromolecules. 5 (2004) 895–902.

[117] Y. He, G. Cheng, L. Xie, Y. Nie, B. He, Z. Gu, Polyethyleneimine/DNA polyplexes with reduction-sensitive hyaluronic acid derivatives shielding for targeted gene delivery, Biomaterials. 34 (2013) 1235–1245.

[118] B. Wirostko, B.K. Mann, D.L. Williams, G.D. Prestwich, Ophthalmic Uses of a Thiol-Modified Hyaluronan-Based Hydrogel., Adv. Wound Care. 3 (2014) 708–716.

[119] G. Yang, G.D. Prestwich, B.K. Mann, G. Yang, G.D. Prestwich, B.K. Mann, Thiolated Carboxymethyl-Hyaluronic-Acid-Based Biomaterials Enhance Wound Healing in Rats, Dogs, and Horses, ISRN Vet. Sci. 2011 (2011) 1–7.

Chapter 4

The impact of a hyaluronic acid-grafted layer on the surface properties of model silicone hydrogel contact lenses

Authors: Myrto Korogiannaki, Lyndon Jones, Heather Sheardown

Publication information:

This chapter has been submitted for peer-review (Manuscript ID: am-2018-09755d) and is reproduced/reprinted with permission from *ACS Applied materials & Interfaces.*

Abstract

The introduction of high oxygen transmissibility silicone hydrogel (SiHy) lenses ameliorated hypoxia-related complications, making them the most prescribed type of contact lens. Despite the progress made over the last two decades to improve their clinical performance, symptoms of ocular dryness and discomfort and a variety of adverse clinical events are still reported. Consequently, the rate of contact lens wear discontinuation has not been appreciably diminished by their introduction. Aiming to improve the interfacial interactions of SiHy contact lenses with the ocular surface, a biomimetic layer of the hydrophilic glycosaminoglycan hyaluronic acid (HA) (100 kDa), was covalently attached to the surface of model poly(2-hydroxyethyl methacrylate-*co*-3-methacryloxypropyl-tris-(trimethylsiloxy)silane) (pHEMA-*co*-TRIS) SiHy materials via UV-induced thiol-ene "click" chemistry. The surface structural changes after each modification step were studied by FTIR-ATR and XPS. Successful grafting of a homogenous HA layer to the surface of the model silicone hydrogels was confirmed by the consistent appearance of N (1s) and the significant decrease of the Si (2p) peaks, as determined by the low-resolution angle-resolved XPS. The HA-grafted surfaces demonstrated reduced contact angles, dehydration rate and nonspecific deposition of lysozyme and albumin, while maintaining their optical transparency (>90%). *In vitro* studies demonstrated that the HA-grafted pHEMA-*co*-TRIS materials did not show any toxicity to

human corneal epithelial cells. These results suggest that surface immobilization of HA via thiol-ene "click" chemistry can be used as a promising surface treatment for SiHy contact lenses.

Keywords

Silicone hydrogel, contact lenses, surface modification, hyaluronic acid, thiol-ene chemistry, dehydration, protein deposition, MTT assay

4.1. Introduction

The contact lens industry was revolutionized by the development of silicone hydrogel (SiHy) lenses, which were first marketed in 1999. The introduction of silicone domains into the composition of soft contact lenses was a pivotal step in the development of contact lenses with superior oxygen permeability (Dk), while retaining the benefits of conventional hydrogel lens materials [1,2]. Consequently, SiHy contact lenses provide sufficient oxygen supply to the cornea to allow normal metabolic requirements to be met [3], eliminating the hypoxia-related complications exhibited by earlier hydrogel-based contact lens materials, particularly when worn overnight [4]. However, due to the inherent hydrophobicity of silicone components, surface or bulk modification is necessary for SiHy lenses to avoid such compromised surface properties as decreased surface wettability, accentuated lens-binding, and increased tear-film related biofouling [5,6] which, in turn, lead to poor compatibility of the contact lens materials with the ocular environment.

Various techniques have been used for the improvement of the surface wettability and hydrophilicity of SiHy lenses, including plasma surface treatments in the form of plasma coating or plasma oxidation [7,8] as well as the inclusion of a hydrophilic internal wetting agent [9,10]. More recently, SiHy materials based on either silicone-based macromers that impart naturally wettable surfaces that do not require further surface modification [11] or novel " water gradient" materials have been commercialised [12]. As evidenced by market trends, SiHy lenses are now the most widely prescribed soft contact lens category, accounting for approximately 65% of new soft lens fits worldwide [13]. Despite the different techniques developed to optimize the interactions between the SiHy lens and the ocular surface, resistance to protein and lipid deposition [14,15] and bacterial adhesion remains problematic, especially with overnight wear, potentially leading to

sight-threatening microbial infections [16]. In addition, contact lens-induced dryness and discomfort, particularly at the end of the day, remain a major impediment to contact lens adoption [17,18].

It is therefore clear that there remains considerable room for improvement in the performance of SiHy lenses. Although the factors that determine contact lens "biocompatibility" are numerous, complex, and interconnected, controlling the interactions of the eye-contact lens biointerface is of substantial importance [19,20]. To improve these interfacial interactions, SiHy-based materials have been typically coated or grafted with hydrophilic polymers, such as PEG or PVP [21–23]. Clinical data showed that PEG surface-modified SiHy contact lenses reduced biofouling *in vivo* compared to unmodified commercial SiHy contact lenses [21]. Another approach was the development of zwitterionic surfaces based on the biomimetic polymer pMPC, a phosphorylcholine containing phospholipid polymer. These materials exhibited improved surface wettability, as well as highly repellent protein characteristics [24]. Taking advantage of the zwitterionic nature of hydrophilic natural amino acids, Xu et al. [25] developed serine-grafted SiHy materials that demonstrated good hydrophilicity *in vitro* and better protein resistance than commercial SiHy contact lenses *in vivo* after a month of continuous wear.

Hyaluronic acid (HA) is a linear, anionic, non-sulfated glycosaminoglycan of the extracellular matrix (ECM) naturally present in many tissues. In the eye, HA is found in the vitreous humour, the lacrimal gland as well as in the conjunctiva, corneal epithelium and tear film [26–29]. Its ocular compatibility in combination with its unique viscoelastic, hygroscopic, shear-thinning and lubricating properties render HA well-suited for ophthalmic applications, especially for the anterior ocular segment [30]. HA promotes tear film stability, ocular hydration and effective lubrication [31–33]. It has been used effectively for the treatment of dry-eye [34], and in contact lens products as a conditioning agent to alleviate dryness and discomfort during wear [35].

The incorporation of HA into the bulk of model SiHy materials either as an internal or releasable wetting agent or in the structure of an interpenetrating network (IPN) led to enhanced wettable surfaces, which not only showed reduced non-specific protein deposition [36–38] but also reduced lysozyme denaturation [39]. Surface immobilization of contact lenses with HA binding peptides was found to locally attract and concentrate exogenous HA, creating a thin HA coating that is able to retain moisture on the surface of the material [40]. Deposition of a self-assembled chitosan/HA multilayer coating, via electrostatic interactions using the layer-by-layer (LbL)

technique, also improved surface characteristics such as wettability, dehydration and resistance to protein sorption [41]. Finally, the bacteriostatic, antimicrobial and antiviral properties of HA when used as a surface layer [42–44] further support its functionality as an efficacious surface layer for contact lens applications.

Thiol–ene "click" chemistry has been widely explored for biomaterials applications, including drug delivery, tissue engineering and surface modification, owing to its rapid, cytocompatible, and bio-orthogonal reactivity [45,46]. Thiol-ene chemistry can be catalyst-mediated (Michael addition) or radical mediated (anti-Markovnikov radical addition). Radical-mediated thiol-ene reactions can be initiated either thermally or photochemically. Recently, photochemical routes have gained increased attention in the surface modification of polymeric materials for the development of controlled interfacial properties. Benefiting from the simplicity, robust nature, excellent chemoselectivity as well as the high reaction efficiency of "click" reactions, radical mediated thiol-ene chemistry allows for reliable surface modification in a fast, modular fashion without compromising the material's bulk properties [47]. In addition, it can be performed under mild reaction conditions and it is tolerant to oxygen and water with minimal or no by-product formation, allowing for the modification of various types of surfaces, including that of living human cervical carcinoma cells (HeLa), without affecting their viability [48]. Further, it follows a step-growth radical addition coupling mechanism that can be spatially and temporary controlled [45]. Photoinitiated thiol-ene reactions have been successfully established for photochemical surface modification processes, thus allowing for applications in biomaterials, biomedicine and biotechnology [45,46]. For instance, surface immobilization of HA on glass and silicon surfaces via UV-induced thiol-ene "click" chemistry resulted in more wettable surfaces with reduced protein deposition as well as cell adhesion and spreading characteristics [49].

It has been recently demonstrated that covalent immobilization of HA on the surface of model poly(hydroxyethyl methacrylate) (pHEMA) hydrogels using thiol-acrylate "click" chemistry, resulted in non-cytotoxic materials with increased surface wettability, protein resistant properties and decreased dehydration rate [50]. This current study, aims to investigate the impact that the surface grafted HA has on the surface properties of model SiHy materials. Surface immobilization of HA was achieved by UV initiated radical-mediated thiol-acrylate "click" chemistry, a versatile chemistry for the surface modification which enables efficient formation of

the corresponding thioether bond with high specificity and fine control over the spatial arrangement of the surface chemical composition in synthetic processes [51].

4.2. Experimental Section

4.2.1. Materials and Chemical Reagents

Hyaluronic acid (HA) (sodium hyaluronate) with an average molecular weight (MW) of 100 kDa was obtained from LifeCore Biomedical (Chaska, MN, USA). Hydroxybenzotriazole (HOBt) was purchased from Toronto Research Chemicals Inc. (Toronto, ON, Canada), while the monomer 3-methacryloxypropyl-tris-(trimethylsiloxy) silane (TRIS, ≥95%) was supplied by Gelest (Morrisville, PA, USA). In addition, the photoinitiators 1-hydroxy-cyclohexyl-phenyl-ketone (Irgacure® 184) and 2-hydroxy-1-[4-(2-hydroxyethoxy)phenyl]-2-methyl- 1-propanone) (Irgacure® 2959) were generously donated by BASF Chemical Company (Vandalia, IL, USA). The human corneal epithelial cell line (HCE-2 [50.B1] ATCC® CRL-11135™) was purchased from the American Type Culture Collection (Rockville, MD, USA). All other chemicals, reagents and proteins were purchased from Sigma Aldrich (Oakville, ON, Canada).

4.2.2. Synthesis and Characterization of thiolated HA (HA-SH)

For the synthesis of HA-SH, the protocol followed was similar to that described previously [50]. Briefly, an aqueous solution of HA (100 kDa) (16.6mg/ml, pH 7.4) was mixed with EDC/HOBt (1:1 molar ratio) (3 equivalents to -COOH of HA) at room temperature under stirring conditions for 1.5 hours, while maintaining a pH of 6.8-7 (NaOH 1M). Then, cysteamine dihydrochloride solution (3 equivalents to -COOH of HA, 10 ml water) was added dropwise while the pH was kept stable at 7 (NaOH 1M) (HA-SS-R) and the coupling reaction was allowed to proceed for 36 hours at room temperature (pH 7, NaOH 0.1M). The intermediate product HA-SS-R was exhaustively dialyzed against Milli-Q water using a dialysis membrane (MWCO 3.5 kDa, Spectrapore, Spectrum Labs, CA). For the disulfide bond reduction, TCEP HCl (35 mM, 5 equivalents to -COOH of HA) was added in the HA-SS-R solution (pH 5, NaOH 1M). After stirring for 7 hours, the pH was reduced to 3.5 and the final solution was then purified by dialyzing (MWCO 3.5 kDa, Spectrapore, Spectrum Labs, CA) in Milli-Q water (pH 3.5) for 5 days. The final product was freeze-dried and stored in the freezer (-20^{o}C) under nitrogen to protect the free

thiols from oxidation. The structure of the HA-SH product was determined by ^{1}HNMR (20 mg/ml) using a Bruker AVANCE 600 MHz (256 scans, room temperature) spectrometer using D_2O as the solvent (D, 99.96%, Cambridge Isotope Laboratories, Inc.).

4.2.3. Ellman's Test – Quantification of free thiols of HA-SH

The quantification of the free thiols of HA-SH was assessed spectrophotometrically, using Ellman's reagent (5,5'-dithiobis (2-nitrobenzoic acid), DTNB) [52]. Briefly, unmodified HA and HA-SH were dissolved in sodium phosphate buffer (0.1M, pH 8) containing 1 mM ethylenediaminetetraacetic acid (EDTA). L-cysteine was used for the calibration curve (2-20nmol, R^2=0.9987). After mixing the samples and L-cysteine standards with a solution of Ellman's reagent for 15 minutes at room temperature under dark conditions, the absorbance was measured at 412 nm using a UV-vis spectrophotometer (Spectramax Plus 384, Molecular Devices Corp.).

4.2.4. Synthesis of model pHEMA-*co*-TRIS hydrogel materials

The monomers HEMA and TRIS, as well as the crosslinker ethylene glycol dimethylacrylate (EGDMA) were passed through a polymerization inhibitor remover column prior to use. For the synthesis of the model pHEMA-*co*-TRIS hydrogels, HEMA and TRIS (90:10 wt%) as well as EGDMA (3.5 mol%) were mixed together vigorously for 30 minutes under a N_2 atmosphere. In turn, the photoinitiator Irgacure® 184 (0.5 wt%) was added and upon its dissolution, the prepolymer mixture was injected into a custom-made UV-transparent acrylic mold equipped with a 0.5 mm thick spacer. For the polymerization reaction, the prepolymer containing-mold was placed into a 400 W UV chamber (λ=365 nm) (Cure Zone 2 Con-trol-cure, Chicago, IL, USA) for 10 minutes. Following an overnight post-curing period at room temperature, the model SiHy were taken out of the mold, placed into Milli-Q water to swell and then punched into discs of 6.35mm (1/4") diameter. For extraction, the discs were soaked in a 1:1 (v/v) methanol:water solution for 12 hours and subsequently in Milli-Q water for 24 hours. Finally, model SiHy discs were dried under ambient conditions and stored at room temperature.

4.2.5. Surface acrylation of pHEMA-*co*-TRIS hydrogel materials

Initially, pHEMA-*co*-TRIS discs were dried overnight under vacuum. Taking advantage of the surface active hydroxyl (-OH) groups of the HEMA domains, the introduction of α, β-unsaturated carbonyls on the surface of the model SiHy was achieved by the esterification reaction between the -OH groups and acryloyl chloride (Acr Cl). More specifically, the dried SiHy discs were immersed into an anhydrous dichloromethane (DCM) solution following dropwise addition of Acr Cl (29 mM per disc) and pyridine (Pyr) (0.1 equivalent to Acr Cl used). The reaction proceeded for 3 hours at room temperature and under N_2 and dark conditions. The surface acrylated model SiHy discs (AcrpHEMA-*co*-TRIS) were then rinsed in DMF for 5 minutes (3 changes) and washed in DCM and in Milli-Q water (3 cycles each), with the washing procedure lasting for 24 hours in total, to remove any unreacted chemicals as well as reaction by-products. Finally, the hydrogels were stored at room temperature in foil covered glass vials containing Milli-Q water until further use.

4.2.6. Synthesis of surface grafted HA-pHEMA-*co*-TRIS hydrogel materials.

In a 20 ml glass vial, HA-SH (0.5 wt%) and the photoinitiator I2959 (0.1wt%) were initially dissolved into MilliQ-water. Into this solution, fully hydrated in MilliQ-water AcrpHEMA-*co*-TRIS discs were submerged and the glass vial was immediately placed into a 400W UV light chamber (Cure Zone 2 Con-trol-cure, Chicago, IL, USA), allowing for the surface grafting thiol-acrylate reaction to proceed at 365 nm for 10 minutes. At the end of the reaction, the surface modified HA-pHEMA-*co*-TRIS discs were thoroughly washed for 24 hours with MilliQ-water to ensure that only grafted HA remained on the surface.

4.2.7. Surface Chemistry Characterization

4.2.7.1. Fourier Transform Infrared Spectroscopy - Attenuated Total Reflectance (FTIR – ATR)

The surface chemistry of dry pHEMA discs after each surface modification step was analyzed using FTIR-ATR (Vertex 70 FTIR spectrometer, Bruker Instruments, Billerica, MA, USA) equipped with a diamond ATR cell. The absorption spectra used for the characterization

were obtained at 64 scans with the resolution 4 cm^{-1} ranging from 600 to 4000 cm^{-1}. A background spectrum was run and subtracted from the spectrum collected for each sample.

4.2.7.2. Angle-resolved X-ray Photoelectron Spectroscopy – AR-XPS

The chemical composition of the control and modified pHEMA-*co*-TRIS surfaces was determined by XPS. XPS measurements were performed using a PHI Quantera II XPS spectrometer (Physical Electronics (Phi), Chanhassen, MN, USA) equipped with a monochromatic Al K-α X-ray source ($h\nu$=1486.7 eV). The X-ray anode was operated at 50 W and the high voltage was kept at 15 kV while the operating pressure of the analyzer chamber remained below 2.0 $x10^{-8}$ Torr. The pass energy was fixed at 280 eV to ensure sufficient sensitivity, while a dual beam charge compensation system was used for neutralization of all samples (beam diameter 200 μm), improving energy resolution of the respective peaks [53]. Angle-resolved XPS (AR-XPS) was applied to obtain survey spectra at photoelectron take-off angles (defined as the angle between surface normal and the position of the analyzer) of 30 °, 45 ° and 90° for an in-depth analysis of the surface structure over a range of 3-10 nm [54]. All binding energies were referenced to the neutral C (1s) hydrocarbon peak at 284.8 eV. Survey scans were obtained in the 0-1350 eV range. Data manipulation of low resolution spectra was performed using PHI MultiPak Version 9.4.0.7 software. The survey spectra of three different spots per sample surface were collected to minimize error (n=3 discs per sample).

4.2.8. Contact angle measurements – Static captive bubble and sessile drop techniques

The contact angle was measured using the captive bubble as well as the sessile drop technique (Optical Contact Angle Analyzer - OCA 35, Dataphysics, Germany). Initially, the surface of fully swollen discs was blotted with a Kimwipe® to remove free water. For the captive bubble technique, the disc was initially immersed into a chamber filled with Milli-Q water and a 5 μl air bubble was placed on the surface of the disc. The Milli-Q water in the chamber was replaced prior to measuring the contact angle of each set of samples. For the sessile drop technique, a 5 μl drop of Milli-Q water was placed on the surface of the disc. In both techniques, the drop was allowed to settle on the surface and the contact angle between the bubble/drop and the hydrogel surface was calculated with a video-based software (SCA 20, Dataphysics Instruments,

Germany). To account for potential inhomogeneities on the surface of the samples, the contact angle of two different spots from both sides of each disc was measured (n=6 discs per sample). All measurements were made at ambient humidity and temperature.

4.2.9. Dehydration kinetics and Equilibrium water content (EWC)

The impact of surface grafting of HA on the dehydration rate of the pHEMA-*co*-TRIS samples was determined by measuring the mass change over time. Briefly, samples equilibrated in Milli-Q water were gently blotted with a Kimwipe® to remove excess water and placed in a closed chamber digital balance with an incorporated digital hygrometer (La Crosse Technology, WT-137U, RH=32 ± 2% at 24ºC) using a custom-made holder which allows for exposure of both surfaces of the discs for evaporation. The samples were weighed immediately after placement ($W_{wet,}$ t=0) as well as at different time intervals ($W_{t,}$ t=1-150 mins). Finally, the discs were dried overnight in a 50ºC oven and re-weighed (W_{dry}).

The water loss (%) used to express the dehydration rate was calculated based on:

$$\text{water loss (\%)} = \frac{W_{wet} - W_t}{W_{wet} - W_{dry}} \cdot 100\% \qquad (4.1)$$

The equilibrium water content (EWC) of the model SiHy was also calculated:

$$\text{EWC (\%)} = \frac{W_{wet} - W_{dry}}{W_{wet}} \cdot 100\% \qquad (4.2)$$

4.2.10. Optical Transparency

The optical properties of the model SiHy materials after each modification step were assessed by measuring the transmittance (%) of fully hydrated pHEMA-*co*-TRIS SiHy discs immersed into 100 μl Milli-Q water for the range of 400-750 nm, using a UV–Vis spectrophotometer (Spectramax Plus 384, Molecular Devices, Corp, Sunnyvale, CA, USA).

4.2.11. *In vitro* protein deposition – Lysozyme and human serum albumin

For the quantification of the non-specifically adhered lysozyme (from chicken egg white) and human serum albumin (HSA) on the surface of the pHEMA-*co*-TRIS surfaces, proteins were radiolabeled with $I^{125}Na$ using the iodine monochloride method (ICl) [55]. After the iodination

reaction, unbound I^{125} was removed by passing the labeled protein through a column packed with AG 1-X4 (Bio-Rad, Hercules, CA, USA). The percentage of free iodide, which was determined by the trichloroacetic acid precipitation assay, was found to be less than 0.5% of the total activity for both labeled protein solutions. A single protein solution (1mg/ml) of each protein of interest was prepared in PBS (pH 7.4) containing 5 wt% of the radiolabeled I^{125}-protein.

The pHEMA-*co*-TRIS discs, equilibrated in PBS (pH 7.4), were individually incubated into each single protein solution (250 μl/disc) for 6 hours at room temperature. The samples were then washed three times with fresh PBS (pH 7.4) (5-minute intervals) to remove loosely adherent protein. Each disc was then blotted dry with a Kimwipe®, placed in a counting vial (5 ml non-pyrogenic, polypropylene round-bottom tube) and counted for radioactivity using a Gamma Counter (Perkin Elmer Wallac Wizard 1470 Automatic Gamma Counter, Wellesley, MA, USA). The radioactivity associated with the surfaces was converted into a protein amount using a standard calibration curve. The results are presented as the mass of protein sorbed per disc surface area (n=6 discs per sample).

4.2.12. In vitro cell viability

The cytocompatibility of the pHEMA-*co*-TRIS model SiHy after each modification step was determined using immortalized human corneal epithelial cells (HCEC) and the 3-(4,5-dimethylthiazol-2-yl)-2,5-diphenyltetrazolium bromide (MTT) assay. This colorimetric assay is based on the reduction of yellow tetrazolium salt MTT to water-insoluble dark blue formazan salt by metabolically active cells. Briefly, immortalized human corneal epithelial cells (HCECs) (HCE-2 [50.B1] ATCCR CRL-11135TM from the American Type Culture Collection, Rockville, MD) were suspended in culture medium (1.5×10^5 cells/ml) and seeded in a flat bottom 96-well culture plate (100 μl culture medium per well). Culture medium included Keratinocyte Serum Free Medium (KSFM) supplemented with human recombinant Epidermal Growth Factor 1-53 (EGF 1-53) and Bovine Pituitary Extract (BPE). After incubating the HCECs in a humidified 5% CO_2 environment at 37°C for 24 hours to ensure adhesion, the culture medium was removed and replaced with fresh KSFM (250 μl). The swollen pHEMA-*co*-TRIS SiHy that previously were extensively washed with sterile PBS (pH 7.4) for 6 hours at room temperature, were then inserted in the HCEC-containing wells vertically and away from the bottom of the well. The positive control of this study was cultured cells without pHEMA-*co*-TRIS discs. At the end of a 24-hour

incubation period in a cell culture incubator (5% CO_2, 37°C), the discs were discarded and the media was aspirated while each well was gently rinsed with PBS pH 7.4. For the assay, 10 μl of the MTT solution (5 mg/ml in PBS pH 7.4) and 100 μl of PBS were added in each well, the plate was then covered with foil and placed in the cell incubator for 4 hours. Subsequently, 85 μl of the above solution was removed, while the resulting formazan salt was dissolved in 50 μl of DMSO. The absorbance of the solubilized formazan product was measured at 540 nm using a UV–Vis spectrophotometer (Spectramax Plus 384, Molecular Devices, Corp, Sunnyvale, CA, USA), with the absorbance value being proportional to the number of viable cells remaining following the incubation period. The reported cell viability (%) was expressed by the ratio of absorbance of the cells in the presence of the SiHy discs to that of the cells incubated with culture medium only (positive control). For cell viability values lower than 70%, the materials were considered potentially cytotoxic [56].

4.2.13. Statistical Analysis

Data are presented as mean ± standard deviation (SD). Statistical analysis was determined/performed by a single-factor analysis of variance (ANOVA) with post-hoc Tukey HSD test in Statistica 10.0 (StatSoft Inc., Tulsa, OK, USA). A p value<0.05 was considered to be statistically significant.

4.3. Results and Discussion

4.3.1. Synthesis and Characterization of Thiolated HA (HA-SH)

The functionalization of HA with thiol groups included a condensation and a reduction reaction, as previously described by Korogiannaki et al. [50] (Figure 4.1). Taking advantage of the carboxyl group (-COOH) in the HA backbone, the amidation reaction between HA and cystamine dihydrochloride was accomplished by a carbodiimide-mediated reaction resulting in the formation of the intermediate HA-SS-R. Commercially available TCEP was chosen for the subsequent reduction reaction (HA-SH) instead of the commonly used 1,4-dithiothreitol (DTT) because it is a faster and stronger reducing agent [57]. The yield of this two-step reaction was approximately 90%.

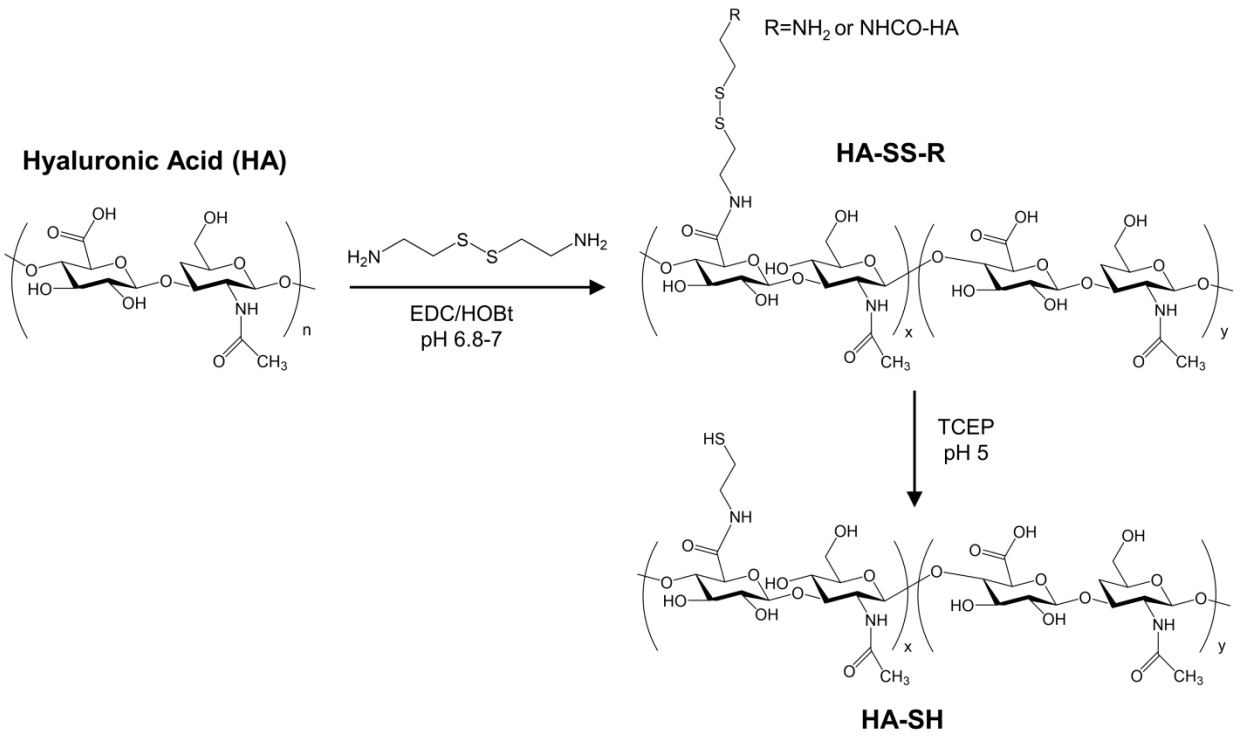

Figure 4.1: Schematic illustration of the synthesis of thiolated-HA (HA-SH).

The structure of the final thiomer HA-SH was confirmed by ^{1}HNMR in D_2O. In Figure 3.2, the resonance at 2.03 ppm (δ_a) was attributed to the acetamide moiety of the N-acetyl-D-glucosamine residue (-NHC(O)C**H**3) group and the peaks from 3.3 to 4 ppm correspond to the methine groups on the six-membered rings of HA backbone respectively (Figure 4.2A). Compared to the ^{1}HNMR spectrum of the native HA, the new signals centered at 2.93 ppm and 2.72 ppm were assigned to the methylene protons (C**H**$_2$C**H**$_2$S**H**) (δ_{b+c}) of the cysteamine moieties (Figure 4.2B), indicating the successful modification of HA with thiol functional groups (HA-SH). Finally, the free thiol content of HA-SH, quantified by the Ellman's method, was 793.1 ± 34.3 nmol SH/mg HA, which in turn corresponds approximately to 32 ± 1.3 free thiols per 100 repeat/disaccharide units of HA. No free thiols were detected in the native HA and in the intermediate HA-SS-R product. This moderate degree of HA thiolation is not expected to affect its hydrophilic anionic character, bioactivity and toxicity while providing adequate anchoring sites with the surface of interest for the modification of the model SiHy materials.

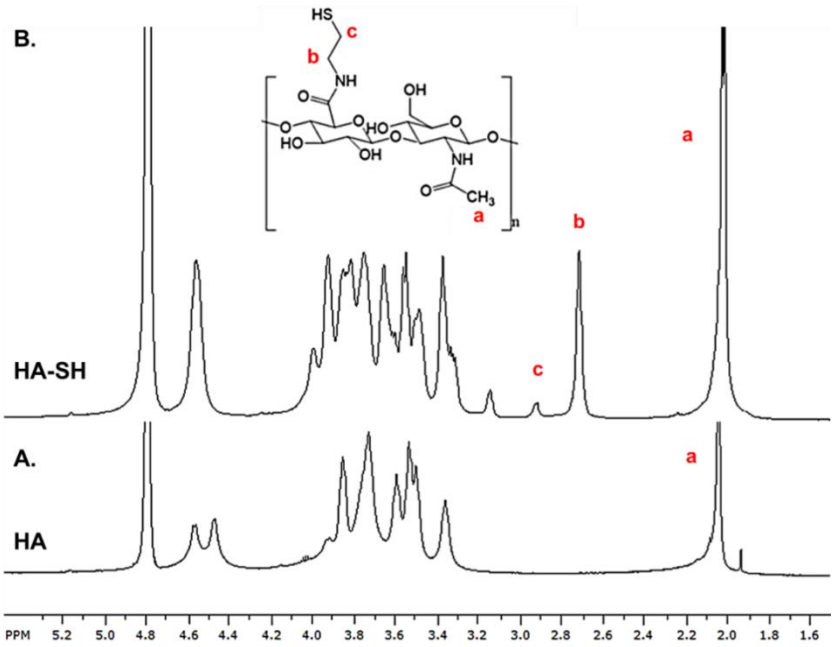

Figure 4.2: A characteristic ^{1}HNMR spectrum (600 MHz) of (A) unmodified HA (100 kDa) and (B) thiolated HA (HA-SH)**.**

4.3.2. Synthesis and surface chemistry characterization of the HA-grafted pHEMA-*co*-TRIS (HA-pHEMA-*co*-TRIS) hydrogel materials

Surface immobilization of HA on the model SiHy substrate was achieved by free-radical thiol-ene "click" chemistry. Figure 4.3 shows a schematic diagram of the procedure followed for the development of the HA-pHEMA-*co*-TRIS materials. The coupling reaction of HA-SH with the acrylate groups present on the pHEMA-*co*-TRIS surface was photochemically induced in the presence of Irgacure 2959 (I2959). For the surface modification reaction with HA, the commercially available I2959 was selected since it is water-soluble and widely used in thiol-acrylate reactions without causing any cellular toxicity [58]. Upon exposure to 365 nm UV light, I2959 undergoes homolytic bond cleavage resulting in the formation of thiyl radicals (RS$^{\cdot}$). The direct addition of the thiyl radical across the C=C double bond of the acrylate group yields an intermediate β-thioether carbon-centred radical, which in turn is able to abstract a hydrogel from another thiol moiety resulting in the formation of a new thiyl radical as well as the final hydrothiolation product that exhibits anti-Markovnikov orientation (Figure 4.3C). This type of reaction generally exhibits step-growth radical addition mechanism, with the propagation and

chain transfer steps occurring consecutively, ensuring quantitative formation of the desired thioether in a modular fashion [59]. In thiol-acrylate chemistry, apart from the hydrothiolation reaction, there is a chance of homopolymerization of the acrylate groups upon UV exposure [45], leading to a combination of step and chain-growth mechanisms. This homopolymerization reaction, however, is considered to be minimal in the present work due to steric hindrance of the surface acrylate groups. The limiting step of the surface modification reaction is therefore considered to be the chain transfer step of the thiol-acrylate grafting reaction [60]. The organic solvent (DCM) was selected for the intermediate acrylation reaction because it did not cause a change of mass for the pHEMA-*co*-TRIS hydrogels. In addition, the grafting reaction occurred in fully swollen samples. Finally, the surface grafting reaction proceeded under ambient atmosphere, since thiol-ene photoreactions have been reported to be relatively unaffected by oxygen [45]. As a result, this facile approach enables the formation of a HA-grafted layer to the surface of the model SiHy materials.

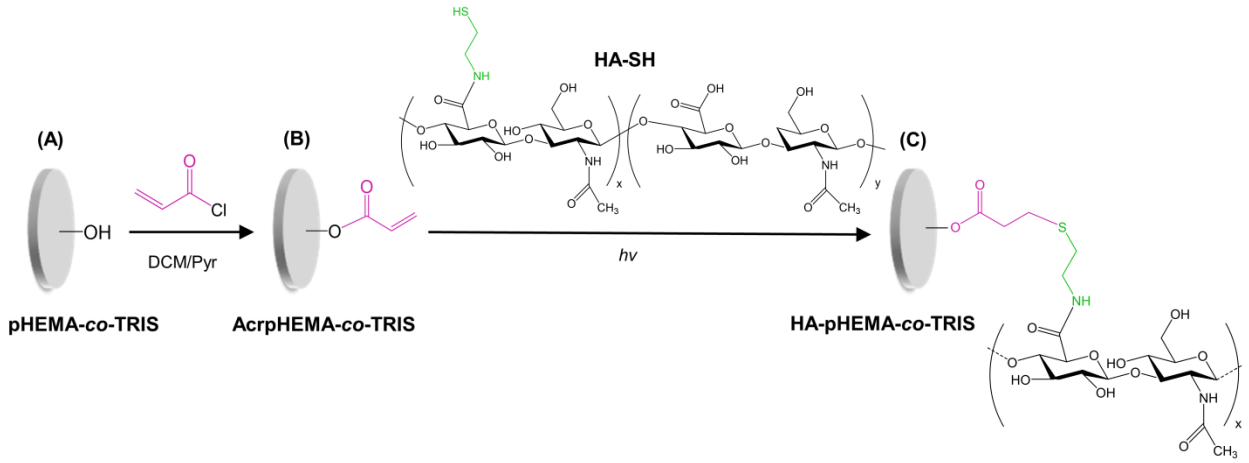

Figure 4.3: Schematic illustration of grafting HA to pHEMA-*co*-TRIS surface via UV-induced free-radical thiol-ene "click" chemistry. (A) pristine pHEMA-*co*-TRIS, (B) acrylated pHEMA-*co*-TRIS (AcrpHEMA-*co*-TRIS) and (C) HA-grafted pHEMA-*co*-TRIS (HA-pHEMA-*co*-TRIS) surfaces.

4.3.3. Surface chemistry characterization of HA-SH grafted to AcrpHEMA-*co*-TRIS (FTIR-ATR and XPS)

The chemistry of the model SiHy surfaces before and after each modification step was determined by FTIR-ATR and XPs (Figures 4.4 and 4.5). All FTIR-ATR measurements were performed on dehydrated samples in order to avoid the impact of bound water on the spectra. Upon reaction of the pHEMA-*co*-TRIS with the Acr Cl, a decrease in the broad absorbance band at approximately 3405 cm^{-1} of the -OH stretching vibration in combination of the presence of a new absorption band at 1635 cm^{-1} which was assigned to the bending vibrations of C=C bonds, suggested successful surface acrylation of pHEMA-*co*-TRIS surfaces (Figure 4.4B). This procedure introduced α,β-unsaturated carbonyls to the surface of the model SiHy allowing for further reaction with the -SH groups of HA (HA-pHEMA-*co*-TRIS). For the HA-modified samples, however, the surface sensitivity of FTIR-ATR was not adequate to detect the expected modifications associated with the covalent attachment of HA on their surface (Figure 4.4C), as the sampling depth of FTIR-ATR is a few hundred nanometers, whereas the surface grafted HA layer is expected to have a thickness of several tens of nanometers. Hence, XPS was used to confirm the surface conjugation reaction.

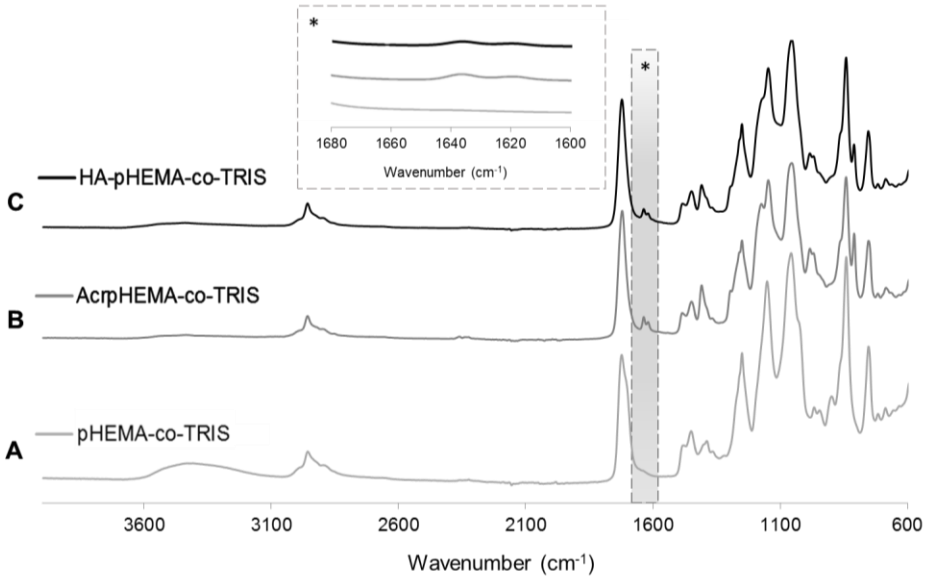

Figure 4.4: FTIR-ATR spectra from (A) pristine pHEMA-*co*-TRIS (B) AcrpHEMA-*co*-TRIS and (C) HA-pHEMA-*co*-TRIS surfaces.

Due to its exceptional surface sensitivity, XPS analyses were performed to gain more insight into the chemical functionalization of the outermost (10 nm) surface layer of the model SiHy surfaces, with up to 0.1 % sensitivity [54]. A typical XPS survey spectrum of the unmodified, acrylated and HA-grafted pHEMA-*co*-TRIS surfaces at 45° take-off angles is depicted in Figure 4.5. As anticipated, the distinct peaks observed for the pristine and acrylated pHEMA-*co*-TRIS surfaces (Figure 4.5A and B) at 530 eV, 283 eV as well as 151 and 100 eV were assigned to oxygen (O_{1s}), carbon (C_{1s}) and silicon (Si_{2s} and Si_{2p}) respectively. The presence of the new peak at approximately 397 eV in the HA-pHEMA-*co*-TRIS surface spectrum was attributed to the nitrogen (N_{1s}) (Figure 4.5C), indicating that the hydrophilic HA had been grafted to the surface of the model SiHy by UV-induced thiol-acrylate chemistry.

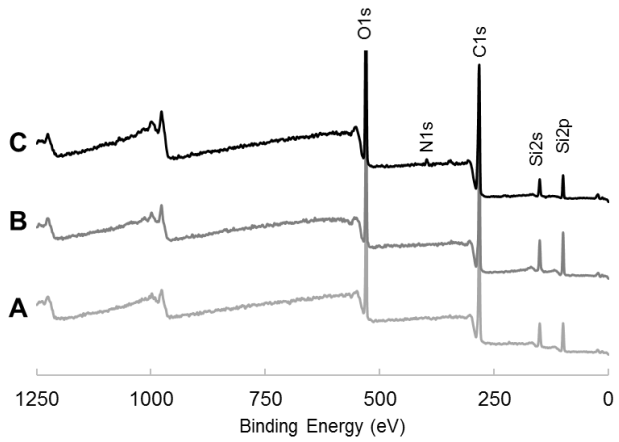

Figure 4.5: Representative XPS survey spectrum at 45° take-off angle for dehydrated (A) pristine pHEMA-*co*-TRIS (B) AcrpHEMA-*co*-TRIS and (C) HA-pHEMA-*co*-TRIS surfaces.

In addition, the presence of concentration gradients in the near-surface region was qualitatively evaluated by angle resolved-XPS (AR-XPS). Table 4.1 shows the composition of the examined surfaces at different take-off angles. Apart from the presence of the N_{1s} signal, the O/C ratio of the HA-pHEMA-*co*-TRIS surfaces was significantly higher for all three take-off angles compared to those of the pristine and the intermediate surface acrylated SiHy ($p<0.001$), in a similar manner to that previously observed for HA-linked surfaces [61,62]. AR-XPS is an effective tool for non-destructive depth-profile analysis of the elemental composition of the near surface regions of the model SiHy materials (usually from 3 to 10 nm of the outermost surface) by

manipulating the photoelectron angle of take-off with respect to the surface normal [63]. Accordingly, by decreasing the take-off angle, the penetration depth from which the photoelectrons are accepted is shallower, therefore enhancing the surface sensitivity of the XPS analysis [64]. AR-XPS, unlike AFM or sputtering methods, can also provide a non-destructive measurement of the thickness of a thin surface-film or the thickness of an overlayer [64].

Moreover, the Si signal of the HA-pHEMA-co-TRIS was significantly decreased ($p<0.0001$), even in the case of the 90° take-off angle, which represents an approximate 10 nm depth of penetration, further confirming the presence of a thick graft layer of HA able to effectively mask the underlying substrate, which in turn limited the silicon detection even in the high vacuum environment of the XPS. Similar or even higher Si content was also detected at the outermost surface region of commercial surface treated SiHy contact lenses (balafilcon A and lotrafilcon A) [53,65]. This is thought to be the result of the high flexibility and mobility of the silicone-oxygen chains, often resulting in their migration to the outer interface, even if they have to overcome a surface layer of a hydrophilic polymer [66,67]. Finally, the O/C as well as the Si/C ratio of the model SiHy surfaces remained almost the same when the take-off angle was increased, suggesting that the samples were characterized by a consistent and homogenous chemical composition throughout their near-surface region.

Table 4.1: Surface elemental compositions (%) of the HA-grafted silicone hydrogels determined

sample	Angle	C (1s)	N(1s)	O(1s)	Si(2p)	O/C	Si/C
control	30°	67.1 ± 1.6	0	21.9 ± 1.0	11.0± 1.1	0.33 ± 0.02	0.16 ± 0.02
Acrylated		66.0 ± 4.7	0	21.9 ± 2.6	12.1 ± 2.3	0.34 ± 0.06	0.19 ± 0.05
HA-grafted		64.7 ± 1.6	**1.7 ± 0.2**	28.0 ± 1.0	**5.7 ± 1.0**	**0.43 ± 0.02**	**0.09 ± 0.02**
control	45°	66.7 ± 2.4	0	23.0 ± 1.9	10.2 ± 0.6	0.35 ± 0.04	0.15 ± 0.01
Acrylated		69.5 ± 2.9	0	20.3 ± 2.3	10.2 ± 1.7	0.29 ± 0.04	0.15 ± 0.03
HA-grafted		65.1 ± 1.4	**2.0 ± 0.6**	27.3 ± 1.2	**5.7 ± 0.7**	**0.42 ± 0.03**	**0.09 ± 0.01**
control	90°	66.3 ± 3.0	0	24.0 ± 2.0	9.6 ± 1.8	0.36 ± 0.04	0.15 ± 0.03
Acrylated		65.2 ± 2.1	0	24.7 ± 1.3	9.8 ± 1.4	0.37 ± 0.03	0.14 ± 0.03
HA-grafted		65.2 ± 1.2	**1.1 ± 0.3**	28.9 ± 1.1	**4.5 ± 0.9**	**0.45 ± 0.02**	**0.07 ± 0.01**

4.3.4. Surface Wettability

Surface wettability is a particularly relevant property for contact lenses as it is associated with tear film spreading and stability upon insertion [68]. In this study, the surface wettability of the model SiHy was evaluated *in vitro* as a function of the contact angle measured by the sessile drop and the captive bubble techniques. According to Maldonaldo–Codina et al. [68], the sessile drop can be used to measure advancing contact angle, which can be indicative of the ease with which the eyelids can reform the tear film (initial tear-film spreading) over a fully or partially dehydrated lens surface, while the captive bubble technique is presumably an indication of the tear film stability on the fully hydrated lens surface during the blinking cycles. Hence, these two techniques are considered of equal importance for a good estimation of the *in vivo* wetting properties of the model SiHy surfaces, even though they measure two different types of contact angle. For both techniques, decrease in the measured contact angle implies improved surface wettability.

As shown in Figure 4.6, substitution of the surface hydroxyl groups with the α,β-unsaturated carbonyls slightly increased the contact angle of the AcrpHEMA-*co*-TRIS ($p<0.04$) for both sessile drop and captive bubble techniques. The HA-pHEMA-*co*-TRIS sample, however, exhibited significantly reduced contact angles (sessile drop: 60%, $p<0.0002$ and captive bubble: 40%, $p<0.002$), suggesting improved surface wettability. This observation can also be used as another indication of the successful covalent attachment of HA on the surface of the model SiHy. Improved surface wettability is of great importance for SiHy contact lenses, since their inherently hydrophobic silicone components can migrate to the surface and cause poor *in vivo* wettability, leading to visual disturbances, increased lens surface deposition and ocular dryness [69,70]. Of note, a 4-fold increase in the concentration of either HA-SH or the initiator I2959 did not cause any further decrease in the contact angle (sessile drop) (data not shown), suggesting that the concentration of HA-SH (0.5 wt%) and I2959 (0.1wt%) resulted in the maximum grafting density under the conditions examined. Interestingly, increasing the I2959 concentration to above 0.1wt% led to was found to cause gelation of the HA-SH solution, even in the presence of TCEP (pH 5) and under N_2 conditions. To the best of our knowledge, this has not been reported before in the research literature. Lower concentrations for either HA-SH or I2959 were not examined.

Finally, the hysteresis, defined as the difference between the advancing (sessile drop) and receding (captive bubble) contact angle, was also investigated. Specifically, the hysteresis of the

pristine and HA-grafted pHEMA-*co*-TRIS materials was 55.0 ± 3.0º and 12.8 ± 3.6º respectively. The significantly lower hysteresis (~80%) of the surface modified model SiHy suggests lower surface heterogeneity and roughness due to the presence of the rigid hydrophilic layer of the grafted HA at the interface [71,72]. In contact lens applications, the advancing contact angle and the hysteresis are suggested to be a good indication of clinically acceptable wettability and overall performance [73]. Reducing hysteresis is one of ultimate goals in contact lens research and development [6,71]. These results are in agreement with those previously observed for the HA-grafted pHEMA materials, while also surface immobilization of thiolated HA on vinyl-terminated glass surfaces via thiol-ene chemistry demonstrated improved surface wettability [74].

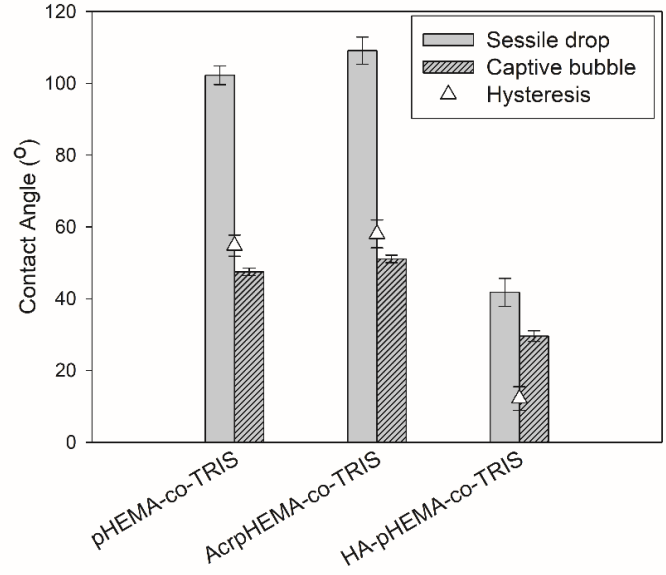

Figure 4.6: Static water contact angle (±SD) of pristine pHEMA-*co*-TRIS, AcrpHEMA-*co*-TRIS and HA-pHEMA-*co*-TRIS hydrogels (n=6) using sessile drop and captive bubble techniques. The hysteresis, defined as the difference between the contact angle of the sessile drop and that of the captive bubble techniques, as a function of surface treatment is also depicted.

4.3.5. Dehydration Profile and Swellability (EWC)

Contact lens dehydration, which occurs mainly due to environmental changes, may increase friction over time and thus can contribute to symptoms of ocular dryness and end-of-day discomfort [75]. Herein, the *in vitro* dehydration profile of the model SiHy was examined by calculating the rate of water evaporation (equation 4.1), using the gravimetric method. As shown in Figure 4.7, HA-grafted pHEMA-*co*-TRIS materials were characterized by a slower dehydration rate compared to the pristine and the intermediate samples. Moreover, the procedure of grafting HA to the surface of the pHEMA-*co*-TRIS SiHy was not found to alter the swellability of the materials, since the EWC of the unmodified pHEMA-*co*-TRIS (29.3±0.8 %) was not statistically different from that of the surface acrylated (27.9±1.0 %) and HA-grafted (29.2±0.7 %) SiHy samples ($p=0.9$). These results are in accordance with previously published results for contact lens materials with HA on the surface [40,50]. Hence, the water-binding properties of the surface grafted-HA layer not only enhanced the surface wettability of the model SiHy but also provided surfaces with improved water retentive properties.

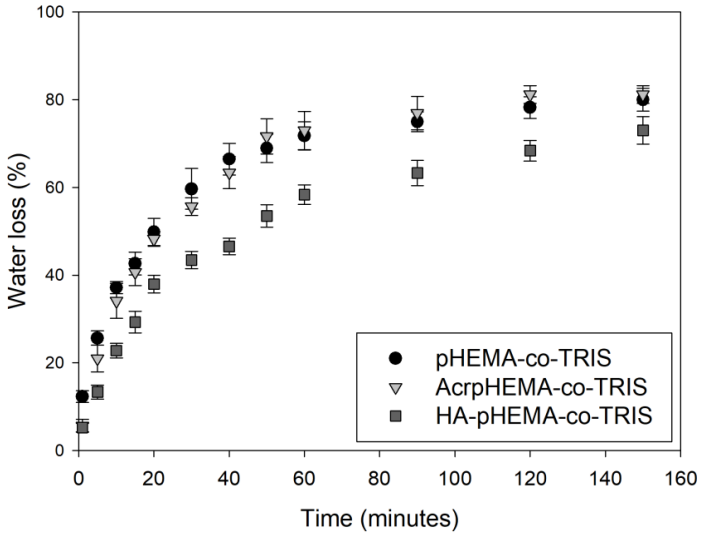

Figure 4.7: Dehydration profile expressed as the water loss (%) (±SD) over time from the pristine pHEMA-*co*-TRIS, Acr pHEMA-*co*-TRIS and HA- pHEMA-*co*-TRIS SiHy in a controlled closed chamber (T=23ºC, RH=32%) (n=6).

4.3.6. Optical Transmittance

The impact of the surface modification process on the optical properties of the HA-grafted pHEMA-*co*-TRIS SiHy is depicted in Figure 4.8. According to the results, the intermediate step of surface acrylation was found to cause a slight decrease (2%, $p<0.0001$) in the measured transmittance. The immobilization reaction of HA on the surface of the pHEMA-*co*-TRIS materials was not found to further impact the optical acuity of the model SiHy with the transparency of these being above the acceptable range for contact lens applications (>90%). In addition, it is important to note that these materials have a thickness approximately five times higher than that of commercial contact lenses, hence the suggested photochemical surface functionalization process described in this work is not expected to affect the optical performance of SiHy contact lenses.

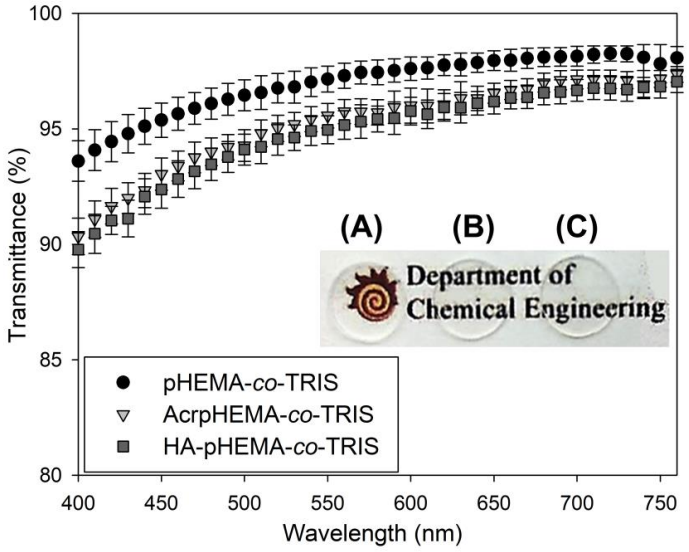

Figure 4.8: The transmittance spectra (±SD) and a photograph) of the (A) pristine pHEMA-*co*-TRIS, (B) AcrpHEMA-*co*-TRIS and (C) HA-pHEMA-*co*-TRIS discs (n=6).

4.3.7. Protein Deposition

The interactions of the contact lens surface with the proteins of the tear film play an important role in the compatibility of the lens with the ocular environment. Lysozyme (MW 14 kDa, pI 11) and HSA (MW 66 kDa, pI 4.7) were chosen as model proteins because they are among the major proteins found on worn SiHy contact lenses, and they are also associated with adverse

effects [14]. Figure 4.9 shows the surface density of lysozyme and HSA on the pHEMA-*co*-TRIS materials. Surface acrylation of pHEMA-*co*-TRIS was found to increase the amount of lysozyme (20%, $p<0.03$), whereas no statistical changes were observed for HSA ($p=0.2$). Contrarily, the amount of lysozyme and HSA deposited on the HA-grafted pHEMA-*co*-TRIS was decreased by 30% ($p<0.002$) and 45% ($p<0.0004$) respectively, when compared to the pristine SiHy materials.

The amount of lysozyme and HSA present on the pHEMA-*co*-TRIS surfaces was determined by protein radiolabeling, since this technique does not affect the absorption profile of the examined protein [76,77] and allows for the direct quantification of low amounts of adhered proteins with no need for prior chemical extraction [78]. According to the results, surface immobilized HA on the surface of model SiHy via thiol-acrylate chemistry was able to retain its known antifouling properties, and thus its bioactivity, rendering it a good candidate for effective contact lens coating. The low protein deposition could be further supported by the improved wettability, as shown by the reduced contact angles, exhibited by the HA-grafted pHEMA-*co*-TRIS surfaces since improving the surface hydrophilicity of biomaterials has been shown in general to reduce non-specific protein deposition [79–82]. Consequently, the surface grafted layer of the hydrophilic HA was speculated to suppress the thermodynamically unfavourable hydrophobic interactions between the proteins and the pHEMA-*co*-TRIS substrate; and thus, steric repulsion in combination with the hydration layer associated with the HA were considered as the primary contributors to the antifouling properties of the HA-modified SiHy surfaces. Parameters, including surface density, chain mobility and conformational freedom of the surface grafted HA layer play key roles in the observed low-fouling properties herein [62,83,84].

In addition, the surface density of lysozyme was consistently higher than the surface density of HSA (~65%, $p<0.0001$) on all samples. This was likely due to the differences in the MW, conformational stability and net charge of the two proteins, as these parameters were previously found to contribute to the protein deposition profile [38]. When compared to surface modified HA-grafted pHEMA hydrogels [50], the amount of lysozyme and HSA deposited on the these SiHy materials was lower. SiHy materials are known to attract less proteins than conventional hydrogel contact lenses. Future studies should also be considered to assess the antifouling properties of the HA-grafted pHEMA-*co*-TRIS surfaces upon incubation in multiprotein solution (artificial tear solution), due to the competitive sorption mechanism (Vroman effect).

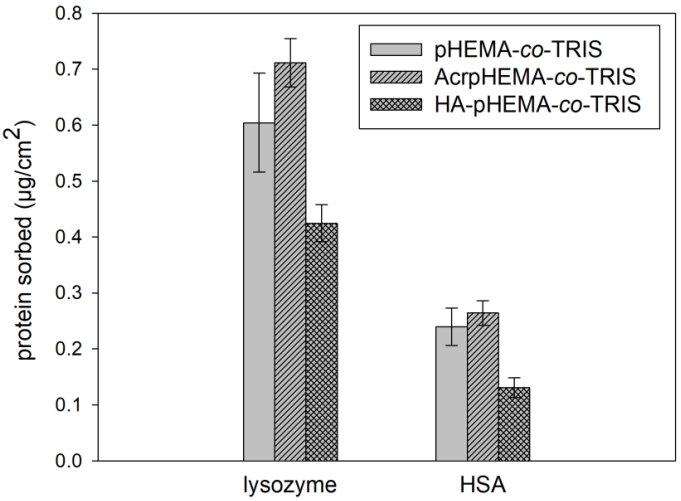

Figure 4.9: The amount (±SD) of lysozyme and human serum albumin (HSA) deposited *in vitro* on the surface of pristine pHEMA-*co*-TRIS, AcrpHEMA-*co*-TRIS and HA-pHEMA-*co*-TRIS discs (n=6) upon a 6-hour incubation period at room temperature.

4.3.8. *In vitro* cytotoxicity study

The cytocompatibility of the pHEMA-*co*-TRIS after each modification step is shown in Figure 4.10. The relative cell viability of all three SiHy samples was almost 100%, indicating that the HA-grafted model SiHy showed little or no cytotoxicity. These results also suggest that the washing steps used during the surface modification procedure were appropriate for the removal of any leachable components that could cause toxic effects to the HCECs. Cytocompatible doses of I2959 were used in this work for the surface modification reaction, since previous studies showed that the viability of living cells was not affected when this concentration of I2959 was used for cell-encapsulation polymerization reactions [58]. Additionally, immortalized HCECs are a well-established tool for screening *in vitro* ocular toxicity [85], while MTT assay allows for reproducible toxicity testing [86]. Hence, the HA-grafting procedure used in this study has good potential for the modification of lens materials to improve surface properties.

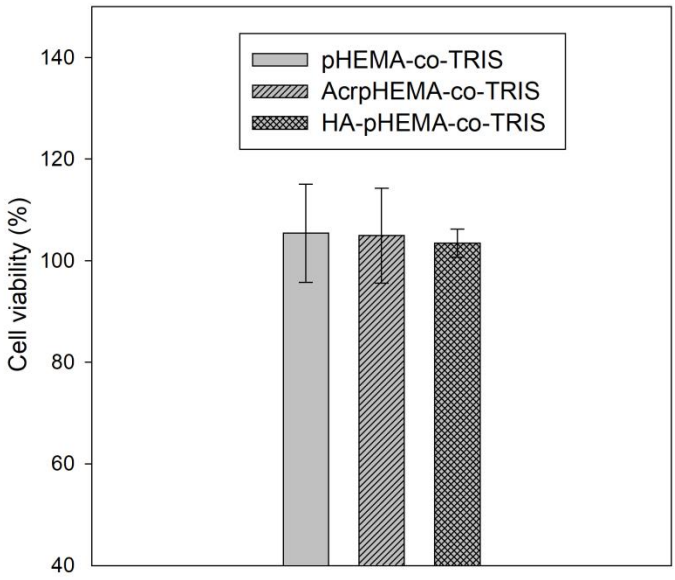

Figure 4.10: Cell viability (%) (±SD) of the HCECs upon incubation with pristine pHEMA-*co*-TRIS, AcrpHEMA-*co*-TRIS and HA-pHEMA-*co*-TRIS discs for 24 hours (n= 4) via MTT assay. Results expressed in respect to positive control (cell-only).

4.4. Conclusions

In this work, HA was successfully grafted on the surface of model pHEMA-*co*-TRIS SiHy by UV-induced thiol-ene "click" chemistry, a versatile technique for tailored surface properties. The intermediate surface acrylation and the presence of the surface bound HA were confirmed by FTIR-ATR and XPS. The results indicated that grafting HA to the surface of the model pHEMA-*co*-TRIS SiHy improved the surface wettability, dehydration profile and antifouling properties. In addition, the HA-grafted pHEMA-*co*-TRIS remained optically transparent and showed good *in vitro* compatibility with HCECs. Therefore, chemical immobilization of HA on the surface of SiHy may offer a promising means of coupling the advantageous bulk properties of SiHy with well-controlled interfacial properties, rendering these materials attractive candidates for biomaterial applications and more specifically as contact lenses.

4.5. Acknowledgements

This work was financially supported by Natural Sciences and Engineering Research Council (NSERC) of Canada and the 20/20 NSERC Ophthalmic Materials Research Network, and is gratefully acknowledged. The authors would also like to thank Dr. Danielle Covelli (Biointerfaces Institute, McMaster University) for her help acquiring the AR-XPS spectra, and Dr. Megan Dodd for her help with the cytotoxicity assay.

4.6. References

[1] L. Jones, Modern contact lens materials: A clinical performance update, Contact Lens Spectr. 17 (2002) 24–35.

[2] D.F. Sweeney, R. du Toit et al., Clinical performance of silicone hydrogel lenses, in: D.F. Sweeney (Ed.), Silicone Hydrogels Contin. Wear Contact Lenses, Butterworth-Heinemann, Oxford, 2004: p. 164–216.

[3] V. Compañ, A. Andrio, A. López-Alemany, E. Riande, M.F. Refojo, Oxygen permeability of hydrogel contact lenses with organosilicon moieties, Biomaterials. 23 (2002) 2767–2772.

[4] M. Covey, D.F. Sweeney, R. Terry, P.R. Sankaridurg, B.A. Holden, Hypoxic effects on the anterior eye of high-Dk soft contact lens wearers are negligible., Optom. Vis. Sci. 78 (2001) 95–9.

[5] G.M. Bruinsma, H.C. van der Mei, H.J. Busscher, Bacterial adhesion to surface hydrophilic and hydrophobic contact lenses., Biomaterials. 22 (2001) 3217–24.

[6] L. Cheng, S.J. Muller, C.J. Radke, Wettability of silicone-hydrogel contact lenses in the presence of tear-film components., Curr. Eye Res. 28 (2004) 93–108.

[7] B. Tighe, Silicone hydrogels: Structure, properties and behaviour, in: D. Sweeney (Ed.), Silicone Hydrogels Contin. Wear Contact Lenses, Butterworth-Heinemann, Oxford, 2004: pp. 1–27.

[8] A. López-Alemany, V. Compañ, M.F. Refojo, Porous structure of Purevision™ versus Focus® Night&Day™ and conventional hydrogel contact lenses, J. Biomed. Mater. Res. 63 (2002) 319–325.

[9] L. Jones, L. Subbaraman, R. Rogers, K. Dumbleton, Surface treatment, wetting and modulus of silicone hydrogels, Optician. (2006) 28–34.

[10] R. Steffen, C. Schnider, A next generation silicone hydrogel lens for daily wear. Part 1 - Material properties., Optician. 227 (2004) 23–25.

[11] L. Jones, Comfilcon A: a new silicone hydrogel material, Contact Lens Spectr. 22 (2007) 21.

[12] R. Stone, Introducing Water Gradient Technology, Contact Lens Spectr. (2013) 34–38.

[13] J.J. Nichols, Continuing upward trends in daily disposable prescribing and other key

segments maintained a healthy industry, Contact Lens Spectr. 33 (2018) 20–25, 42.

[14] D. Luensmann, L. Jones, Protein deposition on contact lenses: The past, the present, and the future, Contact Lens Anterior Eye. 35 (2012) 53–64.

[15] A. Panaser, B.J. Tighe, Function of lipids – their fate in contact lens wear: An interpretive review, Contact Lens Anterior Eye. 35 (2012) 100–111.

[16] F. Stapleton, L. Keay, K. Edwards, B. Holden, The epidemiology of microbial keratitis with silicone hydrogel contact lenses, Eye Contact Lens Sci. Clin. Pract. 39 (2013) 78–84.

[17] K. Richdale, L.T. Sinnott, E. Skadahl, J.J. Nichols, Frequency of and Factors Associated With Contact Lens Dissatisfaction and Discontinuation, Cornea. 26 (2007) 168–174.

[18] K. Dumbleton, C.A. Woods, L.W. Jones, D. Fonn, The impact of contemporary contact lenses on contact lens discontinuation., Eye Contact Lens. 39 (2013) 93–99.

[19] J.T. Jacob, Biocompatibility in the development of silicone-hydrogel lenses., Eye Contact Lens. 39 (2013) 13–19.

[20] L. Jones, N.A. Brennan, J. González-Méijome, J. Lally, C. Maldonado-Codina, T.A. Schmidt, L. Subbaraman, G. Young, J.J. Nichols, The TFOS International Workshop on Contact Lens Discomfort: report of the contact lens materials, design, and care subcommittee., Invest. Ophthalmol. Vis. Sci. 54 (2013) TFOS37-70.

[21] H. Thissen, T. Gengenbach, R. du Toit, D.F. Sweeney, P. Kingshott, H.J. Griesser, L. Meagher, Clinical observations of biofouling on PEO coated silicone hydrogel contact lenses, Biomaterials. 31 (2010) 5510–5519.

[22] J.J. Wang, F. Liu, Imparting antifouling properties of silicone hydrogels by grafting poly(ethylene glycol) methyl ether acrylate initiated by UV light, J. Appl. Polym. Sci. 125 (2012) 548–554.

[23] F. Sun, X. Li, P. Cao, J. Xu, Enhancing hydrophilicity and protein resistance of silicone hydrogels by plasma induced grafting with hydrophilic polymers, Chinese J. Polym. Sci. 28 (2010) 547–554.

[24] T. Goda, K. Ishihara, Soft contact lens biomaterials from bioinspired phospholipid polymers, Expert Rev. Med. Devices. 3 (2006) 167–174.

[25] C. Xu, R. He, B. Xie, M. Ismail, C. Yao, J. Luan, X. Li, Silicone hydrogels grafted with natural amino acids for ophthalmological application, J. Biomater. Sci. Polym. Ed. 27 (2016) 1354–1368.

[26] E.A. Balazs, G. Armand, Glycosaminoglycans and Proteoglycans of Ocular Tissues, in: Glycosaminoglycans Proteoglycans Physiol. Pathol. Process. Body Syst., S. Karger AG, Basel, 1982: pp. 480–499.

[27] K. Yoshida, Y. Nitatori, Y. Uchiyama, Localization of glycosaminoglycans and CD44 in the human lacrimal gland., Arch. Histol. Cytol. 59 (1996) 505–513.

[28] L.E. Lerner, D.M. Schwartz, D.G. Hwang, E.L. Howes, R. Stern, Hyaluronan and CD44 in the Human Cornea and Limbal Conjunctiva, Exp. Eye Res. 67 (1998) 481–484.

[29] M.Y. Fukuda K, Miyamoto Y, Hyaluronic acid in tear fluid and its synthesis by corneal epithelial cells., Asia-Pacific J Ophthalmol. 40 (1998) 62–65.

[30] G. Kogan, L. Soltés, R. Stern, P. Gemeiner, Hyaluronic acid: a natural biopolymer with a broad range of biomedical and industrial applications., Biotechnol. Lett. 29 (2007) 17–25.

[31] J.R.E. Fraser, T.C. Laurent, U.B.G. Laurent, Hyaluronan: its nature, distribution, functions and turnover, J. Intern. Med. 242 (1997) 27–33.

[32] T. Hamano, K. Horimoto, M. Lee, S. Komemushi, Sodium hyaluronate eyedrops enhance tear film stability., Jpn. J. Ophthalmol. 40 (1996) 62.

[33] M.C. Acosta, J. Gallar, C. Belmonte, The influence of eye solutions on blinking and ocular comfort at rest and during work at video display terminals., Exp. Eye Res. 68 (1999) 663–669.

[34] P.D. O'Brien, L.M.T. Collum, Dry eye: diagnosis and current treatment strategies., Curr. Allergy Asthma Rep. 4 (2004) 314–319.

[35] J.M. González-Méijome, A. Carla Da Silva, H. Neves, D. Lopes-Ferreira, A. Queirós, J. Jorge, Clinical performance and "ex vivo" dehydration of silicone hydrogel contact lenses with two new multipurpose solutions, Contact Lens Anterior Eye. 36 (2013) 86–92.

[36] A. Weeks, D. Morrison, J.G. Alauzun, M. a Brook, L. Jones, H. Sheardown, Photocrosslinkable hyaluronic acid as an internal wetting agent in model conventional and silicone hydrogel contact lenses., J. Biomed. Mater. Res. A. 100 (2012) 1972–1982.

[37] A. Weeks, L.N. Subbaraman, L. Jones, H. Sheardown, Physical entrapment of hyaluronic acid during synthesis results in extended release from model hydrogel and silicone hydrogel contact lens materials., Eye Contact Lens. 39 (2013) 179–185.

[38] K.-S. Jeong, H.-J. Kim, H.-L. Lim, G.-C. Ryu, E.-S. Seo, N.-H. You, J. Jun, Synthesis and biocompatibility of silicone hydrogel functionalized with polysaccharide, Bull. Korean Chem. Soc. 36 (2015) 1649–1653.

[39] A. Weeks, A. Boone, D. Luensmann, L. Jones, H. Sheardown, The effects of hyaluronic acid incorporated as a wetting agent on lysozyme denaturation in model contact lens materials., J. Biomater. Appl. 28 (2013) 323–333.

[40] A. Singh, P. Li, V. Beachley, P. McDonnell, J.H. Elisseeff, A hyaluronic acid-binding contact lens with enhanced water retention, Contact Lens Anterior Eye. 38 (2015) 79–84.

[41] C.-H. Lin, H.-L. Cho, Y.-H. Yeh, M.-C. Yang, Improvement of the surface wettability of silicone hydrogel contact lenses via layer-by-layer self-assembly technique, Colloids Surfaces B Biointerfaces. 136 (2015) 735–743.

[42] C. Cassinelli, M. Morra, A. Pavesio, D. Renier, Evaluation of interfacial properties of hyaluronan coated poly(methylmethacrylate) intraocular lenses., J. Biomater. Sci. Polym. Ed. 11 (2000) 961–977.

[43] B. Guan, H. Wang, R. Xu, G. Zheng, J. Yang, Z. Liu, M. Cao, M. Wu, J. Song, N. Li, T. Li, Q. Cai, X. Yang, Y. Li, X. Zhang, Establishing Antibacterial Multilayer Films on the Surface of Direct Metal Laser Sintered Titanium Primed with Phase-Transited Lysozyme, Sci. Rep. 6 (2016) 36408.

[44] M. Morra, Engineering of Biomaterials Surfaces by Hyaluronan, Biomacromolecules. 6 (2005) 1205–1223.

[45] C.E. Hoyle, C.N. Bowman, Thiol-Ene Click Chemistry, Angew. Chemie Int. Ed. 49 (2010) 1540–1573.

[46] C.M. Nimmo, M.S. Shoichet, Regenerative Biomaterials that "Click": Simple, Aqueous-Based Protocols for Hydrogel Synthesis, Surface Immobilization, and 3D Patterning, Bioconjug. Chem. 22 (2011) 2199–2209.

[47] J. Manhart, R. Kramer, R. Schaller, A. Holzner, W. Kern, S. Schlögl, Surface functionalization of natural rubber by UV-induced thiol-ene chemistry, Macromol. Symp. 365 (2016) 32–39.

[48] Y. Iwasaki, H. Matsuno, Metabolic delivery of methacryloyl groups on living cells and cell surface modification via thiol-ene "click" reaction, Macromol. Biosci. 11 (2011) 1478–1483.

[49] A. Köwitsch, Y. Yang, N. Ma, J. Kuntsche, K. Mäder, T. Groth, Bioactivity of immobilized hyaluronic acid derivatives regarding protein adsorption and cell adhesion, Biotechnol. Appl. Biochem. 58 (2011) 376–389.

[50] M. Korogiannaki, J. Zhang, H. Sheardown, Surface modification of model hydrogel contact lenses with hyaluronic acid via thiol-ene "click" chemistry for enhancing surface characteristics, J. Biomater. Appl. 32 (2017) 446–462.

[51] A.B. Lowe, Thiol-ene "click" reactions and recent applications in polymer and materials synthesis, Polym. Chem. 1 (2010) 17–36.

[52] H. Wang, H. Sun, H. Wei, P. Xi, S. Nie, Q. Ren, Biocompatible hyaluronic acid polymer-coated quantum dots for CD44+ cancer cell-targeted imaging, J. Nanoparticle Res. 16 (2014) 2621.

[53] Y. Huo, H. Ketelson, S.S. Perry, Ethylene oxide-block-butylene oxide copolymer uptake by silicone hydrogel contact lens materials, Appl. Surf. Sci. 273 (2013) 472–477.

[54] P.J. Cumpson, Angle-resolved XPS and AES: Depth-resolution limits and a general comparison of properties of depth-profile reconstruction methods, J. Electron Spectros. Relat. Phenomena. 73 (1995) 25–52.

[55] A.S. McFarlane, Efficient Trace-labelling of Proteins with Iodine, Nature. 182 (1958) 53–53.

[56] R. Mencucci, D.E. Pellegrini-Giampietro, I. Paladini, E. Favuzza, U. Menchini, T. Scartabelli, Azithromycin: assessment of intrinsic cytotoxic effects on corneal epithelial cell cultures., Clin. Ophthalmol. 7 (2013) 965–971.

[57] E.B. Getz, M. Xiao, T. Chakrabarty, R. Cooke, P.R. Selvin, A comparison between the sulfhydryl reductants tris(2-carboxyethyl)phosphine and dithiothreitol for use in protein biochemistry, Anal. Biochem. 273 (1999) 73–80.

[58] S.J. Bryant, C.R. Nuttelman, K.S. Anseth, Cytocompatibility of UV and visible light photoinitiating systems on cultured NIH/3T3 fibroblasts in vitro., J. Biomater. Sci. Polym. Ed. 11 (2000) 439–457.

[59] C.E. Hoyle, A.B. Lowe, C.N. Bowman, Thiol-click chemistry: a multifaceted toolbox for small molecule and polymer synthesis, Chem. Soc. Rev. 39 (2010) 1355–1387.

[60] N.B. Cramer, C.N. Bowman, Kinetics of thiol-ene and thiol-acrylate photopolymerizations with real-time fourier transform infrared, J. Polym. Sci. Part A Polym. Chem. 39 (2001) 3311–3319.

[61] R.A. Stile, T.A. Barber, D.G. Castner, K.E. Healy, Sequential robust design methodology and X-ray photoelectron spectroscopy to analyze the grafting of hyaluronic acid to glass substrates, J. Biomed. Mater. Res. 61 (2002) 391–398.

[62] M. Morra, C. Cassineli, Non-fouling properties of polysaccharide-coated surfaces, J. Biomater. Sci. Polym. Ed. 10 (1999) 1107–1124.

[63] S. Hajati, S. Tougaard, XPS for non-destructive depth profiling and 3D imaging of surface nanostructures, Anal. Bioanal. Chem. 396 (2010) 2741–2755.

[64] C. Ton-That, A. A. G. Shard, R.H. Bradley, Thickness of spin-cast polymer thin films determined by angle-resolved XPS and AFM tip-scratch methods, Langmuir. 16 (2000) 2281–2284.

[65] C. Karlgard, D.K. Sarkar, L.W. Jones, C. Moresoli, K.T. Leung, Drying methods for XPS analysis of PureVision™, Focus® Night&Day™ and conventional hydrogel contact lenses, Appl. Surf. Sci. 230 (2004) 106–114.

[66] B.J. Tighe, A decade of silicone hydrogel development: surface properties, mechanical properties, and ocular compatibility., Eye Contact Lens. 39 (2013) 4–12.

[67] A.S. Mikhail, J.J. Ranger, L. Liu, R. Longenecker, D.B. Thompson, H.D. Sheardown, M.A. Brook, Rapid and Efficient Assembly of Functional Silicone Surfaces Protected by PEG: Cell Adhesion to Peptide-Modified PDMS, J. Biomater. Sci. Polym. Ed. 21 (2010) 821–842.

[68] C. Maldonado-codina, P.B. Morgan, In vitro water wettability of silicone hydrogel contact lenses determined using the sessile drop and captive bubble techniques, J. Biomed. Mater. Res. Part A. 83A (2007) 496–502.

[69] N. Keir, L. Jones, Wettability and silicone hydrogel lenses: a review., Eye Contact Lens. 39 (2013) 100–108.

[70] L.C. Thai, A. Tomlinson, W.H. Ridder, Contact lens drying and visual performance: the vision cycle with contact lenses., Optom. Vis. Sci. 79 (2002) 381–388.

[71] S. Tonge, L. Jones, S. Goodall, B. Tighe, The ex vivo wettability of soft contact lenses., Curr. Eye Res. 23 (2001) 51–59.

[72] O.N. Tretinnikov, Y. Ikada, Dynamic wetting and contact angle hysteresis of polymer surfaces studied with the modified Wilhelmy balance method, Langmuir. 10 (1994) 1606–1614.

[73] M.L. Read, P.B. Morgan, J.M. Kelly, C. Maldonado-Codina, Dynamic contact angle analysis of silicone hydrogel contact lenses., J. Biomater. Appl. 26 (2011) 85–99.

[74] A. Köwitsch, M. Jurado Abreu, A. Chhalotre, M. Hielscher, S. Fischer, K. Mäder, T. Groth, Synthesis of thiolated glycosaminoglycans and grafting to solid surfaces., Carbohydr. Polym. 114 (2014) 344–351.

[75] B. Tighe, Silicone hydrogel materials – How do they work?, in: D.F. Sweeney (Ed.),

Silicone Hydrogels Rebirth Contin. Wear Contact Lenses, Butterworth-Heinemann, Oxford, 2000: pp. 1–21.

[76] E. Regoeczi, Iodine-Labeled Plasma Proteins Vol. 1, CRC Press, Boca Raton, FL, 1984.

[77] F.P. Carney, C.A. Morris, B. Milthorpe, J.L. Flanagan, M.D.P. Willcox, In Vitro Adsorption of Tear Proteins to Hydroxyethyl Methacrylate-Based Contact Lens Materials, Eye Contact Lens Sci. Clin. Pract. 35 (2009) 320–328.

[78] B. Hall, L.W. Jones, J.A. Forrest, Competitive Effects from an Artificial Tear Solution to Protein Adsorption, Optom. Vis. Sci. 92 (2015) 781–789.

[79] J.L. Court, R.P. Redman, J.H. Wang, S.W. Leppard, V.J. Obyrne, S. a Small, a L. Lewis, S. a Jones, P.W. Stratford, A novel phosphorylcholine-coated contact lens for extended wear use., Biomaterials. 22 (2001) 3261–3272.

[80] H. Chen, M.A. Brook, Y. Chen, H. Sheardown, Surface properties of PEO-silicone composites: Reducing protein adsorption, J. Biomater. Sci. Polym. Ed. 16 (2005) 531–548.

[81] W. Feng, J.L. Brash, S. Zhu, Non-biofouling materials prepared by atom transfer radical polymerization grafting of 2-methacryloloxyethyl phosphorylcholine: Separate effects of graft density and chain length on protein repulsion, Biomaterials. 27 (2006) 847–855.

[82] J.D. Andrade, Interfacial phenomena and biomaterials., Med. Instrum. 7 (1973) 110–120.

[83] S. Chen, L. Li, C. Zhao, J. Zheng, Surface hydration: Principles and applications toward low-fouling/nonfouling biomaterials, Polymer (Guildf). 51 (2010) 5283–5293.

[84] Z. Ademović, S. Marić, P. Kingshott, Z. Iličković, Hydrogels from polyacrylic acid for reduction of bioadhesion on silicone contact lenses, Contemp. Mater. 1 (2014) 95–100.

[85] A. Huhtala, L. Salminen, H. Tähti, H. Uusitalo, Corneal models for the toxicity testing of drugs and drug releasing materials, in: Top. Multifunct. Biomater. Devices, 2008: pp. 1–24.

[86] E.A. Offord, N.A. Sharif, K. Macé, Y. Tromvoukis, E.A. Spillare, O. Avanti, W.E. Howe, A.M. Pfeifer, Immortalized human corneal epithelial cells for ocular toxicity and inflammation studies., Invest. Ophthalmol. Vis. Sci. 40 (1999) 1091–1101.

Chapter 5

Surface functionalized model contact lenses with a bioinspired Proteoglycan 4 grafted layer.

Authors: Myrto Korogiannaki, Michael Samsom, Tannin A. Schmidt, Heather Sheardown

Publication information:

This chapter has been submitted for peer-review (Manuscript ID: la-2018-01693k) and is reproduced/reprinted with permission from *ACS Langmuir*.

Abstract

Ocular dryness and discomfort is the primary reason for the discontinuation of contact lens wear. This is mainly due to poorly hydrated contact lens surfaces and increased friction, particularly at the end of the day, and can potentially cause reduced vision or even inflammation. Proteoglycan 4 (PRG4), also known as lubricin, is a mucinous glycoprotein with boundary lubricating properties, naturally found in the eye. It is able to prevent tear film evaporation and protect the ocular surface during blinking. Aiming to improve the interfacial interactions between the ocular surface and the contact lens, the synthesis and characterization of surface modified model contact lenses with PRG4 is described. Full-length recombinant human PRG4 (rhPRG4) was successfully grafted to the surface of model conventional and silicone hydrogel (SiHy) contact lenses via its somatomedin B-like end-domain using N,N'-carbonyldiimidazole (CDI) linking chemistry. Grafting was assessed by Fourier transform infrared spectroscopy - attenuated total reflectance (FTIR-ATR), X-ray photoelectron spectroscopy (XPS) and radioactive (I^{131}) labeling. Surface immobilization of rhPRG4 led to model conventional and SiHy materials with improved antifouling properties, without impacting optical transparency or causing any toxic effects to human corneal epithelial cells in vitro. The surface wettability and the boundary friction against human corneal tissue were found to be substrate-dependent, with only the rhPRG4-grafted model SiHy exhibiting reduced contact angle and kinetic friction coefficient compared to the unmodified

surfaces. Hence, clinical grade rhPRG4 can be an attractive candidate for the development of novel bioinspired SiHy contact lenses, providing improved comfort and overall lens performance.

Keywords

2-hydroxyethyl methacrylate (HEMA); silicone hydrogel; contact lens; proteoglycan 4 (PRG4)/lubricin; surface modification; protein deposition; lubrication

5.1. Introduction

Despite years of research, soft contact lens materials still suffer from significant limitations. Conventional hydrogel contact lenses are comprised of 2-hydroxyethyl methacrylate (HEMA) as well as methacrylic acid (MA), N-vinylpyrrolidone (NVP), vinyl alcohol (VA) or synthetic analogues, such as phosphorylcholine (PC) or glycerol methacrylate (GMA) to obtain high water content and low modulus [1]. However, even the highest water content conventional hydrogel contact lens materials do not possess sufficient oxygen permeability for extended wear. Moreover, high-water-content hydrogel contact lenses exhibit low tear strength, increased protein deposits and high dehydration rates [2]. Silicone hydrogel (SiHy) contact lenses were developed to overcome the oxygen permeability limitations of conventional hydrogel materials. Containing siloxane and/or fluorine polymer segments, these materials were designed to allow for overnight wear [3]. The biggest issue with these materials, though, is the surface mobility of the inherently hydrophobic siloxane components which compromise the surface hydrophilicity of silicone hydrogels and in turn may cause issues in surface wettability and fouling as occurs in biological environments [4].

Yet, ocular dryness and discomfort remain significant problems for wearers of both contact lens types, especially towards the end of the day [5], despite the progress made to improve the composition and surface characteristics of commercial contact lenses. Such symptoms are a major factor limiting their use or even leading to the discontinuation of contact lens wear [6,7]. Upon contact lens insertion in the eye, there is a dynamic interaction between the ocular surface, the tear film and the contact lens surface that plays an important role for the overall contact lens performance [8,9]. Therefore, tear related factors such as changes in biophysical and biochemical properties [10] as well as contact lens related properties, including surface wettability, effective

lens modulus and lubricity [11] must be considered. Clinical signs of the ocular surface, such as lid-wiper epitheliopathy and lid parallel conjunctival folds, that are associated with dryness and discomfort during contact lens wear [12,13] have been studied to determine their relationship with the contact lens properties, including friction. Interestingly, contact lens lubricity was found in some studies to be the principal contact lens property associated with contact lens discomfort [11,14–17].

In this study, surface modification was used to create an interface inspired by the corneal surface and tear film using a lubricating mucin-like glycoprotein that is naturally found on the ocular surface. Proteoglycan 4 (PRG4), also known as lubricin, is an extended polymeric nanostructured protein with a molecular weight of approximately 230 kDa. It has a hydrophobic globular somatomedin B (SMB)-like (N-terminus) and a hemopexin (PEX)-like (C-terminus) end domain, and a central mucinous region that is extensively glycosylated with β(1–3)Gal-GalNAc and partially capped with sialic acid (NeuAc) [18]. The abundant negatively charged and hydrated sugars of the central domain generate strong steric forces as well as repulsive forces through hydration that play an essential role in lubricin's lubricating property, while providing high degree of hydrophilicity [19]. PRG4 is able to also lubricate in the absence of a thick fluid film and hence acts as a boundary lubricant. Under physiological conditions (pH 7.4), PRG4 has a small net positive charge (pI 7.8–8.1) [20].

Lubricin is a major component of synovial fluid and as a boundary lubricant in the joints plays a critical role in the protection of cartilaginous surfaces against frictional forces, cell adhesion and protein deposition [21]. In the eye, PRG4 was found to be transcribed, translated and expressed by corneal and conjunctival epithelial cells [22] and in human meibomian gland secretions [23], suggesting that this molecule is responsible for preventing tear film evaporation and for protecting the ocular surface against the significant shear forces generated during blinking. Recently, a two-week, randomized double-masked study showed that lubricin supplementation rapidly led to significantly reduced signs and symptoms of dry eye disease without causing any adverse events, by improving the damage of the ocular surface epithelium, reducing inflammation on the eyelid and the conjunctiva as well as restoring a competent tear film [24]. PRG4 has also been previously shown to reduce the friction between the cornea-eyelid interface *in vitro,* further supporting its role as a natural boundary lubricant [22,25]. Interestingly, when the lubrication properties of PRG4 were examined for a hydrogel-cornea biointerface the results observed varied

with the contact lenses, depending on the nature of the hydrogel material and more specifically its surface properties [26–28]. Despite the good boundary lubrication of PRG4 for SiHy, the surface lubricity of conventional hydrogel contact lenses with hydrophilic surfaces was not improved by the presence of physiosorbed PRG4 [28,29]. Therefore, it is suggested that not all surfaces are good candidates for PRG4 to function as boundary lubricant. Depending on the surface chemistry and charge, the conformational and lubricating properties of PRG4 differ [18,30,31]. The lubricating properties of PRG4 are postulated to occur due to glycoprotein's ability to strongly adhere to the surface in an appropriate conformation. It has been shown that physical sorption of PRG4 on a hydrophobic or negatively charged surfaces results in the formation of a loop-like conformation with friction-lowering behavior, whereas on hydrophilic surfaces the molecule adopts an extended tail-like conformation mitigating its lubricating properties [18,30,31]. For positively charged surfaces, the conformation was speculated to be more complicated as both the central mucin domain and the end domain can be adsorbed [18,30]. Overall, PRG4 adhesion to the substrate is thought to occur by hydrogen bonding, hydrophobic as well as electrostatic interactions [18,30,31].

In this work, full-length recombinant human PRG4 (rhPRG4) was covalently tethered to model conventional and SiHy contact lens materials. We hypothesize that covalent attachment of rhPRG4 on the surface would improve the surface wettability, lubricity and resistance to protein deposition under physiological conditions, without compromising the bulk properties of the materials. PRG4 was grafted to the surface via its somatomedin B (SMB)-like (N-terminus) end-domain using N,N'-carbonyldiimidazole (CDI) linking chemistry. Full-length rhPRG4 was selected as it is characterized by appropriate high order structure, O-linked glycosylation, and boundary lubricating properties consistent with those of native PRG4 found on the ocular surface [27]. Recently, clinically tested full-length rhPRG4 was found to effectively reduce dry eye signs and symptoms, when applied in the form of eye drops [24]. In addition, using CDI linking chemistry allowed for the activity of surface tethered biological molecules to be maintained [32–34] without causing any adverse effect on human corneal epithelial cells [35]. It is therefore expected that these coated hydrogel materials may show better ocular compatibility than previous surface modified contact lenses, providing insight into the nature of surfaces necessary for end-of-day comfort in contact lens wearers. To the best of our knowledge, this is the first time that PRG4 has been grafted to the surface of soft polymeric materials.

5.2. Experimental Section

5.2.1. Chemicals and Reagents

3-methacryloxypropyl-tris-(trimethylsiloxy) silane (TRIS, ≥95%) was supplied by Gelest (Morrisville, PA, USA). The photoinitiator 1-hydroxy-cyclohexyl-phenyl-ketone (Irgacure® 184) was generously donated by BASF Chemical Company (Vandalia, IL, USA). Keratinocyte serum free medium (K-SFM) supplemented with human recombinant epidermal growth factor 1-53 (EGF 1-53) and bovine pituitary extract (BPE) was purchased from Thermo Fisher Scientific (Burlington, ON, Canada). The human corneal epithelial cell line (HCE-2 [50.B1] ATCC® CRL-11135™) was purchased from the American Type Culture Collection (Rockville, MD, USA). Full-length recombinant human PRG4 (rhPRG4) was a kind gift of Lubris BioPharma LLC (Boston, MA, USA) [27,36]. Human corneas (age: 63- 86) that were harvested and stored in Optisol-GS (Bausch & Lomb, Rochester, NY) at 4˚C prior to testing [26], were provided by the Southern Alberta Lions Eye Bank. These tissues were tested within 2 weeks of harvest. Approval for tissue use was granted by the University of Calgary Conjoint Health Research Ethics Board. All other chemicals, reagents and proteins used were obtained from Sigma Aldrich (Oakville, ON, Canada).

5.2.2. Synthesis of model pHEMA and pHEMA-*co*-TRIS hydrogel materials

Prior to synthesis, 2-hydroxyethylmethacylate (HEMA), TRIS and ethylene glycol dimethacrylate (EGDMA) were passed through a custom-made column filled with inhibitor remover for the removal of monomethyl ether hydroquinone (MEHQ). Model pHEMA hydrogels were generated by mixing the HEMA monomer, the EGDMA crosslinker (2 mol%) and the photoinitiator Irg.184 (0.5 wt%) together for 15 minutes. For the synthesis of model SiHy pHEMA-*co*-TRIS, HEMA and TRIS were added in a 90:10 weight ratio and mixed with EGDMA (3.5 mol%) under vigorous stirring conditions for 30 minutes, followed by the dissolution of the photoinitiator Irg.184 (0.5 wt%). The prepolymer mixture of either pHEMA or pHEMA-*co*-TRIS was then injected into a custom-made UV-transparent acrylic mold which was in turn placed into a 400 W UV chamber (365 nm, Cure Zone 2 Con-trol-cure, Chicago, IL, USA) for 10 minutes for the polymerization reaction. The thickness of the resulting disks could be controlled by the using an adjustable spacer in the acrylic mold. Following initiation of polymerization, the hydrogel materials were post-cured overnight at room temperature, demolded and immersed in Milli-Q

water for 18 hours. Swollen hydrogels were cut using a cork borer into discs with a diameter 6.35 mm (1/4“) and thickness 0.5mm and used for all the experiments with the exception of the friction measurement where the discs used were 7.94 mm (5/16“) in diameter and 1 mm thick due to experimental restrictions. For the extraction of unreacted chemicals, discs were initially placed into a 1:1 vol% methanol:water solution for 12 hours and then into Milli-Q water for 36 hours. Discs were dried at room temperature until further use.

5.2.3. Synthesis of CDI-activated pHEMA and pHEMA-*co*-TRIS hydrogels

Prior to the CDI activation step, both pHEMA and pHEMA-*co*-TRIS discs were dried under vacuum overnight at 25ºC, while the vials and pipettes used were rinsed with acetone and dried overnight at 70ºC to eliminate any trace of humidity. For the surface activation reaction, CDI in anhydrous 1,4-dioxane (40 mM per disc) was added dropwise in a 20 ml glass vial that contained the pHEMA or pHEMA-*co*-TRIS discs, under a dry N_2 atmosphere. After stirring for 3 hours at 37ºC, samples were rinsed 3 times with anhydrous 1,4-dioxane, with a 5 minute sonication between each rinse, to remove any unreacted CDI. The discs were dried under N_2 and used immediately for the immobilization reaction of rhPRG4.

5.2.4. Synthesis of surface rhPRG4-grafted pHEMA and pHEMA-*co*-TRIS hydrogels

For the surface grafting reaction, each disc was placed vertically into an eppendorf tube filled with 1ml of rhPRG4 aqueous solution (0.3 mg/ml, pH 9.2). The eppendorf tubes were vortexed (800 rpm) for 24 hours at 4ºC for the completion of the immobilization procedure. The discs were then washed with an excess of PBS (pH 7.4) to remove ungrafted rhPRG4. Samples were stored in Milli-Q water at 4ºC until further use.

5.2.5. Surface Chemistry Characterization

5.2.5.1. Fourier Transform Infrared Spectroscopy - Attenuated Total Reflectance (FTIR – ATR)

The surface chemistry of dehydrated unmodified, CDI-activated and surface rhPRG4-grafted pHEMA and pHEMA-*co*-TRIS discs was determined using Fourier transform infrared spectroscopy (FTIR) in attenuated total reflectance (ATR) mode (Vertex 70 FTIR spectrometer,

Bruker Instruments, Billerica, MA, USA) equipped with a diamond ATR cell. Measurements on dehydrated samples were performed in the frequency range of 600-3000 cm^{-1} (64 scans, 4 cm^{-1} resolution) at room temperature.

5.2.5.2. X-ray Photoelectron Spectroscopy (XPS)

The elemental composition of unmodified and rhPRG4-grafted pHEMA and pHEMA-*co*-TRIS surfaces was determined on vacuum-dried discs using the PHI Quantera II XPS scanning spectrometer (Physical Electronics (Phi), Chanhassen, MN, USA) equipped with a monochromatic anode Al Kα X-ray source (1486.7 eV) operating at 50W 15kV. The survey spectra used for elemental analysis were collected from scans taken over a binding energy range of 0-1100 eV with the photoelectron take-off angle set at 45°. An analyzer pass energy of 280 eV allowed for rapid data acquisition and accurate quantitative analysis. A dual beam charge compensation system was used for neutralization of all samples (beam diameter 200 μm). The instrument was calibrated using a sputter-cleaned piece of Ag, where the Ag $3d_{5/2}$ peak had a binding energy of 368.3 ± 0.1 eV and full width at half maximum for the Ag $3d_{5/2}$- peak was at least 0.52 eV. High resolution N_{1s} scans were obtained with a pass energy set at 55 eV for higher energy resolution. The binding energy scale was referenced to the C_{1s} peak set at 285.0 eV. The operating pressure did not exceed 2 x 10^{-8} Torr. Data analysis of low-resolution spectra was performed using PHI MultiPak Version 9.4.0.7 software in order to calculate the elemental compositions of the surfaces from the integrated intensities of the XPS peaks and to peak fit the high-resolution spectra. At least two different spots per disc were examined for each sample.

5.2.6. Quantification of surface grafted rhPRG4 – I^{131}-rhPRG4

For the quantification of the rhPRG4 that was present on the surface of the pHEMA and pHEMA-*co*-TRIS materials, rhPRG4 was radiolabeled with $I^{131}Na$ using the iodine monochloride method (ICl) [37]. After the radiolabeling reaction, the I^{131}-rhPRG4 solution was dialyzed extensively against PBS (pH 7.4) using Slide-A-Lyzer™ Dialysis Cassette (Thermo Fisher Scientific, Burlington, ON, Canada) for two days to remove unreacted iodide and glycine. Glycine buffer (2 M, pH 8.8) was used during the radiolabeling procedure and contains primary amines that can react with CDI-target groups, impeding the surface grafting of rhPRG4. The percentage

of free iodine, determined by the trichloroacetic acid precipitation assay, was less than 3% of the total radioactivity of I^{131}-rhPRG4. For the reaction incubation solution, 5% I^{131}-rhPRG4 was mixed with rhPRG4 solution to give a final concentration of 0.3 mg/ml. All other conditions for the surface grafting reaction were the same as above. At the end of the reaction, samples were washed with PBS (pH 7.4) (5 ml/disc for 12 hours, 2 cycles). The discs were further stored in PBS (pH 7.4, 2 ml/disc) for the next 7 days at room temperature, with PBS being changed daily. For the quantification of the chemically attached rhPRG4 on the surface of CDI-activated pHEMA and pHEMA-*co*-TRIS discs, the radioactivity of the discs was measured immediately after the immobilization reaction, after the first two PBS wash steps (wash 1: 12 hours and wash 2: day 1) and on the 2nd, 4th and 7th day of incubation using a gamma counter (Perkin Elmer Wallac Wizard 1470 Automatic Gamma Counter, Wellesley, MA, USA). Before each reading, the discs were gently blotted with a Kimwipe® and placed in a counting vial (5 ml non-pyrogenic, polypropylene round-bottom tube). At the end of the reading, the discs were then placed back in the medium for the next measurement. A standard calibration curve was used to convert the measured radioactivity (cpm) into the surface density of rhPRG4 ($\mu g/cm^2$). The decay of the isotope over time was taken into consideration by measuring the radioactivity of the standard solutions at each time point. The surface density of physically sorbed rhPRG4 on the surface of unmodified pHEMA and pHEMA-*co*-TRIS discs was also determined, following the protocol above.

5.2.7. Contact Angle Measurements

The contact angles of unmodified and rhPRG4-grafted pHEMA and pHEMA-*co*-TRIS surfaces were measured using static captive bubbles on an Optical Contact Angle Analyzer - OCA 35 (Dataphysics Instruments, Germany). Briefly, an air bubble with a volume of 10 µl was dispensed on the surface of a fully hydrated disc which had been previously immersed into a chamber filled with Milli-Q water. The contact angle of both sides of each disc was measured. The Milli-Q water in the chamber was replaced every time a new set of samples was assessed. All measurements were done at room temperature.

5.2.8. Quantification of Protein Deposition – Lysozyme and Human Serum Albumin

Radiolabeled lysozyme (from chicken egg white) and human serum albumin (HSA) were used for the quantification of the amount of protein sorbed on the surface of the pHEMA and pHEMA-*co*-TRIS hydrogels. The proteins were radiolabeled with $Na^{125}I$ using the iodine monochloride (ICl) method; the iodination procedure was that same as was used with the I^{131}-rhPRG4. The protein deposition protocol and data analysis were as previously described [38]. The percentage of free iodine determined by the trichloroacetic acid precipitation assay was less than 1% of total radioactivity for both proteins.

For the quantification of the deposited protein, a single protein solution (1 mg/ml, PBS pH 7.4) was prepared, containing 5% I^{125}-lysozyme or I^{125}-HSA. Initially, fully hydrated unmodified and rhPPRG4-grafted pHEMA and pHEMA-*co*-TRIS hydrogel discs were individually incubated in 250 μl of the single protein-containing solution at room temperature for 6 hours. Discs were placed vertically in 96-well plates to ensure that both surfaces were exposed to solution. At the end of the incubation time, the discs gently blotted with a Kimwipe® and then rinsed 3 times with PBS (pH 7.4) (10-minute wash intervals) to remove any loosely bound protein. The rest of the procedure for the determination of the surface density of each protein sorbed was the same as that followed for the quantification of rhPRG4 surface density above.

5.2.9. *In vitro* friction measurement – Boundary Lubrication Test Setup

The boundary lubricating ability of the rhPRG4 grafted layer was investigated using an *in vitro* ocular friction test at a human cornea-hydrogel disc biointerface. The experimental setup and protocol used herein were as previously described [26,39,40]. Briefly, samples were tested using the BOSE ELF3200 biomechanical testing machine equipped with axial and rotational actuators, and axial load (N) and torque (τ) sensors. The resected cornea was prepared and placed on the bottom rotational actuator compartment. The annulus of fully hydrated unmodified (control) and rhPRG4-grafted pHEMA and pHEMA-*co*-TRIS discs was firmly fixed to a custom holder which in turn was placed on the linear actuator, forming the upper articulating surface. The linear actuator was used to articulate the hydrogel disc with the cornea and to control axial load, while the rotational actuator was used to slide the cornea against the material. Axial load (N) and torque (τ) were collected during sliding to calculate the friction coefficients.

After mounting the samples, the two surfaces were immersed and allowed to equilibrate in a chamber containing 300 μl of Bausch & Lomb Saline Plus contact lens solution (Bausch & Lomb, Rochester, NY, USA) at room temperature. A three-position axial compression was followed so as to achieve entire contact of the cornea-disc interface. Once entire contact was achieved in each axial position, a 12 second time interval (dwell time) allowed for stress relaxation of the corneal tissues under load. The cornea-disc samples were subjected to relative articulations (four revolutions in both rotation directions) at four effective sliding velocities (v_{eff}) at 0.3 mm/s, 1.0 mm/s, 10 mm/s, and 30 mm/s, using a repeated measures sequence under pressures of approximately 18 to 25 kPa. Normal load (N) (axial forces) and torque (τ) were recorded at 20 Hz during rotations to calculate the friction coefficients (μ). The boundary lubrication properties of the hydrogels were evaluated by calculating the static (μ_{static}, N_{eq}) (N_{eq}: equilibrium axial load measured the instant after the 12-sec stress relaxation duration) and kinetic ($<\mu_{kinetic}>$) friction coefficients (‹› denotes the kinetic equilibrium mean) of all samples as previously described [26,27,29]. The static friction coefficient (μ_{static}, N_{eq}) measures the force to initiate surface movement while kinetic friction coefficient ($<\mu_{kinetic}>$) measures the force to maintain steady state movement. In each test, a preconditioning run using a PDMS disk in the place of a model hydrogel disc was followed by the unmodified and then the rhPRG4-grafted discs. A full test sequence was done on a single corneal tissue sample and was considered to be one repeat when performing statistical analysis.

5.2.10. Optical Transparency

The impact of the surface immobilization of rhPRG4 on the optical transparency of the pHEMA and pHEMA-*co*-TRIS hydrogels was assessed by measuring the light transmittance (%) of fully hydrated hydrogel discs in the range 400-750 nm at ambient temperature, using a UV–Vis spectrophotometer (Spectramax Plus 384, Molecular Devices, Corp, Sunnyvale, CA, USA). The discs were immersed in 100 μl of Milli-Q water in a 96-well plate during the measurement.

5.2.11. Equilibrium Water Content (EWC)

The hydrogel discs were soaked in Milli-Q water for 24 hours, under stirring conditions at ambient temperature to achieve equilibrium. The fully hydrated discs were removed, blotted with a Kimwipe® to remove any excess water and weighed (W_{wet}). The samples were then placed into

a 37ºC oven overnight and then into a vacuum oven for 12 hours to completely remove any traces of water and subsequently weighed (W_{dry}) again. The equilibrium water content (EWC) of the hydrogels was determined using the equation below:

$$EWC\% = \frac{W_{wet} - W_{dry}}{W_{wet}} \cdot 100\% \qquad (5.1)$$

5.2.12. Cell viability – MTT assay

A study was conducted to assess the effect of rhPRG4 grafting on the pHEMA and pHEMA-*co*-TRIS substrates via CDI chemistry on cell viability using the 3-(4,5-dimethylthiazol-2-yl)-2,5-diphenyltetrazolium bromide (MTT) assay. Briefly, immortalized human corneal epithelial cells (HCEC) were cultured in keratinocyte serum free medium (K-SFM) supplemented with human recombinant epidermal growth factor 1-53 (EGF 1-53) and bovine pituitary extract (BPE) for one week in a 5% CO_2 at 37°C atmosphere. The HCEC were then subcultured and seeded in a flat bottom 96-well polystyrene culture plate (Corning, Costar™, New York, USA) (1.5×10^4 HCEC per well) with 100 µl culture medium and incubated in 5% CO_2 at 37°C. Following a 24-hour incubation period to ensure adhesion of the cells, the cell medium was replaced with fresh K-SFM (250 µl). The hydrogel discs, previously extensively washed with sterilized PBS (pH 7.4) for 6 hours, were then placed vertically in the cell-containing well without touching the bottom and incubated in the cell culture incubator for 24 hours. At the end of the incubation period, the hydrogel discs were discarded and the medium was aspirated. Each well was gently rinsed with PBS (pH 7.4), and 10 µl of MTT solution (5 mg/ml in PBS pH 7.4) with 100 µl of PBS were added. The plate was then covered with foil and placed in the cell incubator for 4 hours (5% CO_2, 37°C) to allow the soluble yellow MTT to be reduced into dark blue insoluble formazan crystals by the metabolically active cells. The formazan crystals were dissolved into 50 µl of DMSO per well, and after 5 minutes of shaking at room temperature under dark conditions, the absorbance was measured spectrophotometrically at 540 nm (Spectramax Plus 384, Molecular Devices, Corp, Sunnyvale, CA, USA). All results were normalized to cells grown in wells without hydrogel discs which were assumed to possess 100% cell viability.

5.2.13. Statistical Analysis

Experiments were performed with a minimum of 4 repeats (discs) and data were verified in at least 2 independent experiments, unless otherwise stated. For comparative studies, statistical analysis was conducted using a one-way analysis of variance (ANOVA) and Tukey's HSD for post-hoc comparisons using Statistica 10 (StatSoft Inc. Tulsa, OK, USA). A p value of 0.05 was set as the threshold of statistical significance. All data were expressed as mean ± standard deviation (SD) with the exception of friction coefficients where data were expressed as mean ± standard error of the mean (SEM).

5.3. Results and Discussion

5.3.1. Synthesis of surface rhPRG4-grafted pHEMA and pHEMA-*co*-TRIS hydrogels via CDI chemistry

The reaction scheme illustrating the surface CDI linking chemistry for rhPRG4 immobilization on pHEMA and pHEMA-*co*-TRIS hydrogels is depicted in Scheme 1. CDI functionalization promotes the condensation between the hydroxyl (–OH) and amine ($–NH_2$) groups to covalently attach the glycoprotein onto the model hydrogel contact lens surfaces via covalent bonds [41].

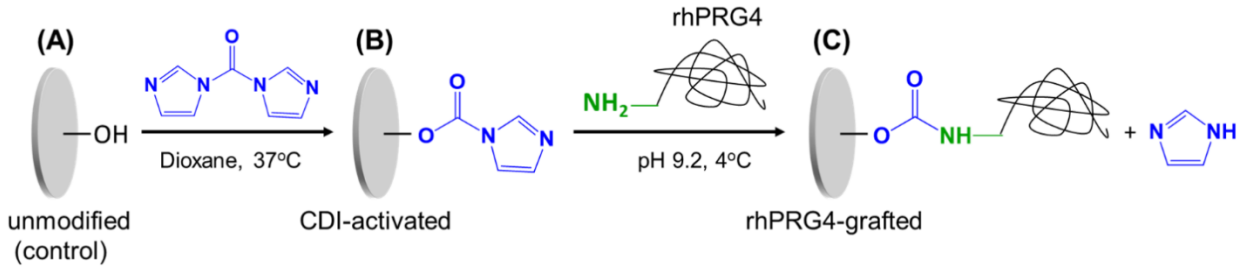

Figure 5.1: Schematic illustration of the synthesis of rhPRG4-grafted pHEMA and pHEMA-*co*-TRIS hydrogels via CDI linking chemistry. (rhPRG4: recombinant human proteoglycan 4; CDI: N,N'-carbonyldiimidazole)

The chemistry of the surfaces was initially determined by FTIR-ATR. The observed decrease in the broad band of the -OH groups at approximately 3405 cm^{-1} in combination with the appearance of two new peaks at approximately 1765 cm^{-1} and 1475 cm^{-1} which were attributed to

the asymmetric stretch of the CDI carbonyl groups and the imidazole cycle characteristic bands respectively [42], indicated successful incorporation of imidazolyl-carbamate groups on the surface of both hydrogels (Figures 5.2A and 5.2B, graph (b)). The peaks at 3130 cm^{-1} and 1530 cm^{-1} which were due to the presence of the amide II of the carbamate in activated surfaces as well as the disappearance of the typical HEMA stretching band of the alcohol group (C-O) at 1074 cm^{-1} upon CDI reaction, also confirmed the successful attachment of the intermediate linkage. For the pHEMA-*co*-TRIS hydrogels, the additional adsorption peaks at approximately 1276 cm^{-1}, 1025 cm^{-1} and 876 cm^{-1} were attributed to Si-CH_3 and Si-O groups of the SiHy materials [43] (Figure 5.2B). Finally, successful covalent attachment of rhPRG4 on both pHEMA and pHEMA-*co*-TRIS surfaces was indicated by the broad peak of 3600-3250 cm^{-1} which was reinforced by hydrogen stretching vibrations of O-H and N-H from the hydroxyl, carboxyl, amine and amide groups of rhPRG4 [41], while the new peak at approximately 1640 cm^{-1} was assigned to the amide groups of the glycoprotein (Figures 5.2A and B, graph (c)).

The atomic composition of the surfaces before and after each modification step was also determined by XPS. Since the unmodified (control) pHEMA and pHEMA-*co*-TRIS do not contain nitrogen (N) in their structure, the presence of an N_{1s} peak in the low resolution XPS spectra was used to monitor the CDI-tethered to the surfaces (Table 5.1). The further increase in the N_{1s} signal on the rhPRG4-modified surfaces was attributed to the successful covalent attachment of the glycoprotein on the pretreated surfaces. The decreasing trend of the Si_{2p} percentage for the pHEMA-*co*-TRIS sample was another indication of successful rhPRG4 grafting, with the glycoprotein layer masking the underlying silicone-based substrate. To further confirm the covalent attachment of the glycoprotein on the CDI-modified surfaces, high resolution N_{1s} spectra were collected before and after the rhPRG4 conjugation reaction and compared. Analysis of the N_{1s} high resolution spectra showed that CDI-activated surfaces had the characteristic imidazole derived-doublet peak with maxima at approximately 399 eV and 401 eV for pHEMA, and 399.4 eV and 401.3 eV for pHEMA-*co*-TRIS (Figures 5.2C and D), attributed to the two distinct molecular environments of the imidazole-carbamate nitrogens [32]. More precisely, the first peak centered around 399.1 eV included the contribution of the nitrogen of the carbamate groups and likely the nitrogen of unreacted imidazole groups, while the other peak at 400.8 eV was assigned to the inner imidazole-ring nitrogen [44]. Upon rhPRG4 grafting reaction, the peak at 401 eV was significantly decreased whereas the other was shifted, forming a more dominant peak at 399.8 eV

for both pHEMA and pHEMA-*co*-TRIS hydrogels (Figures 5.2E and F). The latter peak corresponded to the replacement of the imidazole ring structure with the amide bond [45], suggesting the successful covalent attachment of rhPRG4 on the material surface.

CDI treatment has been shown to be an easy, effective, and rapid method for surface modification with biomolecules with little effect on the bulk properties of the materials [32,41,46]. In contrast to other immobilization methods [47–49], CDI chemistry is advantageous for affinity adsorbent preparation processes because there is no need for an intermediate basic catalyst as the alkyl carbamate linkage formed between the hydroxyl support and the amine-containing ligand is neutral, decreasing thus the chance of non-specific adsorption by ion exchange [50]. For the surface grafting reaction of rhPRG4 to the model pHEMA and pHEMA-*co*-TRIS hydrogels, basic pH was chosen so as to increase the degree of deprotonation of the glycoprotein amine groups, allowing for a more efficient reaction with the imidazole ring. The literature suggests that the remaining active CDI groups upon surface grafting reaction can be removed by hydrolysis using carbonate buffer [50].

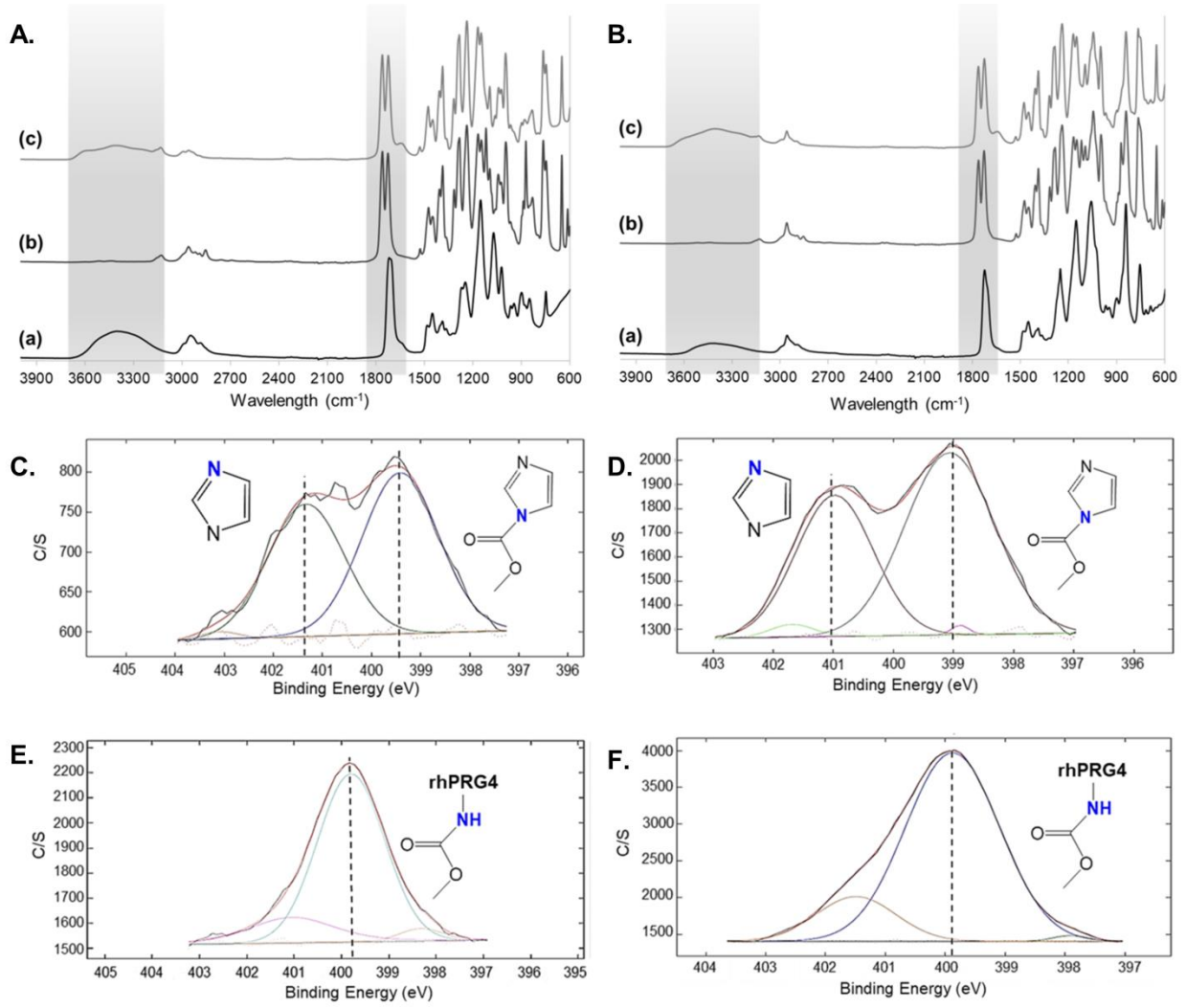

Figure 5.2: Characterization of surface chemistry. FTIR-ATR adsorption spectra of (A) pHEMA and (B) pHEMA-*co*-TRIS for (a) unmodified (control), (b) CDI-activated and (c) rhPRG4-grafted hydrogel surfaces (600-4000 cm^{-1})**.** High-resolution N_{1s} XPS spectra for (C, D) CDI-activated and (E, F) rhPRG4-grafted pHEMA and pHEMA-*co*-TRIS hydrogel surfaces respectively (395-405 eV).

Table 5.1: Atomic composition (%) of the surface of non-modified, CDI-activated and surface rhPRG4-grafted pHEMA and pHEMA-*co*-TRIS hydrogel discs from low resolution XPS spectra (n=3).

sample	C_{1s}	O_{1s}	N_{1s}	Si_{2p}	S_{2p}
pHEMA	70.6 ± 0.9	28.2 ± 0.8	-	1.3 ± 0.04	-
CDI-pHEMA	72.2 ± 1.2	21.5 ± 0.8	4.9 ± 0.1	1.4 ± 0.1	-
rhPRG4-pHEMA	63.8 ± 0.1	23.8 ± 0.03	10.6 ± 0.3	1.2 ± 0.1	0.27 ± 0.01
pHEMA-*co*-TRIS	67.0 ± 1.8	23.3 ± 1.9	-	9.8+0.6	-
CDI-pHEMA-*co*-TRIS	63.8 ± 0.2	23.1 ± 0.4	3.5 ± 0.2	9.6 ± 0.05	-
rhPRG4-pHEMA-*co*-TRIS	62.0 ± 0.3	23.2 ± 0.1	5.1 ± 0.29	8.8 ± 0.2	-

5.3.2. Surface density of rhPRG4 – Quantification of I^{131}-rhPRG4

Figure 5.3 demonstrates the surface density of rhPRG4 on each sample as a function of the time. Immediately after the reaction (24 hours), the amount of rhPRG4 on the rhPRG4-grafted pHEMA sample was found to be 857.8 ± 64.5 ng/cm^2 while the surface density of the physically sorbed rhPRG4 for the unmodified (control) pHEMA sample was 577.3 ± 24.5 ng/cm^2, a 33% difference ($p<0.0003$). In contrast, the surface density of rhPRG4 for the rhPRG4-grafted pHEMA-*co*-TRIS hydrogels (727.4 ± 22.9 ng/cm^2) was similar to that of the physically sorbed rhPRG4 for the unmodified (control) pHEMA-*co*-TRIS sample (751.8 ± 39.8 ng/cm^2) ($p=0.9$). After the first 24 hours of incubation in PBS (pH 7.4), the surface density of rhPRG4 for the surface modified pHEMA and pHEMA-*co*-TRIS samples did not change significantly over time (rhPRG4-grafted pHEMA: 582.8 ± 19.7 ng/cm^2 and rhPRG4-grafted pHEMA-*co*-TRIS: 492.2 ± 10.0 ng/cm^2) ($p>0.05$), suggesting that the 24-hour washing step with PBS was adequate for the effective removal of the loosely bound rhPRG4. However, for the unmodified pHEMA and pHEMA-*co*-TRIS samples, the amount of physically sorbed rhPRG4 was gradually decreased over the course of the 7-day wash period.

Quantification of the rhPRG4 on the surface modified hydrogels further confirmed that the surface density of rhPRG4 on the rhPRG4-grafted pHEMA samples was slightly higher than that

of the respective model SiHy ($p<0.01$). Interestingly, the amount of the glycoprotein detected on the unmodified (control) hydrogels was not completely removed over the course of 7 days, suggesting that some of the physically sorbed rhPRG4 was tightly and irreversibly bound on these surfaces. Moreover, the affinity of the amphiphilic rhPRG4 for the unmodified (control) pHEMA-*co*-TRIS sample was significantly stronger than that of the respective pHEMA surface ($p<0.0003$), indicating that partitioning may occur between the silicone domains of the SiHy and the hydrophobic domains of the rhPRG4. A recent study by Samsom et al. [29] demonstrated that rhPRG4 had higher affinity for PDMS and for commercial SiHy contact lenses (senofilcon A) than for the hydrophilic conventional contact lenses (etafilcon A). In fact, PRG4 is proposed to strongly adsorb on hydrophobic surfaces through the non-polar amino acid residues of the globular end-domains regions of the glycoprotein via hydrophobic interactions [18,19,31,51]. On the other hand, the low degree of rhPRG4 physical deposition on pHEMA surfaces may reflect the absence of strong long-range electrostatic or hydrophobic interactions between rhPRG4 molecules and the relatively hydrophilic non-polar pHEMA surfaces [51], as well as potentially weak van der Waals forces or hydrogen bonding between the pHEMA bonding active sites (-OH and C=O groups) [52–54] and the rich in hydrogen bond donor site of the galactose and sialic acid groups of the glycosylation layer of the rhPRG4 mucin domain [51]. It was therefore assumed that the amount of rPRG4 determined for the CDI-activated pHEMA and pHEMA-*co*-TRIS surfaces was not only covalently attached and but also physically adsorbed. Finally, it is important to note that PRG4 in its native state can form intra- and intermolecular disulfide bonds because of the availability of cysteine in the C- and N-termini domains. Therefore, since rhPRG4 was in its native form and not reduced or alkylated, dimers and possibly oligomers can be present in the reaction solution potentially impeding the degree of surface grafting.

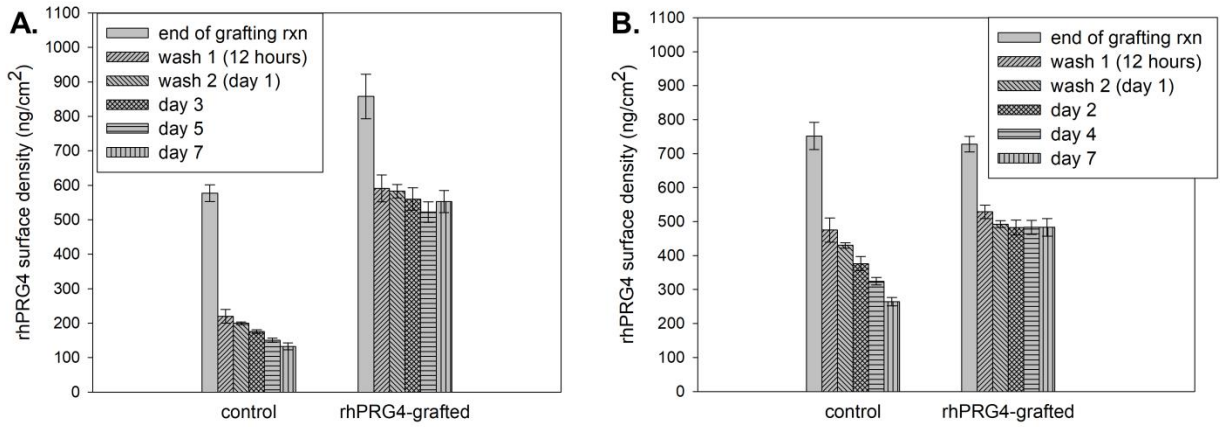

Figure 5.3: Quantification of the surface bound rhPRG4. The surface density (±SD) of physisorbed or grafted rhPRG4 for (A) pHEMA and (B) pHEMA-*co*-TRIS hydrogels was determined (n=4).

5.3.3. Contact angle measurements

An important property for contact lenses is sufficient surface wettability so that the tear film can spread and remain stable on the surface of the lens, without breaking up prematurely [11]. Contact lenses exhibiting poor wettability have been associated with reduced optical quality, increased surface deposition and discomfort [3,55]. In this work, we utilized the captive-bubble technique in order to maintain fully hydrated conditions during the contact angle measurement, since this should correlate more realistically with the on-eye conditions. Another advantage of this technique is that neither the air bubble nor the lens surface is susceptible to surrounding atmospheric conditions.

In vitro measurement of the surface wettability was achieved by measurement of the contact angle using the captive bubble technique. As shown in Figure 5.4, the contact angle of the rhPRG4-grafted pHEMA sample was slightly higher than that of the unmodified (control) pHEMA sample ($p<0.002$). However, the contact angle on rhPRG4-grafted pHEMA-*co*-TRIS was decreased (35%) when compared to the unmodified (control) sample ($p<0.0002$). Lower contact angles suggest improved surface wettability.

The immobilization of its hydrophobic and positively charged N-terminus, made the amphiphilic glycoprotein adopt an energetically favorable conformation that rendered the rhPRG4-grafted pHEMA surfaces less wettable compared to the unmodified (control) pHEMA surfaces. On the contrary, the wettability of the pHEMA-*co*-TRIS surfaces was improved by

covalently attaching rhPRG4. Interestingly, the contact angle for the rhPRG4-modifed model SiHy was lower than that of the unmodified (control) pHEMA hydrogels ($p<0.001$), suggesting better surface wettability. This observation can be explained by considering the structure of the amphiphilic rhPRG4, which mimics that of a surfactant [31]. The contact angle increase for rhPRG4-grafted pHEMA surfaces, was therefore attributed to presence of free hydrophobic hemopexin-like end-domains, whereas for the rhPRG4-grafted pHEMA-*co*-TRIS samples, the wettability enhancement was due to the highly glycosylated and thus highly hydrated mucinous central domain of the glycoprotein [18].

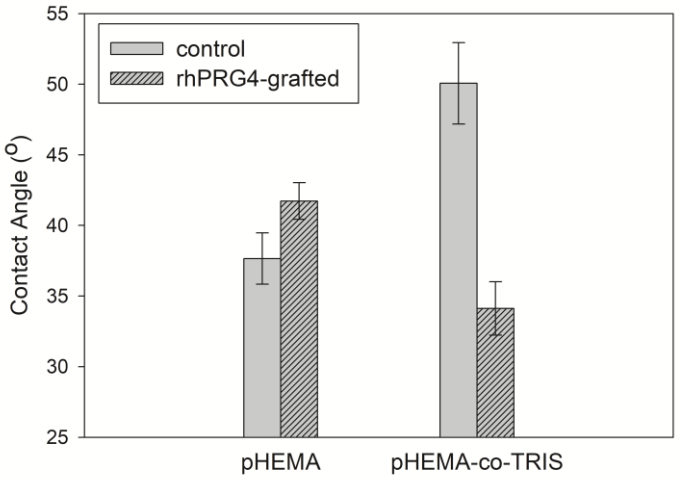

Figure 5.4: The impact of surface rhPRG4-grafted on the surface wettability. The static water contact angles (±SD) of unmodified (control) and rhPRG4-grafted pHEMA and pHEMA-*co*-TRIS hydrogel surfaces, swollen in Milli-Q water, using the captive bubble technique (n=6).

5.3.4. *In vitro* protein sorption study

Tear film components, including proteins and lipids, adhere on the contact lens surface within minutes following lens insertion, while the contact lens-tear film interface remains in a dynamic interaction throughout the period of wear. The process of protein deposition on the contact lens surface is complex including both non-specific adsorption and absorption [56]. Thus, to avoid confusion, protein uptake is herein referred to as protein sorption or deposition.

The materials investigated in this study were incubated in a non-competitive, single protein solution of either lysozyme or human serum albumin (HSA) to establish their individual non-specific binding properties (Figure 5.5). The amount of lysozyme and HSA physically sorbed on the rhPRG4-grafted pHEMA surfaces was reduced by approximately 60% and 45% respectively when compared to that of the unmodified (control) pHEMA hydrogels ($p<0.0004$ and $p<0.001$ respectively). For the pHEMA-*co*-TRIS materials, the presence of the surface grafted rhPRG4 layer led to a 75% reduction in the non-specific deposition of both lysozyme and HSA ($p<0.001$ and $p<0.0002$ respectively).

The conformation of the adsorbed rhPRG4 layer, as a result of the affinity of the glycoprotein with the respective substrate, was previously found to be responsible for the antifouling properties of rhPRG4 [51]. Additionally, the chain flexibility of the surface grafted layer plays an important role in the development of antifouling properties [57]. Reduction in non-specific IgG and bovine serum albumin binding to rhPRG4 coated surfaces was previously attributed to the telechelic brush-like layer formed upon rhPRG4 adsorption that effectively can hide the underlying substrate while exposing the heavily glycosylated and low adhesion mucin-like central domain to the surrounding solutions [51]. Therefore, in a similar manner to the high natural resistance of the glycocalyx [58] and other glycocalyx-mimetic peptoids [59] toward nonspecific protein interactions, the observed decrease in protein sorption is believed to be mainly the synergistic outcome of steric repulsion and surface hydration forces provided by the heavily glycosylated mucin-like domain of rhPRG4 [57], inhibiting thus the protein−surface interactions. It is worth noting that the work presented herein is the first, to our knowledge, to examine the behavior of rhPRG4-grafted surfaces toward lysozyme deposition. Despite the expected strong ionic interactions between the highly positively charged and relatively small lysozyme (MW 14.3 kDa, pI 11.35) [60] and the negatively charged mucin-like central domain of rhPRG4, as previously observed between mucin and lysozyme under physiological conditions [61,62], lysozyme sorption was decreased in all cases with rhPRG4 immobilization. Similarly, interactions between the larger negatively charged albumin (MW 66 kDa, pI 4.9) [63] and the positively charged and hydrophobic end-domains of PRG4, which would also be expected to thermodynamically favour protein deposition, did not overcome the protein repellent properties of the glycoprotein.

These results in combination with the ability of PRG4 to also reduce deposition of IgG [51], another protein that causes adverse effects when sorbed on contact lenses, suggest that rhPRG4 could be an effective antifouling coating useful for contact lens applications.

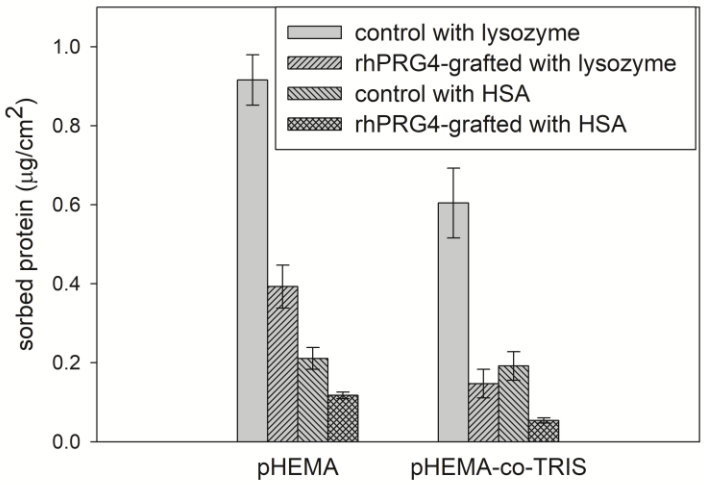

Figure 5.5: The impact of surface rhPRG4-grafted on protein deposition. The amount (±SD) of physisorbed lysozyme and human serum albumin (HSA) on the surface of unmodified (control) and rhPRG4-grafted pHEMA and pHEMA-*co*-TRIS hydrogels upon a 6-hour incubation period at room temperature (n=6).

5.3.5. *In vitro* friction coefficient under boundary lubrication conditions

For contact lens applications, friction is considered the principle material-related property shown to be highly correlated to *in vivo* discomfort [14–17]. During contact lens wear, tear film lubrication of the ocular surface is believed to reduce the significant shear forces between the contact lens and the ocular surface developed during blinking, by preventing surface-to-surface contact at the eyelid-lens and lens-cornea biointerfaces [64]. Contact lenses can provide hydrodynamic lubrication during the fastest part of the blinking with continuous tear film maintenance at the eye-lens interface. At lower ocular movement speeds, boundary lubrication occurs and the contact lens is in direct contact with the ocular tissues, especially if the tear film break up happens prior to blinking, resulting in significantly higher friction [65]. Increased mechanical interactions between the contact lens and the ocular surface are postulated to be

associated clinically with lid-wiper epitheliopathy, lid parallel conjunctival epithelial folds and contact lens associated papillary conjunctivitis, provoking symptoms of dryness and discomfort [12,13,66].

The impact of surface immobilization of rhPRG4 on the friction coefficients of pHEMA and pHEMA-*co*-TRIS samples was determined at a human cornea-disc biointerface, under boundary conditions. The applied sliding velocities and loads during the friction measurement experiments were within the physiological range observed in the eye during blinking [65,67]. All of the data presented herein were log transformed to improve the uniformity of variance for statistical analysis [26]. The μ_{static} of the rhPRG4-grafted pHEMA sample was similar to that of the unmodified (control) pHEMA hydrogels ($p=0.14$), whereas the $\langle\mu_{kinetic}\rangle$ of the rhPRG4-grafted pHEMA hydrogels was slightly higher than of the unmodified (control) pHEMA materials ($p<0.05$) (Figures 5.6A and B). For the pHEMA-*co*-TRIS sample, even though surface immobilization of rhPRG4 did not alter the μ_{static}, a friction lowering effect was observed for the $\langle\mu_{kinetic}\rangle$ on the rhPRG4-grafted sample ($p<0.05$) (Figures 5.6C and D). For both pHEMA and pHEMA-*co*-TRIS samples, μ_{static} increased significantly by increasing the sliding velocity ($p<0.05$), whereas no effect of velocity was observed for $\langle\mu_{kinetic}\rangle$.

The rhPRG4-grafted pHEMA hydrogels were characterized by similar (μ_{static}) or slightly higher friction coefficients ($\langle\mu_{kinetic}\rangle$) than the unmodified (control) pHEMA sample. This is not the first time that PRG4 has been reported as not an effective lubricating agent for relatively hydrophilic surfaces. Previous work showed that physically adherent rhPRG4 on the surface of pHEMA hydrogels did not reduce boundary friction for a human corneal-disc biointerface [39], while Chang et al. [31,68] found that physically adsorbed PRG4 on hydroxyl-terminated self-assembled monolayer hydrophilic surfaces showed an increase in the overall friction force, in a concentration-dependent manner. Conversely, the reduced friction noted for the rhPRG4-grafted pHEMA-*co*-TRIS samples was also observed for the same model SiHy when rhPRG4 was physically sorbed [39], suggesting that covalent attachment of rhPRG4 did not adversely affect its boundary lubricating ability. Likewise, Abubacker et al. [69,70] showed that covalent attachment of aldehyde modified-PRG4 on depleted articular surfaces through its N-terminus, enhanced its binding ability without significantly affecting the structure of the glycoprotein, while also exhibiting a friction reducing cartilage boundary lubricating property similar to the physisorbed PRG4. The velocity dependent profile of μ_{static}, which has been previously observed for similar

setups when PRG4 was used in solution [22,26,29], was attributed to interdigitations between the two soft material surfaces of the biointerface prior to sliding [29].

One of the basic requirements for rhPRG4 to act as a boundary lubricant is the development of strong interactions with the substrate through its hydrophobic end-domains, allowing for its central highly glycosylated mucinous domain to create a low friction layer [31]. Since the surface density of grafted rhPRG4 to pHEMA and pHEMA-*co*-TRIS surfaces was found to be similar, the difference in the friction profile of these two samples is thought to derive from the difference in the surface chemistry between pHEMA and pHEMA-*co*-TRIS materials. The increase in the friction coefficients of rhPRG4-grafted pHEMA samples could be due to weak adhesive interactions (hydrogen bonding) between the mucinous domain of rhPRG4 and pHEMA [51] or an unfavourable hydrophobic interaction between PRG4 end-domains and pHEMA substrate, resulting in a poorly formed extended tail-like steric mucin layer [18] with the free hydrophobic hemopexin-like end-domains (C-termini) exposed to the sliding biointerface [71]. On the other hand, the presence of the hydrophobic TRIS domains in the model SiHy presumably resulted in a conformation that allowed rhPRG4 to present as an effective friction-lowering boundary lubricant. More specifically, surface grafted rhPRG4 on pHEMA-*co*-TRIS surfaces was presumably able to organize into a telechelic brush-like layer (loop-like) conformation where the central mucinous domain is exposed to the biointerface providing strong repulsion through steric and hydration forces [19,51,72,73]. This speculated conformation of the grafted rhPRG4 layer on the pHEMA and pHEMA-*co*-TRIS surfaces was also supported by the contact angle results presented above. Moreover, the friction behavior would not be expected to be significantly different for eyelid-hydrogel biointerface as the choice of ocular tissue was not found to affect PRG4 lubrication to a large extent [29,39].

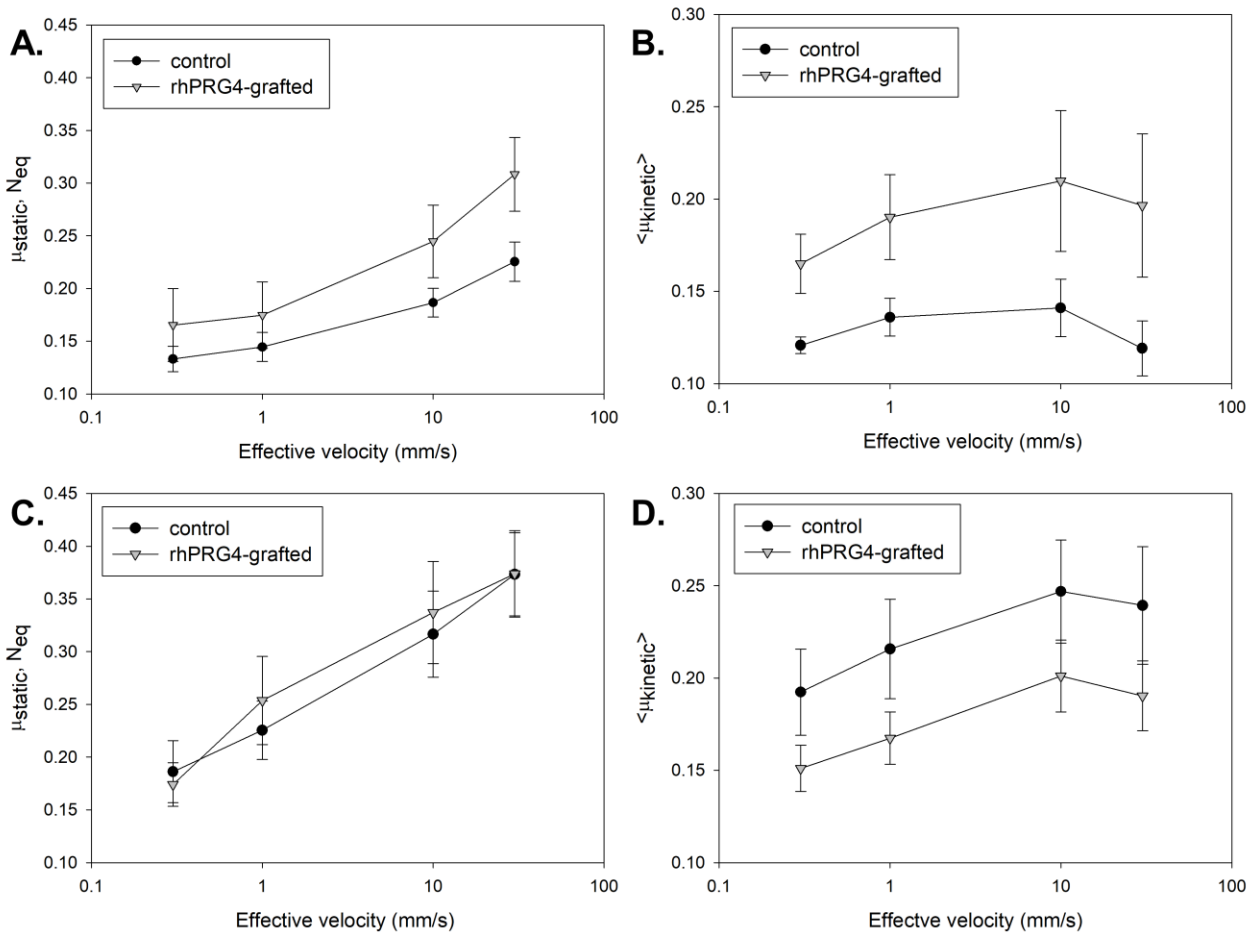

Figure 5.6: The effect of surface rhPRG4-grafted on boundary lubrication at a human cornea-hydrogel disc biointerface. The static ($\mu_{static,}$ N_{eq}) and kinetic ($<\mu_{kinetic}>$) friction coefficients (±SEM) of unmodified (control) and rhPRG4-grafted for (A, B) pHEMA (n=3) and (C, D) pHEMA-*co*-TRIS (n=6) hydrogel surfaces in saline bath at room temperature. The average normal stress (±SD) was 20.6 ± 2.5kPa for pHEMA and 20.1 ± 1.9kPa for pHEMA-*co*-TRIS. Sliding velocity values were log transformed to improve the uniformity of variance for statistical analysis.

5.3.6. Optical Transparency and Equilibrium Water Content (EWC)

The optical properties of unmodified (control) and rhPRG4-grafted pHEMA and pHEMA-*co*-TRIS discs are shown in Figure 5.7. Surface immobilization of rhPRG4 led to a minor reduction in the optical acuity of the materials (approximately 4% for both cases). The model SiHy used in

this study was found to be slightly more opaque than the pHEMA due to microphase separation between the hydrophilic HEMA and hydrophobic TRIS domains. The optical transparency is an important parameter that needs to be considered for the design of contact lens-based applications. While the rhPRG4-grafted pHEMA-*co*-TRIS samples had transmittance values that were slightly lower than 90%, it should be noted that the all discs used in this study were almost five times thicker than commercially available contact lenses (0.5 mm thickness). Therefore, despite the decrease observed in the optical transmittance upon the surface modification step, grafting rhPRG4 to the surface of contact lenses would not be expected to have clinically an impact on their optical transparency.

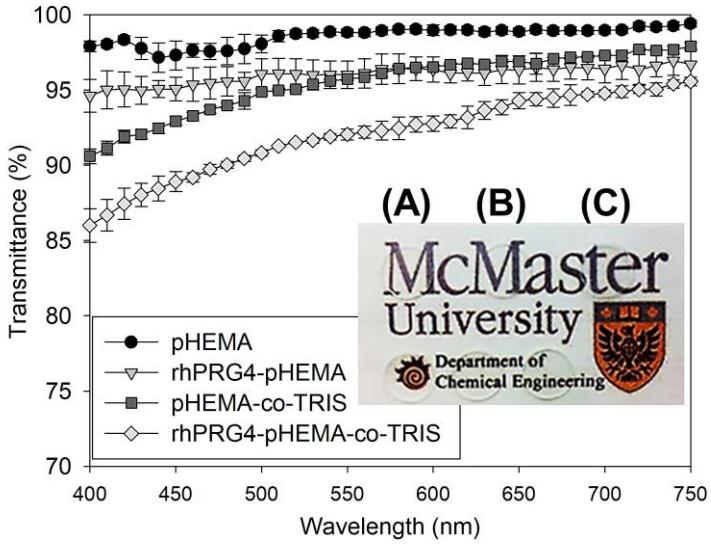

Figure 5.7: The impact of surface modification on optical transparency. Transmittance spectrum (±SD) for the unmodified (control) and rhPRG4-grafted pHEMA and pHEMA-*co*-TRIS hydrogel discs (n=6). Inset: a photograph of (A) unmodified, (B) CDI-activated and (C) rhPRG4-grafted pHEMA (top) and pHEMA-*co*-TRIS (bottom) hydrogel materials.

Water content is another influential property for both conventional and SiHy contact lenses, playing a role in oxygen permeability, ion transport and mechanical properties [74]. The equilibrium water content (EWC) of the pHEMA and pHEMA-*co*-TRIS hydrogel materials was determined using equation (1). The results, presented in Table 2, demonstrate that the modification procedure did not change the EWC of the surface rhPRG4-grafted hydrogel materials when

compared to the unmodified (control) samples ($p>0.05$). The EWC of the hydrogels remained within an acceptable range for contact lens wear. In general, the bulk properties of the surface modified materials are not expected to differ from those of the pristine samples because the 1,4-Dioxane used as the solvent for the intermediate CDI activation reaction did not cause any swelling of the hydrogels.

Table 5.2: Equilbrium water content (EWC) (%) (±SD) of the unmodified (control) and rhPRG4-grafted pHEMA and pHEMA-*co*-TRIS hydrogel discs (n=6).

sample	**EWC (%)**
pHEMA - control	34.2 ± 0.78
rhPRG4-grated pHEMA	34.73 ± 0.94
pHEMA-*co*-TRIS – control	26.9 ± 2.40
rhPRG4-grafted pHEMA-*co*-TRIS	28.3 ± 1.51

5.3.7. Cell viability – MTT assay

The cytotoxicity of potentially leachable components arising from the surface modification procedure was assessed using an MTT assay with human corneal epithelial cells (HCEC). Immortalized HCEC have been shown to be an appropriate *in vitro* model of the human ocular surface for assessing toxicity of front-of-the-eye biomaterials, such as contact lenses [75]. As shown in Figure 5.8, there was no statistical difference in the cell viability of HCEC cultured in the presence of unmodified (control) or surface rhPRG4-grafted pHEMA and pHEMA-*co*-TRIS hydrogels. These results demonstrate that the rhPRG4-grafted pHEMA and pHEMA-*co*-TRIS hydrogel materials were not cytotoxic and the washing steps following synthesis as well as after each modification step were sufficient for the removal of any leachable component that would affect the HCEC viability. According to previous work, CDI as a linking agent did not exhibit any significant toxic effect *in vitro* on human corneal epithelial cells [35] and *in vivo* [76–78], while rhPRG4-containing eye drops were used successfully in a clinical trial for the treatment of dry eye symptoms [24] .

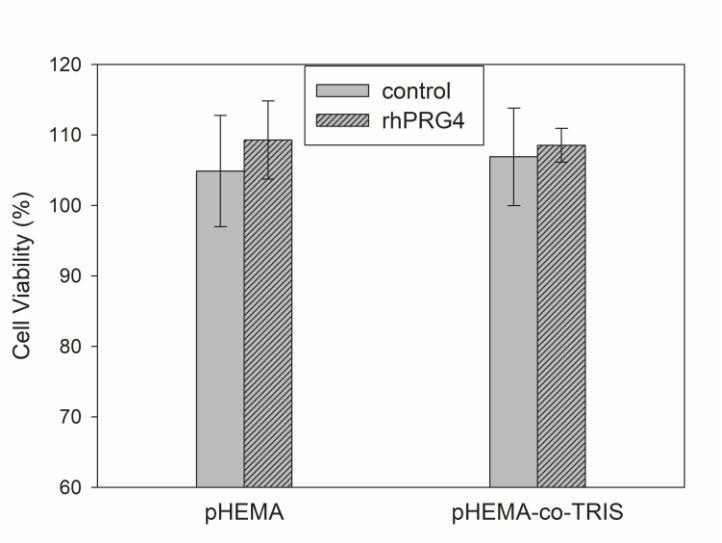

Figure 5.8: Cytotoxicity of rhPRG4-grafted hydrogel materials. Cell viability (%) (± SD) of the human corneal epithelial cells (HCEC) upon incubation with unmodified (control) and surface rhPRG4-grafted pHEMA and pHEMA-*co*-TRIS discs for 24 hours. Results expressed relative cell viability in respect to cells grown in the absence of hydrogel discs (n=4).

5.4. Conclusions

In conclusion, in this study full-length human recombinant rhPRG4 was successfully covalently attached to the surface of model pHEMA and pHEMA-*co*-TRIS hydrogel contact lenses from its somatomedin B-like N-terminus via CDI linking chemistry. The rhPRG4-grafted model contact lenses remained optically clear and were found to be non-cytotoxic. Quantification of the rhPRG4 on the surfaces indicated that the grafting density of rhPRG4 on pHEMA substrates was slightly higher than that on the pHEMA-*co*-TRIS, while a strong interaction was observed between the physically sorbed amphiphilic glycoprotein and the hydrophobic TRIS domains of the unmodified model SiHy. Surface immobilized rhPRG4 was found to acquire a substrate-specific conformation, which was dependent on the composition substrate materials. Even though covalently bound rhPRG4 formed a protein protective layer against lysozyme and albumin sorption for both pHEMA and pHEMA-*co*-TRIS hydrogels, it was found to be more effective as a wetting and boundary lubricating agent only for the model SiHy used in this study. These results suggest that the full-length rhPRG4 tested herein is a good candidate for the development of novel

bioinspired SiHy contact lenses. Future studies should examine the impact of sterilization and shelf-life on the properties of the modified model contact lens materials.

5.5. Acknowledgements

The authors would like to thank Dr. Danielle Covelli (Biointerfaces Institute, McMaster University) for her contribution to XPS spectra acquisition and Dr. Megan Dodd for her help with the cytotoxicity assay. Funding support for this work was provided by the Natural Sciences and Engineering Research Council (NSERC) of Canada, the 20/20 NSERC Ophthalmic Materials Research Network and the Canada Research Chairs Program, and is gratefully acknowledged.

5.6. References

[1] L. Jones, Modern contact lens materials: A clinical performance update, Contact Lens Spectr. 17 (2002) 24–35.

[2] C. Maldonado-Codina, Soft lens materials, in: N. Efron (Ed.), Contact Lens Pract., Butterworth-Heineman, 2010: pp. 67–86.

[3] P.C. Nicolson, J. Vogt, Soft contact lens polymers: an evolution., Biomaterials. 22 (2001) 3273–3283.

[4] N. Keir, L. Jones, Wettability and silicone hydrogel lenses: a review., Eye Contact Lens. 39 (2013) 100–108.

[5] J.J. Nichols, L.T. Sinnott, Tear film, contact lens, and patient-related factors associated with contact lens-related dry eye., Invest. Ophthalmol. Vis. Sci. 47 (2006) 1319–1328.

[6] K. Dumbleton, C.A. Woods, L.W. Jones, D. Fonn, The impact of contemporary contact lenses on contact lens discontinuation., Eye Contact Lens. 39 (2013) 93–99.

[7] K. Richdale, L.T. Sinnott, E. Skadahl, J.J. Nichols, Frequency of and Factors Associated With Contact Lens Dissatisfaction and Discontinuation, Cornea. 26 (2007) 168–174.

[8] J.P. Craig, M.D.P. Willcox, P. Argüeso, C. Maissa, U. Stahl, A. Tomlinson, J. Wang, N. Yokoi, F. Stapleton, The TFOS International Workshop on Contact Lens Discomfort: report of the contact lens interactions with the tear film subcommittee., Invest. Ophthalmol. Vis. Sci. 54 (2013) TFOS123-156.

[9] N. Efron, L. Jones, A.J. Bron, E. Knop, R. Arita, S. Barabino, A.M. McDermott, E. Villani, M.D.P. Willcox, M. Markoulli, The TFOS International Workshop on Contact Lens Discomfort: Report of the Contact Lens Interactions With the Ocular Surface and Adnexa Subcommittee, Investig. Opthalmology Vis. Sci. 54 (2013) TFOS98-122.

[10] A. Tomlinson, Tear film changes with contact lens wear, in: A. Tomlinson (Ed.), Complicat.

Contact Lens Wear, Mosby, St Louis, MO, 1992: pp. 195–218.

[11] L. Jones, N.A. Brennan, J. González-Méijome, J. Lally, C. Maldonado-Codina, T.A. Schmidt, L. Subbaraman, G. Young, J.J. Nichols, The TFOS International Workshop on Contact Lens Discomfort: report of the contact lens materials, design, and care subcommittee., Invest. Ophthalmol. Vis. Sci. 54 (2013) TFOS37-70.

[12] D.R. Korb, J. V Greiner, J.P. Herman, E. Hebert, V.M. Finnemore, J.M. Exford, T. Glonek, M.C. Olson, Lid-wiper epitheliopathy and dry-eye symptoms in contact lens wearers., CLAO J. 28 (2002) 211–216.

[13] H. Pult, C. Purslow, M. Berry, P.J. Murphy, Clinical Tests for Successful Contact Lens Wear: Relationship and Predictive Potential, Optom. Vis. Sci. 85 (2008) E924–E929.

[14] N. Brennan, C. Coles-Brennan, Contact lens-based correlates of soft lens wearing comfort, Optom. Vis. Sci. 86 (2009) E-abstract 90957.

[15] C. Coles, N. Brennan, Coefficient of friction and soft contact lens comfort, Optom Vis Sci. 89 (2012) E-abstract 125603.

[16] J. Kern, J. Rappon, E. Bauman, B. Vaughn, Assessment of the relationship between contact lens coefficient of friction and subject lens comfort, Invest. Ophthalmol. Vis. Sci. 54 (2013) 494.

[17] N.A. Brennan, C. Coles, Supportive data linking coefficient of friction and comfort, Contact Lens Anterior Eye. 36 (2013) e10.

[18] B. Zappone, M. Ruths, G.W. Greene, G.D. Jay, J.N. Israelachvili, Adsorption, lubrication, and wear of lubricin on model surfaces: polymer brush-like behavior of a glycoprotein., Biophys. J. 92 (2007) 1693–1708.

[19] G.D. Jay, D.A. Harris, C.J. Cha, Boundary lubrication by lubricin is mediated by O-linked beta(1-3)Gal-GalNAc oligosaccharides., Glycoconj. J. 18 (2001) 807–815.

[20] G.D. Jay, Joint lubrication: A physicochemical study of a purified lubricating factor from bovine synovial fluid, State University of New York, Stony Brook, NY, 1990.

[21] F. Mantelli, P. Argüeso, Functions of ocular surface mucins in health and disease, Curr. Opin. Allergy Clin. Immunol. 8 (2008) 477–483.

[22] T.A. Schmidt, D.A. Sullivan, E. Knop, S.M. Richards, N. Knop, S. Liu, A. Sahin, R.R. Darabad, S. Morrison, W.R. Kam, B.D. Sullivan, Transcription, translation, and function of lubricin, a boundary lubricant, at the ocular surface., JAMA Ophthalmol. 131 (2013) 766–776.

[23] T. Cheriyan, T.M. Schmid, M. Spector, Presence and distribution of the lubricating protein, lubricin, in the meibomian gland in rabbits, Mol. Vis. 17 (2011) 3055–3061.

[24] A. Lambiase, B.D. Sullivan, T.A. Schmidt, D.A. Sullivan, G.D. Jay, E.R. Truitt, A. Bruscolini, M. Sacchetti, F. Mantelli, A Two-Week, Randomized, Double-masked Study to Evaluate Safety and Efficacy of Lubricin (150 μg/mL) Eye Drops Versus Sodium Hyaluronate (HA) 0.18% Eye Drops (Vismed®) in Patients with Moderate Dry Eye

Disease, Ocul. Surf. 15 (2017) 77–87.

[25] S.C. Regmi, M.L. Samsom, M.L. Heynen, G.D. Jay, B.D. Sullivan, S. Srinivasan, B. Caffery, L. Jones, T.A. Schmidt, Degradation of proteoglycan 4/lubricin by cathepsin S: Potential mechanism for diminished ocular surface lubrication in Sjögren's syndrome, Exp. Eye Res. 161 (2017) 1–9.

[26] S. Morrison, D.A. Sullivan, B.D. Sullivan, H. Sheardown, T.A. Schmidt, Dose-dependent and synergistic effects of proteoglycan 4 on boundary lubrication at a human cornea-polydimethylsiloxane biointerface., Eye Contact Lens. 38 (2012) 27–35.

[27] M.L. Samsom, S. Morrison, N. Masala, B.D. Sullivan, D.A. Sullivan, H. Sheardown, T.A. Schmidt, Characterization of full-length recombinant human Proteoglycan 4 as an ocular surface boundary lubricant, Exp. Eye Res. 127 (2014) 14–19.

[28] T.A. Schmidt, H. Sheardown, M.L. Samsom, Human Ocular Surface Boundary Lubrication of Model Conventional and Silicone Hydrogels by Proteoglycan 4, Invest. Ophthalmol. Vis. Sci. 55 (2014) 4651.

[29] M. Samsom, A. Chan, Y. Iwabuchi, L. Subbaraman, L. Jones, T.A. Schmidt, In vitro friction testing of contact lenses and human ocular tissues: Effect of proteoglycan 4 (PRG4), Tribol. Int. 89 (2015) 27–33.

[30] B. Zappone, G.W. Greene, E. Oroudjev, G.D. Jay, J.N. Israelachvili, Molecular aspects of boundary lubrication by human lubricin: effect of disulfide bonds and enzymatic digestion., Langmuir. 24 (2008) 1495–1508.

[31] D.P. Chang, N.I. Abu-Lail, F. Guilak, G.D. Jay, S. Zauscher, Conformational Mechanics, Adsorption, and Normal Force Interactions of Lubricin and Hyaluronic Acid on Model Surfaces., Langmuir. 24 (2008) 1183–1193.

[32] S.M. Martin, R. Ganapathy, T.K. Kim, D. Leach-Scampavia, C.M. Giachelli, B.D. Ratner, Characterization and analysis of osteopontin-immobilized poly(2-hydroxyethyl methacrylate) surfaces., J. Biomed. Mater. Res. A. 67 (2003) 334–343.

[33] J. Bi, J.C. Downs, J.T. Jacob, Tethered protein/peptide-surface-modified hydrogels., J. Biomater. Sci. Polym. Ed. 15 (2004) 905–916.

[34] S. Bauer, J. Park, A. Pittrof, Y.-Y. Song, K. von der Mark, P. Schmuki, Covalent functionalization of TiO2 nanotube arrays with EGF and BMP-2 for modified behavior towards mesenchymal stem cells, Integr. Biol. 3 (2011) 927–936.

[35] S. Park, S.H. Nam, W.-G. Koh, Preparation of collagen-immobilized poly(ethylene glycol)/poly(2-hydroxyethyl methacrylate) interpenetrating network hydrogels for potential application of artificial cornea, J. Appl. Polym. Sci. 123 (2012) 637–645.

[36] S.M. Iqbal, C. Leonard, S. C. Regmi, D. De Rantere, P. Tailor, G. Ren, H. Ishida, C. Hsu, S. Abubacker, D.S. Pang, P. T. Salo, H.J. Vogel, D.A. Hart, C.C. Waterhouse, G.. Jay, T.A. Schmidt, R.J. Krawetz, Lubricin/Proteoglycan 4 binds to and regulates the activity of Toll-Like Receptors In Vitro, Sci. Rep. 6 (2016) 18910.

[37] E. Regoeczi, Iodine-Labeled Plasma Proteins Vol. 1, CRC Press, Boca Raton, FL, 1984.

[38] A. Weeks, L.N. Subbaraman, L. Jones, H. Sheardown, The Competing Effects of Hyaluronic and Methacrylic Acid in Model Contact Lenses, J. Biomater. Sci. Polym. Ed. 23 (2012) 1021–1038.

[39] M. Samsom, Y. Iwabuchi, H. Sheardown, T.A. Schmidt, Proteoglycan 4 and hyaluronan as boundary lubricants for model contact lens hydrogels, J. Biomed. Mater. Res. Part B Appl. Biomater. 00B (2017) 000–000. doi:10.1002/jbm.b.33895.

[40] M. Samsom, M. Korogiannaki, L.N. Subbaraman, H. Sheardown, T.A. Schmidt, Hyaluronan incorporation into model contact lens hydrogels as a built-in lubricant: Effect of hydrogel composition and proteoglycan 4 as a lubricant in solution, J. Biomed. Mater. Res. Part B Appl. Biomater. 00B (2017) 000–000. doi:10.1002/jbm.b.33989.

[41] T. Yan, R. Sun, C. Li, B. Tan, X. Mao, N. Ao, Immobilization of type-I collagen and basic fibroblast growth factor (bFGF) onto poly (HEMA-co-MMA) hydrogel surface and its cytotoxicity study, J. Mater. Sci. Mater. Med. 21 (2010) 2425–2433.

[42] H.J. Lee, D. Nedelkov, R.M. Corn, Surface Plasmon Resonance Imaging Measurements of Antibody Arrays for the Multiplexed Detection of Low Molecular Weight Protein Biomarkers, Anal. Chem. 78 (2006) 6504–6510.

[43] W. Lin, J. Zhang, Z. Wang, S. Chen, Development of robust biocompatible silicone with high resistance to protein adsorption and bacterial adhesion, Acta Biomater. 7 (2011) 2053–2059.

[44] S. Boufi, M. Rei Vilar, V. Parra, A.M. Ferraria, A.M. Botelho do Rego, Grafting of Porphyrins on Cellulose Nanometric Films, Langmuir. 24 (2008) 7309–7315.

[45] B.L. Beckstead, J.C. Tung, K.J. Liang, Z. Tavakkol, M.L. Usui, J.E. Olerud, C.M. Giachelli, Methods to promote Notch signaling at the biomaterial interface and evaluation in a rafted organ culture model., J. Biomed. Mater. Res. A. 91 (2009) 436–446.

[46] S.L. McArthur, M.W. Halter, V. Vogel, D.G. Castner, Castner David G., Covalent Coupling and Characterization of Supported Lipid Layers, Langmuir. 19 (2003) 8316–8324.

[47] S.M. Rezaei, Z.A. Mohd Ishak, Grafting of collagen onto interpenetrating polymer networks of poly(2-hydroxyethyl methacrylate) and poly(dimethyl siloxane) polymer films for biomedical applications, Express Polym. Lett. 8 (2014) 39–49.

[48] K. Nilsson, K. Mosbach, Immobilization of ligands with organic sulfonyl chlorides., Methods Enzymol. 104 (1984) 56–69.

[49] M. Kavoshchian, R. Üzek, S.A. Uyanık, S. Şenel, A. Denizli, HSA immobilized novel polymeric matrix as an alternative sorbent in hemoperfusion columns for bilirubin removal, React. Funct. Polym. 96 (2015) 25–31.

[50] S.C. Crowley, K.C. Chan, R.R. Walters, Optimization of protein immobilization on 1,1′-carbonyldiimidazole-activated diol-bonded silica, J. Chromatogr. A. 359 (1986) 359–368.

[51] G.W. Greene, L.L. Martin, R.F. Tabor, A. Michalczyk, L.M. Ackland, R. Horn, Lubricin: A versatile, biological anti-adhesive with properties comparable to polyethylene glycol, Biomaterials. 53 (2015) 127–136.

[52] S. Morita, Hydrogen-bonds structure in poly(2-hydroxyethyl methacrylate) studied by temperature-dependent infrared spectroscopy., Front. Chem. 2 (2014) 10.

[53] G.A. Jeffrey, An introduction to hydrogen bonding, Oxford University Press, Oxford and New York, 1997.

[54] Y. Maréchal, The hydrogen bond and the water molecule : the physics and chemistry of water, aqueous and bio media, Elsevier, Amsterdam, 2007.

[55] B. Tighe, Silicone hydrogels: Structure, properties and behaviour, in: D. Sweeney (Ed.), Silicone Hydrogels Contin. Wear Contact Lenses, Butterworth-Heinemann, Oxford, 2004: pp. 1–27.

[56] Z. Zhao, X. Wei, Y. Aliwarga, N.A. Carnt, Q. Garrett, M.D.P. Willcox, Proteomic analysis of protein deposits on worn daily wear silicone hydrogel contact lenses., Mol. Vis. 14 (2008) 2016–2024.

[57] S. Chen, L. Li, C. Zhao, J. Zheng, Surface hydration: Principles and applications toward low-fouling/nonfouling biomaterials, Polymer (Guildf). 51 (2010) 5283–5293.

[58] S. Reitsma, D.W. Slaaf, H. Vink, M.A.M.J. van Zandvoort, M.G.A. oude Egbrink, The endothelial glycocalyx: composition, functions, and visualization, Pflugers Arch. 454 (2007) 345–359.

[59] H.O. Ham, S.H. Park, J.W. Kurutz, I.G. Szleifer, P.B. Messersmith, Antifouling Glycocalyx-Mimetic Peptoids, J. Am. Chem. Soc. 135 (2013) 13015–13022.

[60] L.R. Wetter, H.F. Deutsch, Immunological studies on egg white proteins. IV. Immunochemical and physical studies of lysozyme., J. Biol. Chem. 192 (1951) 237–42.

[61] C. Lu, L. Kostanski, H. Ketelson, D. Meadows, R. Pelton, Hydroxypropyl Guar−Borate Interactions with Tear Film Mucin and Lysozyme, Langmuir. 21 (2005) 10032–10037.

[62] J.M. Creeth, J.L. Bridge, J.R. Horton, An interaction between lysozyme and mucus glycoproteins. Implications for density-gradient separations., Biochem. J. 181 (1979) 717–724.

[63] D. Luensmann, L. Jones, Albumin adsorption to contact lens materials: A review, Contact Lens Anterior Eye. 31 (2008) 179–187.

[64] M.B. Jones, G.R. Fulford, C.P. Please, D.L.S. McElwain, M.J. Collins, Elastohydrodynamics of the Eyelid Wiper, Bull. Math. Biol. 70 (2008) 323–43.

[65] A.C. Dunn, J.M. Urueña, Y. Huo, S.S. Perry, T.E. Angelini, W.G. Sawyer, Lubricity of Surface Hydrogel Layers, Tribol. Lett. 49 (2013) 371–378.

[66] P.C. Donshik, Contact lens chemistry and giant papillary conjunctivitis., Eye Contact Lens. 29 (2003) S37-39-59, S192-194.

[67] A.C. Dunn, J.A. Tichy, J.M. Urueña, W.G. Sawyer, Lubrication regimes in contact lens wear during a blink, Tribol. Int. 63 (2013) 45–50.

[68] D.P. Chang, N.I. Abu-Lail, J.M. Coles, F. Guilak, G.D. Jay, S. Zauscher, Friction Force

Microscopy of Lubricin and Hyaluronic Acid between Hydrophobic and Hydrophilic Surfaces., Soft Matter. 5 (2009) 3438–3445.

[69] K. Chawla, H.O. Ham, T. Nguyen, P.B. Messersmith, Molecular resurfacing of cartilage with proteoglycan 4., Acta Biomater. 6 (2010) 3388–3394.

[70] S. Abubacker, H.O. Ham, P.B. Messersmith, T.A. Schmidt, Cartilage boundary lubricating ability of aldehyde modified proteoglycan 4 (PRG4-CHO)., Osteoarthr. Cartil. 21 (2013) 186–189.

[71] J.M. Coles, D.P. Chang, S. Zauscher, Molecular mechanisms of aqueous boundary lubrication by mucinous glycoproteins, Curr. Opin. Colloid Interface Sci. 15 (2010) 406–416.

[72] J. Klein, Molecular mechanisms of synovial joint lubrication, Proc. Inst. Mech. Eng. Part J. 220 (2006) 691–710.

[73] D.B. Schaefer, D. Wendt, M. Moretti, M. Jakob, G.D. Jay, M. Heberer, I. Martin, Lubricin reduces cartilage–cartilage integration, Biorheology. 41 (2004) 503–508.

[74] B.J. Tighe, A decade of silicone hydrogel development: surface properties, mechanical properties, and ocular compatibility., Eye Contact Lens. 39 (2013) 4–12.

[75] E.A. Offord, N.A. Sharif, K. Macé, Y. Tromvoukis, E.A. Spillare, O. Avanti, W.E. Howe, A.M. Pfeifer, Immortalized human corneal epithelial cells for ocular toxicity and inflammation studies., Invest. Ophthalmol. Vis. Sci. 40 (1999) 1091–1101.

[76] L. Ling, Y. Du, M. Ismail, R. He, Y. Hou, Z. Fu, Y. Zhang, C. Yao, X. Li, Self-assembled liposomes of dual paclitaxel-phospholipid prodrug for anticancer therapy, Int. J. Pharm. 526 (2017) 11–22.

[77] S.N. Isenhath, Y. Fukano, M.L. Usui, R.A. Underwood, C.A. Irvin, A.J. Marshall, K.D. Hauch, B.D. Ratner, P. Fleckman, J.E. Olerud, A mouse model to evaluate the interface between skin and a percutaneous device, J. Biomed. Mater. Res. Part A. 83A (2007) 915–922.

[78] J.-Q. Gao, Q.-Q. Zhao, T.-F. Lv, W.-P. Shuai, J. Zhou, G.-P. Tang, W.-Q. Liang, Y. Tabata, Y.-L. Hu, Gene-carried chitosan-linked-PEI induced high gene transfection efficiency with low toxicity and significant tumor-suppressive activity, Int. J. Pharm. 387 (2010) 286–294.

Chapter 6

Investigating the synergistic interactions of surface immobilized and free natural ocular lubricants for contact lens applications: A comparative study between hyaluronic acid and proteoglycan 4 (Lubricin)

Authors: Myrto Korogiannaki, Michael Samsom, Austyn Matheson, Tannin A. Schmidt, Heather Sheardown

Abstract

The development of contact lens materials with biomimetic surfaces that work synergistically with naturally occurring ocular agents can be advantageous for alleviating ocular dryness and discomfort, the two primary reasons for discontinuation of contact lens wear. Proteoglycan 4 (PRG4), a mucinous glycoprotein, and hyaluronic acid (HA), a non-sulfated linear glycosaminoglycan, are naturally present in the ocular environment and play an essential role in ocular hydration and lubrication. PRG4 and HA were previously found to interact with each other, forming a complex with boundary lubricating properties. Therefore, the aim of this study was to investigate the impact of the structure of the rhPRG4/HA complex on important contact lens properties, when one agent is grafted and the counterpart is physisorbed (HA_{sol} or $rhPRG4_{sol}$) to the surface of 2-hydroxyethylmethacrylate (HEMA)-based conventional and model silicone hydrogel contact lenses. Surface analysis showed that the affinity of the HA and rhPRG4 in solution was stronger toward the respective rhPRG4 and HA-grafted surfaces than for unmodified hydrogels. For conventional hydrogels, the HA-grafted+$rhPRG4_{sol}$ sample exhibited better antifouling and tribological properties than the rhPRG4-grafted+HA_{sol} sample, with the latter demonstrating slower dehydration rates. The configuration of the rhPRG4/HA complex did not affect the surface wettability of these hydrogels. For model silicone hydrogels, the rhPRG4-grafted+HA_{sol} sample demonstrated more wettable surfaces with superior antifouling and water retentive properties than the respective HA-grafted+$rhPRG4_{sol}$. The friction lowering properties between HA and rhPRG4 were not dependent on the arrangement of the rhPRG4/HA complex for these samples. According to these results, rhPRG4/HA interactions as well as the degree of their synergism on the examined properties were found to vary with the composition of the underlying

hydrogel substrate used (conventional versus model silicone samples), potentially due to the different conformations that the rhPRG4/HA complex can acquire when associated with surfaces of differing hydrophobicity.

Keywords

2-hydroxyethyl methacrylate (HEMA); contact lens; proteoglycan 4 (PRG4)/lubricin; hyaluronic acid; surface immobilization; synergistic effect; protein deposition; lubrication

6.1. Introduction

Approximately half of the population of contact lens wearers experiences symptoms of ocular dryness and discomfort, especially towards the end of the day [1–3]. The need to develop ocular solutions and contact lens materials that will provide relief from discomfort has become one of the greatest driving forces within the field. To date, wetting and lubricant agents have been used in the form of eye drops or contact lens solutions. They have also been incorporated in the bulk of the lens, as releasable or internal agents, or have been attached to the surface of the contact lens material in an effort to increase levels of comfort during wear [4]. Despite the progress made in this field, contact lens-related dryness and discomfort remain the primary reasons leading to the discontinuation of contact lens wear [2,3]. The factors affecting contact lens performance are complex and multifactorial; and they can independently or synergistically lead to a specific etiology for poor ocular compatibility [5]. Among them, contact lens dehydration and poor surface wettability, uncontrolled protein and lipid deposition, modulus (stiffness), oxygen deprivation; and compromised tear film stability and quality are considered to play essential roles in ocular dryness and discomfort during contact lens wear [6,7]. In addition, disruption of the tear film structure during contact lens wear is likely to cause friction-related damage to ocular tissues due to inadequate lubrication. Lack of lubrication is postulated to the be related to clinical signs of the ocular surface, including lid wiper epitheliopathy and lid parallel conjunctival folds, signs associated with the symptoms of dryness and discomfort during contact lens wear [8–10]. Studies also suggest that the shear-induced forces developed between the contact lens, the eyelid and the cornea/conjunctiva may be well correlated with *in vivo* comfort and overall contact lens performance [11–13]. Therefore, contact lens materials should be characterized by adequate wettability promoting tear film stability and hydration, resistance to accumulation of tear deposits

and to biofouling, and low friction to minimize the adverse interactions with the ocular environment and thus achieve a higher degree of comfort during wear.

One promising method with the potential for improving the compatibility of a contact lens with the ocular surface is to modify the lens surface with natural ocular lubricating agents. Proteoglycan 4 (PRG4) and hyaluronic acid (HA) are characterized by antiadhesive [14–16], antifouling [17–19] as well as wetting and lubricating properties [20–22], and are naturally present at the human ocular surface. PRG4, a mucin-like glycoprotein present in meibomian gland secretions and at the corneal surface [23,24], is considered to likely play a critical role in preventing tear film evaporation and in reducing friction on the ocular surface during blinking [23,25,26]. A recent clinical study [27] showed that instillation of full-length recombinant human PRG4 (rhPRG4) eye drops to patients suffering from dry eye disease led to improved tear film homeostasis, thus alleviating the signs and symptoms of discomfort. It was speculated that this occurred by restoring the glycocalyx layer, which is considered crucial in maintaining the wettability and lubrication of the ocular surface [28]. Hyaluronic acid (HA), a linear, anionic non-sulfated glycosaminoglycan naturally found in the lacrimal gland as well as in the conjunctiva, corneal epithelium and tear film [29–32], has also been widely used for the treatment of dry eye disease due to its ocular compatibility and unique hygroscopic, rheological and lubricating properties [33–35]. HA has also been used in contact lens products, including artificial tears, and packaging and multipurpose solutions, and has been shown to promote tear film stability, ocular hydration and lubrication, thus alleviating symptoms of ocular dryness and discomfort [36,37].

Boundary lubrication is one of multiple lubrication mechanisms that protects biological surfaces, including the articular and ocular surfaces, from friction and wear. During contact lens wear, boundary lubrication occurs at lower ocular movement speeds and/or high contact pressure. The contact lens can be in direct contact with the ocular tissues, especially in the case of a compromised tear film, leading to significantly higher friction [38–40]. To function as an effective boundary lubricant, a lubricating agent should result in low work of adhesion with the substrate of interest in order to either adhere strongly and avoid from being sheared away or be able to adsorb sufficiently quickly from solution to the surface allowing for those interfacial elements that have been sheared off to be readily replaced [41]. In the case of contact lenses, therefore, the friction coefficient is influenced by both the properties of the surface-bound lubricating agent and the

contact lens [40]. Since nearly all wear and thus damage occurs in the boundary lubrication regime, successful boundary lubrication is considered vital [42].

PRG4 is a major component of synovial fluid providing boundary lubrication in the joints [43]. It has also been found to reduce the boundary friction between several synthetic surfaces [44,45] as well as at cartilage [46] and cornea-eyelid [23] biointerfaces *in vitro*. Interestingly, for contact lens materials, the boundary lubricating properties of rhPRG4 were effective only for the non surface-pretreated silicone hydrogels (SiHy) and not for the more hydrophilic conventional hydrogel materials [47–50]. The observed reduction in boundary friction and wear by PRG4 has been attributed to the steric repulsive hydration forces caused by the central, extensively glycosylated, mucinous domain that gains a "polymer brush-like" conformation once the end C', N'-terminal protein domains of the glycoprotein are strongly bound to the surface [51]. As a boundary lubricant, HA was found to effectively reduce boundary friction and wear when it was physically attached (mechanically trapped) to soft porous surfaces, such as articular cartilage [52,53] and cornea-PDMS or SiHy [47,49] biointerfaces or when it was chemically surface grafted and/or crosslinked [54,55]. However, the poor adsorption behavior of free HA has been suggested to the be the cause of the reported minimal impact on both boundary lubrication and wear protection [42].

PRG4 and HA were first reported to interact under boundary lubricating conditions by synergistically reducing friction to a greater extent than either alone for a latex-glass interface [22]. This synergistic effect was further observed in tribological studies that examined cartilage–cartilage [52,56], cornea-eyelid [23], as well as cornea-PDMS [47] biointerfaces, but was not seen for idealized model surfaces [42,57,58]. In addition, when HA was covalently attached to these model substrates, the presence of physisorbed PRG4 led to a further decrease in boundary friction and wear [58,59]. Determination of the exact mechanism for the PRG4-HA boundary synergy has been challenging and the molecular basis for PRG4-HA interactions remains to be fully elucidated. Previous work showed that PRG4 altered the rheological properties of HA, either when both were in solution [60] or when HA was used as a grafted layer [58], potentially by forming an entangled and physically crosslinked network via non-covalent interactions. Using the quartz crystal microbalance with dissipation (QCM-D), Majd et. al showed that PRG4 could bind strongly to HA-grafted surfaces [61]. Conversely, HA was not reported to bind to PRG4-coated idealized substrates, whereas the PRG4-HA complex was found to adhere to model substrates to a greater

extent than PRG4 alone [57]. Additionally, when more complicated systems were examined, the interactions between PRG4 and HA were affected by the presence of other biomolecules, such as albumin [61], which in turn could potentially have an impact on the synergistic lubrication. Greene at al. [53] suggested that the PRG4-HA complex functioned as an effective boundary lubricant by becoming mechanically trapped at the cartilage porous interface under compression. However, for the formation of the PRG4-HA complex at the interface, which is eventually responsible for providing synergistic boundary lubrication, some studies suggested that PRG4 acted as the surface anchor for HA to the substrate [60,62] whereas others proposed the opposite [53,63]. Therefore, it is not clear which agent should be immobilized on the substrate first in order to achieve optimum conditions for synergistic interaction.

For model contact lens materials, the PRG4-HA synergy in boundary lubrication has been detected only for SiHy materials and not for the more hydrophilic conventional ones, when both agents were used in solution [49]. Similar results were observed when HA was covalently tethered into the bulk of model contact lens with and PRG4 was in solution [50]. In an effort to further understand PRG4-HA interactions, we recently developed rhPRG4 and HA surface-modified model contact lenses by covalently attaching rhPRG4 or HA to the surface of pHEMA and pHEMA-*co*-TRIS hydrogels. The resulting materials showed no cytotoxicity as well as improved *in vitro* surface wettability and protein antifouling properties [64]. Taking advantage of the natural presence of PRG4 and HA in the eye, the existence of HA containing ophthalmic solutions, the fact that full-length recombinant human PRG4 (rhPRG4) has been used in a clinical setting [28], and the aforementioned PRG4-HA synergy in boundary lubrication for these materials, the aim of this study was to assess the impact of the PRG4/HA complex and its configuration on the surface properties of contact lens materials. Enhancing the understanding of boundary lubrication with these molecules could aid in the development of contact lens materials characterized by improved ocular compatibility and higher degree of comfort.

6.2. Materials and Methods

6.2.1. Chemicals and Reagents

The monomer 3-methacryloxypropyl-tris-(trimethylsiloxy) silane (TRIS, ≥95%) was supplied by Gelest (Morrisville, PA, USA), while the photoinitiators 1-hydroxy-cyclohexyl-

phenyl-ketone (Irgacure® 184) and 2-hydroxy-1-[4-(2-hydroxyethoxy)phenyl]-2-methyl- 1-propanone) (Irgacure® 2959) were generously donated by BASF Chemical Company (Vandalia, IL, USA). Hyaluronic acid (HA) (sodium hyaluronate) of two different molecular weights (MW) of 100 kDa and 1.6 MDa was obtained from LifeCore Biomedical (Chaska, MN, USA). Hydroxybenzotriazole (HOBt) was purchased from Toronto Research Chemicals Inc (Toronto, ON, Canada). Full-length recombinant human PRG4 (rhPRG4) was provided by Lubris BioPharma LLC (Framingham, MA, USA) [48,65]. Human corneas (age: 63-86) that were harvested and stored in Optisol-GS (Bausch & Lomb, Rochester, NY) at 4˚C prior to testing [47], were obtained from the Southern Alberta Lions Eye Bank. These tissues were tested within 2 weeks of harvest. Approval for tissue use was granted by the University of Calgary Conjoint Health Research Ethics Board. All other chemicals, reagents and proteins used were purchased from Sigma Aldrich (Oakville, ON, Canada).

6.2.2. Synthesis of model pHEMA and pHEMA-*co*-TRIS hydrogel materials

Prior to synthesis, 2-hydroxyethylmethacylate (HEMA), TRIS and ethylene glycol dimethacrylate (EGDMA) were passed through a custom-made column filled with inhibitor remover for the removal of monomethyl ether hydroquinone (MEHQ). For the model pHEMA hydrogels, the monomer HEMA, crosslinker EGDMA (2 mol% based on HEMA) and the photoinitiator Irgacure® 184 (0.5 wt% based on HEMA) were mixed for 15 minutes. For the model SiHy pHEMA-*co*-TRIS, HEMA (10 wt%), TRIS (90 wt%) and EGDMA (3.5 mol% based on monomer' mixture) were vigorously stirred for 30 minutes, followed by the addition of Irgacure® 184 (0.5 wt% based on the monomer mixture). Following, the prepolymer mixture was transferred into a custom-made UV-transparent acrylic mold equipped with a spacer of adjustable thickness (0.5mm and 1 mm). The mold was then placed into a 400 W UV chamber (365 nm, Cure Zone 2 Con-trol-cure, Chicago, IL, USA) for 10 minutes to allow the hydrogel to cure. Samples were demolded 12 hours post curing, immersed in Milli-Q water for a minimum of 24 hours to ensure complete swelling and then punched into discs of 6.35 mm (1/4“) diameter and 0.5 mm thickness. For friction measurement, the discs used were 7.94 mm (5/16“) in diameter and 1 mm thick due to experimental restrictions. Discs were placed into a 1:1 vol% methanol:water solution and then into Milli-Q water to remove any unreacted monomers and photoinitiator. Discs were subsequently dried and stored at room temperature.

6.2.3. Synthesis of surface rhPRG4- grafted pHEMA and pHEMA-*co*-TRIS hydrogels

For the immobilization of rhPRG4 on the surface of pHEMA and pHEMA-*co*-TRIS hydrogels, N,N'-carbonyldiimidazole (CDI) linking chemistry was performed. The protocol followed was as previously described. Briefly, CDI in anhydrous 1,4-dioxane solution (40 mM per disc) was added dropwise to a 20 ml glass vial that contained vacuum dried pHEMA or pHEMA-*co*-TRIS discs, under a dry N_2 atmosphere. The reaction duration was three hours under stirring conditions, followed by sample washing and sonication (5 minutes) with anhydrous 1,4-dioxane. The discs were then dried under N_2 and used immediately for the immobilization of rhPRG4.

For the surface rhPRG4-grafting reaction, each CDI-activated hydrogel disc was placed into an eppendorf tube filled with 1ml of rhPRG4 solution (0.3 mg/ml, pH 9.2). The eppendorf tubes were vortexed (800 rpm) for 24 hours at 4^{o}C. After this incubation period, discs were washed extensively with PBS (pH 7.4) to remove ungrafted rhPRG4. To investigate the impact of physisorbed HA on the surface properties of rhPRG4-grafted hydrogels, fully hydrated rhPRG4-grafted pHEMA and pHEMA-*co*-TRIS discs were preconditioned in a 300 μl/disc HA (1.6kDa) solution (1.5 mg/ml, pH 7.4) that had the same concentration and similar MW of HA to Blink Contacts® lubricant eye drops (Abbott Medical Optics), for 3 hours at room temperature (sample denoted as rhPRG4-grafted+HA_{sol}).

6.2.4. Synthesis of surface HA-grafted pHEMA and pHEMA-*co*-TRIS hydrogels

HA was covalently attached to the surface of the pHEMA and pHEMA-*co*-TRIS via thiol-ene chemistry using a procedure previously described [64]. For the surface acrylation of the hydrogels, discs were immersed in a solution containing acryloyl chloride (29 mM per disc) and pyridine (0.1 equivalent to acryloyl chloride) dissolved in anhydrous dichloromethane for 3 hours at room temperature under N_2 and dark conditions. The acrylated hydrogels were then washed in DMF for 5 minutes (3 changes) and in Milli-Q water (3 changes) for 24 hours. Following this, the fully hydrated acrylated hydrogels were immersed in a solution containing thiolated HA (HA-SH) (0.5 wt%, 30% free thiols) as well as the photoinitiator Irgacure® 2959 (0.05 wt%) and then placed into an UV oven (80 mW/cm^2 at 365 nm, Cure Zone 2 Con-trol-cure, Chicago, IL, USA) for 10 minutes under constant stirring to allow for the surface grafting reaction. To remove the unattached HA-SH, the discs were thoroughly washed for 24 hours with PBS (pH 7.4). To investigate the

impact of physisorbed rhPRG4 on the surface properties of HA-grafted hydrogels, fully swollen HA-grafted pHEMA and pHEMA-*co*-TRIS were incubated in 300 μg/disc rhPRG4 solution (300 μg/ml, pH 7.4) for 3 hours at room temperature (rhPRG4 preconditioning step, samples noted as HA-grafted+rhPRG4$_{sol}$). Since the concentration and distribution of PRG4 protein both in the tear film and on the ocular surface are currently unknown, the concentration of rhPRG4 used in this study was based on the physiologic levels in normal synovial fluid [52] in accordance with previous work on similar ocular biointerfaces where synergistic boundary lubrication between PRG4 and HA was observed [47,50,66].

6.2.5. Surface chemistry characterization - X-ray Photoelectron Spectroscopy (XPS)

The surface chemical composition of unmodified and surface modified pHEMA and pHEMA-*co*-TRIS samples before and after the preconditioning with HA or rhPRG4 solution respectively, was analyzed by XPS. At the end of the preconditioning step, the discs were gently blotted with a Kimwipe® and then washed for 5 minutes in Milli-Q water (3 cycles) to remove any loosely bound preconditioning agent. A PHI Quantera II XPS scanning spectrometer (Physical Electronics (Phi), Chanhassen, MN, USA) operating at 50W 15kV and equipped with an Al Kα X-ray source (1486.7 eV) and pass energy 280 eV was used. The operating pressure in the chamber was below 3.0×10^{-6} Pa before and during the measurement. The take-off angle was set at 45°, while the survey spectra used for the elemental analysis were collected from scans taken over a binding energy range of 0-1100 eV. The binding energy scale was referenced to the C_{1s} peak set at 285.0 eV. Data analysis of low-resolution spectra was performed using PHI MultiPak Version 9.4.0.7 software. At least two different spots were examined on three different disks for each sample.

6.2.6. Quantification of rhPRG4 (I^{125}-rhPRG4) on the surface HA-grafted hydrogel samples

For the quantification of the rhPRG4 deposited on the surface of the HA-grafted pHEMA and pHEMA-*co*-TRIS hydrogels, rhPRG4 was radiolabeled with I^{125}Na using the iodine monochloride method (ICl) [67]. At the end of the radiolabeling reaction, the I^{125}-rhPRG4 solution was dialyzed extensively against PBS (pH 7.4) using Slide-A-Lyzer™ Dialysis Cassette (Thermo Fisher Scientific, Burlington, ON, Canada) for two days. The percentage of free iodide,

determined by trichloroacetic acid precipitation, was less than 4% of the total radioactivity. In a similar manner to the aforementioned rhPRG4 preconditioning step, fully hydrated HA-grafted pHEMA and pHEMA-*co*-TRIS discs were incubated for 3 hours in a rhPRG4 solution (300 μg/ml, I^{125}-rhPRG4 5%, pH 7.4). Following this, the radioactivity of the samples was measured at the end of the incubation step and after the washing step (5-minute intervals in PBS pH 7.4, 3 cycles) using a gamma counter (Perkin Elmer Wallac Wizard 1470 Automatic Gamma Counter, Wellesley, MA, USA). The surface density of rhPRG4 was also determined over the course of 6 days. Briefly, after measuring the radioactivity of the samples after the incubation step, the discs were stored in PBS (pH 7.4, 2ml/disc) that was exchanged after every radioactivity reading in order to maintain sink conditions. For all measurements, the discs were gently blotted with a Kimwipe® before each reading and placed in a counting vial (5 ml non-pyrogenic, polypropylene round-bottom tube). Standard solutions were used at each time point for the calculation of the rhPRG4 mass present on the surface of the HA-pHEMA and HA-pHEMA-*co*-TRIS surface, accounting for the decay of the isotope over time. The surface density of physically sorbed rhPRG4 on the surface of unmodified (control) pHEMA and pHEMA-*co*-TRIS discs was determined respectively.

6.2.7. Dynamic contact angle measurement

The contact angle of the modified surfaces was measured using the dynamic sessile drop method (Optical Contact Angle Analyzer - OCA 35, Dataphysics, Germany). Prior to measuring the contact angle, each disc was taken out the HA or rhPRG4 preconditioning solutions respectively, and was gently blotted with Kimwipe® to remove excess liquid. The disc was immediately placed on the stage of the OCA 20 instrument and the dosing needle was positioned. The advancing (droplet diameter increases until it attains its maximum) and the receding (droplet diameter decreases until it attains its minimum) phases of a 10 μl drop of PBS (rate 1 μl/sec) were recorded. The advancing (θ_a) (maximum contact angle for maximum drop diameter) and receding (θ_r) (minimum contact angle for maximum drop diameter-until retraction of the contact line) contact angles were calculated using the instrument's software (SCA 20, Dataphysics Instruments, Germany). After each measurement, the disc was returned to the incubating solution for rehydration and the next disc of the same sample was measured. Measurements were made for 6 discs (n=6) of each hydrogel sample both for pHEMA and pHEMA-*co*-TRIS materials and the

process was repeated for both sides of each disc to account for potential non-homogeneity between the surfaces. All contact angles were obtained at ambient temperature and humidity. The contact angle hysteresis (H), the difference between the advancing and the receding contact angles ($H=\theta_a - \theta_r$), was also calculated.

6.2.8. Dehydration Study

The dehydration rate of the surface rhPRG4 and HA-grafted pHEMA-*co*-TRIS samples was determined before and after the preconditioning step in the HA and rhPRG4 solution, by measuring the change in mass over time. Briefly, samples equilibrated in PBS were removed from the vial, gently blotted with a Kimwipe® and placed on a custom-made holder that allowed both surfaces of the disc to be equally exposed for evaporation. The gravimetric measurement began immediately after the holder was placed in a closed chamber digital balance ($W_{wet,}$ t=0) equipped with an incorporated digital hygrometer (La Crosse Technology, WT-137U, RH=40 ± 2% at 23°C). The samples were also weighed at different time intervals ($W_{t,}$ t=1-150 mins). Finally, the discs were dried for 48 hours in a 50°C oven and re-weighed (W_{dry}).

The water loss (%) used herein to express the dehydration rate was calculated based on the equation below:

$$\text{water loss (\%)} = \frac{W_{wet} - W_t}{W_{wet} - W_{dry}} \cdot 100\% \qquad (6.1)$$

6.2.9. Quantification of Protein Deposition – Lysozyme and Human Serum Albumin

For the quantification of the protein deposition on the pHEMA and pHEMA-*co*-TRIS hydrogel surfaces, lysozyme (chicken egg white) and human serum albumin (HSA) were radiolabeled separately with with $Na^{125}I$ using the iodine monochloride (ICl) method as previously described [Papers 1-3]. Unbound I^{125} was removed by passing the labeled samples through a 6 ml column packed with AG 1-X4 (100–200 dry mesh in chloride form; Bio-Rad, Hercules, CA) followed by dialysis with a Slide-A-Lyzer™ Dialysis Cassette (Thermo Fisher Scientific, Burlington, ON, Canada) (7000 MWCO; Pierce, Rockford, IL) against PBS pH 7.4 for 24 hours. Using the trichloroacetic precipitation assay [68], the free I^{125} was determined to be less than 0.5% for both I^{125}-lysozyme and I^{125}-HSA. Aiming to better mimic the composition of the tear film, an

artificial tear solution (ATS) containing salts, glucose, urea and proteins was prepared at pH 7.4, as previously described [69] (Table 6.1). In the ATS, only one protein at a time was radiolabeled with I^{125}. The fraction of the I^{125}-labeled protein in both cases was 5% of the desired final concentration.

For protein deposition experiments, each fully hydrated disc was removed from the incubation solution, dabbed gently to remove any excess liquid and then immersed into 250 μl of the ATS in a 96-well plate. Discs were placed vertically in the wells of the plate to ensure that both surfaces were exposed to solution. The incubation period was 12 hours for the pHEMA and 24 hours for the pHEMA-*co*-TRIS samples. At the end of the incubation time, the discs were gently blotted with a Kimwipe® and then rinsed 3 times with PBS (pH 7.4) (10-minute wash intervals) to remove any loosely bound protein. The discs were then dabbed again and placed in a counting vial (5 ml non-pyrogenic, polypropylene round-bottom tube). The radioactivity was measured using a Gamma Counter (Perkin Elmer Wallac Wizard 1470 Automatic Gamma Counter, Wellesley, MA, USA). For the determination of the surface density of lysozyme and HSA, a standard calibration curve was used to convert the measured radioactivity (cpm) into mass of protein ($\mu g/cm^2$).

Table 6. 1: Artificial tear solution (ATS) components**.**

Salt components	Concentration (mg/ml)	Proteins	Concentration (mg/ml)
Sodium chloride (NaCl)	5.26	Human Serum Albumin (HAS)	0.2
Potassium chloride (KCl)	1.19	Hen Egg Lysozyme	1.9
Sodium carbonate (Na_2CO_3)	1.27	Bovine colostrum lactoferrin	1.8
Potassium bicarbonate ($KHCO_3$)	0.30	Bovine β-Lactoglobulin A	1.6
Calcium chloride ($CaCl_2$)	0.07	Human IgG	0.02
Trisodium citrate ($Na_3C_6H_5O_7$)	0.44	Bovine submaxillary Mucin	0.15
Sodium phosphate dibasic (Na_2HPO_4)	3.41		
Hydrochloric acid (HCl)	0.94		
Glucose	0.036		
Urea	0.072		
Proclin 300	200 μl per liter of solution		

6.2.10. *In vitro* friction measurement

To investigate the potential synergy of physisorbed HA and rhPRG4 on the lubricating properties of the respective rhPRG4 and HA-modified pHEMA and pHEMA-*co*-TRIS materials, *in vitro* ocular biomechanical friction tests were conducted before and after the preconditioning step with the counterpart agent, under boundary conditions at a human cornea-disc biointerface. The experimental setup, procedure and data analysis was as previously described [23,47,48,66]. In this study, the control saline used was Bausch and Lomb Saline Plus® (Bausch and Lomb, Rochester, NY, USA), the rhPRG4 solution ($rhPRG4_{sol}$) was based on rhPRG4 (0.3 mg/ml) dissolved in the control saline and the HA solution (HA_{sol}) used was Blink Contacts® lubricating eye drops (HA 1.5 mg/ml) (Abbott Medical Optics, Santa Ana, CA, USA) [37]. Briefly, fully

swollen in PBS rhPRG4-grafted samples were initially preconditioned in the solution of interest for one hour. Testing was performed using the biomechanical BOSE ELF3200 machine which was equipped with axial and rotational actuators where the hydrogel disc and the cornea were mounted respectively. The axial load (N) and torque (τ) were recorded at a rate of 20 Hz for the calculation of static (μ_{static}, N_{eq}) (N_{eq}: equilibrium axial load) and kinetic ($<\mu_{kinetic}>$) ($\langle\rangle$ denotes the kinetic equilibrium mean) friction coefficients at four different sliding velocities (0.3, 1, 10, 30 mm/s) under normal loads of approximately 12-25 kPa. During the friction testing, the cornea-disc interface was immersed in a lubricating bath (0.3 ml) containing the same solution as the preconditioning step. The two test sequences that were the same for pHEMA and pHEMA-*co*-TRIS materials are shown below:

1. control and rhPRG4-grafted in saline bath, control+HA_{sol} and rhPRG4-grafted+HA_{sol} in HA_{sol} bath
2. control and HA-grafted in saline bath, control+$rhPRG4_{sol}$ and HA-grafted+$rhPRG4_{sol}$ in $rhPRG4_{sol}$ bath

Each full test sequence was done using the same human cornea sample and was considered a one repeat for the statistical analysis results. The test sequence was based on previously employed sequences followed for a similar test set-up where hydrogel material-dependent interactions between rhPRG4 and HA were investigated [47,49,50]. All of the data presented were transformed into log scale to improve the uniformity of variance for statistical analysis [47].

6.2.11. Statistical Analysis

The results are presented as mean ± standard deviation (SD) with the exception of the friction coefficients where results are presented as mean ± standard error of the mean (SEM) to conform with previous studies. One-way ANOVA with Tukey's HSD for post-hoc comparisons using Statistica 10 (StatSoft Inc. Tulsa, OK, USA) was performed among groups to determine any statistical significance in mean values. Statistically significant values were determined for $p<0.05$.

6.3. Results

6.3.1. X-ray photoelectron spectroscopy (XPS) analysis

The elemental composition of the pHEMA and pHEMA-*co*-TRIS surfaces from the low resolution XPS spectra is reported in terms of percent atomic composition in Tables 6.2 and 6.3 respectively. After the HA preconditioning step, the C_{1s} and O_{1s} content of the unmodified pHEMA and pHEMA-*co*-TRIS samples (pHEMA or pHEMA-*co*-TRIS +HA_{sol}) was not altered ($p=0.3$). However, for the rhPRG4-grafted+HA_{sol} pHEMA and pHEMA-*co*-TRIS samples the N_{1s} percentage and the O/C ratio were significantly decreased ($p<0.001$). It is thus speculated that the lower-nitrogen-containing coating of HA was able to physically adhere to the surface of the rhPRG4-grafted materials, indicating higher affinity of the HA for the rhPRG4-grafted layer than for the unmodified substrates. This is further supported by the observed decrease in the Si_{2p} percentage for the rhPRG4-grafted+HA_{sol} pHEMA-*co*-TRIS hydrogels. On the other hand, the presence of the N_{1s} signal as well as the increase in the O/C ratio ($p<0.008$) for the unmodified pHEMA and pHEMA-*co*-TRIS samples that are preconditioned with rhPRG4 (pHEMA or pHEMA-*co*-TRIS + $rhPRG4_{sol}$) are attributed to the presence of physically sorbed rhPRG4 on these surfaces. For the HA-grafted+$rhPRG4_{sol}$ pHEMA and pHEMA-*co*-TRIS materials, the N_{1s} content is further increased whereas the O/C ratio is slightly decreased ($p<0.003$), suggesting that the rhPRG4 can adhere to the HA-grafted layer of the substrates. The Si_{2p} content of the HA-grafted+$rhPRG4_{sol}$ pHEMA-*co*-TRIS sample is also reduced ($p<0.02$), which in turn further indicates the interaction of the glycoprotein with the HA-grafted layer.

Table 6.2: Atomic composition (%) of the surface of the unmodified, rhPRG4-grafted and HA-grafted pHEMA samples before and after the preconditioning step in the HA and rhPRG4 solution respectively from low resolution XPS spectra (n=3).

Sample	**C_{1s}**	**O_{1s}**	**N_{1s}**	**Si_{2p}**	**S_{2p}**	**O/C**
pHEMA control	73.7 ± 2.1	25.1 ± 2.2	-	1.2 ± 0.4	-	0.36 ± 0.05
pHEMA + HA_{sol}	72.7 ± 2.8	27.0 ± 2.7	-	0.6 ± 0.2	-	0.37 ± 0.05
rhPRG4-grafted	63.8 ± 0.7	24.8 ± 0.9	**10.1 ± 0.5**	1.0 ± 0.3	**0.3 ± 0.03**	0.39 ± 0.02
rhPRG4-grafted + HA_{sol}	68.9 ± 1.3	23.6 ± 1.6	**6.7 ± 0.9**	0.8 ± 0.3	**0.1 ± 0.07**	0.34 ± 0.03
pHEMA + $rhPRG4_{sol}$	69.4 ± 2.3	28.5 ± 2.4	**0.4 ± 0.1**	0.8 ± 0.3	-	0.41 ± 0.05
HA-grafted	67.4 ± 2.0	26.0 ± 1.4	**3.1 ± 0.5**	0.6 ± 0.4	0.1 ± 0.02	0.43 ± 0.05
HA-grafted + $rhPRG4_{sol}$	67.3 ± 1.9	26.3 ± 1.1	**4.7 ± 0.5**	0.7 ± 0.2	0.2 ± 0.06	0.39 ± 0.03

Table 6.3: Atomic composition (%) of the surface of the unmodified, rhPRG4-grafted and HA-grafted pHEMA-*co*-TRIS samples before and after the preconditioning step in the HA and rhPRG4 solution respectively from low resolution XPS spectra (n=3).

Sample	**C_{1s}**	**O_{1s}**	**N_{1s}**	**Si_{2p}**	**O/C**
pHEMA-*co*-TRIS control	66.5 ± 1.7	23.3 ± 1.6	-	10.2 ± 0.5	0.35 ± 0.03
pHEMA-*co*-TRIS + HA_{sol}	65.7 ± 1.4	24.3 ± 1.3	-	10.1 ± 0.4	0.37 ± 0.03
rhPRG4-gtafted	63.7 ± 1.4	24.1 ± 1.3	**6.0 ± 0.6**	**6.4 ± 0.6**	0.38 ± 0.02
rhPRG4-grafted+HA_{sol}	72.0 ± 2.3	24.1 ± 1.1	**3.9 ± 0.9**	**3.4 ± 1.1**	0.29 ± 0.03
pHEMA-*co*-TRIS + $rhPRG4_{sol}$	64.1 ± 1.2	26.4 ± 1.4	**0.9 ± 0.2**	9.0 ± 1.0	0.41 ± 0.03
HA-grafted	64.7 ± 1.0	27.0 ± 1.1	**2.1 ± 0.6**	**6.1 ± 0.5**	0.42 ± 0.02
HA-grafted + $rhPRG4_{sol}$	65.3 ± 3.2	23.9 ± 2.1	**4.0 ± 0.4**	**5.4 ± 0.3**	0.37 ± 0.05

6.3.2. Quantification of rhPRG4 (I^{125}-rhPRG4) on the surface HA-grafted hydrogel samples

The amount of rhPRG4 physically sorbed to the surface of the unmodified (control) and HA-grafted pHEMA and pHEMA-*co*-TRIS materials after the rhPRG4 preconditioning step is shown in Figure 6.1. At the end of the preconditioning step, the surface density of rhPRG4 is slightly higher for the unmodified pHEMA discs compared to the HA-grafted samples (unmodified: 577.3 ± 22.4 ng/cm^2 and HA-grafted+rhPRG4$_{sol}$: 498.0 ± 22.9 ng/cm^2, $p<0.003$). The opposite trend was observed for the pHEMA-*co*-TRIS materials (unmodified: 648.0 ± 22.7 ng/cm^2 and HA-grafted+rhPRG4$_{sol}$: 720.9 ± 20.3 ng/cm^2, $p<0.006$). After the removal of the loosely bound rhPRG4 with the PBS washing procedure however, the HA-grafted samples were characterized by higher amounts of rhPRG4 than the unmodified samples for both pHEMA (unmodified: 261.5 ± 10.6 ng/cm^2 and HA-grafted+rhPRG4$_{sol}$: 320.0 ± 14.7 ng/cm^2) and pHEMA-*co*-TRIS (unmodified: 366.0 ng/cm^2 ± 12.3 ng/cm^2 and HA-grafted+rhPRG4$_{sol}$: 500.0 ± 140.0 ng/cm^2) hydrogels ($p<0.002$). The surface density of rhPRG4 was also determined as a function of time (Figure 6.2). Incubation of the unmodified pHEMA and pHEMA-*co*-TRIS samples in PBS presumably led to a slow release of the non-specifically sorbed rhPRG4 from their surface over the course of 6 days. However, the amount of rhPRG4 present on the surface of the HA-grafted samples remained the same after the first 48 hours of incubation in PBS.

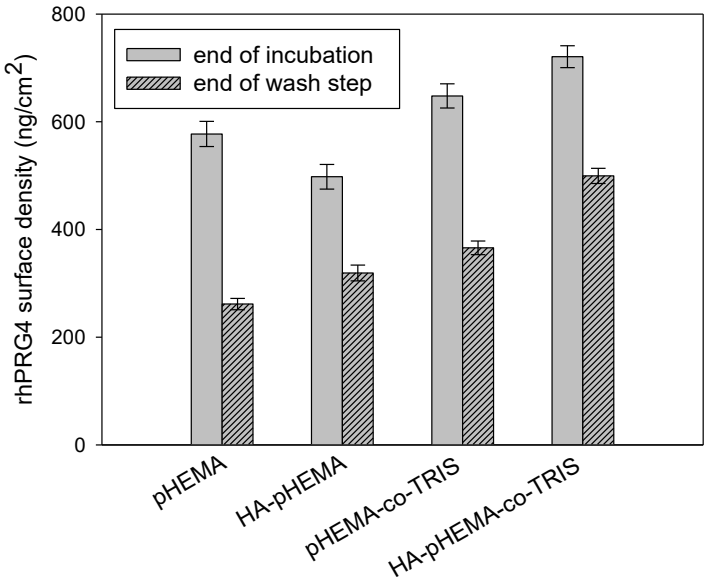

Figure 6.1: The surface density (±SD) of rhPRG4 for the unmodified (control) and HA-grafted pHEMA and pHEMA-*co*-TRIS hydrogels (n=4), at the end of preconditioning step (2.5 hours) and the wash step respectively.

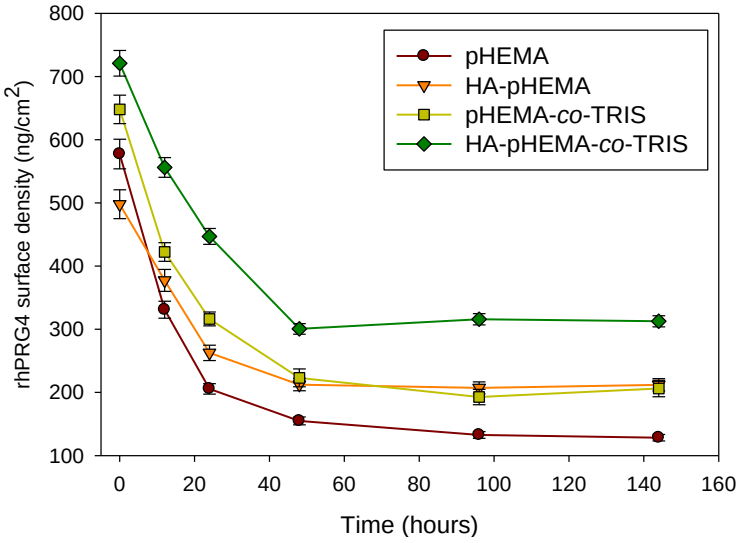

Figure 6.2: The profile of the rhPRG4 surface density (±SD) over time, for the unmodified (control) and HA-grafted pHEMA and pHEMA-*co*-TRIS hydrogels (n=4) respectively.

6.3.3. Dynamic contact angle

The advancing and receding contact angles as well as their hystereses before and after the preconditioning step are depicted in Figure 6.3. Surface immobilization of rhPRG4 reduced the contact angles, especially for the pHEMA-*co*-TRIS materials ($p<0.0002$), however, the HA-grafted pHEMA and pHEMA-*co*-TRIS samples exhibited the lowest advancing and receding contact angles, and thus the smallest hysteresis ($p<0.0005$). Preconditioning rhPRG4-grafted discs with HA (rhPRG4-grafted+HA_{sol}) further decreased the dynamic contact angles and hysteresis, particularly for the rhPRG4-grafted+HA_{sol} pHEMA hydrogels ($p<0.0003$). On the contrary, the presence of the amphiphilic rhPRG4 coating increased the dynamic contact angles and the hysteresis of the HA-grafted+$rhPRG4_{sol}$ samples for both pHEMA and pHEMA-*co*-TRIS materials ($p<0.0002$). Overall, the surface wettability of rhPRG4-grafted+HA_{sol} and HA-grafted+$rhPRG4_{sol}$ pHEMA hydrogels was similar ($p=1$), whereas rhPRG4-grafted+HA_{sol} pHEMA-*co*-TRIS hydrogels were characterized by a lower advancing contact angle, and thus hysteresis, than the respective HA-grafted+$rhPRG4_{sol}$ materials ($p<0.001$).

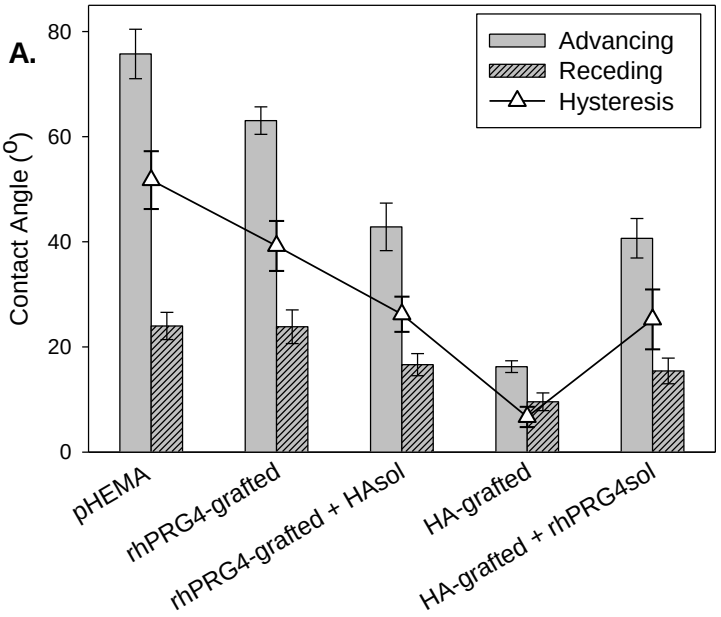

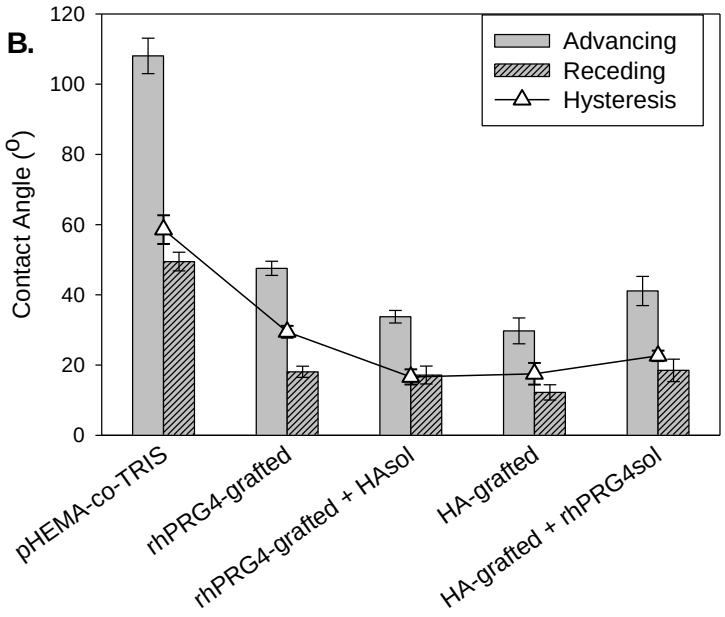

Figure 6.3: The impact of surface treatment and preconditioning step on the surface wettability. Advancing and receding contact angles (and their hysteresis) of (A) pHEMA and (B) pHEMA-*co*-TRIS hydrogel discs (n=8).

6.3.4. Dehydration rate

The impact of the rhPRG4/HA interactions on the dehydration profile of the model contact lens materials was determined based on the rate of mass change (%) over time (equation 6.2) using the gravimetric method (Figure 6.4). According to the results, the water evaporation rate for the rhPRG4-grafted pHEMA and pHEMA-*co*-TRIS samples was significantly slower than that of the HA-grafted samples ($p<0.05$), which also exhibited reduced dehydration compared to the unmodified (control) hydrogels ($p<0.05$). Preconditioning the rhPRG4-grafted pHEMA sample with HA (rhPRG4-grafted+HA_{sol}) further delayed its water evaporation rate ($p<0.05$), whereas the impact of a rhPRG4 preconditioning step on the dehydration profile of the HA-grafted-$rhPRG4_{sol}$ pHEMA hydrogels was not significant (Figure 6.4A). For the pHEMA-*co*-TRIS materials, the presence of the HA coating on the rhPRG4-grafted (rhPRG4-grafted+HA_{sol}) sample as well as the presence of the rhPRG4 coating on the HA-grafted (HA-grafted+$rhPRG4_{sol}$) sample further restricted the water evaporation rate ($p<0.05$) (Figure 6.4B). Interestingly, the percentage decrease in the water evaporation rate of rhPRG4-grafted+HA_{sol} compared to the rhPRG4-grafted sample

was similar to that of the HA-grafted+rhPRG4$_{sol}$ and HA-grafted pHEMA-*co*-TRIS samples. Overall, the rhPRG4-grafted+HA$_{sol}$ pHEMA and pHEMA-*co*-TRIS samples were characterized by the slowest dehydration rate.

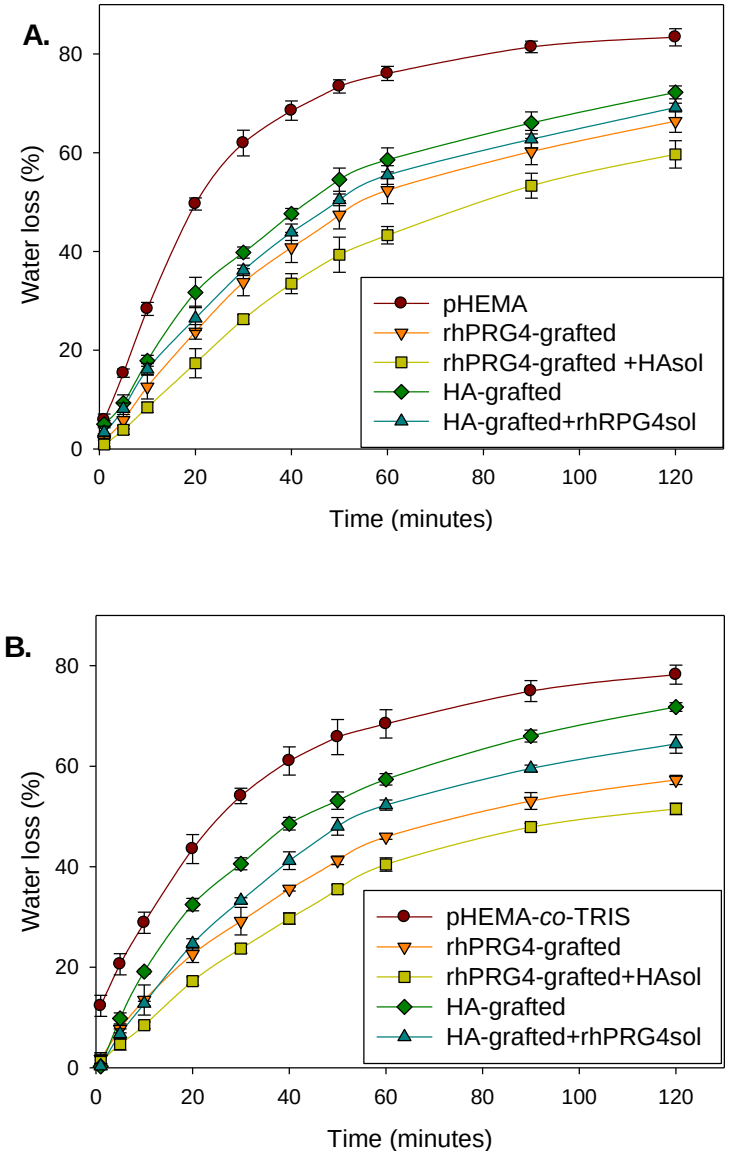

Figure 6.4: Dehydration profile of rhPRG4 and HA-grafted A. pHEMA and B. pHEMA-*co*-TRIS hydrogels, before and after the preconditioning step with the counterpart agent. The water loss (%) (±SD) was calculated over time in a closed chamber (T=22^{o}C, RH=40 ± 2%) (n=6).

6.3.5. *In vitro* lysozyme and human serum albumin (HSA) deposition

The effect of the preconditioning step on the protein deposition profile of the rhPRG4 and HA-grafted layers was assessed *in vitro* using an ATS that contained major tear film proteins, mucins and electrolytes. Figure 6.5 shows the surface density of lysozyme and albumin (HSA) on the pHEMA and pHEMA-*co*-TIRS hydrogel materials for the various surface treatments. Overall, the rhPRG4-grafted samples exhibited the least amount of non-specifically sorbed proteins when compared to the respective HA-grafted and unmodified (control) hydrogels ($p<0.02$) prior to the preconditioning step.

In order to better understand the results after the preconditioning step, the impact of rhPRG4/HA configuration on the percentage change of the lysozyme and albumin (HSA) surface density is shown in Table 6.4. More specifically, the stated change (%) in the quantity of each of the examined proteins due to the rhPRG4 or HA-grafted layer is compared to that of the unmodified (control) samples, whereas the change (%) in the protein surface density caused by the physisorbed HA or rhPRG4 coating (HA_{sol} or $rhPRG4_{sol}$) is compared to that of the respective rhPRG4 or HA-grafted sample, so as to show the impact of the preconditioning step on the non-specific protein sorption. The presence of physisorbed HA coating on the rhPRG4-grafted+HA_{sol} pHEMA hydrogels further reduced the lysozyme (30%, $p<0.002$) but not the albumin sorption ($p=0.94$). The opposite was observed for the rhPRG4-grafted+HA_{sol} pHEMA-*co*-TRIS materials where physisorbed HA significantly decreased the amount of non-specifically sorbed albumin (60%, $p<0.0002$) but not that of lysozyme ($p=0.45$). On the other hand, the presence of the rhPRG4 coating was found to further reduce the surface density of both proteins for both HA-grafted+$rhPRG4_{sol}$ pHEMA (lysozyme: $p<0.0003$, albumin: $p<0.004$) and pHEMA-*co*-TRIS hydrogel samples (lysozyme: $p<0.0005$, albumin: $p<0.02$). Overall, less albumin was deposited on the HA-grafted+$rhPRG4_{sol}$ pHEMA compared to the rhPRG4-grafted+HA_{sol} pHEMA ($p<0.02$) while the lysozyme amount was the same, whereas for the pHEMA-*co*-TRIS hydrogels the surface density of both proteins was significantly lower for rhPRG4-grafted+HA_{sol} hydrogels ($p<0.0005$).

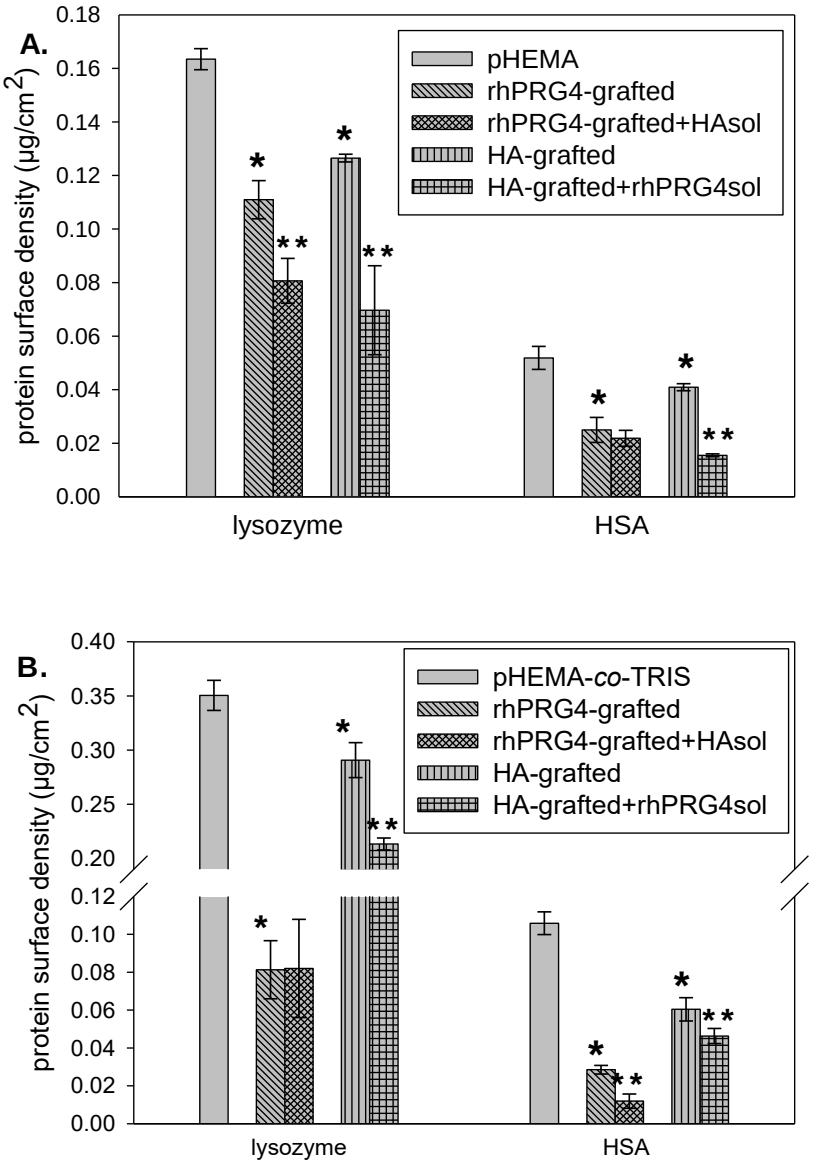

Figure 6.5: The surface density (±SD) of lysozyme and albumin (HSA) from an artificial tear solution (ATS) on (A) pHEMA and (B) pHEMA-*co*-TRIS hydrogels (n=6), before and after the preconditioning step, after 12 hours and 24 hours of incubation.
(*$p<0.05$ compared to the unmodified control samples, ** $p<0.05$ compared to the rhPRG4 and HA-grafted samples).

Table 6.4: The impact of rhPRG4 and HA as a grafted-layer and as a coating on the percentage decrease in lysozyme and albumin deposition for the pHEMA and pHEMA-*co*-TRIS materials respectively (n=6).

sample	pHEMA		pHEMA-*co*-TRIS	
	lysozyme	HSA	lysozyme	HSA
rhPRG4-grafted	↓ 30%	↓ 55%	↓ 80%	↓ 75%
rhPRG4-grafted+HA_{sol}	↓ 30%	none	none	↓ 60%
HA-grafted	↓ 25%	↓ 20%	↓ 20%	↓ 50%
HA-grafted+$rhPRG4_{sol}$	↓ 45%	↓ 60%	↓ 30%	↓ 25%

6.3.6. *In vitro* friction coefficients under boundary lubrication conditions

In this work, the ability of rhPRG4 and HA to synergistically reduce boundary friction in soft polymeric material materials, such as the model contact lenses used herein, was determined under physiologically relevant contact pressures and sliding velocities observed during les wear [70]. The impact of the configuration of the rhPRG4/HA complex on the friction profile of the examined hydrogels was assessed as well.

The μ_{static} and $\langle\mu_{kinetic}\rangle$ for both pHEMA and pHEMA-*co*-TRIS are shown Figures 6.5 and 6.6 and summarized in Table 6.5 (mean over all velocities). The μ_{static} of rhPRG4 and HA-grafted samples was similar to that of the unmodified (control) pHEMA sample ($p>0.5$). Although not statistically significant, the $\langle\mu_{kinetic}\rangle$ of the rhPRG4-grafted sample was higher ($p=0.5$), whereas the $\langle\mu_{kinetic}\rangle$ of the HA-grafted sample was slightly lower than that of the unmodified (control) pHEMA hydrogels ($p=0.2$). After the HA preconditioning step, the μ_{static} and $\langle\mu_{kinetic}\rangle$ of the rhPRG4-grafted+HA_{sol} pHEMA samples were further increased without however leading to friction coefficients higher than those of the unmodified (control) sample (μ_{static}: $p>0.2$; $\langle\mu_{kinetic}\rangle$: $p>0.5$) (Figure 6.6). The opposite was observed for the HA-grafted pHEMA samples, where the μ_{static} and $\langle\mu_{kinetic}\rangle$ of HA-grafted+$rhPRG4_{sol}$ sample were significantly reduced compared to those of the unmodified (control) pHEMA hydrogels, especially for lower sliding speeds (0.3 and 1 mm/s) (μ_{static}: $p<0.02$; $\langle\mu_{kinetic}\rangle$: $p<0.05$). Despite the observed changes, there was no statistically

significant interaction effect in boundary friction between rhPRG4 and HA for either configuration of pHEMA hydrogels; however, the $\langle\mu_{kinetic}\rangle$ of rhPRG4-grafted+HA_{sol} pHEMA sample was significantly higher than that of the HA-grafted+$rhPRG4_{sol}$ pHEMA hydrogels ($p<0.05$). Moreover, the μ_{static} of all pHEMA samples increased significantly by increasing the sliding velocity ($p<0.04$), with the exception of the rhPRG4-grafted+HA_{sol} pHEMA hydrogels ($p=0.3$). There was no effect of velocity for $\langle\mu_{kinetic}\rangle$.

Surface modification of pHEMA-*co*-TRIS hydrogels with either a rhPRG4 or an HA-grafted layer did not cause any significant change in the μ_{static} ($p>0.05$) (Figure 6.7A). However, after the preconditioning step, the μ_{static} of rhPRG4-grafted+HA_{sol} sample was significantly lower than that of the unmodified (control) pHEMA-*co*-TRIS sample ($p<0.03$), while a strong decreasing trend was also observed for the μ_{static} of the HA-grafted+$rhPRG4_{sol}$ sample respectively ($p=0.05$). Moreover, the $\langle\mu_{kinetic}\rangle$ of the rhPRG4-grafted pHEMA-*co*-TRIS sample, which was lower than the unmodified (control) sample ($p<0.03$), was further reduced with the presence of the physisorbed HA (rhPRG4-grafted+HA_{sol} sample, $p<0.01$) (Figure 6.7B). In a similar manner, the presence of the physisorbed rhPRG4 significantly reduced the $\langle\mu_{kinetic}\rangle$ of the HA-grafted+$rhPRG4_{sol}$ sample when compared to the unmodified (control) pHEMA-*co*-TRIS hydrogels ($p<0.03$). Hence, the $\langle\mu_{kinetic}\rangle$ of the rhPRG4-grafted+HA_{sol} and HA-grafted+$rhPRG4_{sol}$ pHEMA-*co*-TRIS samples were characterized by similar boundary friction coefficients (μ_{static}: $p=0.65$; $\langle\mu_{kinetic}\rangle$: $p=0.8$). Despite the friction lowering synergistic interactions between rhPRG4 and HA for the model SiHy, there was no statistically significant interaction effect in boundary friction between rhPRG4 and HA for either configuration of pHEMA-*co*-TRIS samples ($p>0.2$). In a similar manner to pHEMA hydrogels, the μ_{static} of the human cornea-disc biointerface for the developed pHEMA-*co*-TRIS samples was characterized by a velocity dependent profile ($p<0.01$), whereas their $\langle\mu_{kinetic}\rangle$ was not ($p>0.05$).

Table 6.5: Summary of the values of the static μ_{static} and kinetic $\langle\mu_{kinetic}\rangle$ (±SEM) friction coefficients (mean over all velocities) for unmodified (control), rhPRG4 and HA-grafted pHEMA hydrogels in baths of saline, HA (rhPRG4-grafted+HA_{sol}) or rhPRG4 (HA-grafted+$rhPRG4_{sol}$) respectively at a cornea-disc biointerface (pHEMA: n=3; pHEMA-*co*-TRIS: n=5).

sample	pHEMA		pHEMA-*co*-TRIS	
	μ_{static}	$\langle\mu_{kinetic}\rangle$	μ_{static}	$\langle\mu_{kinetic}\rangle$
control	0.21 ± 0.03	0.16 ± 0.03	0.35 ± 0.04	0.25 ± 0.02
rhPRG4-grafted	0.22 ± 0.03	0.19 ± 0.3	0.25 ± 0.03	0.18 ± 0.01
rhPRG4-grafted+HA_{sol}	0.38 ± 0.14	0.24 ± 0.05	0.21 ± 0.02	0.15 ± 0.02
HA-grafted	0.19 ± 0.02	0.14 ± 0.02	0.29 ± 0.05	0.20 ± 0.03
HA-grafted+$rhPRG4_{sol}$	0.15 ± 0.02	0.12 ± 0.01	0.20 ± 0.03	0.16 ± 0.02

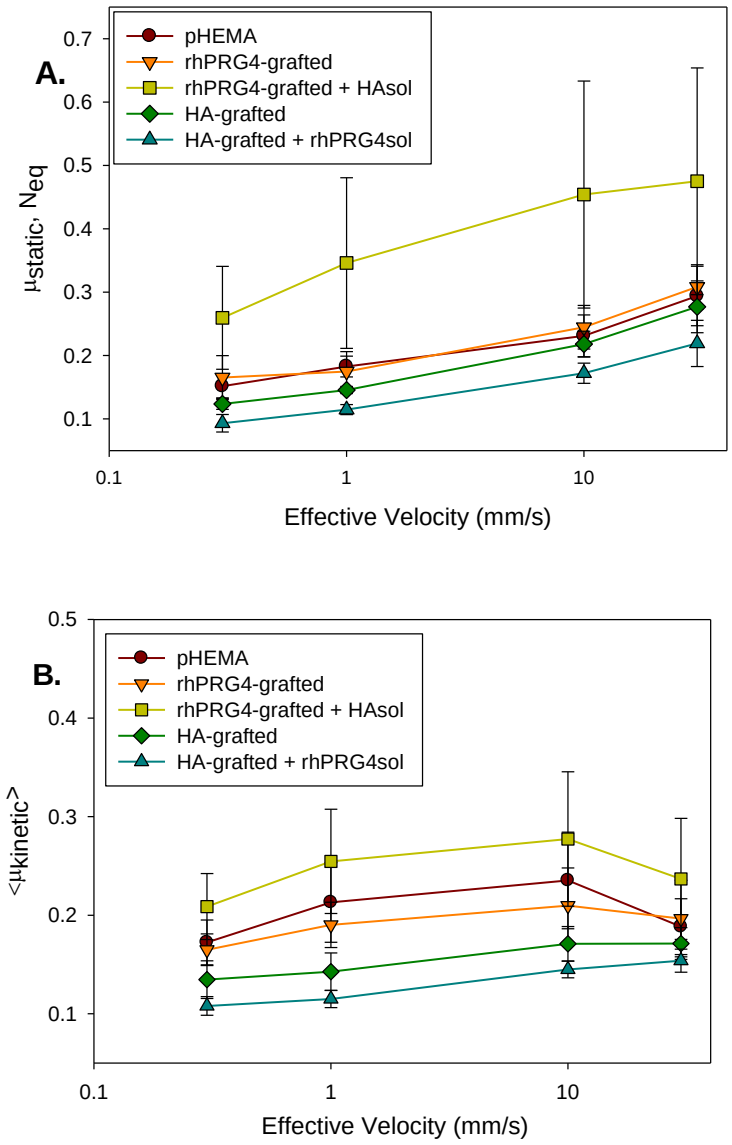

Figure 6.6: Effect of the preconditioning step on the *in vitro* boundary lubrication at a human cornea-hydrogel disc biointerface. (A) static $\mu_{static,}$ N_{eq} (±SEM) and (B) kinetic $<\mu_{kinetic}>$ (±SEM) friction coefficients for unmodified (control) and rhPRG4 and HA-grafted pHEMA hydrogels in baths of saline and HA (rhPRG4-grafted+HA_{sol}) or rhPRG4 (HA-grafted+$rhPRG4_{sol}$) respectively. The average normal stress was 21.4 ± 4.5kPa (±SD). Sliding velocity values were log transformed to improve the uniformity of variance for statistical analysis.

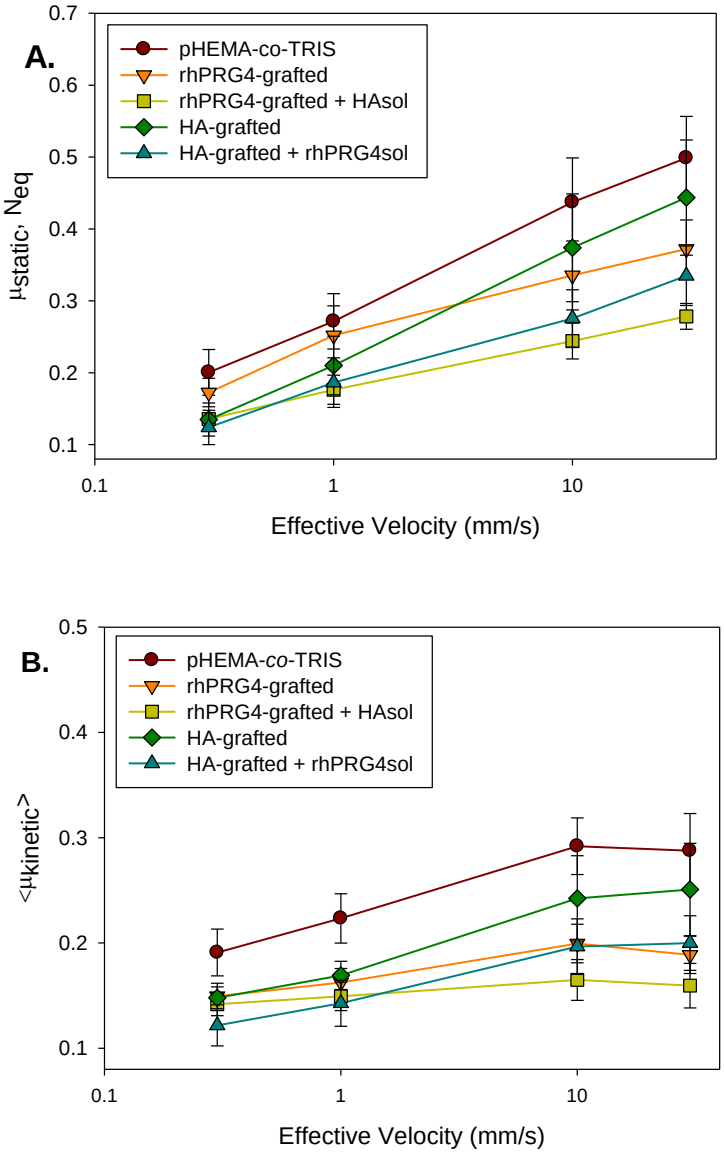

Figure 6.7: Effect of the preconditioning step on the *in vitro* boundary lubrication at a human cornea-SiHy disc biointerface. (A) static $\mu_{static,}$ N_{eq} (±SEM) and (B) kinetic $<\mu_{kinetic}>$ (±SEM) friction coefficients for unmodified (control) and rhPRG4 and HA-grafted pHEMA-*co*-TRIS hydrogels in baths of saline and HA (rhPRG4-grafted+HA_{sol}) or rhPRG4 (HA-grafted+$rhPRG4_{sol}$) respectively. The average normal stress was 20.1 ± 1.9kPa (±SD). Sliding velocity values were log transformed to improve the uniformity of variance for statistical analysis.

6.4. Discussion

6.4.1. Surface chemistry analysis

The changes observed in the N_{1s} content as well as the O/C ratio of the low resolution XPS spectra for the rhPRG4 and HA-grafted pHEMA and pHEMA-*co*-TRIS samples, in combination with the reduction in the Si_{2p} percentage of the model SiHy materials, indicated that rhPRG4 and HA interact with each other when either is surface grafted or free in solution. Previous work suggested that surface bound PRG4 may function as a surface anchor for HA [60,62], leading to subsequent aggregation and cross-linking with rhPRG4 [53], thus aiding joint lubrication. However, Chang et al. [57] demonstrated that physical deposition of a PRG4-HA complex was greater than PRG4 alone, whereas no interaction between HA and a PRG4-coated model non-porous surface was observed. On the other hand, earlier studies showed that PRG4 can adhere strongly on HA-modified model substrates [53,58,61]. The increased affinity of rhPRG4 with the HA-grafted surfaces was attributed to previously observed non-covalent molecular interactions between the end-domains of physisorbed rhPRG4 and the HA chains [58,71]. Furthermore, interactions between PRG4 and HA may also be mediated by the hemopexin-like domain of rhPRG4, which is free for the rhPRG4-grafted samples, since purified hemopexin has been previously found to interact with HA [71]. This may result in the formation of a partially entangled and physically crosslinked rhPRG4/HA complex on the surface of the hydrogel materials, as previously reported [53]. Finally, it is worth noting that the Si_{2p} percentage detected on the rhPRG4-grafted+HA_{sol} pHEMA-*co*-TRIS surfaces was lower than that of that of the HA-grafted+$rhPRG4_{sol}$ SiHy ($p<0.003$). It was thus speculated that the rhPRG4-grafted/HA-coated surface may form a more compact layer better able to mask the silicone domains of the model SiHy materials.

6.4.2. Surface density of the physically sorbed rhPRG4 ($rhPRG4_{sol}$)

Quantification of the rhPRG4 amount present on the surface of HA-grafted hydrogel samples showed increased affinity between physically sorbed rhPRG4 and an HA-grafted layer compared to the unmodified (control) pHEMA and pHEMA-*co*-TRIS surfaces. These results are in agreement with the XPS results presented above. Moreover, the surface density of rhPRG4 for the SiHy materials, and more importantly for the HA-grafted pHEMA-*co*-TRIS sample, was

significantly higher than that of the respective pHEMA sample ($p<0.003$). Taking into consideration that the glycoprotein is characterized by a greater affinity for hydrophobic surfaces [57], it is postulated that upon saturation of rhPRG4/HA binding sites due to rhPRG4 accumulation on the HA-grafted surface over time, the glycoprotein may also interact with the substrate of the model contact lens materials.

The surface density profile of rhPRG4 over time indicated that the HA layer could hold and trap the physically bound glycoprotein at the interface over time via molecular interactions, leading to strong and irreversible binding as previously observed [53,58,60,61]. This would be expected to improve the on-eye residence time of rhPRG4 *in vivo*. Future studies should also determine the surface density of the physisorbed HA on the surface of rhPRG4-grafted pHEMA and pHEMA-*co*-TRIS materials respectively, so as to better understand the HA-rhPRG4 interactions on soft polymeric materials, such as the model hydrogel materials examined herein.

6.4.3. Surface wettability

The impact of the rhPRG4/HA configuration on the surface wettability of the examined materials was assessed by measuring the advancing (θ_a) and receding (θ_r) contact angles of rhPRG4 and HA-grafted materials before and after the preconditioning step. The advancing contact angle reflects to the ease with which the pre-lens tear film (PrLTF) spreads over a partially or fully dehydrated lens when the upper lid is closing, while the receding contact angle can be used for the determination of the tear film integrity and stability upon eye lid retraction (lid opening) at the interblink period of a blinking cycle. Lower contact angles suggest improved surface wetting. Hence, determination of the dynamic contact angle is considered relevant for gauging on-eye contact lens wettability. Contact angle hysteresis can provide a macroscopic indication of molecular mobility at the material interface [72]. It may also reflect surface roughness, chemical heterogeneity or potential surface defects as well as the rearrangement of the surface structure through the reorientation of the polymer chains at the surface in order to minimize the interfacial free energy when exposed to either water or air [72,73].

Previous work suggested that the hydrophilic central mucin-like domain of the surface immobilized rhPRG4 would obtain a poorly formed tail-like conformation with the free hydrophobic C'-terminal exposed to the interface for pHEMA hydrogels, whereas for the pHEMA-*co*-TRIS materials a loop-like conformation was presumed with the central mucin-like domain

being exposed to the interface and the C'-terminal being physically bound to the substrate. Therefore, the deposited HA coating had an energetically favourable conformation able to cover the hydrophobic end domains present, particularly the free hemopexin-like end-domain, on the pHEMA surfaces. As well, it was able to reinforce the hydrophilic mucin-like domains of rhPRG4 surface layer, improving the surface wettability, homogeneity and potentially roughness of the model rhPRG4-grafted contact lenses. Interestingly, the calculated increase in the contact angle for the HA-grafted+rhPRG4$_{sol}$ pHEMA was significantly higher than that of the HA-grafted+rhPRG4$_{sol}$ pHEMA-*co*-TRIS sample ($p<0.0004$), even though the HA-grafted+rhPRG4$_{sol}$ pHEMA-*co*-TRIS were characterized by a higher rhPRG4 surface density as shown above. This was attributed to the potentially different conformations obtained by the rhPRG4/HA complex on the HA-grafted pHEMA and pHEMA-*co*-TRIS substrates. For the HA-grafted+rhPRG4$_{sol}$ pHEMA sample, the observed increase in the contact angle was attributed to the hydrophobic end domains of the deposited rhPRG4 that were assumed to protrude out of the HA-grafted/PRG4-coating complex thus reducing the surface free energy. For the pHEMA-*co*-TRIS sample, the end domains of the glycoprotein are considered to interact with the HA-grafted layer, leaving the highly glycosylated central domain exposed to the surface.

6.4.4. Dehydration profile

Contact lens dehydration was found to be influenced *in vitro* by a number of factors, including the water content of the hydrogel material and its water binding properties (free-to-bound water ratio), the thickness of the contact lens, the ambient relative humidity as well as the air flow over the lens during measurement [74]. Dehydration reflects the structure of water in the material with more tightly bound water molecules producing strong binding; this tightly bound water is less prone to evaporation under the examined conditions [75]. Herein, the water content of the rhPRG4 and HA-grafted pHEMA and pHEMA-*co*-TRIS hydrogels, which was previously found to be similar to that of the unmodified samples [64], did not change after the preconditioning step ($p=0.1$) (data not shown). In addition, the discs were all characterized by the same thickness and the water evaporation profile was determined under the same experimental conditions of controlled temperature and relative humidity. Therefore, the observed delay in the dehydration rate of the rhPRG4 and HA-grafted pHEMA and pHEMA-*co*-TRIS hydrogels was attributed to the hygroscopic nature of the heavily glycosylated central mucinous domain of the rhPRG4 [76] and

the glycosaminoglycan HA [77]. Changes in the dehydration profile after the preconditioning step were speculated to be dependent on the different conformations obtained for the rhPRG4/HA complex. Thus, the results support that the rhPRG4/HA complex, particularly that of the rhPRG4-grafted+HA_{sol} samples, obtained a favourable conformation of reinforced water retentive properties and can effectively shield the surface of the model contact lenses when exposed to air.

Although the *in vitro* contact lens dehydration profile has not been directly correlated to *in vivo* dryness and discomfort [78,79], it might give information about material properties that might further affect lens performance [80]. Designing contact lens materials capable of maintaining a well-hydrated surface has been suggested to contribute to improved surface wettability and lubricity. This would allow for improved tear film stability, potentially preventing ocular dryness and end-of-day discomfort [81,82].

6.4.5. Antifouling properties

The rhPRG4 and HA-grafted pHEMA and pHEMA-co-TRIS hydrogel materials were able to retain their previously observed antifouling properties when a single-protein solution was used [64] even in the presence of a more complex multiprotein solution, such as the ATS used herein. Moreover, based on the reported results, it was postulated that rhPRG4 was generally superior to HA in terms of antifouling properties when used either as a grafted layer or as a coating for the HA-grafted surfaces of the hydrogel materials.

Improved surface wettability and thus high surface free energy has been associated with a reduced thermodynamic driving forces (lower interfacial tension) at the contact lens-tear film interface for protein adherence and denaturation, allowing for higher degree of compatibility [83,84]. For the surfaces examined herein, the rhPRG4/HA complex obtained a conformation that allowed for a reduction in the work of adhesion between the protein and the substrate. The observed reduction in non-specific protein sorption associated with these surfaces is considered to be the outcome of steric repulsion and the presence of a water barrier at the highly glycosylated central domain of rhPRG4 and the hydrophilic HA. Future studies should also include lipids in the ATS composition, since they play a significant role in protein deposition on both conventional and SiHy contact lenses [85]. In addition, the state of the sorbed protein should also be examined as certain sorbed proteins, such as lysozyme, tend to denature potentially causing further protein aggregation or triggering immunological responses [86,87].

6.4.6. In vitro friction coefficients under boundary lubrication conditions

Contact lens friction has been shown to correlate well with *in vivo* contact lens discomfort [11–13]. In addition, determination of the friction coefficient provides a good indication of the quality of lubrication, since wear measurements of biological surfaces are challenging [11]. The results of this study suggest that the configuration of the rhPRG4/HA complex plays an important role in determining the frictional properties for pHEMA hydrogels. The HA-grafted+rhPRG4$_{sol}$ sample exhibited a more favourable conformation, similar to that observed in biological surfaces, synergistically allowing for reduced boundary friction when compared to the unmodified pHEMA hydrogels. This could be attributed to strong interactions and thus adherence of physisorbed rhPRG4 on the HA-grafted layer that prevent the glycoprotein from being sheared away from the contact biointerface under boundary conditions. The number of repeats performed for the pHEMA samples, however, were low compared to the other samples as well as other studies using similar methodologies [23,47,48,45,49]. On the other hand, the friction coefficients of the rhPRG4-grafted+HA$_{sol}$ and HA-grafted+rhPRG4$_{sol}$ pHEMA-*co*-TRIS samples were similar, and lower than those of the unmodified model SiHy, indicating a friction lowering synergistic effect between, under boundary conditions, rhPRG4 and HA independent of the rhPRG4/HA complex configuration.

The results of this study are in agreement with previously published data where rhPRG4 and HA lubricants were in solution and a human cornea-hydrogel disc biointerface was used [47,50]. This suggests that the natural synergistic interactions between PRG4 and HA were able to fully or partially occur even with the covalent attachment of either rhPRG4 or HA to the surface of the model contact lens materials, particularly for the model SiHy materials. In the case of reduced boundary friction, it is speculated that rhPRG4 and HA were able to sufficiently interact with each other through molecular interactions, forming a partially entangled and physically crosslinked rhPRG4/HA complex that was in turn characterized by a reinforced hydration layer. As a result, the developed extended steric and increased electrostatic repulsive forces of the rhPRG4/HA complex facilitated the molecular distribution of shear, thus preventing the adhesion of the human corneal-disc biointerface [52].

Before this work, it was not known whether the PRG4/HA synergy was dependent on a structure-function relationship induced by the surface bound agent. According the results herein, the impact of the configuration of the surface rhPRG4/HA complex on boundary friction lowering

synergistic effect was found to be dependent on the chemistry of the underlying substrate material. The synergistic friction-reducing effect of rhPRG4 and HA was previously found to be also material dependent when HA was covalently incorporated in the bulk of model soft contact lenses [49], with the boundary friction of HA-containing pHEMA sample getting further increased upon the physical deposition of rhPRG4 [49]. Therefore, it could be speculated that not only the material of the substrate but also the method of HA incorporation and thus the conformation of the HA chains of the model contact lens surface plays a role in the rhPRG4/HA interactions and thus in boundary lubrication.

Overall, the rhPRG4-grafted pHEMA-*co*-TRIS sample exhibited lower friction profiles than the corresponding HA-grafted sample, while the percentage reduction observed in the $\langle\mu_{kinetic}\rangle$ of the HA-grafted SiHy caused by the physisorbed rhPRG4 coating (HA-grafted+rhPRG4$_{sol}$ sample) was significantly higher than the decrease observed with HA coating (HA-grafted+rhPRG4$_{sol}$ sample) ($p<0.01$). This suggests that rhPRG4 can be an advantageous boundary lubricant, either as a grafted layer or as a coating, compared to HA for pHEMA-*co*-TRIS materials. The opposite would be in the case of pHEMA hydrogels. This observation could be beneficial for the development of rhPRG4-grafted model SiHy combined with HA-containing eye drops or contact lens solutions respectively, since previous work found that the molecular weight of HA did not have an impact on the synergistic boundary lubrication of the rhPRG4/HA complex [63]. The effect of the sliding speed on the friction coefficients has been previously observed in similar cornea-hydrogel biointerfaces [47,49,50] and was attributed to the interdigitations between the two soft material surfaces of the biointerface prior to sliding [66]. Finally, the friction behavior of the surfaces would not be expected to be significantly different for human eyelid-disc biointerface since previous results showed that the choice of ocular tissue did not play a significant role to PRG4/HA boundary lubrication, at least for the specific experimental setup employed herein [50,66].

6.5. Conclusions

Overall, the results of this study further demonstrate that potential of PRG4 and HA at the interface of contact lens materials, contributing to our understanding of rhPRG4 and HA interactions and their dependence on the structure-function of the rhPRG4 complex. As well, the study provides evidence for the impact of these interactions on important contact lens properties,

such as surface wettability, dehydration rate, protein deposition and boundary friction at a cornea-hydrogel biointerface. The presence of physisorbed HA and rhPRG4 on the surface of the rhPRG4 and HA-grafted pHEMA and pHEMA-*co*-TRIS hydrogels was confirmed by XPS. Surface analysis also indicated that the affinity of the deposited HA and rhPRG4 was stronger toward the rhPRG4 and HA-grafted than the unmodified surfaces. The amount of physisorbed rhPRG4 remained higher for the HA-grafted surfaces over time, with SiHy exhibiting the highest surface density of rhPRG4 overall. Moreover, the impact of the rhPRG4 and HA synergistic interactions on the examined properties was found to vary with the composition of the hydrogel substrate used. This was potentially attributed to potentially different conformations obtained by the rhPRG4/HA complex depending on the presence of the hydrophobic TRIS domains. Although the configuration of the rhPRG4/HA complex was not found to affect the surface wettability of pHEMA hydrogels, the HA-grafted+rhPRG4$_{sol}$ sample was characterized by lower protein deposition and boundary friction compared to the respective rhPRG4-grafted+HA$_{sol}$ sample which demonstrated slower dehydration rates. For the model pHEMA-*co*-TRIS hydrogels, the rhPRG4-grafted+HA$_{sol}$ sample exhibited improved surface wettability, antifouling and water retentive properties compared to the respective HA-grafted+rhPRG4$_{sol}$ sample. Interestingly, the synergistic interactions between rhPRG4 and HA for effective boundary lubrication were not found to be dependent on the configuration of the rhPRG4/HA complex for the SiHy materials. Overall, rhPRG4 either as a grafting layer or as a physisorbed coating exhibited superior antifouling and lubricating properties for the model SiHy only, when compared to HA. These results along with the recently demonstrated therapeutic and protective effect of rhPRG4 in dry eye disease and the presence of HA in the ocular environment as well as in ophthalmic solutions, give rise to the potential for the design of biomimetic contact lens surfaces that work synergistically with ocular fluid-phase biological agents, in an effort to enhance compatibility between the contact lens and the ocular environment that could alleviate dry eye symptoms and improve comfort.

6.6. Funding

Funding support for this work was provided by the Natural Sciences and Engineering Research Council (NSERC) of Canada, the Canadian Institutes of Health Research Collaborative Health Research Program, the 20/20 NSERC Ophthalmic Materials Research Network and the Canada Research Chairs Program, and is gratefully acknowledged.

6.7. Acknowledgements

The authors would like to thank Dr. Danielle Covelli (Biointerfaces Institute, McMaster University) for her contribution to XPS spectra acquisition. This work was financially supported by Natural Sciences and Engineering Research Council (NSERC) of Canada and the 20/20 NSERC Ophthalmic Materials Research Network.

6.8. References

[1] K. Richdale, L.T. Sinnott, E. Skadahl, J.J. Nichols, Frequency of and Factors Associated With Contact Lens Dissatisfaction and Discontinuation, Cornea. 26 (2007) 168–174.

[2] G. Young, J. Veys, N. Pritchard, S. Coleman, A multi-centre study of lapsed contact lens wearers, Ophthalmic Physiol. Opt. 22 (2002) 516–527.

[3] K. Dumbleton, B. Caffery, M. Dogru, S. Hickson-Curran, J. Kern, T. Kojima, P.B. Morgan, C. Purslow, D.M. Robertson, J.D. Nelson, The TFOS International Workshop on Contact Lens Discomfort: Report of the Subcommittee on Epidemiology, Investig. Opthalmology Vis. Sci. 54 (2013) TFOS20-36.

[4] C.J. White, C.R. Thomas, M.E. Byrne, Bringing comfort to the masses: A novel evaluation of comfort agent solution properties, Contact Lens Anterior Eye. 37 (2014) 81–91.

[5] G. Young, R. Chalmers, L. Napier, J. Kern, C. Hunt, K. Dumbleton, Soft Contact Lens-Related Dryness with and without Clinical Signs, Optom. Vis. Sci. 89 (2012) 1125–1132.

[6] A. Mann, B. Tighe, Contact lens interactions with the tear film, Exp. Eye Res. 117 (2013) 88–98.

[7] R. Chalmers, Overview of factors that affect comfort with modern soft contact lenses, Contact Lens Anterior Eye. 37 (2014) 65–76.

[8] H. Pult, C. Purslow, M. Berry, P.J. Murphy, Clinical Tests for Successful Contact Lens Wear: Relationship and Predictive Potential, Optom. Vis. Sci. 85 (2008) E924–E929.

[9] B. Yeniad, M. Beginoglu, L.K. Bilgin, Lid-Wiper Epitheliopathy in Contact Lens Users and Patients With Dry Eye, Eye Contact Lens Sci. Clin. Pract. 36 (2010) 140–143.

[10] D.R. Korb, J.P. Herman, J. V Greiner, R.C. Scaffidi, V.M. Finnemore, J.M. Exford, C.A. Blackie, T. Douglass, Lid wiper epitheliopathy and dry eye symptoms., Eye Contact Lens.

31 (2005) 2–8.

[11] L. Jones, N.A. Brennan, J. González-Méijome, J. Lally, C. Maldonado-Codina, T.A. Schmidt, L. Subbaraman, G. Young, J.J. Nichols, The TFOS International Workshop on Contact Lens Discomfort: report of the contact lens materials, design, and care subcommittee., Invest. Ophthalmol. Vis. Sci. 54 (2013) TFOS37-70.

[12] C. Coles, N. Brennan, Coefficient of friction and soft contact lens comfort, Optom Vis Sci. 89 (2012) E-abstract 125603.

[13] J. Kern, J. Rappon, E. Bauman, B. Vaughn, Assessment of the relationship between contact lens coefficient of friction and subject lens comfort, Invest. Ophthalmol. Vis. Sci. 54 (2013) 494.

[14] G.E. Aninwene, E. Taylor, A. Mei, G.D. Jay, T.J. Webster, Decreased Attachment of Bacteria to Lubricin Coated Intraocular Lenses, MRS Proc. 1316 (2011) mrsf10-1316-qq12-31.

[15] G.E. Aninwene Ii, E. Taylor, T.J. Webster, G.D. Jay, Decreased Infection and Epithelial Cell Attachment to Lubricin Coated Intraocular Lenses, (n.d.).

[16] C.L. Romanò, E. De Vecchi, M. Bortolin, I. Morelli, L. Drago, Hyaluronic Acid and Its Composites as a Local Antimicrobial/Antiadhesive Barrier., J. Bone Jt. Infect. 2 (2017) 63–72.

[17] A. Weeks, L.N. Subbaraman, L. Jones, H. Sheardown, The Competing Effects of Hyaluronic and Methacrylic Acid in Model Contact Lenses, J. Biomater. Sci. Polym. Ed. 23 (2012) 1021–1038.

[18] G.W. Greene, L.L. Martin, R.F. Tabor, A. Michalczyk, L.M. Ackland, R. Horn, Lubricin: A versatile, biological anti-adhesive with properties comparable to polyethylene glycol, Biomaterials. 53 (2015) 127–136.

[19] M. van Beek, A. Weeks, L. Jones, H. Sheardown, Immobilized hyaluronic acid containing model silicone hydrogels reduce protein adsorption., J. Biomater. Sci. Polym. Ed. 19 (2008) 1425–1436.

[20] F. Mantelli, P. Argüeso, Functions of ocular surface mucins in health and disease, Curr. Opin. Allergy Clin. Immunol. 8 (2008) 477–483.

[21] D.B. Schaefer, D. Wendt, M. Moretti, M. Jakob, G.D. Jay, M. Heberer, I. Martin, Lubricin reduces cartilage–cartilage integration, Biorheology. 41 (2004) 503–508.

[22] G.D. Jay, B.P. Lane, L. Sokoloff, Characterization of a bovine synovial fluid lubricating factor III. The interaction with hyaluronic acid, Connect. Tissue Res. 28 (1992) 245–255.

[23] T.A. Schmidt, D.A. Sullivan, E. Knop, S.M. Richards, N. Knop, S. Liu, A. Sahin, R.R. Darabad, S. Morrison, W.R. Kam, B.D. Sullivan, Transcription, translation, and function of lubricin, a boundary lubricant, at the ocular surface., JAMA Ophthalmol. 131 (2013) 766–776.

[24] S.C. Regmi, M.L. Samsom, M.L. Heynen, G.D. Jay, B.D. Sullivan, S. Srinivasan, B. Caffery, L. Jones, T.A. Schmidt, Degradation of proteoglycan 4/lubricin by cathepsin S: Potential mechanism for diminished ocular surface lubrication in Sjögren's syndrome, Exp. Eye Res. 161 (2017) 1–9.

[25] T. Cheriyan, T.M. Schmid, M. Spector, Presence and distribution of the lubricating protein, lubricin, in the meibomian gland in rabbits, Mol. Vis. 17 (2011) 3055–3061.

[26] P.S. Tsai, J.E. Evans, K.M. Green, R.M. Sullivan, D.A. Schaumberg, S.M. Richards, M.R. Dana, D.A. Sullivan, Proteomic analysis of human meibomian gland secretions., Br. J. Ophthalmol. 90 (2006) 372–377.

[27] A. Lambiase, B.D. Sullivan, T.A. Schmidt, D.A. Sullivan, G.D. Jay, E.R. Truitt, A. Bruscolini, M. Sacchetti, F. Mantelli, A Two-Week, Randomized, Double-masked Study to Evaluate Safety and Efficacy of Lubricin (150 μg/mL) Eye Drops Versus Sodium Hyaluronate (HA) 0.18% Eye Drops (Vismed®) in Patients with Moderate Dry Eye Disease, Ocul. Surf. 15 (2017) 77–87.

[28] I.K. Gipson, P. Argüeso, Role of mucins in the function of the corneal and conjunctival epithelia., Int. Rev. Cytol. 231 (2003) 1–49.

[29] M.Y. Fukuda K, Miyamoto Y, Hyaluronic acid in tear fluid and its synthesis by corneal epithelial cells., Asia-Pacific J Ophthalmol. 40 (1998) 62–65.

[30] M. Fukuda, Y. Miyamoto, Y. Miyara, H. Mishima, T. Otori, Hyaluronic acid concentration in human tear fluids, Invest. Ophthalmol. Vis. Sci. 37 (1996) 3916–3916.

[31] K. Yoshida, Y. Nitatori, Y. Uchiyama, Localization of glycosaminoglycans and CD44 in the human lacrimal gland., Arch. Histol. Cytol. 59 (1996) 505–513.

[32] L.E. Lerner, D.M. Schwartz, D.G. Hwang, E.L. Howes, R. Stern, Hyaluronan and CD44 in the Human Cornea and Limbal Conjunctiva, Exp. Eye Res. 67 (1998) 481–484.

[33] M.J. Doughty, S. Glavin, Efficacy of different dry eye treatments with artificial tears or

ocular lubricants: a systematic review., Ophthalmic Physiol. Opt. 29 (2009) 573–583.

[34] M.E. Johnson, P.J. Murphy, M. Boulton, Effectiveness of sodium hyaluronate eyedrops in the treatment of dry eye, Graefe's Arch. Clin. Exp. Ophthalmol. 244 (2006) 109–112.

[35] P.D. O'Brien, L.M.T. Collum, Dry eye: diagnosis and current treatment strategies., Curr. Allergy Asthma Rep. 4 (2004) 314–319.

[36] D. Fonn, Targeting contact lens induced dryness and discomfort: what properties will make lenses more comfortable., Optom. Vis. Sci. 84 (2007) 279–285.

[37] Szczotka-Flynn LB, Chemical properties of contact lens rewetters., Contact Lens Spectr. 21 (2006) 11–9.

[38] R. Stone, Introducing Water Gradient Technology, Contact Lens Spectr. (2013) 34–38.

[39] M. Guillon, Are Silicone Hydrogel Contact Lenses More Comfortable Than Hydrogel Contact Lenses?, Eye Contact Lens Sci. Clin. Pract. 39 (2013) 85–91.

[40] J.A. Nairn, T.J. Jiang, Measurement Of The Friction And Lubricity Properties Of Contact Lenses, Proc. ANTEC '95. May 7-11 (1995) 1–5.

[41] J.M. Coles, D.P. Chang, S. Zauscher, Molecular mechanisms of aqueous boundary lubrication by mucinous glycoproteins, Curr. Opin. Colloid Interface Sci. 15 (2010) 406–416.

[42] D.P. Chang, N.I. Abu-Lail, J.M. Coles, F. Guilak, G.D. Jay, S. Zauscher, Friction Force Microscopy of Lubricin and Hyaluronic Acid between Hydrophobic and Hydrophilic Surfaces., Soft Matter. 5 (2009) 3438–3445.

[43] G.D. Jay, K.A. Waller, The biology of Lubricin: Near frictionless joint motion, Matrix Biol. 39 (2014) 17–24.

[44] G.D. Jay, D.A. Harris, C.J. Cha, Boundary lubrication by lubricin is mediated by O-linked beta(1-3)Gal-GalNAc oligosaccharides., Glycoconj. J. 18 (2001) 807–815.

[45] B. Zappone, G.W. Greene, E. Oroudjev, G.D. Jay, J.N. Israelachvili, Molecular aspects of boundary lubrication by human lubricin: effect of disulfide bonds and enzymatic digestion., Langmuir. 24 (2008) 1495–1508.

[46] J.P. Gleghorn, A.R.C. Jones, C.R. Flannery, L.J. Bonassar, Boundary mode lubrication of articular cartilage by recombinant human lubricin, J. Orthop. Res. 27 (2009) 771–777.

[47] S. Morrison, D.A. Sullivan, B.D. Sullivan, H. Sheardown, T.A. Schmidt, Dose-dependent and synergistic effects of proteoglycan 4 on boundary lubrication at a human cornea-

polydimethylsiloxane biointerface., Eye Contact Lens. 38 (2012) 27–35.

[48] M.L. Samsom, S. Morrison, N. Masala, B.D. Sullivan, D.A. Sullivan, H. Sheardown, T.A. Schmidt, Characterization of full-length recombinant human Proteoglycan 4 as an ocular surface boundary lubricant, Exp. Eye Res. 127 (2014) 14–19.

[49] M. Samsom, M. Korogiannaki, L.N. Subbaraman, H. Sheardown, T.A. Schmidt, Hyaluronan incorporation into model contact lens hydrogels as a built-in lubricant: Effect of hydrogel composition and proteoglycan 4 as a lubricant in solution, J. Biomed. Mater. Res. Part B Appl. Biomater. 00B (2017) 000–000. doi:10.1002/jbm.b.33989.

[50] M. Samsom, Y. Iwabuchi, H. Sheardown, T.A. Schmidt, Proteoglycan 4 and hyaluronan as boundary lubricants for model contact lens hydrogels, J. Biomed. Mater. Res. Part B Appl. Biomater. 106 (2018) 1329–1338.

[51] B. Zappone, M. Ruths, G.W. Greene, G.D. Jay, J.N. Israelachvili, Adsorption, lubrication, and wear of lubricin on model surfaces: polymer brush-like behavior of a glycoprotein., Biophys. J. 92 (2007) 1693–1708.

[52] T.A. Schmidt, N.S. Gastelum, Q.T. Nguyen, B.L. Schumacher, R.L. Sah, Boundary lubrication of articular cartilage: Role of synovial fluid constituents, Arthritis Rheum. 56 (2007) 882–891.

[53] G.W. Greene, X. Banquy, D.W. Lee, D.D. Lowrey, J. Yu, J.N. Israelachvili, Adaptive mechanically controlled lubrication mechanism found in articular joints., Proc. Natl. Acad. Sci. U. S. A. 108 (2011) 5255–5259.

[54] J. Yu, X. Banquy, G.W. Greene, D.D. Lowrey, J.N. Israelachvili, The Boundary Lubrication of Chemically Grafted and Cross-Linked Hyaluronic Acid in Phosphate Buffered Saline and Lipid Solutions Measured by the Surface Forces Apparatus, Langmuir. 28 (2012) 2244–2250.

[55] A. Singh, M. Corvelli, S.A. Unterman, K.A. Wepasnick, P. McDonnell, J.H. Elisseeff, Enhanced lubrication on tissue and biomaterial surfaces through peptide-mediated binding of hyaluronic acid, Nat. Mater. 13 (2014) 988–995.

[56] T.E. Ludwig, M.M. Hunter, T.A. Schmidt, Cartilage boundary lubrication synergism is mediated by hyaluronan concentration and PRG4 concentration and structure, BMC Musculoskelet. Disord. 16 (2015) 386.

[57] D.P. Chang, N.I. Abu-Lail, F. Guilak, G.D. Jay, S. Zauscher, Conformational Mechanics,

Adsorption, and Normal Force Interactions of Lubricin and Hyaluronic Acid on Model Surfaces., Langmuir. 24 (2008) 1183–1193.

[58] S. Das, X. Banquy, B. Zappone, G.W. Greene, G.D. Jay, J.N. Israelachvili, Synergistic Interactions between Grafted Hyaluronic Acid and Lubricin Provide Enhanced Wear Protection and Lubrication, Biomacromolecules. 14 (2013) 1669–1677.

[59] D.W. Lee, X. Banquy, S. Das, N. Cadirov, G. Jay, J. Israelachvili, Effects of molecular weight of grafted hyaluronic acid on wear initiation, Acta Biomater. 10 (2014) 1817–1823.

[60] G.D. Jay, J.R. Torres, M.L. Warman, M.C. Laderer, K.S. Breuer, The role of lubricin in the mechanical behavior of synovial fluid., Proc. Natl. Acad. Sci. U. S. A. 104 (2007) 6194–6199.

[61] S.E. Majd, R. Kuijer, A. Köwitsch, T. Groth, T.A. Schmidt, P.K. Sharma, Both hyaluronan and collagen type II keep proteoglycan 4 (lubricin) at the cartilage surface in a condition that provides low friction during boundary lubrication., Langmuir. 30 (2014) 14566–14572.

[62] J. Seror, L. Zhu, R. Goldberg, A.J. Day, J. Klein, Supramolecular synergy in the boundary lubrication of synovial joints, Nat. Commun. 6 (2015) 6497.

[63] J.J. Kwiecinski, S.G. Dorosz, T.E. Ludwig, S. Abubacker, M.K. Cowman, T.A. Schmidt, The effect of molecular weight on hyaluronan's cartilage boundary lubricating ability – alone and in combination with proteoglycan 4, Osteoarthr. Cartil. 19 (2011) 1356–1362.

[64] M. Korogiannaki, J. Zhang, H. Sheardown, Surface modification of model hydrogel contact lenses with hyaluronic acid via thiol-ene "click" chemistry for enhancing surface characteristics, J. Biomater. Appl. 32 (2017) 446–462.

[65] S.M. Iqbal, C. Leonard, S. C. Regmi, D. De Rantere, P. Tailor, G. Ren, H. Ishida, C. Hsu, S. Abubacker, D.S. Pang, P. T. Salo, H.J. Vogel, D.A. Hart, C.C. Waterhouse, G.. Jay, T.A. Schmidt, R.J. Krawetz, Lubricin/Proteoglycan 4 binds to and regulates the activity of Toll-Like Receptors In Vitro, Sci. Rep. 6 (2016) 18910.

[66] M. Samsom, A. Chan, Y. Iwabuchi, L. Subbaraman, L. Jones, T.A. Schmidt, In vitro friction testing of contact lenses and human ocular tissues: Effect of proteoglycan 4 (PRG4), Tribol. Int. 89 (2015) 27–33.

[67] E. Regoeczi, Iodine-Labeled Plasma Proteins Vol. 1, CRC Press, Boca Raton, FL, 1984.

[68] B. Hall, M. Heynen, L.W. Jones, J.A. Forrest, Analysis of Using I 125 Radiolabeling for Quantifying Protein on Contact Lenses, Curr. Eye Res. 41 (2016) 456–465.

[69] A. Ng, M. Heynen, D. Luensmann, L.N. Subbaraman, L. Jones, Impact of tear film components on the conformational state of lysozyme deposited on contact lenses, J. Biomed. Mater. Res. Part B Appl. Biomater. 101 (2013) 1172–1181.

[70] A.C. Dunn, J.A. Tichy, J.M. Urueña, W.G. Sawyer, Lubrication regimes in contact lens wear during a blink, Tribol. Int. 63 (2013) 45–50.

[71] Z. Hrkal, K. Kuzelová, U. Muller-Eberhard, R. Stern, Hyaluronan-binding properties of human serum hemopexin., FEBS Lett. 383 (1996) 72–4.

[72] S. Tonge, L. Jones, S. Goodall, B. Tighe, The ex vivo wettability of soft contact lenses., Curr. Eye Res. 23 (2001) 51–59.

[73] C. Maldonado-codina, P.B. Morgan, In vitro water wettability of silicone hydrogel contact lenses determined using the sessile drop and captive bubble techniques, J. Biomed. Mater. Res. Part A. 83A (2007) 496–502.

[74] L. Jones, C. May, L. Nazar, T. Simpson, In vitro evaluation of the dehydration characteristics of silicone hydrogel and conventional hydrogel contact lens materials., Cont. Lens Anterior Eye. 25 (2002) 147–156.

[75] C. Maldonado-Codina, Soft lens materials, in: N. Efron (Ed.), Contact Lens Pract., Butterworth-Heineman, 2010: pp. 67–86.

[76] A. Guzman-Aranguez, P. Argüeso, Structure and biological roles of mucin-type O-glycans at the ocular surface., Ocul. Surf. 8 (2010) 8–17.

[77] M. Nakamura, M. Hikida, T. Nakano, S. Ito, T. Hamano, S. Kinoshita, Characterization of water retentive properties of hyaluronan., Cornea. 12 (1993) 433–436.

[78] P. McConville, J.M. Pope, J.W. Huff, Limitations of in vitro contact lens dehydration/rehydration data in predicting on-eye dehydration., CLAO J. 23 (1997) 117–21.

[79] P.B. Morgan, N. Efron, Hydrogel contact lens ageing., CLAO J. 26 (2000) 85–90.

[80] K. Krysztofiak, A. Szyczewski, Study of dehydration and water states in new and worn soft contact lens materials, Opt. Appl. XLIV (2014).

[81] J.M.G.- Méijome, J. González - Pérez, P.R.B. Fernandes, D.P.L.- Ferreira, S. Mollá, V. Compañ, Silicone Hydrogels Materials for Contact Lens Applications, in: Concise Encycl. High Perform. Silicones, John Wiley & Sons, Inc., Hoboken, NJ, USA, 2014: pp. 293–308.

[82] B. Tighe, Silicone hydrogel materials – How do they work?, in: D.F. Sweeney (Ed.),

Silicone Hydrogels Rebirth Contin. Wear Contact Lenses, Butterworth-Heinemann, Oxford, 2000: pp. 1–21.

[83] J.D. Andrade, Interfacial phenomena and biomaterials., Med. Instrum. 7 (1973) 110–120.

[84] Y. Ikada, M. Suzuki, Y. Tamada, Polymer Surfaces Possessing Minimal Interaction with Blood Components, in: Polym. as Biomater., Shalaby SW, Springer US, New York, NY, 1984: pp. 135–147.

[85] H. Lorentz, M. Heynen, D. Trieu, S.J. Hagedorn, L. Jones, The Impact of Tear Film Components on In Vitro Lipid Uptake, Optom. Vis. Sci. 89 (2012) 856–867.

[86] D. Luensmann, L. Jones, Protein deposition on contact lenses: The past, the present, and the future, Contact Lens Anterior Eye. 35 (2012) 53–64.

[87] C. Skotnitsky, P.R. Sankaridurg, D.F. Sweeney, B.A. Holden, General and local contact lens induced papillary conjunctivitis (CLPC)., Clin. Exp. Optom. 85 (2002) 193–197.

Chapter 7

7.1. Concluding Remarks

Contact lens related dryness and discomfort remain the primary reasons for limiting or even discontinuing contact lens wear [307,308], despite the effort to develop new contact lens materials with improved characteristics and overall performance. This is attributed to the poor ocular compatibility of the contact lens with the tear film and the ocular surface [176], primarily due to inadequately hydrated contact lens surfaces and increased friction, causing a cascade of adverse events from low quality of vision to inflammation. The primary incentive for this research work was the reported direct association of friction with contact lens discomfort [22] along with the clinically demonstrated therapeutic and protective effect of topically applied rhPRG4 and HA in dry eye symptoms [38].

The overall goal of the work presented in this thesis was to create biomimetic surfaces of hydrogel materials for soft contact lens applications in an effort to minimize the adverse interactions between the contact lens and the ocular surface. It was thus hypothesized that the development of contact lens materials with controlled interfacial and biomimetic properties could allow for enhanced compatibility between the lens and the ocular environment under physiological conditions and ultimately these materials could alleviate contact lens induced dryness and discomfort during wear. This was achieved by modifying the surface of model conventional and silicone hydrogel contact lens materials with the natural, ocular wetting and lubricating agents, HA and PRG4. The surfaces were covalently modified with the wetting agents in order to achieve long-term improvement of surface characteristics. HA is a linear non-sulfated glycosaminoglycan naturally found in the ocular environment contributing to tear film stability and has been widely used in ophthalmic applications, as in the treatment of dry eye symptoms, and more importantly in contact lens products, such as artificial tears, packaging and multipurpose solutions in order to alleviate symptoms of dryness and discomfort. PRG4 is a mucin-like glycoprotein able to prevent tear film evaporation and protect the ocular surface during blinking due to its boundary lubricating properties. Moreover, a recent clinical study showed that instillation of rhPRG4-containing eye drops is capable of alleviating signs and symptoms of dry eye disease.

Initially, HA was covalently attached to the surface of model pHEMA conventional hydrogel via a nucleophile-mediated Michael addition thiol-ene “click” chemistry. Surface chemistry

analysis through FTIR-ATR and low resolution XPS techniques confirmed the successful grafting of thiolated-HA to the acrylated surface of pHEMA hydrogels in the presence of TCEP catalyst. The presence of the hydrophilic HA layer on the surface of pHEMA hydrogels resulted in significantly lower water contact angles, as well as lysozyme and albumin deposition and dehydration rates *in vitro*. Moreover, the surface modification procedure followed herein did not affect the optical transparency of the HA-grafted pHEMA hydrogels or the *in vitro* viability of human corneal epithelial cells. Therefore, surface immobilization of HA via thiol-ene "click" chemistry was shown to be an effective method for the development of pHEMA hydrogels with improved surface wettability, resistance to non-specific protein deposition and water retentive properties, while retaining the optical acuity of the hydrogel material.

In a similar manner, HA was covalently attached the surface of model pHEMA-*co*-TRIS silicone hydrogels in order to improve their surface characteristics without affecting their bulk properties. The surface immobilization reactions involved the covalent attachment of thiolated-HA to the acrylated pHEMA-*co*-TRIS surface via UV-induced thiol-ene "click" chemistry. As indicated by the low-resolution angle-resolved XPS spectra and water contact angle measurements, a homogenous HA layer was grated to the surface of the pHEMA-*co*-TRIS materials successfully masking the hydrophobic silicone domains and thus significantly improving the surface wettability of the model silicone hydrogels. In turn, the HA-grafted pHEMA-*co*-TRIS materials were characterized by significantly improved protein antifouling properties and dehydration profile when compared to the unmodified model silicone hydrogels. Furthermore, the materials remained optically transparent and demonstrated good *in vitro* compatibility with human corneal epithelial cells. Hence, surface functionalization with HA via thiol-ene "click" chemistry, a versatile technique with high specificity and fine control for tailored surface properties, can be used as a promising method for the development of novel contact lenses with well-controlled interfacial properties under physiological conditions.

Following, the synthesis and characterization of rhPRG4-grafted pHEMA and pHEMA-*co*-TRIS hydrogel surfaces was described. Covalent attachment of rhPRG4 via its SMB-like end-domain using CDI linking chemistry was confirmed by high-resolution XPS spectra. Radiolabeled I^{131}-rhPRG4 was used to determine the amount of the glycoprotein present at the pHEMA and pHEMA-*co*-TRIS materials. The rhPRG4-grafted pHEMA hydrogels exhibited slightly higher levels of rhPRG4 than the respective surface-modified model silicone hydrogels. In contrast, the

strong affinity observed between the amphiphilic glycoprotein and the hydrophobic silicone domains of the unmodified pHEMA-*co*-TRIS hydrogels resulted in model silicone hydrogels with higher amount of physically bound rhPRG4 than the pHEMA materials. Furthermore, surface-tethered rhPRG4 exhibited substrate-specific wetting and boundary lubricating properties depending on the composition of the hydrogel material used. More specifically, the surface-grafted rhPRG4 was found to effectively reduce the static water contact angle and boundary friction of a hydrogel-human cornea biointerface for the pHEMA-*co*-TRIS but not for the pHEMA hydrogels, when compared to the unmodified hydrogel materials. Despite the conformation obtained, however, the rhPRG4-grafted layer was able to inhibit lysozyme and albumin deposition for both pHEMA and pHEMA-*co*-TRIS hydrogels. Moreover, the surface immobilization process of rhPRG4 did not compromise the optical properties of the examined model contact lens materials or caused any cytotoxic effect against human corneal epithelial cells.

Previous work reported that PRG4 and HA can interact with each other and synergistically reduce further boundary friction. Hence, the interactions between these two agents when either was associated with a lens material and their impact on contact lens specific properties were assessed. Physisorbed HA and rhPRG4 (HA_{sol} and $PRG4_{sol}$) exhibited stronger affinity toward the respective rhPRG4 and HA-grafted pHEMA and pHEMA-*co*-TRIS hydrogels than the unmodified surfaces. Quantification of the deposited rhPRG4 over time by radiolabeling further supported the strength of the interactions between the glycoprotein and the HA-grafted surfaces, with the highest amount of physically bound rhPRG4 being detected at the HA-grafted pHEMA-*co*-TRIS materials. *In vitro* characterization of the pHEMA hydrogels showed that the rhPRG4/HA complex formed by the physisorbed rhPRG4 and HA-grafted layer (HA-grafted+$rhPRG4_{sol}$ sample) synergistically led to the least amount of non-specifically sorbed lysozyme and albumin and boundary friction coefficient, whereas the rhPRG4/HA complex formed by the opposite configuration (rhPRG4-grafted+HA_{sol} sample) resulted in the slowest dehydration rate. In addition, the surface wettability of the HA-grafted+$rhPRG4_{sol}$ and rhPRG4-grafted+HA_{sol} samples was similar and significantly improved compared to the unmodified hydrogel. For pHEMA-*co*-TRIS materials, the rhPRG4/HA complex formed by the physisorbed HA and rhPRG4-grafted layer (rhPRG4-grafted+HA_{sol} sample) was characterized by higher wettability with superior water retentive and antifouling properties than the rhPRG4/HA complex obtained by the opposite configuration (HA-grafted+$rhPRG4_{sol}$ sample), and the unmodified silicone hydrogel surface. The

configuration of the rhPRG4/HA complex did not have an impact on the tribological properties of the surface modified pHEMA-*co*-TRIS samples, with rhPRG4 and HA interactions synergistically contributing to a boundary friction lowering effect compared to the unmodified silicone hydrogel. Overall, rhPRG4 either as a grafting layer or as a physisorbed coating presented superior protein repelling and lubricating properties for the model pHEMA-*co*-TRIS materials, when compared to HA.

Concluding, the results of this thesis demonstrate the potential of natural, ocular friendly wetting and lubricating agents, such as HA and rhPRG4, to be used for the surface treatment of soft contact lens materials. Furthermore, it contributed to the understanding of rhPRG4 and HA interactions with different contact lens-based hydrogel compositions, their *in vitro* performance as grafted layers against properties pertinent to the ocular compatibility and overall performance of soft contact lenses. Finally, the dependence of these properties on the structure-function of the formed rhPRG4/HA complex when one agent is surface bound and the other is in solution was shown.

The development of contact lens materials with novel biomimetic surfaces that work synergistically with naturally occurring ocular agents can be advantageous, allowing for the management of ocular dryness and discomfort, thus optimizing the overall contact lens performance.

7.2. Future work

Moving forward, future work should consider the impact of sterilization process of the surface modified model contact lens materials and the stability of the grafted layer over time (shelf-life). Although the developed HA and rhPRG4-grafted pHEMA and pHEMA-*co*-TRIS hydrogels did not show any cytotoxic effect on human corneal epithelial cells, material sterilization would be necessary prior to proceeding with *in vivo* studies. Taking into consideration that the wetting and frictional properties of rhPRG4 under boundary conditions were dependent on the contact lens substrate chemistry, when commercial and model soft contact lenses were examined [386,570], it would be useful to further develop a library of suitable contact lens components that would allow PRG4 to obtain the necessary conformation resulting in its natural boundary lubrication properties. This would also facilitate the process of moving closer to *in vivo* studies.

This thesis work is a proof-of-concept in order to evaluate the impact of surface grafted HA and rhPRG4 on important contact lens properties. To simplify and understand the properties of the examined engineered surfaces and the direct interactions between rhPRG4 and HA, the experiments concerning the surface wettability and boundary friction coefficients were conducted in the presence of water or a simple saline solution, while *in vitro* protein deposition was assessed using PBS and a multiprotein and mucin containing solution. However, previous studies showed that all tear film components, particularly proteins and lipids, contribute individually and synergistically to the contact lens-related interfacial phenomena [297,571,572]. Therefore, to better mimic *in vivo* conditions it would be useful for the future characterization of these properties to use an artificial tear film solution, containing multiple proteins, mucins, lipids and salts [362].

Although protein deposition profile is important in assessing *in vitro* the efficacy of the surface treatment for contact lenses, evaluation the degree of protein activity upon sorption is of equal significance and may be correlated with contact lens discomfort and other ocular adverse effects [22]. Finally, future studies on the biotribology of these materials should also investigate the wear (fatigue wear/damage) of both contact lens surface and ocular tissue apart from friction at the tissue-hydrogel biointerface, in order to determine the durability and the protective role of the surface grafted layer to the ocular surface respectively. Even though the factor of friction may impact the subjective feeling of comfort, it is questionable if the symptoms observed in contact lens induced dry eye are directly related to increased friction or tissue damage [573]. There is increasing evidence that wear prevention and low friction are not necessarily correlated [493,574,575], thus deducing wear generation from friction measurements alone is not possible. Local tissue damage or even wear of the corneal surface and/or eyelid could be responsible for the symptoms of irritation and inflammation reported for the dry eye patients.

Bibliography

[1] J.J. Nichols, Contact lenses 2014., Contact Lens Spectr. 30 (2015) 22–27.

[2] P.B. Morgan, C.A. Woods, I.G. Tranoudis, M. Helland, N. Efron, L. Jones, N.L. Merchan, M. Teufl, M. van Beusekom, et al., International Contact Lens Prescribing in 2017: Our 17th annual report in Contact Lens Spectrum reveals current global trends in contact lens prescribing., Contact Lens Spectr. 33 (n.d.) 28–33.

[3] C. Maldonado-Codina, Soft lens materials, in: N. Efron (Ed.), Contact Lens Pract., Butterworth-Heineman, 2010: pp. 67–86.

[4] J.P. Craig, M.D.P. Willcox, P. Argüeso, C. Maissa, U. Stahl, A. Tomlinson, J. Wang, N. Yokoi, F. Stapleton, The TFOS International Workshop on Contact Lens Discomfort: report of the contact lens interactions with the tear film subcommittee., Invest. Ophthalmol. Vis. Sci. 54 (2013) TFOS123-156.

[5] F. Stapleton, S. Stretton, E. Papas, C. Skotnitsky, D.F. Sweeney, Silicone Hydrogel Contact Lenses and the Ocular Surface, Ocul. Surf. 4 (2006) 24–43.

[6] N. Keir, L. Jones, Wettability and silicone hydrogel lenses: a review., Eye Contact Lens. 39 (2013) 100–108.

[7] G. Young, R. Bowers, B. Hall, M. Port, Six month clinical evaluation of a biomimetic hydrogel contact lens., CLAO J. 23 (1997) 226–236.

[8] U. Businger, A New Material on the Block of Frequent Replacement Lenses, Contact Lens Spectr. . 15 (200AD) 49–51.

[9] B.J. Tighe, A decade of silicone hydrogel development: surface properties, mechanical properties, and ocular compatibility., Eye Contact Lens. 39 (2013) 4–12.

[10] L. Jones, Modern contact lens materials: A clinical performance update, Contact Lens Spectr. 17 (2002) 24–35.

[11] G. Young, J. Veys, N. Pritchard, S. Coleman, A multi-centre study of lapsed contact lens wearers, Ophthalmic Physiol. Opt. 22 (2002) 516–527.

[12] K. Dumbleton, C.A. Woods, L.W. Jones, D. Fonn, The impact of contemporary contact lenses on contact lens discontinuation., Eye Contact Lens. 39 (2013) 93–99.

[13] R.L. Chalmers, C.G. Begley, Dryness symptoms among an unselected clinical population with and without contact lens wear., Cont. Lens Anterior Eye. 29 (2006) 25–30. doi:10.1016/j.clae.2005.12.004.

[14] D. Fonn, P. Situ, T. Simpson, Hydrogel lens dehydration and subjective comfort and dryness ratings in symptomatic and asymptomatic contact lens wearers., Optom. Vis. Sci. 76 (1999) 700–704.

[15] N. Efron, N.A. Brennan, A.S. Bruce, D.I. Duldig, N.J. Russo, Dehydration of hydrogel lenses under normal wearing conditions., CLAO J. 13 (1987) 152–156.

[16] D. Fonn, Targeting contact lens induced dryness and discomfort: what properties will make lenses more comfortable., Optom. Vis. Sci. 84 (2007) 279–285.

[17] L.W. Jones, M. Byrne, J.B. Ciolino, J. Legerton, M. Markoulli, E. Papas, L. Subbaraman,

Revolutionary Future Uses of Contact Lenses, Optom. Vis. Sci. 93 (2016) 325–327.

[18] G. Young, R. Chalmers, L. Napier, J. Kern, C. Hunt, K. Dumbleton, Soft Contact Lens-Related Dryness with and without Clinical Signs, Optom. Vis. Sci. 89 (2012) 1125–1132.

[19] L.C. Thai, A. Tomlinson, M.G. Doane, Effect of contact lens materials on tear physiology., Optom. Vis. Sci. 81 (2004) 194–204. http://www.ncbi.nlm.nih.gov/pubmed/15017179.

[20] E. Faber, T.R. Golding, R. Lowe, N.A. Brennan, Effect of hydrogel lens wear on tear film stability., Optom. Vis. Sci. 68 (1991) 380–384.

[21] P.L. Valint, D.M. Ammon, G.L. Grobe, J.A. McGee, In-Situ Surface Modification of Contact Lens Polymers, in: Surf. Modif. Polym. Biomater., Springer US, Boston, MA, 1996: pp. 21–26.

[22] L. Jones, N.A. Brennan, J. González-Méijome, J. Lally, C. Maldonado-Codina, T.A. Schmidt, L. Subbaraman, G. Young, J.J. Nichols, The TFOS International Workshop on Contact Lens Discomfort: report of the contact lens materials, design, and care subcommittee., Invest. Ophthalmol. Vis. Sci. 54 (2013) TFOS37-70.

[23] A. Mann, B. Tighe, Contact lens interactions with the tear film, Exp. Eye Res. 117 (2013) 88–98.

[24] R. Chalmers, Overview of factors that affect comfort with modern soft contact lenses, Contact Lens Anterior Eye. 37 (2014) 65–76.

[25] M.Y. Fukuda K, Miyamoto Y, Hyaluronic acid in tear fluid and its synthesis by corneal epithelial cells., Asia-Pacific J Ophthalmol. 40 (1998) 62–65.

[26] M. Fukuda, Y. Miyamoto, Y. Miyara, H. Mishima, T. Otori, Hyaluronic acid concentration in human tear fluids, Invest. Ophthalmol. Vis. Sci. 37 (1996) 3916–3916.

[27] K. Yoshida, Y. Nitatori, Y. Uchiyama, Localization of glycosaminoglycans and CD44 in the human lacrimal gland., Arch. Histol. Cytol. 59 (1996) 505–513.

[28] L.E. Lerner, D.M. Schwartz, D.G. Hwang, E.L. Howes, R. Stern, Hyaluronan and CD44 in the Human Cornea and Limbal Conjunctiva, Exp. Eye Res. 67 (1998) 481–484.

[29] M.J. Rah, A review of hyaluronan and its ophthalmic applications., Optometry. 82 (2011) 38–43.

[30] M.J. Doughty, S. Glavin, Efficacy of different dry eye treatments with artificial tears or ocular lubricants: a systematic review., Ophthalmic Physiol. Opt. 29 (2009) 573–583.

[31] M.E. Johnson, P.J. Murphy, M. Boulton, Effectiveness of sodium hyaluronate eyedrops in the treatment of dry eye, Graefe's Arch. Clin. Exp. Ophthalmol. 244 (2006) 109–112.

[32] P.D. O'Brien, L.M.T. Collum, Dry eye: diagnosis and current treatment strategies., Curr. Allergy Asthma Rep. 4 (2004) 314–319.

[33] Szczotka-Flynn LB, Chemical properties of contact lens rewetters., Contact Lens Spectr. 21 (2006) 11–9.

[34] T.A. Schmidt, D.A. Sullivan, E. Knop, S.M. Richards, N. Knop, S. Liu, A. Sahin, R.R. Darabad, S. Morrison, W.R. Kam, B.D. Sullivan, Transcription, translation, and function of lubricin, a boundary lubricant, at the ocular surface., JAMA Ophthalmol. 131 (2013) 766–

776.

[35] S.C. Regmi, M.L. Samsom, M.L. Heynen, G.D. Jay, B.D. Sullivan, S. Srinivasan, B. Caffery, L. Jones, T.A. Schmidt, Degradation of proteoglycan 4/lubricin by cathepsin S: Potential mechanism for diminished ocular surface lubrication in Sjögren's syndrome, Exp. Eye Res. 161 (2017) 1–9.

[36] T. Cheriyan, T.M. Schmid, M. Spector, Presence and distribution of the lubricating protein, lubricin, in the meibomian gland in rabbits, Mol. Vis. 17 (2011) 3055–3061.

[37] P.S. Tsai, J.E. Evans, K.M. Green, R.M. Sullivan, D.A. Schaumberg, S.M. Richards, M.R. Dana, D.A. Sullivan, Proteomic analysis of human meibomian gland secretions., Br. J. Ophthalmol. 90 (2006) 372–377.

[38] A. Lambiase, B.D. Sullivan, T.A. Schmidt, D.A. Sullivan, G.D. Jay, E.R. Truitt, A. Bruscolini, M. Sacchetti, F. Mantelli, A Two-Week, Randomized, Double-masked Study to Evaluate Safety and Efficacy of Lubricin (150 μg/mL) Eye Drops Versus Sodium Hyaluronate (HA) 0.18% Eye Drops (Vismed®) in Patients with Moderate Dry Eye Disease, Ocul. Surf. 15 (2017) 77–87.

[39] G.E. Aninwene, E. Taylor, A. Mei, G.D. Jay, T.J. Webster, Decreased Attachment of Bacteria to Lubricin Coated Intraocular Lenses, MRS Proc. 1316 (2011) mrsf10-1316-qq12-31.

[40] G.E. Aninwene Ii, E. Taylor, T.J. Webster, G.D. Jay, Decreased Infection and Epithelial Cell Attachment to Lubricin Coated Intraocular Lenses, (n.d.).

[41] C.L. Romanò, E. De Vecchi, M. Bortolin, I. Morelli, L. Drago, Hyaluronic Acid and Its Composites as a Local Antimicrobial/Antiadhesive Barrier., J. Bone Jt. Infect. 2 (2017) 63–72.

[42] A. Weeks, L.N. Subbaraman, L. Jones, H. Sheardown, The Competing Effects of Hyaluronic and Methacrylic Acid in Model Contact Lenses, J. Biomater. Sci. Polym. Ed. 23 (2012) 1021–1038.

[43] M. van Beek, A. Weeks, L. Jones, H. Sheardown, Immobilized hyaluronic acid containing model silicone hydrogels reduce protein adsorption., J. Biomater. Sci. Polym. Ed. 19 (2008) 1425–1436.

[44] G.W. Greene, L.L. Martin, R.F. Tabor, A. Michalczyk, L.M. Ackland, R. Horn, Lubricin: A versatile, biological anti-adhesive with properties comparable to polyethylene glycol, Biomaterials. 53 (2015) 127–136.

[45] D.B. Schaefer, D. Wendt, M. Moretti, M. Jakob, G.D. Jay, M. Heberer, I. Martin, Lubricin reduces cartilage–cartilage integration, Biorheology. 41 (2004) 503–508.

[46] F. Mantelli, P. Argüeso, Functions of ocular surface mucins in health and disease, Curr. Opin. Allergy Clin. Immunol. 8 (2008) 477–483.

[47] G.D. Jay, B.P. Lane, L. Sokoloff, Characterization of a bovine synovial fluid lubricating factor III. The interaction with hyaluronic acid, Connect. Tissue Res. 28 (1992) 245–255.

[48] S. Morrison, D.A. Sullivan, B.D. Sullivan, H. Sheardown, T.A. Schmidt, Dose-dependent and synergistic effects of proteoglycan 4 on boundary lubrication at a human cornea-

polydimethylsiloxane biointerface., Eye Contact Lens. 38 (2012) 27–35.

[49] M. Samsom, Y. Iwabuchi, H. Sheardown, T.A. Schmidt, Proteoglycan 4 and hyaluronan as boundary lubricants for model contact lens hydrogels, J. Biomed. Mater. Res. Part B Appl. Biomater. 106 (2018) 1329–1338.

[50] D.W. Lee, X. Banquy, S. Das, N. Cadirov, G. Jay, J. Israelachvili, Effects of molecular weight of grafted hyaluronic acid on wear initiation, Acta Biomater. 10 (2014) 1817–1823.

[51] S. Das, X. Banquy, B. Zappone, G.W. Greene, G.D. Jay, J.N. Israelachvili, Synergistic Interactions between Grafted Hyaluronic Acid and Lubricin Provide Enhanced Wear Protection and Lubrication, Biomacromolecules. 14 (2013) 1669–1677.

[52] M. Korogiannaki, J. Zhang, H. Sheardown, Surface modification of model hydrogel contact lenses with hyaluronic acid via thiol-ene "click" chemistry for enhancing surface characteristics, J. Biomater. Appl. 32 (2017) 446–462.

[53] N. Efron, L. Jones, A.J. Bron, E. Knop, R. Arita, S. Barabino, A.M. McDermott, E. Villani, M.D.P. Willcox, M. Markoulli, The TFOS International Workshop on Contact Lens Discomfort: Report of the Contact Lens Interactions With the Ocular Surface and Adnexa Subcommittee, Investig. Opthalmology Vis. Sci. 54 (2013) TFOS98-122.

[54] C.S. McCaa, The eye and visual nervous system: anatomy, physiology and toxicology., Environ. Health Perspect. 44 (1982) 1–8.

[55] S.C. Pflugfelder, R.W. Beuerman, M.E. Stern, Dry eye and ocular surface disorders, Marcel Dekker Inc, New York , 2004.

[56] R.C. Tripathi, B.J. Tripathi, Anatomy of the Human Eye, Orbit, and Adnexa, in: Eye, Elsevier, 1984: pp. 1–268.

[57] I.K. Gipson, P. Argüeso, Role of mucins in the function of the corneal and conjunctival epithelia., Int. Rev. Cytol. 231 (2003) 1–49.

[58] M.K. Tsilimbaris, E. Lesniewska, S. Lydataki, C. Le Grimellec, J.P. Goudonnet, I.G. Pallikaris, The use of atomic force microscopy for the observation of corneal epithelium surface., Invest. Ophthalmol. Vis. Sci. 41 (2000) 680–686.

[59] D. Korb, J. Craig, M. Doughty, J.-P. Guillon, A. Tomlinso, G. Smith, The tear film : structure, function, and clinical examination, BCLA, Butterworth-Heinemann, 2002.

[60] H.F. Li, W.M. Petroll, T. Møller-Pedersen, J.K. Maurer, H.D. Cavanagh, J. V Jester, Epithelial and corneal thickness measurements by in vivo confocal microscopy through focusing (CMTF)., Curr. Eye Res. 16 (1997) 214–221.

[61] S. Hayashi, T. Osawa, K. Tohyama, Comparative observations on corneas, with special reference to bowman's layer and descemet's membrane in mammals and amphibians, J. Morphol. 254 (2002) 247–258.

[62] S.E. Wilson, J.W. Hong, Bowman's layer structure and function: critical or dispensable to corneal function? A hypothesis., Cornea. 19 (2000) 417–420.

[63] D.M. Maurice, The Cornea and Sclera, in: H. Davson (Ed.), Eye, Academic Press, New York, NY, 1962: pp. 289–367.

[64] N.C. Joyce, Proliferative capacity of the corneal endothelium., Prog. Retin. Eye Res. 22

(2003) 359–389.

[65] M.M. Stiemke, H.F. Edelhauser, D.H. Geroski, The developing corneal endothelium: Correlation of morphology, hydration and Na/K ATPase pump site density, Curr. Eye Res. 10 (1991) 145–156. doi:10.3109/02713689109001742.

[66] M.A. Watsky, M.L. McDermott, H.F. Edelhauser, In vitro corneal endothelial permeability in rabbit and human: the effects of age, cataract surgery and diabetes., Exp. Eye Res. 49 (1989) 751–67.

[67] D.M. Maurice, The location of the fluid pump in the cornea., J. Physiol. 221 (1972) 43–54.

[68] T.G. Rowsey, D. Karamichos, The role of lipids in corneal diseases and dystrophies: a systematic review., Clin. Transl. Med. 6 (2017) 30.

[69] F.W. Newell, Ophthalmology : principles and concepts, 6th ed., Mosby, St. Louis, MO, 1986.

[70] G.E. Marshall, A.G.P. Konstas, W.R. Lee, Collagens in the aged human macular sclera, Curr. Eye Res. 12 (1993) 143–153.

[71] E.M. Van Buskirk, The anatomy of the limbus, Eye. 3 (1989) 101–108.

[72] M.A. Watsky, M.M. Jablonski, H.F. Edelhauser, Comparison of conjunctival and corneal surface areas in rabbit and human, Curr. Eye Res. 7 (1988) 483–486.

[73] M.R. Allansmith, R.S. Baird, J. V. Greiner, Density of Goblet Cells in Vernal Conjunctivitis and Contact Lens-Associated Giant Papillary Conjunctivitis, Arch. Ophthalmol. 99 (1981) 884–885.

[74] N. Knop, D.R. Korb, C.A. Blackie, E. Knop, The Lid Wiper Contains Goblet Cells and Goblet Cell Crypts for Ocular Surface Lubrication During the Blink, Cornea. 31 (2012) 668–679.

[75] S.V. Kessing, A New Division of the Conjunctiva on the basis of X-Ray Examination, Acta Ophthalmol. 45 (1967) 680–683.

[76] J.P. Sand, B.Z. Zhu, S.C. Desai, Surgical Anatomy of the Eyelids., Facial Plast. Surg. Clin. North Am. 24 (2016) 89–95.

[77] E. Knop, N. Knop, T. Millar, H. Obata, D.A. Sullivan, The international workshop on meibomian gland dysfunction: report of the subcommittee on anatomy, physiology, and pathophysiology of the meibomian gland., Invest. Ophthalmol. Vis. Sci. 52 (2011) 1938–1978.

[78] C. Donald, L. Hamilton, M.J. Doughty, C. Hughes, A quantitative assessment of the location and width of Marx's line along the marginal zone of the human eyelid., Optom. Vis. Sci. 80 (2003) 564–572.

[79] B.D. Kels, A. Grzybowski, J.M. Grant-Kels, Human ocular anatomy, Clin. Dermatol. 33 (2015) 140–146.

[80] J.J. Dutton, B.R. Frueh, Eyelid Anatomy and Physiology with Reference to Blepharoptosis, in: Eval. Manag. Blepharoptosis, Springer New York, New York, NY, 2011: pp. 13–26.

[81] X. Zhang, V.J. M, Y. Qu, X. He, S. Ou, J. Bu, C. Jia, J. Wang, H. Wu, Z. Liu, W. Li, Dry

Eye Management: Targeting the Ocular Surface Microenvironment., Int. J. Mol. Sci. 18 (2017).

[82] F.J. Holly, Tear film physiology., Am. J. Optom. Physiol. Opt. 57 (1980) 252–257. http://www.ncbi.nlm.nih.gov/pubmed/7386586.

[83] D.A. Benedetto, D.O. Shah, H.E. Kaufman, The instilled fluid dynamics and surface chemistry of polymers in the preocular tear film, Invest. Ophthalmol. Vis. Sci. 14 (1975) 887–902.

[84] P.E. King-Smith, B.A. Fink, N. Fogt, K.K. Nichols, R.M. Hill, G.S. Wilson, The thickness of the human precorneal tear film: evidence from reflection spectra., Invest. Ophthalmol. Vis. Sci. 41 (2000) 3348–3359.

[85] N. Yokoi, A.J. Bron, J.M. Tiffany, K. Maruyama, A. Komuro, S. Kinoshita, Relationship Between Tear Volume and Tear Meniscus Curvature, Arch. Ophthalmol. 122 (2004) 1265–1269.

[86] J. Born Anthony, J.M. Tiffany, N. Yokoi, M.S. Gouveia, Using Osmolarity to Diagnose Dry Eye: A Compartmental Hypothesis and Review of Our Assumptions, in: D.A. Sullivan (Ed.), Lacrimal Gland. Tear Film. Dry Eye Syndr. Adv. Exp. Med. Biol., Springer, Boston, MA, Boston, MA, 1994: pp. 1087–1095.

[87] S.M. Gouveia, J.M. Tiffany, Human tear viscosity: An interactive role for proteins and lipids, Biochim. Biophys. Acta - Proteins Proteomics. 1753 (2005) 155–163.

[88] J.M. Tiffany, The viscosity of human tears., Int. Ophthalmol. 15 (1991) 371–6.

[89] J.M. Tiffany, N. Winter, G. Bliss, Tear film stability and tear surface tension, Curr. Eye Res. 8 (1989) 507–515.

[90] M. Yamada, H. Mochizuki, M. Kawai, M. Yoshino, Y. Mashima, Fluorophotometric measurement of pH of human tears in vivo., Curr. Eye Res. 16 (1997) 482–486.

[91] E. Wolff, The anatomy of the eye and orbit, Blakinston , New York , 1954.

[92] S.C. Pflugfelder, Z. Liu, D. Monroy, D. Li, M.E. Carvajal, S.A. Price–Schiavi, N. Idris, A. Solomon, A. Perez, K.L. Carraway, Detection of Sialomucin Complex (MUC4) in Human Ocular Surface Epithelium and Tear Fluid, C.V. Mosby Co, 2000.

[93] P.N. Dilly, Structure and Function of the Tear Film, in: D.A. Sullivan (Ed.), Lacrimal Gland. Tear Film. Dry Eye Syndr. Adv. Exp. Med. Biol., Springer, Boston, MA, 1994: pp. 239–247. doi:10.1007/978-1-4615-2417-5_41.

[94] S.T. Tragoulias, P.J. Anderton, G.R. Dennis, F. Miano, T.J. Millar, Surface pressure measurements of human tears and individual tear film components indicate that proteins are major contributors to the surface pressure., Cornea. 24 (2005) 189–200.

[95] I.A. Butovich, T.J. Millar, B.M. Ham, Understanding and analyzing meibomian lipids--a review., Curr. Eye Res. 33 (2008) 405–420.

[96] J.-P. Guillon, Tear film photography and contact lens wear, J. Br. Contact Lens Assoc. 5 (1982) 84–87.

[97] F.J. Holly, Formation and rupture of the tear film, Exp. Eye Res. 15 (1973) 515–525.

[98] J.M. Tiffany, The role of meibomian secretion in the tears., Trans. Ophthalmol. Soc. U. K. 104 (Pt 4) (1985) 396–401.

[99] L.M. Grant, F. Tiberg, Normal and lateral forces between lipid covered solids in solution: correlation with layer packing and structure., Biophys. J. 82 (2002) 1373–1385.

[100] B. Nagyová, J.M. Tiffany, Components responsible for the surface tension of human tears., Curr. Eye Res. 19 (1999) 4–11.

[101] J.P. Craig, A. Tomlinson, Importance of the lipid layer in human tear film stability and evaporation., Optom. Vis. Sci. 74 (1997) 8–13.

[102] T.J. Millar, B.S. Schuett, The real reason for having a meibomian lipid layer covering the outer surface of the tear film – A review, Exp. Eye Res. 137 (2015) 125–138.

[103] S. Mishima, Some Physiological Aspects of the Precorneal Tear Film., Arch. Ophthalmol. (Chicago, Ill. 1960). 73 (1965) 233–41.

[104] R.M. Herranz, R.M. Corrales Herran, Ocular Surface: Anatomy and Physiology, Disorders and Therapeutic Care, Taylor & Francis/ CRC Press, 2013. https://books.google.ca/books?id=cr8KfacHi54C.

[105] K.B. Green-Church, K.K. Nichols, N.M. Kleinholz, L. Zhang, J.J. Nichols, Investigation of the human tear film proteome using multiple proteomic approaches., Mol. Vis. 14 (2008) 456–70.

[106] W.G. Bachman, G. Wilson, Essential ions for maintenance of the corneal epithelial surface., Invest. Ophthalmol. Vis. Sci. 26 (1985) 1484–1488.

[107] M.A. Lemp, Report of the National Eye Institute/Industry workshop on Clinical Trials in Dry Eyes., CLAO J. . 21 (1995) 221–232. http://www.ncbi.nlm.nih.gov/pubmed/8565190.

[108] F. Murillo-Lopez, S.C. Pflugfelder, Dry eye, in: J.H. Krachmer, M.J. Mannis, E.J. Holland (Eds.), Cornea, Mosby, St Louis, MI, 1997: pp. 663–668.

[109] J.P. Gilbard, K.L. Gray, S.R. Rossi, A Proposed Mechanism for Increased Tear-Film Osmolarity in Contact Lens Wearers, Am. J. Ophthalmol. 102 (1986) 505–507.

[110] W.D.H. Gillan, W.D. H., Tear biochemistry: a review, African Vis. Eye Heal. 69 (2010) 100–106.

[111] H.J. Davidson, V.J. Kuonen, The tear film and ocular mucins, Vet. Ophthalmol. 7 (2004) 71–77.

[112] H. Watanabe, Significance of mucin on the ocular surface., Cornea. 21 (2002) S17-22.

[113] P.A. Asbell, M.A. Lemp, Dry eye disease : the clinician's guide to diagnosis and treatment, Thieme, 2006.

[114] S. Spurr-Michaud, P. Argüeso, I. Gipson, Assay of mucins in human tear fluid, Exp. Eye Res. 84 (2007) 939–950.

[115] P.N. Dilly, Contribution of the epithelium to the stability of the tear film., Trans. Ophthalmol. Soc. U. K. 104 (Pt 4) (1985) 381–389.

[116] I.K. Gipson, The ocular surface: the challenge to enable and protect vision: the Friedenwald lecture., Invest. Ophthalmol. Vis. Sci. 48 (2007) 4390–4398.

[117] R.R. Hodges, D.A. Dartt, Tear film mucins: front line defenders of the ocular surface; comparison with airway and gastrointestinal tract mucins., Exp. Eye Res. 117 (2013) 62–78.

[118] F.J. Holly, D.W. Lamberts, D.L. MacKeen, The Preocular tear film in health, disease, and contact lens wear, Dry Eye Institute, 1986.

[119] E.A. Fick, Eine Contact-Brille, Arch. Für Augenheilkd. 18 (1888) 279–289.

[120] A. Müller, Brillenglaser und Hornhautlinsen Part III [inaugural Dissertation]., Germany, Kiel Handorff, 1889.

[121] J.E. Key, Development of Contact Lenses and Their Worldwide Use, Eye Contact Lens Sci. Clin. Pract. 33 (2007) 343–345. http://www.ncbi.nlm.nih.gov/pubmed/17975417.

[122] N. Efron, Contact lens practice, 3rd ed., Elsevier Heatlh Sciences , 2016.

[123] T.J. Bowden, Contact Lenses: The Story., Bower House Publications, 2009.

[124] O. Wichterle, D. Lim, Hydrophilic Gels for Biological Use, Nature. 185 (1960) 117–118. doi:10.1038/185117a0.

[125] N. Annabi, A. Tamayol, J.A. Uquillas, M. Akbari, L.E. Bertassoni, C. Cha, G. Camci-Unal, M.R. Dokmeci, N.A. Peppas, A. Khademhosseini, 25th Anniversary Article: Rational design and applications of hydrogels in regenerative medicine., Adv. Mater. 26 (2014) 85–123.

[126] E. Caló, V. V. Khutoryanskiy, Biomedical applications of hydrogels: A review of patents and commercial products, Eur. Polym. J. 65 (2015) 252–267.

[127] N.A. Peppas, R. Langer, New challenges in biomaterials., Sci. . 263 (1994) 1715–20.

[128] K. Park, Controlled drug delivery : challenges and strategies, American Chemical Society, Washington, DC, 1997.

[129] N. Efron, Contact lens complications, Butterworth-Heinemann, Edinburgh, United Kingdom, 2004.

[130] S.M.J. Fleiszig, The Pathogenesis of Contact Lens-Related Keratitis, Optom. Vis. Sci. . 83 (2005) 866–873.

[131] L. Minarik, J. Rapp, Protein deposits on individual hydrophilic contact lenses: effects of water and ionicity., CLAO J. 15 (1989) 185–8.

[132] Q. Garrett, R.C. Chatelier, H.J. Griesser, B.K. Milthorpe, Effect of charged groups on the adsorption and penetration of proteins onto and into carboxymethylated poly(HEMA) hydrogels., Biomaterials. 19 (1998) 2175–2186.

[133] S. Hosaka, H. Ozawa, H. Tanzawa, H. Ishida, K. Yoshimura, T. Momose, H. Magatani, A. Nakajima, Analysis of deposits on high water content contact lenses, J. Biomed. Mater. Res. 17 (1983) 261–274.

[134] R.C. Tripathi, B.J. Tripathi, R.A. Silverman, G.N. Rao, Contact lens deposits and spoilage: identification and management., Int. Ophthalmol. Clin. 31 (1991) 91–120.

[135] J.J. Nichols, L.T. Sinnott, Tear film, contact lens, and patient-related factors associated with contact lens-related dry eye., Invest. Ophthalmol. Vis. Sci. 47 (2006) 1319–1328.

[136] G.N. Orsborn, S.G. Zantos, Corneal desiccation staining with thin high water content contact lenses., CLAO J. 14 (1988) 81–85.

[137] L. Jones, C.A. Woods, N. Efron, Life expectancy of rigid gas permeable and high water content contact lenses., CLAO J. 22 (1996) 258–261.

[138] J. Kunzler, Silicone-based hydrogels for contact lens applications, Contact Lens Spectr. 14 (1999) 9s–11s.

[139] D. Sweeney, Silicone hydrogels: the rebirth of continuous wear contact lenses, Butterworth-Heinemann Medical, 2000.

[140] P.C. Nicolson, J. Vogt, Soft contact lens polymers: an evolution., Biomaterials. 22 (2001) 3273–3283.

[141] T. Goda, K. Ishihara, Soft contact lens biomaterials from bioinspired phospholipid polymers, Expert Rev. Med. Devices. 3 (2006) 167–174.

[142] P.C. Nicolson, Continuous wear contact lens surface chemistry and wearability, Eye Contact Lens. 29 (2003) S30–S32.

[143] A. López-Alemany, V. Compañ, M.F. Refojo, Porous structure of Purevision™ versus Focus® Night&Day™ and conventional hydrogel contact lenses, J. Biomed. Mater. Res. 63 (2002) 319–325.

[144] L. Jones, Comfilcon A: a new silicone hydrogel material, Contact Lens Spectr. 22 (2007) 21.

[145] K.P. McCabe, F.F. Molock, G.A. Hill, A. Alli, R.B. Steffen, D.G. Vanderlaan, K.A. Young, J.D. Ford, Biomedical devices containing internal wetting agents, US Patent 7052131, 2006.

[146] R. Steffen, K. McCabe, Finding the comfort zone, Contact Lens Spectr. 13 (2004).

[147] K. Wygladacz, D. Hook, R. Steffen, W. Reindel, Breaking the Cycle of Discomfort, Contact Lens Spectr. 29 (2014) 33–38.

[148] H. Griffiths, A new silicone hydrogel daily disposable lens, Opt. . 238 (2009) 16–19.

[149] B. Chou, The Evolution of Silicone Hydrogel Lenses, Contact Lens Spectr. . (n.d.).

[150] B.A. Holden, D.F. Sweeney, P.R. Sankaridurg, N. Carnt, K. Edwards, S. Stretton, F. Stapleton, Microbial keratitis and vision loss with contact lenses., Eye Contact Lens. 29 (2003) S131-4-144, S192-194.

[151] O.D. Schein, J.J. McNally, J. Katz, R.L. Chalmers, J.M. Tielsch, E. Alfonso, M. Bullimore, D. O'Day, J. Shovlin, The Incidence of Microbial Keratitis among Wearers of a 30-Day Silicone Hydrogel Extended-Wear Contact Lens, Ophthalmology. 112 (2005) 2172–2179.

[152] J.K.G. Dart, C.F. Radford, D. Minassian, S. Verma, F. Stapleton, Risk Factors for Microbial Keratitis with Contemporary Contact Lenses, Ophthalmology. 115 (2008) 1647-1654–3.

[153] F. Stapleton, L. Keay, K. Edwards, T. Naduvilath, J.K.G. Dart, G. Brian, B.A. Holden, The Incidence of Contact Lens–Related Microbial Keratitis in Australia, Ophthalmology. 115 (2008) 1655–1662.

[154] F. Stapleton, L. Keay, K. Edwards, B. Holden, The epidemiology of microbial keratitis with silicone hydrogel contact lenses, Eye Contact Lens Sci. Clin. Pract. 39 (2013) 78–84.

[155] L. Lim, M.S. Loughnan, L.J. Sullivan, Microbial keratitis associated with extended wear of silicone hydrogel contact lenses., Br. J. Ophthalmol. 86 (2002) 355–7.

[156] L. Szczotka-Flynn, M. Diaz, Risk of Corneal Inflammatory Events with Silicone Hydrogel and Low Dk Hydrogel Extended Contact Lens Wear: A Meta-Analysis, Optom. Vis. Sci. 84 (2007) 247–256.

[157] N. Carnt, D. Sweeney, J. Stern, M. Willcox, R. Wong, Factors associated with unusual cases of acute infiltrative keratitis in silicone hydrogel extended wear, Invest. Ophthalmol. Vis. Sci. 43 (2002) 3111.

[158] R.L. Chalmers, L. Keay, J. McNally, J. Kern, Multicenter Case-Control Study of the Role of Lens Materials and Care Products on the Development of Corneal Infiltrates, Optom. Vis. Sci. 89 (2012) 316–325.

[159] D. Jones, C. Woods, L. Jones, N. Efron, P. Morgan, A sixteen year survey of Canadian contact lens prescribing, Contact Lens Anterior Eye. 39 (2016) 402–410. doi:10.1016/j.clae.2016.09.002.

[160] N. Pence, What's new in silicone hydrogel lenses?, Contact Lens Spectr. 28 (2013) 19.

[161] L. Jones, N. MacDougall, L.G. Sorbara, Asymptomatic corneal staining associated with the use of balafilcon silicone-hydrogel contact lenses disinfected with a polyaminopropyl biguanide-preserved care regimen., Optom. Vis. Sci. 79 (2002) 753–61.

[162] N. Efron, P.B. Morgan, M. Helland, M. Itoi, D. Jones, J.J. Nichols, E. van der Worp, C.A. Woods, Daily disposable contact lens prescribing around the world, Contact Lens Anterior Eye. 33 (2010) 225–227.

[163] K. Dumbleton, C. Woods, L. Jones, D. Fonn, D.B. Sarwer, Patient and Practitioner Compliance With Silicone Hydrogel and Daily Disposable Lens Replacement in the United States, Eye Contact Lens Sci. Clin. Pract. 35 (2009) 164–171.

[164] R. Stone, Introducing Water Gradient Technology, Contact Lens Spectr. (2013) 34–38.

[165] J. Pruitt, E. Bauman, The development of Dailies Total1 water gradient contact lenses., Contact Lens Spectr. . (2013) 40–44.

[166] J. Pruitt, Y. Qiu, S. Thekveli, R. Hart, Surface characterisation of a water gradient silicone hydrogel contact lens (delefilcon A)., Invest. Ophthalmol. Vis. Sci. 53 (2012) 6107.

[167] A.C. Dunn, J.M. Urueña, Y. Huo, S.S. Perry, T.E. Angelini, W.G. Sawyer, Lubricity of Surface Hydrogel Layers, Tribol. Lett. 49 (2013) 371–378.

[168] J. Kern, J. Rappon, E. Bauman, B. Vaughn, Assessment of the relationship between contact lens coefficient of friction and subject lens comfort, Invest. Ophthalmol. Vis. Sci. 54 (2013) 494.

[169] C. Coles, N. Brennan, Coefficient of friction and soft contact lens comfort, Optom Vis Sci. 89 (2012) E-abstract 125603.

[170] D. Fonn, Clinical Relevance of Contact Lens Lubricity, Contact Lens Spectr. 28 (2013) 25–27.

[171] L. Jones, L. Subbaraman, R. Rogers, K. Dumbleton, Surface treatment, wetting and modulus of silicone hydrogels, Optician. (2006) 28–34.

[172] K. Dumbleton, Noninflammatory silicone hydrogel contact lens complications., Eye Contact Lens. 29 (2003) S186-9–1, S192-4.

[173] M.C. Lin, T.N. Yeh, Mechanical Complications Induced by Silicone Hydrogel Contact Lenses, Eye Contact Lens Sci. Clin. Pract. 39 (2013) 115–124.

[174] K. Dumbleton, Adverse events with silicone hydrogel continuous wear., Cont. Lens Anterior Eye. 25 (2002) 137–146.

[175] N. Pritchard, D. Fonn, D. Brazeau, Discontinuation of contact lens wear: a survey, Int. Contact Lens Clin. 26 (1999) 157–162.

[176] J.J. Nichols, M.D.P. Willcox, A.J. Bron, C. Belmonte, J.B. Ciolino, J.P. Craig, M. Dogru, G.N. Foulks, L. Jones, J.D. Nelson, K.K. Nichols, C. Purslow, D.A. Schaumberg, F. Stapleton, D.A. Sullivan, The TFOS International Workshop on Contact Lens Discomfort: executive summary., Invest. Ophthalmol. Vis. Sci. 54 (2013) TFOS7-13.

[177] A. Sulley, G. Young, C. Hunt, Factors in the success of new contact lens wearers, Contact Lens Anterior Eye. 40 (2017) 15–24.

[178] R.L. Chalmers, S.B. Hickson-Curran, L. Keay, W.J. Gleason, R. Albright, Rates of Adverse Events With Hydrogel and Silicone Hydrogel Daily Disposable Lenses in a Large Postmarket Surveillance Registry: The TEMPO Registry, Invest. Ophthalmol. Vis. Sci. 56 (2015) 654–663.

[179] Food Drug Adminsitration, Premarket Notification [510(k)] Guidance Document for Class II Daily Wear Contact Lenses, (n.d.) Issued May 1994.

[180] D. Hampton, J.A. Green, M. Robboy, M. Eydelman, Food and Drug Administration Efforts to Mitigate Contact Lens Discomfort, Eye Contact Lens Sci. Clin. Pract. 43 (2017) 2–4.

[181] J.C. Hutter, FDA Group V: Is a Single Grouping Sufficient to Describe SiH Performance

[182] J.A. Green, K.S. Phillips, V.M. Hitchins, A.D. Lucas, M.E. Shoff, J.C. Hutter, E.M. Rorer, M.B. Eydelman, Material Properties That Predict Preservative Uptake for Silicone Hydrogel Contact Lenses, Eye Contact Lens Sci. Clin. Pract. 38 (2012) 350–357.

[183] J.C. Hutter, J.A. Green, M.B. Eydelman, Proposed Silicone Hydrogel Contact Lens Grouping System for Lens Care Product Compatibility Testing, Eye Contact Lens Sci. Clin. Pract. 38 (2012) 358–362.

[184] ISO 18369-1:2017 - Ophthalmic optics -- Contact lenses -- Part 1: Vocabulary, classification system and recommendations for labelling specifications

[185] D.M. Robertson, The Effects of Silicone Hydrogel Lens Wear on the Corneal Epithelium and Risk for Microbial Keratitis, Eye Contact Lens Sci. Clin. Pract. 39 (2013) 66–71.

[186] J.P. Beygmanson, Effects of contact lens wear on corneal ultrastructure., Cont. Lens Anterior Eye. 24 (2001) 115–120.

[187] M. Markoulli, E. Papas, N. Cole, B. Holden, Corneal erosions in contact lens wear., Cont. Lens Anterior Eye. 35 (2012) 2–8.

[188] B.A. Holden, D.F. Sweeney, A. Vannas, K.T. Nilsson, N. Efron, Effects of long-term extended contact lens wear on the human cornea., Invest. Ophthalmol. Vis. Sci. 26 (1985) 1489–14501.

[189] N. Hine, A. Back, B. Holden, Aetiology of arcuate epithelial lesions induced by hydrogels, J. Br. Contact Lens Assoc. 10 (1987) 48–50.

[190] J.A. Bonanno, K.A. Polse, Hypoxic changes in the corneal epithelium and stroma, in: A. Tomlinson (Ed.), Complicat. Contact Lens Wear, Mosby, St Louis, MO, 1991: pp. 21–36.

[191] N. Efron, Corneal neovascularization, in: N. Efron (Ed.), Contact Lens Complicat., 3rd ed., Elsevier, London, UK, 2012: pp. 214–224.

[192] A.S. Bruce, N.A. Brennan, Corneal pathophysiology with contact lens wear., Surv. Ophthalmol. 35 (n.d.) 25–58.

[193] D. Fonn, R. du Toit, T.L. Simpson, J.A. Vega, P. Situ, R.L. Chalmers, Sympathetic swelling response of the control eye to soft lenses in the other eye., Invest. Ophthalmol. Vis. Sci. 40 (1999) 3116–3121.

[194] R.A. Thoft, J. Friend, Biochemical Aspects of Contact Lens Wear, Am. J. Ophthalmol. 80 (1975) 139–145.

[195] W.H. Ridder III, Anatomy and Physiology, in: M.M. Hom, A.S. Bruce (Eds.), Man. Contact Lens Prescr. Fitting, 3rd ed., Butterworth-Heinemann Medical, 2006: pp. 3–22.

[196] L. Cheng, S.J. Muller, C.J. Radke, Wettability of silicone-hydrogel contact lenses in the presence of tear-film components., Curr. Eye Res. 28 (2004) 93–108.

[197] J.J. Nichols, G.L. Mitchell, P.E. King-Smith, Thinning Rate of the Precorneal and Prelens Tear Films, Investig. Opthalmology Vis. Sci. 46 (2005) 2353.

[198] P. Situ, T.L. Simpson, L.W. Jones, D. Fonn, Effects of Silicone Hydrogel Contact Lens Wear on Ocular Surface Sensitivity to Tactile, Pneumatic Mechanical, and Chemical Stimulation, Investig. Opthalmology Vis. Sci. 51 (2010) 6111–6117.

[199] N.A. McNamara, K.A. Polse, S.A. Fukunaga, J.S. Maebori, R.M. Suzuki, Soft lens extended wear affects epithelial barrier function11The authors have no proprietary interests in the materials mentioned in the article., Ophthalmology. 105 (1998) 2330–2335.

[200] M.C. Lin, G.N. Soliman, M.J. Song, J.P. Smith, C.T. Lin, Y.Q. Chen, K.A. Polse, Soft contact lens extended wear affects corneal epithelial permeability: hypoxic or mechanical etiology?, Contact Lens Anterior Eye. 26 (2003) 11–16.

[201] E. Papas, On the Relationship Between Soft Contact Lens Oxygen Transmissibility and Induced Limbal Hyperaemia, Exp. Eye Res. 67 (1998) 125–131.

[202] N.A. Brennan, M.-L.C. Coles, J.H.-B. Ang, An evaluation of silicone-hydrogel lenses worn on a daily wear basis, Clin. Exp. Optom. 89 (2006) 18–25.

[203] K.A. Dumbleton, R.L. Chalmers, D.B. Richter, D. Fonn, Vascular response to extended wear of hydrogel lenses with high and low oxygen permeability., Optom. Vis. Sci. 78 (2001) 147–51.

[204] E.B. Papas, C.M. Vajdic, R. Austen, B.A. Holden, High-oxygen-transmissibility soft contact lenses do not induce limbal hyperaemia., Curr. Eye Res. 16 (1997) 942–948.

[205] D. Fonn, K.E. MacDonald, D. Richter, N. Pritchard, The ocular response to extended wear of a high Dk silicone hydrogel contact lens., Clin. Exp. Optom. 85 (2002) 176–82.

[206] B.H. Jeng, C.P. Halfpenny, D.M. Meisler, E.L. Stock, Management of Focal Limbal Stem Cell Deficiency Associated With Soft Contact Lens Wear, Cornea. 30 (2011) 18–23.

[207] R.P. Bhatia, R. Srivastava, A. Ghosh, Limbal stem cell study in contact lens wearers., Ann. Ophthalmol. (Skokie). 41 (2009) 87–92.

[208] E. Knop, H. Brewitt, Induction of conjunctival epithelial alterations by contact lens wearing. A prospective study., Ger. J. Ophthalmol. 1 (1992) 125–34.

[209] N. Efron, M. Al-Dossari, N. Pritchard, Confocal Microscopy of the Bulbar Conjunctiva in Contact Lens Wear, Cornea. 29 (2010) 43–52.

[210] M. Guillon, C. Maissa, Bulbar conjunctival staining in contact lens wearers and non lens wearers and its association with symptomatology, Contact Lens Anterior Eye. 28 (2005) 67–73.

[211] J.P.G. Bergmanson, J. Tukler, N.E. Leach, M. Alabdelmoneam, W.L. Miller, Morphology of contact lens-induced conjunctival epithelial flaps: A pilot study, Contact Lens Anterior Eye. 35 (2012) 185–188.

[212] C. Maïssa, M. Guillon, R.J. Garofalo, Contact Lens–Induced Circumlimbal Staining in Silicone Hydrogel Contact Lenses Worn on a Daily Wear Basis, Eye Contact Lens Sci. Clin. Pract. 38 (2012) 16–26.

[213] T. Lofstrom, A. Kruse, A Conjunctival Response to Silicone Hydrogel Lens Wear: A new finding reveals how silicone hydrogel lenses may affect the conjunctival epithelium., Contact Lens Spectr. (n.d.) 42–44.

[214] H. Pult, W. Sickenberger, LIPCOF and contact lens wearers: a new tool of forecast subjective dryness and degree of comfort of contact lens wearers, Contactologia. 22 (2000) 74–9.

[215] M. Berry, H. Pult, C. Purslow, P.J. Murphy, Mucins and Ocular Signs in Symptomatic and Asymptomatic Contact Lens Wear, Optom. Vis. Sci. 85 (2008) E930–E938.

[216] P.E. Allaire, R.D. Flack, Squeeze forces in contact lenses with a steep base curve radius., Am. J. Optom. Physiol. Opt. 57 (1980) 219–227.

[217] J.L. Creech, A. Chauhan, C.J. Radke, Dispersive mixing in the posterior tear film under a soft contact lens, Ind. Eng. Chem. Res. 40 (2001) 3015–3026.

[218] A.J. Shaw, M.J. Collins, B.A. Davis, L.G. Carney, Eyelid Pressure and Contact with the Ocular Surface, Investig. Opthalmology Vis. Sci. 51 (2010) 1911–1917.

[219] E. Sakai, A. Shiraishi, M. Yamaguchi, K. Ohta, Y. Ohashi, Blepharo-Tensiometer: New Eyelid Pressure Measurement System Using Tactile Pressure Sensor, Eye Contact Lens Sci. Clin. Pract. 38 (2012) 326–330.

[220] H.D. Conway, M.W. Richman, The Effects of Contact Lens Deformation on Tear Film Pressure and Thickness During Motion of the Lens Towards the Eye, J. Biomech. Eng. 105 (1983) 47.

[221] A.C. Dunn, J.A. Tichy, J.M. Urueña, W.G. Sawyer, Lubrication regimes in contact lens wear during a blink, Tribol. Int. 63 (2013) 45–50.

[222] D.R. Korb, J. V Greiner, J.P. Herman, E. Hebert, V.M. Finnemore, J.M. Exford, T. Glonek,

M.C. Olson, Lid-wiper epitheliopathy and dry-eye symptoms in contact lens wearers., CLAO J. 28 (2002) 211–216.

[223] B. Yeniad, M. Beginoglu, L.K. Bilgin, Lid-Wiper Epitheliopathy in Contact Lens Users and Patients With Dry Eye, Eye Contact Lens Sci. Clin. Pract. 36 (2010) 140–143.

[224] H. Pult, C. Purslow, M. Berry, P.J. Murphy, Clinical Tests for Successful Contact Lens Wear: Relationship and Predictive Potential, Optom. Vis. Sci. 85 (2008) E924–E929.

[225] A. Shiraishi, M. Yamaguchi, Y. Ohashi, Prevalence of Upper- and Lower-Lid-Wiper Epitheliopathy in Contact Lens Wearers and Non-wearers, Eye Contact Lens Sci. Clin. Pract. 40 (2014) 220–224.

[226] H. Pult, P.J. Murphy, C. Purslow, The longitudinal impact of soft contact lens wear on lid wiper epitheliopathy and lid-parallel conjunctival folds, in: 6th Int. Conf. Tear Film Ocul. Surf. Basic Sci. Clin. Relev., Florence, Italy, 2010.

[227] H. Pult, P.J. Murphy, C. Purslow, A Novel Method to Predict the Dry Eye Symptoms in New Contact Lens Wearers, Optom. Vis. Sci. 86 (2009) E1042–E1050.

[228] N. Best, L. Drury, J.S. Wolffsohn, Predicting success with silicone-hydrogel contact lenses in new wearers, Contact Lens Anterior Eye. 36 (2013) 232–237. doi:10.1016/j.clae.2013.02.013.

[229] A. Tomlinson, Tear film changes with contact lens wear, in: A. Tomlinson (Ed.), Complicat. Contact Lens Wear, Mosby, St Louis, MO, 1992: pp. 195–218.

[230] G. Young, N. Efron, Characteristics of the pre-lens tear film during hydrogel contact lens wear., Ophthalmic Physiol. Opt. 11 (1991) 53–58.

[231] Q. Chen, J. Wang, A. Tao, M. Shen, S. Jiao, F. Lu, Ultrahigh-resolution measurement by optical coherence tomography of dynamic tear film changes on contact lenses., Invest. Ophthalmol. Vis. Sci. 51 (2010) 1988–1993.

[232] J. Wang, D. Fonn, T.L. Simpson, L. Jones, Precorneal and pre- and postlens tear film thickness measured indirectly with optical coherence tomography., Invest. Ophthalmol. Vis. Sci. 44 (2003) 2524–8.

[233] J.J. Nichols, P.E. King-Smith, The effect of eye closure on the post-lens tear film thickness during silicone hydrogel contact lens wear., Cornea. 22 (2003) 539–544.

[234] F.S. Chen, D.M. Maurice, The pH in the precorneal tear film and under a contact lens measured with a fluorescent probe., Exp. Eye Res. 50 (1990) 251–259.

[235] M.S. Norn, Tear fluid pH in normals, contact lens wearers, and pathological cases., Acta Ophthalmol. 66 (1988) 485–9.

[236] Q. Chen, J. Wang, M. Shen, C. Cai, J. Li, L. Cui, J. Qu, F. Lu, Lower Volumes of Tear Menisci in Contact Lens Wearers with Dry Eye Symptoms, Investig. Opthalmology Vis. Sci. 50 (2009) 3159–3163.

[237] C. Maïssa, M. Guillon, K. Girard-Claudon, P. Cooper, Tear lipid composition of hydrogel contact lens wearers., Adv. Exp. Med. Biol. 506 (2002) 935–938.

[238] M. Guillon, C. Maissa, K. Girard-Claudon, P. Cooper, Influence of the tear film composition on tear film structure and symptomatology of soft contact lens wearers., Adv.

Exp. Med. Biol. 506 (2002) 895–899.

[239] D. Alonso-Caneiro, D.R. Iskander, M.J. Collins, Tear Film Surface Quality With Soft Contact Lenses Using Dynamic-Area High-Speed Videokeratoscopy, Eye Contact Lens Sci. Clin. Pract. 35 (2009) 227–231.

[240] M. Kopf, F. Yi, D. Robert Iskander, M.J. Collins, A.J. Shaw, B. Straker, Tear Film Surface Quality with Soft Contact Lenses Using Dynamic Videokeratoscopy, J. Optom. 1 (2008) 14–21.

[241] G. Tyagi, D. Alonso-Caneiro, M. Collins, S. Read, Tear Film Surface Quality With Rigid and Soft Contact Lenses, Eye Contact Lens Sci. Clin. Pract. 38 (2012) 171–178.

[242] H. Mochizuki, M. Yamada, S. Hatou, K. Tsubota, Turnover rate of tear-film lipid layer determined by fluorophotometry, Br. J. Ophthalmol. 93 (2009) 1535–1538.

[243] M. Guillon, C. Maissa, Contact Lens Wear Affects Tear Film Evaporation, Eye Contact Lens Sci. Clin. Pract. 34 (2008) 326–330.

[244] A. Tomlinson, T.H. Cedarstaff, Tear evaporation from the human eye: The effects of contact lens wear, J. Br. Contact Lens Assoc. 5 (1982) 141–147.

[245] I. Tranoudis, N. Efron, In-eye performance of soft contact lenses made from different materials, Contact Lens Anterior Eye. 27 (2004) 133–148.

[246] P.B. Morgan, N. Efron, In Vivo Dehydration of Silicone Hydrogel Contact Lenses, Eye Contact Lens Sci. Clin. Pract. 29 (2003) 173–176.

[247] J.M. González-Méijome, A. López-Alemany, J.B. Almeida, M.A. Parafita, Dynamic in vitro dehydration patterns of unworn and worn silicone hydrogel contact lenses, J. Biomed. Mater. Res. Part B Appl. Biomater. 90B (2008) 250–258.

[248] D.E. Hart, M.P. Plociniak, G.W. Grimes, Defining the physiologically normal coating and pathological deposit: an analysis of sulfur-containing moieties and pellicle thickness on hydrogel contact lenses., CLAO J. 24 (1998) 85–101.

[249] A. Rohit, M. Willcox, F. Stapleton, Tear Lipid Layer and Contact Lens Comfort, Eye Contact Lens Sci. Clin. Pract. 39 (2013) 247–253.

[250] C. Kramann, N. Boehm, K. Lorenz, N. Wehrwein, B.M. Stoffelns, N. Pfeiffer, F.H. Grus, Effect of contact lenses on the protein composition in tear film: a ProteinChip study, Graefe's Arch. Clin. Exp. Ophthalmol. 249 (2011) 233–243.

[251] C. Baleriola-Lucas, M. Fukuda, M.D. Willcox, D.F. Sweeney, B.A. Holden, Fibronectin concentration in tears of contact lens wearers., Exp. Eye Res. 64 (1997) 37–43.

[252] D.J. Pearce, G. Demirci, M.D. Willcox, Secretory IgA epitopes in basal tears of extended-wear soft contact lens wearers and in non-lens wearers., Aust. N. Z. J. Ophthalmol. 27 (n.d.) 221–223.

[253] B.J. Tighe, V. Franklin, C. Graham, A. Mann, M. Guillon, Vitronectin adsorption in contact lens surfaces during wear: locus and significance., Adv. Exp. Med. Biol. 438 (1998) 769–773.

[254] R.L. Lundh, S. Liotet, Y. Pouliquen, Study of the human blood-tear barrier and the biochemical changes in the tears of 30 contact lens wearers (50 eyes)., Ophthalmologica.

188 (1984) 100–105.

[255] J.J. Nichols, K.B. Green-Church, Mass Spectrometry-Based Proteomic Analyses in Contact Lens-Related Dry Eye, Cornea. 28 (2009) 1109–1117.

[256] G.A. de Souza, L.M.F. Godoy, M. Mann, Identification of 491 proteins in the tear fluid proteome reveals a large number of proteases and protease inhibitors., Genome Biol. 7 (2006) R72.

[257] D. Luensmann, L. Jones, Protein deposition on contact lenses: The past, the present, and the future, Contact Lens Anterior Eye. 35 (2012) 53–64.

[258] N.A. Brennan, M.-L.C. Coles, Deposits and symptomatology with soft contact lens wear, Int. Contact Lens Clin. 27 (2000) 75–100.

[259] G.E. Minno, L. Eckel, S. Groemminger, B. Minno, T. Wrzosek, Quantitative analysis of protein deposits on hydrophilic soft contact lenses: I. Comparison to visual methods of analysis. II. Deposit variation among FDA lens material groups., Optom. Vis. Sci. 68 (1991) 865–872.

[260] L. Jones, K. Evans, R. Sariri, V. Franklin, B. Tighe, Lipid and protein deposition of N-vinyl pyrrolidone-containing group II and group IV frequent replacement contact lenses., CLAO J. 23 (1997) 122–126.

[261] M. Suwala, M.-A. Glasier, L.N. Subbaraman, L. Jones, Quantity and Conformation of Lysozyme Deposited on Conventional and Silicone Hydrogel Contact Lens Materials Using an In Vitro Model, Eye Contact Lens Sci. Clin. Pract. 33 (2007) 138–143.

[262] R.A. Sack, B. Jones, A. Antignani, R. Libow, H. Harvey, Specificity and biological activity of the protein deposited on the hydrogel surface. Relationship of polymer structure to biofilm formation., Invest. Ophthalmol. Vis. Sci. 28 (1987) 842–849.

[263] L. Jones, M. Senchyna, M.-A. Glasier, J. Schickler, I. Forbes, D. Louie, C. May, Lysozyme and lipid deposition on silicone hydrogel contact lens materials., Eye Contact Lens. 29 (2003) S75-9–4, S192-4.

[264] L.N. Subbaraman, M.-A. Glasier, M. Senchyna, H. Sheardown, L. Jones, Kinetics of in vitro lysozyme deposition on silicone hydrogel, PMMA, and FDA Groups I, II, and IV contact lens materials, Curr. Eye Res. 31 (2006) 787–796.

[265] M. Senchyna, L. Jones, D. Louie, C. May, I. Forbes, M.-A. Glasier, Quantitative and conformational characterization of lysozyme deposited on balafilcon and etafilcon contact lens materials, Curr. Eye Res. 28 (2004) 25–36.

[266] L.N. Subbaraman, M.-A. Glasier, J. Varikooty, S. Srinivasan, L. Jones, Protein Deposition and Clinical Symptoms in Daily Wear of Etafilcon Lenses, Optom. Vis. Sci. 89 (2012) 1450–1459.

[267] N.B. Omali, L.N. Subbaraman, C. Coles-Brennan, Z. Fadli, L.W. Jones, Biological and Clinical Implications of Lysozyme Deposition on Soft Contact Lenses., Optom. Vis. Sci. 92 (2015) 750–757.

[268] D.E. Hart, J.A. Schkolnick, S. Bernstein, D. Wallach, D.F. Gross, Contact lens induced giant papillary conjunctivitis: a retrospective study., J. Am. Optom. Assoc. 60 (1989) 195–

204.

[269] C.C. Skotnitsky, T.J. Naduvilath, D.F. Sweeney, P.R. Sankaridurg, Two Presentations of Contact Lens-Induced Papillary Conjunctivitis (CLPC) in Hydrogel Lens Wear: Local and General, Optom. Vis. Sci. 83 (2006) 27–36.

[270] L. Sorbara, L. Jones, D. Williams-Lyn, Contact lens induced papillary conjunctivitis with silicone hydrogel lenses, Contact Lens Anterior Eye. 32 (2009) 93–96.

[271] S.I. Butrus, S.A. Klotz, Contact lens surface deposits increase the adhesion of Pseudomonas aeruginosa, Curr. Eye Res. 9 (1990) 717–724.

[272] L. Michaud, C.J. Giasson, Overwear of contact lenses: increased severity of clinical signs as a function of protein adsorption., Optom. Vis. Sci. 79 (2002) 184–192.

[273] M. Eltis, Contact-lens-related microbial keratitis: case report and review, J. Optom. 4 (2011) 122–127.

[274] D. Dutta, N. Cole, M. Willcox, Factors influencing bacterial adhesion to contact lenses., Mol. Vis. 18 (2012) 14–21.

[275] H. Lorentz, L. Jones, Lipid deposition on hydrogel contact lenses: how history can help us today., Optom. Vis. Sci. 84 (2007) 286–95.

[276] C. Maldonado-Codina, P.B. Morgan, C.M. Schnider, N. Efron, Short-term physiologic response in neophyte subjects fitted with hydrogel and silicone hydrogel contact lenses., Optom. Vis. Sci. 81 (2004) 911–921.

[277] L. Jones, A. Mann, K. Evans, V. Franklin, B. Tighe, An in vivo comparison of the kinetics of protein and lipid deposition on group II and group IV frequent-replacement contact lenses., Optom. Vis. Sci. 77 (2000) 503–510.

[278] B.J. Tighe, L. Jones, K. Evans, V. Franklin, Patient-dependent and material-dependent factors in contact lens deposition processes., Adv. Exp. Med. Biol. 438 (1998) 745–751.

[279] A. Panaser, B.J. Tighe, Evidence of Lipid Degradation During Overnight Contact Lens Wear: Gas Chromatography Mass Spectrometry as the Diagnostic Tool, Investig. Opthalmology Vis. Sci. 55 (2014) 1797–1804.

[280] A.R. Bontempo, J. Rapp, Protein-lipid interaction on the surface of a rigid gas-permeable contact lens in vitro., Curr. Eye Res. 16 (1997) 1258–62. http://www.ncbi.nlm.nih.gov/pubmed/9426961 (accessed February 8, 2017).

[281] K.W. Gellatly, N.A. Brennan, N. Efron, Visual decrement with deposit accumulation of HEMA contact lenses., Am. J. Optom. Physiol. Opt. 65 (1988) 937–941.

[282] O.D. Solomon, M.I. Freeman, E.L. Boshnick, W.M. Cannon, B.W. Dubow, R.T. Kame, J.C. Lanier, R.W. Lopanik, T.G. Quinn, L.E. Rigel, D.D. Sherrill, M.J. Stiegmeier, R.S. Teiche, L.G. Zigler, G.W. Mertz, R.J. Nason, A 3-year prospective study of the clinical performance of daily disposable contact lenses compared with frequent replacement and conventional daily wear contact lenses., CLAO J. 22 (1996) 250–257.

[283] M. Glasson, F. Stapleton, M. Willcox, Lipid, lipase and lipocalin differences between tolerant and intolerant contact lens wearers., Curr. Eye Res. 25 (2002) 227–235.

[284] Z. Zhao, T. Naduvilath, J.L. Flanagan, N.A. Carnt, X. Wei, J. Diec, V. Evans, M.D.P.

Willcox, Contact Lens Deposits, Adverse Responses, and Clinical Ocular Surface Parameters, Optom. Vis. Sci. 87 (2010) 669–674.

[285] N. Yokoi, H. Yamada, Y. Mizukusa, A.J. Bron, J.M. Tiffany, T. Kato, S. Kinoshita, Rheology of tear film lipid layer spread in normal and aqueous tear-deficient dry eyes., Invest. Ophthalmol. Vis. Sci. 49 (2008) 5319–24.

[286] N. Babaei Omali, H. Zhu, Z. Zhao, J. Ozkan, B. Xu, R. Borazjani, M.D.P. Willcox, Effect of Cholesterol Deposition on Bacterial Adhesion to Contact Lenses, Optom. Vis. Sci. 88 (2011) 950–958.

[287] S. Yasueda, K. Yamakawa, Y. Nakanishi, M. Kinoshita, K. Kakehi, Decreased mucin concentrations in tear fluids of contact lens wearers, J. Pharm. Biomed. Anal. 39 (2005) 187–195.

[288] M. Dogru, S.K. Ward, T. Wakamatsu, O. Ibrahim, C. Schnider, T. Kojima, Y. Matsumoto, J. Ogawa, J. Shimazaki, K. Tsubota, The effects of 2 week senofilcon—A silicone hydrogel contact lens daily wear on tear functions and ocular surface health status, Contact Lens Anterior Eye. 34 (2011) 77–82.

[289] P.J. Pisella, F. Malet, S. Lejeune, F. Brignole, C. Debbasch, J. Bara, P. Rat, J. Colin, C. Baudouin, Ocular surface changes induced by contact lens wear., Cornea. 20 (2001) 820–5.

[290] Y. Hori, P. Argüeso, S. Spurr-Michaud, I.K. Gipson, Mucins and contact lens wear., Cornea. 25 (2006) 176–181.

[291] R.M. Corrales, D. Galarreta, J.M. Herreras, V. Saez, I. Arranz, M.J. González, A. Mayo, M. Calonge, F.J. Chaves, Conjunctival Mucin mRNA Expression in Contact Lens Wear, Optom. Vis. Sci. 86 (2009) 1051–1058.

[292] M. Berry, A. Harris, A.P. Corfield, Patterns of mucin adherence to contact lenses., Invest. Ophthalmol. Vis. Sci. 44 (2003) 567–572.

[293] F.C. Wedler, Analysis of biomaterials deposited on soft contact lenses, J. Biomed. Mater. Res. 11 (1977) 525–535.

[294] A.E. Klein, Detection of mucin deposits on hydrogel contact lenses: evaluation of staining procedures and clinical significance., Optom. Vis. Sci. 66 (1989) 56–60.

[295] J.E. Proust, A. Baszkin, M.M. Boissonnade, Adsorption of bovine submaxillary mucin on surface-oxidized polyethylene films, J. Colloid Interface Sci. 94 (1983) 421–429.

[296] T.J. Millar, S.T. Tragoulias, P.J. Anderton, M.S. Ball, F. Miano, G.R. Dennis, P. Mudgil, The surface activity of purified ocular mucin at the air-liquid interface and interactions with meibomian lipids., Cornea. 25 (2006) 91–100.

[297] O. Sterner, C. Karageorgaki, M. Zürcher, S. Zürcher, C.W. Scales, Z. Fadli, N.D. Spencer, S.G.P. Tosatti, Reducing Friction in the Eye: A Comparative Study of Lubrication by Surface-Anchored Synthetic and Natural Ocular Mucin Analogues, ACS Appl. Mater. Interfaces. 9 (2017) 20150–20160.

[298] M. Berry, C. Purslow, P.J. Murphy, H. Pult, Contact Lens Materials, Mucin Fragmentation and Relation to Symptoms, Cornea. 31 (2012) 770–776.

[299] I.K. Gipson, Distribution of mucins at the ocular surface., Exp. Eye Res. 78 (2004) 379–88.

[300] N. Pritchard, L. Jones, K. Dumbleton, D. Fonn, Epithelial inclusions in association with mucin ball development in high-oxygen permeability hydrogel lenses., Optom. Vis. Sci. 77 (2000) 68–72.

[301] J. Tan, L. Keay, I. Jalbert, T.J. Naduvilath, D.F. Sweeney, B.A. Holden, Mucin balls with wear of conventional and silicone hydrogel contact lenses., Optom. Vis. Sci. 80 (2003) 291–297.

[302] C. Fleming, R. Austen, S. Davies, Pre-corneal deposits during soft contact lens wear, Optom. Vis. Sci. 71 (1994) 152–153.

[303] K. Dumbleton, L. Jones, R. Chalmers, D. Williams-Lyn, D. Fonn, Clinical characterization of spherical post-lens debris associated with lotrafilcon high-Dk silicone lenses., CLAO J. 26 (2000) 186–192.

[304] T.J. Millar, E.B. Papas, J. Ozkan, I. Jalbert, M. Ball, Clinical appearance and microscopic analysis of mucin balls associated with contact lens wear., Cornea. 22 (2003) 740–745.

[305] L. Szczotka-Flynn, B.A. Benetz, J. Lass, M. Albright, B. Gillespie, J. Kuo, D. Fonn, A. Sethi, A. Rimm, The Association Between Mucin Balls and Corneal Infiltrative Events During Extended Contact Lens Wear, Cornea. 30 (2011) 535–542.

[306] J. Tanner, N. Efron, Reusable Soft Lenses, in: Contact Lens Pract., 3rd ed., Elsevier Heatlh Sciences , 2018: p. 175–186.e1.

[307] K. Dumbleton, B. Caffery, M. Dogru, S. Hickson-Curran, J. Kern, T. Kojima, P.B. Morgan, C. Purslow, D.M. Robertson, J.D. Nelson, The TFOS International Workshop on Contact Lens Discomfort: Report of the Subcommittee on Epidemiology, Investig. Opthalmology Vis. Sci. 54 (2013) TFOS20-36.

[308] K. Richdale, L.T. Sinnott, E. Skadahl, J.J. Nichols, Frequency of and Factors Associated With Contact Lens Dissatisfaction and Discontinuation, Cornea. 26 (2007) 168–174.

[309] K.K. Nichols, R.L. Redfern, J.T. Jacob, J.D. Nelson, D. Fonn, S.L. Forstot, J.-F. Huang, B.A. Holden, J.J. Nichols, members of the TFOS International Workshop on Contact Lens Discomfort, The TFOS International Workshop on Contact Lens Discomfort: Report of the Definition and Classification Subcommittee, Investig. Opthalmology Vis. Sci. 54 (2013) TFOS14-19.

[310] J.T. Jacob, Biocompatibility in the development of silicone-hydrogel lenses., Eye Contact Lens. 39 (2013) 13–19.

[311] R.E. Johnson, R.H. Dettre, Wetting of Low-Energy Surfaces, in: J.C. Berg (Ed.), Wettability (Surfactant Sci. Ser., CRC Press, New York, 1993: pp. 1–73.

[312] C. Maldonado-codina, P.B. Morgan, In vitro water wettability of silicone hydrogel contact lenses determined using the sessile drop and captive bubble techniques, J. Biomed. Mater. Res. Part A. 83A (2007) 496–502.

[313] B. Tighe, Silicone hydrogels: Structure, properties and behaviour, in: D. Sweeney (Ed.), Silicone Hydrogels Contin. Wear Contact Lenses, Butterworth-Heinemann, Oxford, 2004: pp. 1–27.

[314] L.C. Thai, A. Tomlinson, W.H. Ridder, Contact lens drying and visual performance: the vision cycle with contact lenses., Optom. Vis. Sci. 79 (2002) 381–388.

[315] R. Tutt, A. Bradley, C. Begley, L.N. Thibos, Optical and visual impact of tear break-up in human eyes., Invest. Ophthalmol. Vis. Sci. 41 (2000) 4117–23.

[316] C. Maldonado-Codina, N. Efron, Dynamic wettability of pHEMA-based hydrogel contact lenses., Ophthalmic Physiol. Opt. 26 (2006) 408–18.

[317] M. Guillon, K.A. Dumbleton, P. Theodoratos, S. Wong, K. Patel, G. Banks, T. Patel, Association Between Contact Lens Discomfort and Pre-lens Tear Film Kinetics, Optom. Vis. Sci. 93 (2016) 881–891.

[318] H. Zeng, ed., Polymer Adhesion, Friction, and Lubrication, John Wiley & Sons, Inc., Hoboken, NJ, USA, 2013.

[319] T. Young, An Essay on the Cohesion of Fluids, Philos. Trans. R. Soc. London. 95 (1805) 65–87.

[320] D. Campbell, S.M. Carnell, R.J. Eden, Applicability of Contact Angle Techniques Used in the Analysis of Contact Lenses, Part 1, Eye Contact Lens Sci. Clin. Pract. 39 (2013) 254–262.

[321] A. Marmur, Soft contact: measurement and interpretation of contact angles, Soft Matter. 2 (2006) 12–17.

[322] A.W. Adamson, Physical Chemistry of Surfaces, 5th ed., New York, 1990.

[323] R.E. Johnson, R.H. Dettre, D.A. Brandreth, Dynamic contact angles and contact angle hysteresis, J. Colloid Interface Sci. 62 (1977) 205–212.

[324] L.S. Penn, B. Miller, A study of the primary cause of contact angle hysteresis on some polymeric solids, J. Colloid Interface Sci. 78 (1980) 238–241.

[325] F.J. Holly, M.F. Refojo, Wettability of hydrogels I. Poly(2-hydroxyethyl methacrylate), J. Biomed. Mater. Res. 9 (1975) 315–326.

[326] M. Morra, E. Occhiello, F. Garbassi, Knowledge about polymer surfaces from contact angle measurements, Adv. Colloid Interface Sci. 32 (1990) 79–116.

[327] K.L. Menzies, L. Jones, The impact of contact angle on the biocompatibility of biomaterials., Optom. Vis. Sci. 87 (2010) 387–99.

[328] S. Tonge, L. Jones, S. Goodall, B. Tighe, The ex vivo wettability of soft contact lenses., Curr. Eye Res. 23 (2001) 51–59.

[329] H. Lorentz, R. Rogers, L. Jones, The impact of lipid on contact angle wettability., Optom. Vis. Sci. 84 (2007) 946–53.

[330] C.A. Morris, B.A. Holden, E. Papas, H.J. Griesser, S. Bolis, P. Anderton, F. Carney, The ocular surface, the tear film, and the wettability of contact lenses., Adv. Exp. Med. Biol. 438 (1998) 717–22.

[331] W. Norde, J. Lyklema, Why proteins prefer interfaces., J. Biomater. Sci. Polym. Ed. 2 (1991) 183–202.

[332] T.A. Horbett, J.L. Brash, Proteins at Interfaces: Current Issues and Future Prospects, in:

Proteins at Interfaces, ACS Symposium Series, 1987: pp. 1–33.

[333] W. Norde, C.A. Haynes, Thermodynamics of Protein Adsorption, in: J.L. Brash, P.W. Wojciechowski (Eds.), Interfacial Phenom. Bioprod., Marcel Dekker. Inc, New York, 1996: pp. 123–144.

[334] E.J. Castillo, J.L. Koenig, J.M. Anderson, J. Lo, Protein adsorption on hydrogels: II. Reversible and irreversible interactions between lysozyme and soft contact lens surfaces, Biomaterials. 6 (1985) 338–345.

[335] W. Norde, Energy and Entropy of Protein Adsorption, J. Dispers. Sci. Technol. 13 (1992) 363–377.

[336] W. Norde, Adsorption of proteins from solution at the solid-liquid interface, Adv. Colloid Interface Sci. 25 (1986) 267–340.

[337] M.S. Lord, M.H. Stenzel, A. Simmons, B.K. Milthorpe, The effect of charged groups on protein interactions with poly(HEMA) hydrogels, Biomaterials. 27 (2006) 567–575.

[338] L. Vroman, The Importance of Surfaces in Contact Phase Reactions, Semin. Thromb. Hemost. 13 (1987) 79–85.

[339] Q. Garrett, B.K. Milthorpe, Human serum albumin adsorption on hydrogel contact lenses in vitro., Invest. Ophthalmol. Vis. Sci. 37 (1996) 2594–602.

[340] E.J. Castillo, J.L. Koenig, J.M. Anderson, Characterization of protein adsorption on soft contact lenses. IV. Comparison of in vivo spoilage with the in vitro adsorption of tear proteins., Biomaterials. 7 (1986) 89–96.

[341] Z. Zhao, X. Wei, Y. Aliwarga, N.A. Carnt, Q. Garrett, M.D.P. Willcox, Proteomic analysis of protein deposits on worn daily wear silicone hydrogel contact lenses., Mol. Vis. 14 (2008) 2016–2024.

[342] P. Kingshott, H.A. St John, R.C. Chatelier, H.J. Griesser, Matrix-assisted laser desorption ionization mass spectrometry detection of proteins adsorbed in vivo onto contact lenses., J. Biomed. Mater. Res. 49 (2000) 36–42.

[343] C.E. Soltys-Robitaille, D.M. Ammon, P.L. Valint, G.L. Grobe III, The relationship between contact lens surface charge and in-vitro protein deposition levels, Biomaterials. 22 (2001) 3257–3260. doi:10.1016/S0142-9612(01)00163-6.

[344] D.R. Schmidt, H. Waldeck, W.J. Kao, Protein Adsorption to Biomaterials, in: D. Puleo, R. Bizios (Eds.), Biol. Interact. Mater. Surfaces, Springer, New York, NY, 2009: pp. 1–18.

[345] D.C. Carter, J.X. Ho, Structure of serum albumin., Adv. Protein Chem. 45 (1994) 153–203.

[346] R. Sariri, R. Sabbaghzadeh, Competitive adsorption of proteins on hydrogel contact lenses., CLAO J. 27 (2001) 159–62.

[347] F.P. Carney, C.A. Morris, B. Milthorpe, J.L. Flanagan, M.D.P. Willcox, In Vitro Adsorption of Tear Proteins to Hydroxyethyl Methacrylate-Based Contact Lens Materials, Eye Contact Lens Sci. Clin. Pract. 35 (2009) 320–328.

[348] E. Okada, T. Matsuda, T. Yokoyama, K. Okuda, Lysozyme Penetration in Group IV Soft Contact Lenses, Eye Contact Lens Sci. Clin. Pract. 32 (2006) 174–177.

[349] D. Luensmann, M.-A. Glasier, F. Zhang, V. Bantseev, T. Simpson, L. Jones, Confocal Microscopy and Albumin Penetration into Contact Lenses, Optom. Vis. Sci. 84 (2007) 839–847.

[350] D. Luensmann, L. Jones, Albumin adsorption to contact lens materials: A review, Contact Lens Anterior Eye. 31 (2008) 179–187.

[351] D. Mirejovsky, A.S. Patel, D.D. Rodriguez, Effect of proteins on water and transport properties of various hydrogel contact lens materials, Curr. Eye Res. 10 (1991) 187–196.

[352] S.E. Lee, S.R. Kim, M. Park, Influence of Tear Protein Deposition on the Oxygen Permeability of Soft Contact Lenses, J. Ophthalmol. 2017 (2017) 1–6.

[353] R.W. Bowers, B.J. Tighe, Studies of the ocular compatibility of hydrogels. A review of the clinical manifestations of spoilation., Biomaterials. 8 (1987) 83–88.

[354] D. Luensmann, M. Heynen, L. Liu, H. Sheardown, L. Jones, The efficiency of contact lens care regimens on protein removal from hydrogel and silicone hydrogel lenses., Mol. Vis. 16 (2010) 79–92.

[355] L. Jones, V. Franklin, K. Evans, R. Sariri, B. Tighe, Spoilation and clinical performance of monthly vs. three monthly Group II disposable contact lenses., Optom. Vis. Sci. 73 (1996) 16–21.

[356] J.D. Andrade, Interfacial phenomena and biomaterials., Med. Instrum. 7 (1973) 110–120.

[357] Y. Ikada, M. Suzuki, Y. Tamada, Polymer Surfaces Possessing Minimal Interaction with Blood Components, in: Polym. as Biomater., Shalaby SW, Springer US, New York, NY, 1984: pp. 135–147.

[358] T. Imoto, L. Johnson, A. North, D. Phillips, J. Rupley, Vertebrate Lysozymes, in: P. Boyer (Ed.), Enzyme, Academic Press, New York, 1972: pp. 665–868.

[359] P.T. Janssen, O.P. van Bijsterveld, Origin and biosynthesis of human tear fluid proteins., Invest. Ophthalmol. Vis. Sci. 24 (1983) 623–630.

[360] O.K. Gasymov, A.R. Abduragimov, T.N. Yusifov, B.J. Glasgow, Interaction of Tear Lipocalin with Lysozyme and Lactoferrin, Biochem. Biophys. Res. Commun. 265 (1999) 322–325.

[361] E.C. Leitch, M.D.P. Willcox, Synergic antistaphylococcal properties of lactoferrin and lysozyme, J. Med. Microbiol. 47 (1998) 837–842.

[362] A. Ng, M. Heynen, D. Luensmann, L.N. Subbaraman, L. Jones, Impact of tear film components on the conformational state of lysozyme deposited on contact lenses, J. Biomed. Mater. Res. Part B Appl. Biomater. 101 (2013) 1172–1181.

[363] A. Ng, M. Heynen, D. Luensmann, L. Jones, Impact of Tear Film Components on Lysozyme Deposition to Contact Lenses, Optom. Vis. Sci. 89 (2012) 392–400.

[364] L.C. Winterton, M.M. Gabriel, P.D. Bergenske, Ex vivo protein deposition on bi-weekly silicone hydrogel contact lenses., Optom. Vis. Sci. 87 (2010) 145; author reply 146.

[365] A.R. Bontempo, J. Rapp, Protein and lipid deposition onto hydrophilic contact lenses in vivo., CLAO J. 27 (2001) 75–80.

[366] M.L. Ferrer, R. Duchowicz, B. Carrasco, J.G. de la Torre, A.U. Acuña, The Conformation of Serum Albumin in Solution: A Combined Phosphorescence Depolarization-Hydrodynamic Modeling Study, Biophys. J. 80 (2001) 2422–2430.

[367] F.P. Carney, C.A. Morris, M.D. Willcox, Effect of hydrogel lens wear on the major tear proteins during extended wear., Aust. N. Z. J. Ophthalmol. 25 Suppl 1 (1997) S36-38.

[368] Q. Garrett, B. Laycock, R.W. Garrett, Hydrogel lens monomer constituents modulate protein sorption., Invest. Ophthalmol. Vis. Sci. 41 (2000) 1687–95.

[369] E.J. Castillo, J.L. Koenig, J.M. Andersen, J. Lo, Characterization of protein adsorption on soft contact lenses: I. Conformational changes of adsorbed human serum albumin, Biomaterials. 5 (1984) 319–325.

[370] Q. Garrett, H.J. Griesser, B.K. Milthorpe, R.W. Garrett, Irreversible adsorption of human serum albumin to hydrogel contact lenses: a study using electron spin resonance spectroscopy, Biomaterials. 20 (1999) 1345–1356.

[371] M.G. Baines, F. Cai, H.A. Backman, Adsorption and removal of protein bound to hydrogel contact lenses., Optom. Vis. Sci. 67 (1990) 807–810.

[372] L.N. Subbaraman, R. Borazjani, H. Zhu, Z. Zhao, L. Jones, M.D.P. Willcox, Influence of protein deposition on bacterial adhesion to contact lenses., Optom. Vis. Sci. 88 (2011) 959–66.

[373] R.L. Taylor, M.D.P. Willcox, T.J. Williams, J. Verran, Modulation of Bacterial Adhesion to Hydrogel Contact Lenses by Albumin, Optom. Vis. Sci. 75 (1998) 23–29.

[374] M.E. Tan, G. Demirci, D. Pearce, I. Jalbert, P. Sankaridurg, M.D.P. Willcox, Contact lens-induced papillary conjunctivitis is associated with increased albumin deposits on extended wear hydrogel lenses., Adv. Exp. Med. Biol. 506 (2002) 951–955.

[375] J. Steinhardt, J. Krijn, J.G. Leidy, Differences between bovine and human serum albumins. Binding isotherms, optical rotatory dispersion, viscosity, hydrogen ion titration, and fluorescence effects, Biochemistry. 10 (1971) 4005–4015.

[376] B. Hall, J.A. Forrest, L. Jones, A Review of Techniques to Measure Protein Sorption to Soft Contact Lenses, Eye Contact Lens Sci. Clin. Pract. 43 (2017) 276–286.

[377] A. Guan, Z. Li, K.S. Phillips, The Effect of Fluorescent Labels on Protein Sorption in Polymer Hydrogels, J. Fluoresc. 24 (2014) 1639–1650.

[378] B. Hall, M. Heynen, L.W. Jones, J.A. Forrest, Analysis of Using I 125 Radiolabeling for Quantifying Protein on Contact Lenses, Curr. Eye Res. 41 (2016) 456–465.

[379] B. Hall, L.W. Jones, J.A. Forrest, Competitive Effects from an Artificial Tear Solution to Protein Adsorption, Optom. Vis. Sci. 92 (2015) 781–789.

[380] M. York, J. Ong, J.C. Robbins, Variation in blink rate associated with contact lens wear and task difficulty., Am. J. Optom. Arch. Am. Acad. Optom. 48 (1971) 461–467.

[381] M.E. Jansen, C.G. Begley, N.H. Himebaugh, N.L. Port, Effect of Contact Lens Wear and a Near Task on Tear Film Break-Up, Optom. Vis. Sci. 87 (2010) 350–357.

[382] L.G. Carney, R.M. Hill, Variations in blinking bahaviour during soft lens wear, Int. Contact Lens Clin. 11 (1984) 250–253.

[383] N. Brennan, C. Coles-Brennan, Contact lens-based correlates of soft lens wearing comfort, Optom. Vis. Sci. 86 (2009) E-abstract 90957.

[384] N.A. Brennan, C. Coles, Supportive data linking coefficient of friction and comfort, Contact Lens Anterior Eye. 36 (2013) e10.

[385] M. Roba, E.G. Duncan, G.A. Hill, N.D. Spencer, S.G.P. Tosatti, Friction Measurements on Contact Lenses in Their Operating Environment, Tribol. Lett. 44 (2011) 387–397.

[386] M. Samsom, A. Chan, Y. Iwabuchi, L. Subbaraman, L. Jones, T.A. Schmidt, In vitro friction testing of contact lenses and human ocular tissues: Effect of proteoglycan 4 (PRG4), Tribol. Int. 89 (2015) 27–33.

[387] M. Vidal-Rohr, J.S. Wolffsohn, L.N. Davies, A. Cerviño, Effect of contact lens surface properties on comfort, tear stability and ocular physiology, Contact Lens Anterior Eye. 41 (2018) 117–121.

[388] F.P. Bowden, D. Tabor, The friction and lubrication of solids, Oxford Classic Series, 2001.

[389] B.N.J. Persson, I.M. Sivebaek, V.N. Samoilov, K. Zhao, A.I. Volokitin, Z. Zhang, On the origin of Amonton's friction law, J. Phys. Condens. Matter. 20 (2008) 395006.

[390] A. Faghihnejad, H. Zeng, Fundamentals of Surface Adhesion, Friction, and Lubrication, in: Polym. Adhes. Frict. Lubr., John Wiley & Sons, Inc., Hoboken, NJ, USA, 2013: pp. 1–57.

[391] J.N. Israelachvili, Intermolecular and surface forces: Revised Third Edition, Academic Press, 2011.

[392] G.W. Greene, D.W. Lee, J. Yu, S. Das, X. Banquy, J.N. Israelachvili, Lubrication and Wear Protection of Natural (Bio)Systems, in: Polym. Adhes. Frict. Lubr., John Wiley & Sons, Inc., Hoboken, NJ, USA, 2013: pp. 83–133.

[393] M. Minn, S.K. Sinha, The frictional behavior of UHMWPE films with different surface energies at low normal loads, Wear. 268 (2010) 1030–1036.

[394] L.-H. Lee, Effect of Surface Energetics on Polymer Friction and Wear, in: Adv. Polym. Frict. Wear, Springer US, Boston, MA, 1974: pp. 31–68.

[395] T.W. Secomb, R. Hsu, A.R. Pries, Motion of red blood cells in a capillary with an endothelial surface layer: effect of flow velocity, Am. J. Physiol. Circ. Physiol. 281 (2001) H629–H636.

[396] R. Stribeck, Kugellager für beliebige Belastungen (Ball Bearings for any Stress), Zeitschrift Des Vereins Dtsch. Ingenieure 45. (1901).

[397] J.M. Coles, D.P. Chang, S. Zauscher, Molecular mechanisms of aqueous boundary lubrication by mucinous glycoproteins, Curr. Opin. Colloid Interface Sci. 15 (2010) 406–416.

[398] J. Liu, J.P. Gong, Hydrogel Friction and Lubrication, in: Aqueous Lubr., Co-Published with Indian Institute of Science (IISc), Bangalore, India, 2014: pp. 145–181.

[399] W.B. Hardy, I. Doubleday, Boundary Lubrication. The Paraffin Series, Proc. R. Soc. A Math. Phys. Eng. Sci. 100 (1922) 550–574.

[400] W.B. Hardy, I. Doubleday, Boundary Lubrication. The Temperature Coefficient, Proc. R.

Soc. A Math. Phys. Eng. Sci. 101 (1922) 487–492.

[401] G.W. Greene, X. Banquy, D.W. Lee, D.D. Lowrey, J. Yu, J.N. Israelachvili, Adaptive mechanically controlled lubrication mechanism found in articular joints., Proc. Natl. Acad. Sci. U. S. A. 108 (2011) 5255–5259.

[402] G.A. Ateshian, The role of interstitial fluid pressurization in articular cartilage lubrication., J. Biomech. 42 (2009) 1163–1176.

[403] J. Israelachvili, H. Wennerström, Role of hydration and water structure in biological and colloidal interactions, Nature. 379 (1996) 219–225.

[404] J.N. Israelachvili, Intermolecular and surface forces, Academic Press, 2011.

[405] D. Leckband, J. Israelachvili, Intermolecular forces in biology, Q. Rev. Biophys. 34 (2001).

[406] D. Dowson, A tribological day, Proc. Inst. Mech. Eng. Part J J. Eng. Tribol. 223 (2009) 261–273.

[407] Z.M. Jin, D. Dowson, Elastohydrodynamic Lubrication in Biological Systems, Proc. Inst. Mech. Eng. Part J J. Eng. Tribol. 219 (2005) 367–380.

[408] F.P. Bowden, D. Tabor, Friction, lubrication and wear: a survey of work during the last decade, Br. J. Appl. Phys. 17 (1966) 1521–1544.

[409] H. Pult, S.G.P. Tosatti, N.D. Spencer, J.-M. Asfour, M. Ebenhoch, P.J. Murphy, Spontaneous Blinking from a Tribological Viewpoint, Ocul. Surf. 13 (2015) 236–249.

[410] J.A. Nairn, T.J. Jiang, Measurement Of The Friction And Lubricity Properties Of Contact Lenses, Proc. ANTEC '95. May 7-11 (1995) 1–5.

[411] M. Guillon, Are Silicone Hydrogel Contact Lenses More Comfortable Than Hydrogel Contact Lenses?, Eye Contact Lens Sci. Clin. Pract. 39 (2013) 85–91.

[412] M.J. Giraldez, C. Serra, M. Lira, M.E.C.D. Real Oliveira, E. Yebra-Pimentel, Soft Contact Lens Surface Profile by Atomic Force Microscopy, Optom. Vis. Sci. 87 (2010) E475-481.

[413] S.H. Kim, C. Marmo, G.A. Somorjai, Friction studies of hydrogel contact lenses using AFM: non-crosslinked polymers of low friction at the surface, Biomaterials. 22 (2001) 3285–3294.

[414] Y. Huo, A. Rudy, A. Wang, H. Ketelson, S.S. Perry, Impact of Ethylene Oxide Butylene Oxide Copolymers on the Composition and Friction of Silicone Hydrogel Surfaces, Tribol. Lett. 45 (2012) 505–513.

[415] R.C. Tucker, B. Quinter, D. Patel, J. Pruitt, J. Nelson, Qualitative and Quantitative Lubricity of Experimental Contact Lenses, 2012.

[416] A.C. Rennie, P.L. Dickrell, W.G. Sawyer, Friction coefficient of soft contact lenses: measurements and modeling, Tribol. Lett. 18 (2005) 499–504.

[417] O. Sterner, R. Aeschlimann, S. Zürcher, C. Scales, D. Riederer, N.D. Spencer, S.G.P. Tosatti, Tribological Classification of Contact Lenses: From Coefficient of Friction to Sliding Work, Tribol. Lett. 63 (2016) 63–69.

[418] O. Sterner, R. Aeschlimann, S. Zürcher, K. Osborn Lorenz, J. Kakkassery, N.D. Spencer, S.G.P. Tosatti, Friction Measurements on Contact Lenses in a Physiologically Relevant

Environment: Effect of Testing Conditions on Friction, Investig. Opthalmology Vis. Sci. 57 (2016) 5383–5392.

[419] B. Bhushan, Modern Tribology Handbook, CRC Press , New York, 2001.

[420] H. Thissen, T. Gengenbach, R. du Toit, D.F. Sweeney, P. Kingshott, H.J. Griesser, L. Meagher, Clinical observations of biofouling on PEO coated silicone hydrogel contact lenses, Biomaterials. 31 (2010) 5510–5519.

[421] J.J. Wang, F. Liu, Imparting antifouling properties of silicone hydrogels by grafting poly(ethylene glycol) methyl ether acrylate initiated by UV light, J. Appl. Polym. Sci. 125 (2012) 548–554.

[422] F. Sun, X. Li, P. Cao, J. Xu, Enhancing hydrophilicity and protein resistance of silicone hydrogels by plasma induced grafting with hydrophilic polymers, Chinese J. Polym. Sci. 28 (2010) 547–554.

[423] R.C. Peterson, J.S. Wolffsohn, J. Nick, L. Winterton, J. Lally, Clinical performance of daily disposable soft contact lenses using sustained release technology, Contact Lens Anterior Eye. 29 (2006) 127–134.

[424] N.J. Schwarz S., Effectiveness of lubricating daily disposable lenses with different additives, Optician. 231 (2006) 22–26.

[425] F. Yañez, A. Concheiro, C. Alvarez-Lorenzo, Macromolecule release and smoothness of semi-interpenetrating PVP–pHEMA networks for comfortable soft contact lenses, Eur. J. Pharm. Biopharm. 69 (2008) 1094–1103.

[426] L.N. Subbaraman, S. Bayer, M.-A. Glasier, H. Lorentz, M. Senchyna, L. Jones, Rewetting drops containing surface active agents improve the clinical performance of silicone hydrogel contact lenses., Optom. Vis. Sci. 83 (2006) 143–51.

[427] C.J. White, C.R. Thomas, M.E. Byrne, Bringing comfort to the masses: A novel evaluation of comfort agent solution properties, Contact Lens Anterior Eye. 37 (2014) 81–91.

[428] J.J. Nichols, C.W. Lievens, M.R. Bloomenstein, H. Liu, P. Simmons, J. Vehige, Dual-Polymer Drops, Contact Lens Comfort, and Lid Wiper Epitheliopathy., Optom. Vis. Sci. 93 (2016) 979–986.

[429] K.A. Potter, B. Gui, J.R. Capadona, Biomimicry at the Cell–Material Interface, in: Y. Bar-Cohen (Ed.), Biomimetics Nature-Based Innov., CRC Press, 2012: pp. 95–129.

[430] N.B. Holland, Y. Qiu, M. Ruegsegger, R.E. Marchant, Biomimetic engineering of non-adhesive glycocalyx-like surfaces using oligosaccharide surfactant polymers, Nature. 392 (1998) 799–801.

[431] H.J.A. Egberts, J.F.J.G. Koninkx, J.E. van Dijk, J.M.V.M. Mouwen, Biological and pathobiological aspects of the glycocalyx of the small intestinal epithelium. A review, Vet. Q. 6 (1984) 186–199.

[432] Q. Yang, C. Kaul, M. Ulbricht, Anti-nonspecific Protein Adsorption Properties of Biomimetic Glycocalyx-like Glycopolymer Layers: Effects of Glycopolymer Chain Density and Protein Size, Langmuir. 26 (2010) 5746–5752.

[433] S. Reitsma, D.W. Slaaf, H. Vink, M.A.M.J. van Zandvoort, M.G.A. oude Egbrink, The

endothelial glycocalyx: composition, functions, and visualization, Pflugers Arch. 454 (2007) 345–359.

[434] H.O. Ham, S.H. Park, J.W. Kurutz, I.G. Szleifer, P.B. Messersmith, Antifouling Glycocalyx-Mimetic Peptoids, J. Am. Chem. Soc. 135 (2013) 13015–13022.

[435] C. Perrino, S. Lee, S.W. Choi, A. Maruyama, N.D. Spencer, A Biomimetic Alternative to Poly(ethylene glycol) as an Antifouling Coating: Resistance to Nonspecific Protein Adsorption of Poly(L -lysine)- *graft* -dextran, Langmuir. 24 (2008) 8850–8856.

[436] B. Winkeljann, K. Boettcher, B.N. Balzer, O. Lieleg, Mucin Coatings Prevent Tissue Damage at the Cornea-Contact Lens Interface, Adv. Mater. Interfaces. 4 (2017) 1700186.

[437] C. Perrino, Æ.S. Lee, Æ.N.D. Spencer, End-grafted Sugar Chains as Aqueous Lubricant Additives : Synthesis and Macrotribological Tests of Poly (L -lysine) - graft - Dextran (PLL- g -dex) Copolymers, Tribol. Lett. 33 (2009) 83–96.

[438] M. Milas, M. Rinaudo, I. Roure, S. Al-Assaf, G.O. Phillips, P.A. Williams, Comparative rheological behavior of hyaluronan from bacterial and animal sources with cross-linked hyaluronan (hylan) in aqueous solution, Biopolymers. 59 (2001) 191–204.

[439] K. Meyer, J.W. Palmer, The polysaccharide of the vitreous humor, J. Biol. Chem. 107 (1934) 629–634.

[440] F.E. Kendall, M. Heidelberger, M.H. Dawson, A serologically inactive polysaccharide elaborated by mucoid strains of group A hemolytic streptococcus, J. Biol. Chem. 118 (1937) 61–69.

[441] N. Volpi, J. Schiller, R. Stern, L. Soltés, Role, metabolism, chemical modifications and applications of hyaluronan., Curr. Med. Chem. 16 (2009) 1718–1745.

[442] C.L. Bourlais, L. Acar, H. Zia, P. a Sado, T. Needham, R. Leverge, Ophthalmic drug delivery systems--recent advances., Prog. Retin. Eye Res. 17 (1998) 33–58.

[443] G. Tripodo, A. Trapani, M.L. Torre, G. Giammona, G. Trapani, D. Mandracchia, Hyaluronic acid and its derivatives in drug delivery and imaging: Recent advances and challenges, Eur. J. Pharm. Biopharm. 97 (2015) 400–416.

[444] A.G. Ogston, J.E. Stanier, The physiological function of hyaluronic acid in synovial fluid; viscous, elastic and lubricant properties., J. Physiol. 119 (1953) 244–252.

[445] I. Hargittai, M. Hargittai, Molecular structure of hyaluronan: an introduction, Struct. Chem. 19 (2008) 697–717.

[446] J.R.E. Fraser, T.C. Laurent, U.B.G. Laurent, Hyaluronan: its nature, distribution, functions and turnover, J. Intern. Med. 242 (1997) 27–33.

[447] T.C. Laurent, Structure of hyaluronic acid., in: E. Balasz (Ed.), Chem. Mol. Biol. Intracell. Matrix, Academic Press, London, 1970: pp. 709–732.

[448] P. Gribbon, B.C. Heng, T.E. Hardingham, The analysis of intermolecular interactions in concentrated hyaluronan solutions suggest no evidence for chain-chain association., Biochem. J. 350 (2000) 329.

[449] D.A. Gibbs, E.W. Merrill, K.A. Smith, E.A. Balazs, Rheology of hyaluronic acid, Biopolymers. 6 (2004) 777–791.

[450] L. Lapcík L Jr and, L. Lapcík, S. De Smedt, J. Demeester, P. Chabrecek, Hyaluronan: Preparation, Structure, Properties, and Applications., Chem. Rev. 98 (1998) 2663–2684.

[451] M. Guter, M. Breunig, Hyaluronan as a promising excipient for ocular drug delivery, Eur. J. Pharm. Biopharm. 113 (2017) 34–49.

[452] Y.-H. Liao, S. a Jones, B. Forbes, G.P. Martin, M.B. Brown, Hyaluronan: pharmaceutical characterization and drug delivery., Drug Deliv. 12 (2005) 327–42.

[453] T.C. Laurent, U.B.G. Laurent, J.R.E. Fraser, The structure and function of hyaluronan: An overview, Immunol. Cell Biol. 74 (1996) A1–A7.

[454] J.S. Frenkel, The role of hyaluronan in wound healing, Int. Wound J. 11 (2014) 159–163.

[455] F. Arnold, D.C. West, Angiogenesis in wound healing, Pharmacol. Ther. 52 (1991) 407–422.

[456] M.N. Collins, C. Birkinshaw, Hyaluronic acid based scaffolds for tissue engineering—A review, Carbohydr. Polym. 92 (2013) 1262–1279.

[457] E.A. Balazs, Viscosupplementation for treatment of osteoarthritis: from initial discovery to current status and results., Surg. Technol. Int. 12 (2004) 2782–89.

[458] J.B. Catterall, L.M.H. Jones, G.A. Turner, Membrane protein glycosylation and CD44 content in the adhesion of human ovarian cancer cells to hyaluronan, Clin. Exp. Metastasis. 17 (1999) 583–591.

[459] G. Kogan, L. Soltés, R. Stern, P. Gemeiner, Hyaluronic acid: a natural biopolymer with a broad range of biomedical and industrial applications., Biotechnol. Lett. 29 (2007) 17–25.

[460] E.L. Graue, F.M. Polack, E.A. Balazs, The protective effect of Na-hyaluronate to corneal endothelium., Exp. Eye Res. 31 (1980) 119–27.

[461] F.M. Polack, Healon (R)(Na Hyaluronate): A Review of the Literature, Cornea. 5 (1986) 81–94.

[462] M.F. Saettone, D. Monti, M.T. Torraca, P. Chetoni, Mucoadhesive ophthalmic vehicles: evaluation of polymeric low-viscosity formulations, J. Ocul. Pharmacol. Ther. 10 (1994) 83–92.

[463] N.M. Salwowska, K.A. Bebenek, D.A. Żądło, D.L. Wcisło-Dziadecka, Physiochemical properties and application of hyaluronic acid: a systematic review, J. Cosmet. Dermatol. 15 (2016) 520–526.

[464] G.A. Georgiev, N. Yokoi, S. Ivanova, T. Dimitrov, K. Andreev, R. Krastev, Z. Lalchev, Surface chemistry study of the interactions of hyaluronic acid and benzalkonium chloride with meibomian and corneal cell lipids, Soft Matter. 9 (2013) 10841–10856.

[465] T. Hamano, K. Horimoto, M. Lee, S. Komemushi, Sodium hyaluronate eyedrops enhance tear film stability., Jpn. J. Ophthalmol. 40 (1996) 62.

[466] B.C.H. Ang, J.J. Sng, P.X.H. Wang, H.M. Htoon, L.H.T. Tong, Sodium Hyaluronate in the Treatment of Dry Eye Syndrome: A Systematic Review and Meta-Analysis, Sci. Rep. 7 (2017) 9013.

[467] M.F. Saettone, B. Giannaccini, P. Chetoni, M.T. Torracca, D. Monti, Evaluation of high-

and low-molecular-weight fractions of sodium hyaluronate and an ionic complex as adjuvants for topical ophthalmic vehicles containing pilocarpine, Int. J. Pharm. 72 (1991) 131–139.

[468] C.A. Scheuer, K.M. Fridman, V.L. Barniak, S.E. Burke, S. Venkatesh, Retention of conditioning agent hyaluronan on hydrogel contact lenses, Contact Lens Anterior Eye. 33 (2010) S2–S6.

[469] M.J. Glasson, F. Stapleton, L. Keay, M.D. Willcox, The effect of short term contact lens wear on the tear film and ocular surface characteristics of tolerant and intolerant wearers., Contact Lens Anterior Eye J. Br. Contact Lens Assoc. 29 (2006) 41.

[470] S. Kaya, D. Schmidl, L. Schmetterer, K.J. Witkowska, A. Unterhuber, V. Aranha dos Santos, C. Baar, G. Garhöfer, R.M. Werkmeister, Effect of hyaluronic acid on tear film thickness as assessed with ultra-high resolution optical coherence tomography, Acta Ophthalmol. 93 (2015) 439–443.

[471] S. Garcia-Lázaro, D. Madrid-Costa, T. Ferrer-Blasco, R. Montés-Micó, A. Cerviño, OCT for Assessing Artificial Tears Effectiveness in Contact Lens Wearers, Optom. Vis. Sci. 89 (2012) E62-69.

[472] J.C. Stuart, J.G. Linn, Dilute sodium hyaluronate (Healon) in the treatment of ocular surface disorders., Ann. Ophthalmol. 17 (1985) 190–192.

[473] R.A. Fagehi, A. Tomlinson, V. Manahilov, Comparative study of soft contact lenswetting in vitro after storage in Biotrue MPS, Contact Lens Anterior Eye. 35 (2012) e21.

[474] C. Scheuer, M. Rah, W. Reindel, Increased concentration of hyaluronan in tears after soaking contact lenses in Biotrue multipurpose solution, Clin. Ophthalmol. 10 (2016) 1945–1952.

[475] W. Reindel, G. Cairns, M. Merchea, Assessment of patient and practitioner satisfaction with Biotrue™ multi-purpose solution for contact lenses, Contact Lens Anterior Eye. 33 (2010) S12-17.

[476] M. Van Beek, L. Jones, H. Sheardown, Hyaluronic acid containing hydrogels for the reduction of protein adsorption., Biomaterials. 29 (2008) 780–789.

[477] A. Weeks, D. Morrison, J.G. Alauzun, M. a Brook, L. Jones, H. Sheardown, Photocrosslinkable hyaluronic acid as an internal wetting agent in model conventional and silicone hydrogel contact lenses., J. Biomed. Mater. Res. A. 100 (2012) 1972–1982.

[478] A. Weeks, D. Luensmann, A. Boone, L. Jones, H. Sheardown, Hyaluronic acid as an internal wetting agent in model DMAA/TRIS contact lenses, J. Biomater. Appl. (2011).

[479] M. Ali, M.E. Byrne, Controlled release of high molecular weight hyaluronic Acid from molecularly imprinted hydrogel contact lenses., Pharm. Res. 26 (2009) 714–726.

[480] F.A. Maulvi, T.G. Soni, D.O. Shah, Extended release of hyaluronic acid from hydrogel contact lenses for dry eye syndrome., J. Biomater. Sci. Polym. Ed. 26 (2015) 1035–10350.

[481] A. Weeks, L.N. Subbaraman, L. Jones, H. Sheardown, Physical entrapment of hyaluronic acid during synthesis results in extended release from model hydrogel and silicone hydrogel contact lens materials., Eye Contact Lens. 39 (2013) 179–185.

[482] H.-J. Kim, G.-C. Ryu, K.-S. Jeong, J. Jun, Hydrogel lenses functionalized with polysaccharide for reduction of protein adsorption, Macromol. Res. 23 (2015) 74–78.

[483] A. Weeks, A. Boone, D. Luensmann, L. Jones, H. Sheardown, The effects of hyaluronic acid incorporated as a wetting agent on lysozyme denaturation in model contact lens materials., J. Biomater. Appl. 28 (2013) 323–333.

[484] M. Samsom, M. Korogiannaki, L.N. Subbaraman, H. Sheardown, T.A. Schmidt, Hyaluronan incorporation into model contact lens hydrogels as a built-in lubricant: Effect of hydrogel composition and proteoglycan 4 as a lubricant in solution, J. Biomed. Mater. Res. Part B Appl. Biomater. 00B (2017) 000–000. doi:10.1002/jbm.b.33989.

[485] X.H. Hu, H.P. Tan, D. Li, M.Y. Gu, Surface functionalisation of contact lenses by CS/HA multilayer film to improve its properties and deliver drugs, Mater. Technol. 29 (2014) 8–13.

[486] C.-H. Lin, H.-L. Cho, Y.-H. Yeh, M.-C. Yang, Improvement of the surface wettability of silicone hydrogel contact lenses via layer-by-layer self-assembly technique, Colloids Surfaces B Biointerfaces. 136 (2015) 735–743.

[487] A. Singh, P. Li, V. Beachley, P. McDonnell, J.H. Elisseeff, A hyaluronic acid-binding contact lens with enhanced water retention, Contact Lens Anterior Eye. 38 (2015) 79–84.

[488] C. Cassinelli, M. Morra, A. Pavesio, D. Renier, Evaluation of interfacial properties of hyaluronan coated poly(methylmethacrylate) intraocular lenses., J. Biomater. Sci. Polym. Ed. 11 (2000) 961–977.

[489] B. Guan, H. Wang, R. Xu, G. Zheng, J. Yang, Z. Liu, M. Cao, M. Wu, J. Song, N. Li, T. Li, Q. Cai, X. Yang, Y. Li, X. Zhang, Establishing Antibacterial Multilayer Films on the Surface of Direct Metal Laser Sintered Titanium Primed with Phase-Transited Lysozyme, Sci. Rep. 6 (2016) 36408.

[490] M. Morra, Engineering of Biomaterials Surfaces by Hyaluronan, Biomacromolecules. 6 (2005) 1205–1223.

[491] M. Morra, C. Cassineli, Non-fouling properties of polysaccharide-coated surfaces, J. Biomater. Sci. Polym. Ed. 10 (1999) 1107–1124.

[492] M. Ombelli, L. Costello, C. Postle, V. Anantharaman, Q.C. Meng, R.J. Composto, D.M. Eckmann, Competitive protein adsorption on polysaccharide and hyaluronate modified surfaces., Biofouling. 27 (2011) 505–518.

[493] M. Benz, N. Chen, J. Israelachvili, Lubrication and wear properties of grafted polyelectrolytes, hyaluronan and hylan, measured in the surface forces apparatus, J. Biomed. Mater. Res. 71 (2004) 6–15.

[494] J. Necas, L. Bartosikova, P. Brauner, J. Kolar, Hyaluronic acid (hyaluronan): a review, 2008 (2008) 397–411.

[495] T.A. Schmidt, N.S. Gastelum, Q.T. Nguyen, B.L. Schumacher, R.L. Sah, Boundary lubrication of articular cartilage: Role of synovial fluid constituents, Arthritis Rheum. 56 (2007) 882–891.

[496] D.P. Chang, N.I. Abu-Lail, J.M. Coles, F. Guilak, G.D. Jay, S. Zauscher, Friction Force

Microscopy of Lubricin and Hyaluronic Acid between Hydrophobic and Hydrophilic Surfaces., Soft Matter. 5 (2009) 3438–3445.

[497] R. Tadmor, N. Chen, J.N. Israelachvili, Thin film rheology and lubricity of hyaluronic acid solutions at a normal physiological concentration, J. Biomed. Mater. Res. 61 (2002) 514–523.

[498] J.-T. Wu, C.-H. Huang, W.-C. Liang, Y.-L. Wu, J. Yu, H.-Y. Chen, Reactive Polymer Coatings: A General Route to Thiol-ene and Thiol-yne Click Reactions, Macromol. Rapid Commun. 33 (2012) 922–927.

[499] A. Singh, M. Corvelli, S.A. Unterman, K.A. Wepasnick, P. McDonnell, J.H. Elisseeff, Enhanced lubrication on tissue and biomaterial surfaces through peptide-mediated binding of hyaluronic acid, Nat. Mater. 13 (2014) 988–995.

[500] D. Lee, Q. Lu, S.D. Sommerfeld, A. Chan, N.G. Menon, T.A. Schmidt, J.H. Elisseeff, A. Singh, Targeted delivery of hyaluronic acid to the ocular surface by a polymer-peptide conjugate system for dry eye disease, Acta Biomater. 55 (2017) 163–171.

[501] R. Andresen Eguiluz, R. Schur, D. Gourdon, Lubrication and Adhesion by Charged Biopolymers for Biomedical Applications, in: M. Elnashar (Ed.), Biopolymers, InTech, 2010: pp. 257–270.

[502] B. Zappone, M. Ruths, G.W. Greene, G.D. Jay, J.N. Israelachvili, Adsorption, lubrication, and wear of lubricin on model surfaces: polymer brush-like behavior of a glycoprotein., Biophys. J. 92 (2007) 1693–1708.

[503] B. Zappone, G.W. Greene, E. Oroudjev, G.D. Jay, J.N. Israelachvili, Molecular aspects of boundary lubrication by human lubricin: effect of disulfide bonds and enzymatic digestion., Langmuir. 24 (2008) 1495–1508.

[504] G.D. Jay, U. Tantravahi, D.E. Britt, H.J. Barrach, C.-J. Cha, Homology of lubricin and superficial zone protein (SZP): Products of megakaryocyte stimulating factor (MSF) gene expression by human synovial fibroblasts and articular chondrocytes localized to chromosome 1q25, J. Orthop. Res. 19 (2001) 677–687.

[505] D.A. Swann, R.B. Hendren, E.L. Radin, S.L. Sotman, E.A. Duda, The lubricating activity of synovial fluid glycoproteins., Arthritis Rheum. 24 (1981) 22–30.

[506] G.D.. Jay, Lubricin and surfacing of articular joints., Curr. Opin.Orthop. 15 (2004) 355–359.

[507] G.D. Jay, D.A. Harris, C.J. Cha, Boundary lubrication by lubricin is mediated by O-linked beta(1-3)Gal-GalNAc oligosaccharides., Glycoconj. J. 18 (2001) 807–815.

[508] A.R.C. Jones, J.P. Gleghorn, C.E. Hughes, L.J. Fitz, R. Zollner, S.D. Wainwright, B. Caterson, E.A. Morris, L.J. Bonassar, C.R. Flannery, Binding and localization of recombinant lubricin to articular cartilage surfaces., J. Orthop. Res. 25 (2007) 283–92. doi:10.1002/jor.20325.

[509] G.D. Jay, J.R. Torres, D.K. Rhee, H.J. Helminen, M.M. Hytinnen, C.-J. Cha, K. Elsaid, K.-S. Kim, Y. Cui, M.L. Warman, Association between friction and wear in diarthrodial joints lacking lubricin., Arthritis Rheum. 56 (2007) 3662–9.

[510] D.A. Swann, H.S. Slayter, F.H. Silver, The Molecular Structure of Lubricating Glycoprotein-I, the Boundary Lubricant for Articular Cartilage*, J. Biol. CHEMlSTRY. 256 (n.d.) 5921–5925.

[511] M.L. Samsom, S. Morrison, N. Masala, B.D. Sullivan, D.A. Sullivan, H. Sheardown, T.A. Schmidt, Characterization of full-length recombinant human Proteoglycan 4 as an ocular surface boundary lubricant, Exp. Eye Res. 127 (2014) 14–19.

[512] D.P. Chang, N.I. Abu-Lail, F. Guilak, G.D. Jay, S. Zauscher, Conformational Mechanics, Adsorption, and Normal Force Interactions of Lubricin and Hyaluronic Acid on Model Surfaces., Langmuir. 24 (2008) 1183–1193.

[513] J.P. Gleghorn, A.R.C. Jones, C.R. Flannery, L.J. Bonassar, Boundary mode lubrication of articular cartilage by recombinant human lubricin, J. Orthop. Res. 27 (2009) 771–777.

[514] D.K. Rhee, J. Marcelino, M. Baker, Y. Gong, P. Smits, V. Lefebvre, G.D. Jay, M. Stewart, H. Wang, M.L. Warman, J.D. Carpten, The secreted glycoprotein lubricin protects cartilage surfaces and inhibits synovial cell overgrowth., J. Clin. Invest. 115 (2005) 622–31.

[515] C. Englert, K.B. McGowan, T.J. Klein, A. Giurea, B.L. Schumacher, R.L. Sah, Inhibition of integrative cartilage repair by proteoglycan 4 in synovial fluid, Arthritis Rheum. 52 (2005) 1091–1099.

[516] C. Zhao, Y.-L. Sun, R.L. Kirk, A.R. Thoreson, G.D. Jay, S.L. Moran, K.-N. An, P.C. Amadio, Effects of a Lubricin-Containing Compound on the Results of Flexor Tendon Repair in a Canine Model in Vivo, J. Bone Jt. Surgery-American Vol. 92 (2010) 1453–1461.

[517] T. Webster, G. Aninwene, G. Jay, V. Ravi, Z. Yang, Lubricin as a novel nanostructured protein coating to reduce fibroblast density, Int. J. Nanomedicine. 9 (2014) 3131–3135.

[518] G.E. Aninwene, P.N. Abadian, V. Ravi, E.N. Taylor, D.M. Hall, A. Mei, G.D. Jay, E.D. Goluch, T.J. Webster, Lubricin: A novel means to decrease bacterial adhesion and proliferation, J. Biomed. Mater. Res. Part A. 103 (2015) 451–462.

[519] T.E. Ludwig, M.M. Hunter, T.A. Schmidt, Cartilage boundary lubrication synergism is mediated by hyaluronan concentration and PRG4 concentration and structure, BMC Musculoskelet. Disord. 16 (2015) 386.

[520] J.J. Kwiecinski, S.G. Dorosz, T.E. Ludwig, S. Abubacker, M.K. Cowman, T.A. Schmidt, The effect of molecular weight on hyaluronan's cartilage boundary lubricating ability – alone and in combination with proteoglycan 4, Osteoarthr. Cartil. 19 (2011) 1356–1362.

[521] G.D. Jay, J.R. Torres, M.L. Warman, M.C. Laderer, K.S. Breuer, The role of lubricin in the mechanical behavior of synovial fluid., Proc. Natl. Acad. Sci. U. S. A. 104 (2007) 6194–6199.

[522] J. Seror, L. Zhu, R. Goldberg, A.J. Day, J. Klein, Supramolecular synergy in the boundary lubrication of synovial joints, Nat. Commun. 6 (2015) 6497.

[523] A.C. Maiden, D.G. Vanderlaan, D.C. Turner, R.N. Love, J.D. Ford, F.F. Molock, R.B. Steffen, G.A. Hill, A. Alli, K.P. McCabe, Hydrogel with internal wetting agent, (2002).

[524] S. Minko, Grafting on Solid Surfaces: "Grafting to" and "Grafting from" Methods, in: M.

Stamm (Ed.), Polym. Surfaces Interfaces, Springer, Berlin, Heidelberg, 2008: pp. 215–234.

[525] Y. Ikada, Blood-compatible polymers, in: Polym. Med. Adv. Polym. Sci., Springer, Berlin, Heidelberg, 1984: pp. 103–140.

[526] S.. Jeon, J.. Lee, J.. Andrade, P.. De Gennes, Protein - surface interactions in the presence of polyethylene oxide: I. Simplified theory, J. Colloid Interface Sci. 142 (1991) 149–158.

[527] A.S. Hoffman, Surface modification of polymers: Physical, chemical, mechanical and biological methods, Macromol. Symp. 101 (1996) 443–454.

[528] M.A. Rufin, M.A. Grunlan, Surface-Grafted Polymer Coatings, in: Funct. Polym. Coatings, John Wiley & Sons, Inc, Hoboken, NJ, 2015: pp. 218–238.

[529] B. Zhao, W.. Brittain, Polymer brushes: surface-immobilized macromolecules, Prog. Polym. Sci. 25 (2000) 677–710.

[530] P.G. de Gennes, Polymers at an interface: a simplified view, Adv. Colloid Interface Sci. 27 (1987) 189–209.

[531] J. Klein, Entropic interactions: neutral and end-functionalized chains in confined geometries, J. Phys. Condens. Matter. 12 (2000) A19–A27.

[532] Y. Uyama, K. Kato, Y. Ikada, Surface Modification of Polymers by Grafting, in: Galina H. et al. (Ed.), Grafting/Characterization Tech. Model., Springer , Berlin, Heidelberg, 1998: pp. 1–39.

[533] P. Wyman, Hydrophilic coatings for biomedical applications in and ex vivo, in: M. Driver (Ed.), Coatings Biomed. Appl., Woodhead Publishing Limited, 2012: pp. 3–42.

[534] S.R. Meyers, M.W. Grinstaff, Biocompatible and Bioactive Surface Modifications for Prolonged In Vivo Efficacy, Chem. Rev. 112 (2012) 1615–1632.

[535] E.M. Benetti, N.D. Spencer, Are Lubricious Polymer Brushes Antifouling? Are Antifouling Polymer Brushes Lubricious?, in: Polym. Biopolym. Brushes, John Wiley & Sons, Inc., Hoboken, NJ, USA, 2017: pp. 421–431.

[536] G. Morgese, L. Trachsel, M. Romio, M. Divandari, S.N. Ramakrishna, E.M. Benetti, Topological Polymer Chemistry Enters Surface Science: Linear versus Cyclic Polymer Brushes, Angew. Chemie Int. Ed. 55 (2016) 15583–15588.

[537] G. Gunkel, M. Weinhart, T. Becherer, R. Haag, W.T.S. Huck, Effect of Polymer Brush Architecture on Antibiofouling Properties, Biomacromolecules. 12 (2011) 4169–4172.

[538] M. Krishnamoorthy, S. Hakobyan, M. Ramstedt, J.E. Gautrot, Surface-Initiated Polymer Brushes in the Biomedical Field: Applications in Membrane Science, Biosensing, Cell Culture, Regenerative Medicine and Antibacterial Coatings, Chem. Rev. 114 (2014) 10976–11026.

[539] M. Chen, W.H. Briscoe, S.P. Armes, H. Cohen, J. Klein, Polyzwitterionic brushes: Extreme lubrication by design, Eur. Polym. J. 47 (2011) 511–523.

[540] J. Yang, H. Chen, S. Xiao, M. Shen, F. Chen, P. Fan, M. Zhong, J. Zheng, Salt-Responsive Zwitterionic Polymer Brushes with Tunable Friction and Antifouling Properties, Langmuir. 31 (2015) 9125–9133.

[541] M. Kobayashi, H. Yamaguchi, Y. Terayama, Z. Wang, K. Ishihara, M. Hino, A. Takahara, Structure and Surface Properties of High-density Polyelectrolyte Brushes at the Interface of Aqueous Solution, Macromol. Symp. 279 (2009) 79–87.

[542] T. Kang, X. Banquy, J. Heo, C. Lim, N.A. Lynd, P. Lundberg, D.X. Oh, H.-K. Lee, Y.-K. Hong, D.S. Hwang, J.H. Waite, J.N. Israelachvili, C.J. Hawker, Mussel-Inspired Anchoring of Polymer Loops That Provide Superior Surface Lubrication and Antifouling Properties, ACS Nano. 10 (2016) 930–937.

[543] T. Moro, Y. Takatori, K. Ishihara, T. Konno, Y. Takigawa, T. Matsushita, U. Chung, K. Nakamura, H. Kawaguchi, Surface grafting of artificial joints with a biocompatible polymer for preventing periprosthetic osteolysis, Nat. Mater. 3 (2004) 829–836.

[544] T. Goda, T. Konno, M. Takai, K. Ishihara, Photoinduced phospholipid polymer grafting on Parylene film: Advanced lubrication and antibiofouling properties, Colloids Surfaces B Biointerfaces. 54 (2007) 67–73.

[545] J. Zhang, S. Xiao, M. Shen, L. Sun, F. Chen, P. Fan, M. Zhong, J. Yang, Aqueous lubrication of poly(N-hydroxyethyl acrylamide) brushes: a strategy for their enhanced load bearing capacity and wear resistance, RSC Adv. 6 (2016) 21961–21968.

[546] H.C. Kolb, M.G. Finn, K.B. Sharpless, Click Chemistry: Diverse Chemical Function from a Few Good Reactions., Angew. Chem. Int. Ed. Engl. 40 (2001) 2004–2021.

[547] C.E. Hoyle, A.B. Lowe, C.N. Bowman, Thiol-click chemistry: a multifaceted toolbox for small molecule and polymer synthesis, Chem. Soc. Rev. 39 (2010) 1355–1387.

[548] A.B. Lowe, Thiol-ene "click" reactions and recent applications in polymer and materials synthesis, Polym. Chem. 1 (2010) 17–36.

[549] C.R. Morgan, F. Magnotta, A.D. Ketley, Thiol/ene photocurable polymers, J. Polym. Sci. Polym. Chem. Ed. 15 (1977) 627–645.

[550] C.M. Nimmo, M.S. Shoichet, Regenerative Biomaterials that "Click": Simple, Aqueous-Based Protocols for Hydrogel Synthesis, Surface Immobilization, and 3D Patterning, Bioconjug. Chem. 22 (2011) 2199–2209.

[551] C.E. Hoyle, C.N. Bowman, Thiol-Ene Click Chemistry, Angew. Chemie Int. Ed. 49 (2010) 1540–1573.

[552] Y. Sun, H. Liu, L. Cheng, S. Zhu, C. Cai, T. Yang, L. Yang, P. Ding, Thiol Michael addition reaction: a facile tool for introducing peptides into polymer-based gene delivery systems, Polym Int. 65 (2018) 25–31.

[553] A.E. Rydholm, N.L. Held, D.S.W. Benoit, C.N. Bowman, K.S. Anseth, Modifying network chemistry in thiol-acrylate photopolymers through postpolymerization functionalization to control cell-material interactions, J. Biomed. Mater. Res. Part A. 86A (2008) 23–30.

[554] C.D. Pritchard, T.M. O'Shea, D.J. Siegwart, E. Calo, D.G. Anderson, F.M. Reynolds, J.A. Thomas, J.R. Slotkin, E.J. Woodard, R. Langer, An injectable thiol-acrylate poly(ethylene glycol) hydrogel for sustained release of methylprednisolone sodium succinate, Biomaterials. 32 (2011) 587–597.

[555] S.P. Zustiak, J.B. Leach, Hydrolytically Degradable Poly(Ethylene Glycol) Hydrogel

Scaffolds with Tunable Degradation and Mechanical Properties, Biomacromolecules. 11 (2010) 1348–1357.

[556] A. Köwitsch, Y. Yang, N. Ma, J. Kuntsche, K. Mäder, T. Groth, Bioactivity of immobilized hyaluronic acid derivatives regarding protein adsorption and cell adhesion, Biotechnol. Appl. Biochem. 58 (2011) 376–389.

[557] A. Köwitsch, M. Jurado Abreu, A. Chhalotre, M. Hielscher, S. Fischer, K. Mäder, T. Groth, Synthesis of thiolated glycosaminoglycans and grafting to solid surfaces., Carbohydr. Polym. 114 (2014) 344–351.

[558] L.A. Connal, C.R. Kinnane, A.N. Zelikin, F. Caruso, Stabilization and Functionalization of Polymer Multilayers and Capsules via Thiol−Ene Click Chemistry, Chem. Mater. 21 (2009) 576–578.

[559] P. Lundberg, A. Bruin, J.W. Klijnstra, A.M. Nyström, M. Johansson, M. Malkoch, A. Hult, Poly(ethylene glycol)-Based Thiol-ene Hydrogel Coatings−Curing Chemistry, Aqueous Stability, and Potential Marine Antifouling Applications, ACS Appl. Mater. Interfaces. 2 (2010) 903–912.

[560] S. Beigi Burujeny, M. Atai, H. Yeganeh, Assessments of antibacterial and physico-mechanical properties for dental materials with chemically anchored quaternary ammonium moieties: Thiol–ene–methacrylate vs. conventional methacrylate system, Dent. Mater. 31 (2015) 244–261.

[561] J.W. Chan, C.E. Hoyle, A.B. Lowe, M. Bowman, Nucleophile-initiated thiol-Michael reactions: Effect of organocatalyst, thiol, and ene, Macromolecules. 43 (2010) 6381–6388.

[562] M. Liu, B.H. Tan, R.P. Burford, A.B. Lowe, Nucleophilic thiol-Michael chemistry and hyperbranched (co)polymers: synthesis and ring-opening metathesis (co)polymerization of novel difunctional exo-7-oxanorbornenes with in situ inimer formation, Polym. Chem. 4 (2013) 3300.

[563] J.W. Chan, B. Yu, C.E. Hoyle, A.B. Lowe, The nucleophilic, phosphine-catalyzed thiol–ene click reaction and convergent star synthesis with RAFT-prepared homopolymers, Polymer (Guildf). 50 (2009) 3158–3168.

[564] J.W. Chan, H. Wei, H. Zhou, C.E. Hoyle, The effects of primary amine catalyzed thio-acrylate Michael reaction on the kinetics, mechanical and physical properties of thio-acrylate networks, Eur. Polym. J. 45 (2009) 2717–2725.

[565] G.-Z. Li, R.K. Randev, A.H. Soeriyadi, G. Rees, C. Boyer, Z. Tong, T.P. Davis, C.R. Becer, D.M. Haddleton, Investigation into thiol-(meth)acrylate Michael addition reactions using amine and phosphine catalysts, Polym. Chem. 1 (2010) 1196–1204.

[566] S. Chatani, D.P. Nair, C.N. Bowman, Relative reactivity and selectivity of vinyl sulfones and acrylates towards the thiol–Michael addition reaction and polymerization, Polym. Chem. 4 (2013) 1048–1055.

[567] E. Scanlan, V. Corcé, A. Malone, Synthetic Applications of Intramolecular Thiol-Ene “Click” Reactions, Molecules. 19 (2014) 19137–19151.

[568] N.B. Cramer, C.N. Bowman, Kinetics of thiol-ene and thiol-acrylate photopolymerizations with real-time fourier transform infrared, J. Polym. Sci. Part A Polym. Chem. 39 (2001)

3311–3319.

[569] C.E. Hoyle, T.Y. Lee, T. Roper, Thiol-enes: Chemistry of the past with promise for the future, J. Polym. Sci. Part A Polym. Chem. 42 (2004) 5301–5338.

[570] M.L. Samsom, H. Sheardown, T.A. Schmidt, Proteoglycan 4 and Hyaluronan Lubrication Synergy at Silicone Hydrogel-Human Cornea Biointerfaces, Invest. Ophthalmol. Vis. Sci. 55 (2014) 4655–4655.

[571] S. Tosatti, R. Aeschlimann, J. Kakkassery, K. Lorenz, Dynamic coefficient of friction measurements of contact lenses in tear-like fluid, Contact Lens Anterior Eye. 38 (2015) e29. doi:10.1016/j.clae.2014.11.040.

[572] D. Silva, A.C. Fernandes, T.G. Nunes, R. Colaço, A.P. Serro, The effect of albumin and cholesterol on the biotribological behavior of hydrogels for contact lenses, Acta Biomater. 26 (2015) 184–194.

[573] C.G. Begley, B. Caffery, K.K. Nichols, R. Chalmers, Responses of contact lens wearers to a dry eye survey., Optom. Vis. Sci. 77 (2000) 40–46.

[574] S. Kienle, K. Boettcher, L. Wiegleb, J. Urban, R. Burgkart, O. Lieleg, T. Hugel, Comparison of friction and wear of articular cartilage on different length scales, J. Biomech. 48 (2015) 3052–3058.

[575] J.M. Coles, L. Zhang, J.J. Blum, M.L. Warman, G.D. Jay, F. Guilak, S. Zauscher, Loss of cartilage structure, stiffness, and frictional properties in mice lacking PRG4, Arthritis Rheum. 62 (2010) 1666–1674.